ADVANCED RELIABILITY ANALYSIS OF ROAD-SLOPE STABILITY IN SOFT ROCK GEOLOGICAL TERRAIN

by

FHATUWANI SENGANI

Submitted in fulfilment of the academic requirements for
the Degree of

Doctor of Engineering

in the

Department of Civil Engineering and Geomatics

Faculty of Engineering and the Built Environment

at the

Durban University of Technology

Supervisor: Prof Dhiren Allopi

(January 2023)

DECLARATION

Name: Fhatuwani Sengani

Student number: 22176501

Degree: Doctor of Engineering

ADVANCED RELIABILITY ANALYSIS OF ROAD-SLOPE STABILITY IN SOFT ROCK GEOLOGICAL TERRAIN

I declare that the above research study is my own work and that all the sources that I have used or quoted have been indicated and acknowledged by means of complete references.

I further declare that I submitted the research study to originality checking software and that it falls within the accepted requirements for originality.

I further declare that I have not previously submitted this work, or part of it, for examination at DUT for another qualification or at any other higher education institution.

_____ 11/01/2023

SIGNATURE (Student) DATE

—

_____ 12/01/2023

PROMOTER SIGNATURE DATE

Prof D Allopi

Abstract

Most of the national, regional, and local roads in Limpopo Province have been developed through a rugged topography and artificial slopes have been created with loose rocks scattered across the slopes as a results road slope instability is the common challenge. The objective of this research study is to conduct an advanced reliability analysis of road-slope stability in soft rock geological terrain using the national road (N1) and its tributary (R71) as case studies. Limit analysis, limit equilibrium, finite element methods, finite difference methods, machine learning and GIS-based tools have been used for this purpose. Meanwhile, the accuracy classification chart of limit equilibrium methods in homogenous slope and a new method for predicting the stability of slope in multiple faulted slopes were developed. The reproduction of failure evolution of slope instability was also performed, followed by reliability analysis of the slope based on probabilistic analysis. Lastly, an integrated approach to slope stability assessment based on machine learning, geographic information system-based tools and geotechnical methods was presented. To achieve the above, field observations and measurements, structural mapping, limit equilibrium, limit analysis, Monte Carlo simulation, fuzzy inference analysis, and GIS digitization and analysis were performed. Software packages such as SLIDE, FLACslope, Optimum 2G, DIPS, RocLab, and ArcGIS, were used. The accuracy classification chart for Limit Equilibrium Methods LEM), a new method for performing stability analysis in multiple faulted slopes, reproduction of failure evolution of slope was developed. Monte Carlo simulation was established as the most reliable and effective technique to analyze slope stability. The steepness of the slope, rock and soil properties, extreme rainfall and geological features were demonstrated to influence slope instability based on an integrated approach as stated above. From the above-mentioned major findings, it was concluded that the developed accuracy error classification chart of LEMs and the new method of slope stability in multi-faulted slopes are useful. Though the reproduction of failure evolution of slope was successfully achieved, for material to flow for a longer distance, high kinetic energy and more shearing of material are expected to take place during this process. It is

recommended that other sophisticated methods be utilized to expand the results.

KEY TERMS: Slope stability, Reliability Analysis, Probability Analysis, GIS-based tool, Numerical Modelling

List of publications

The articles below have been published or submitted to peer-reviewed journals for the degree of Doctor of Engineering (Civil Engineering and Geomatics).

Sengani, F.; Allopi, D. Accuracy of Two-Dimensional Limit Equilibrium Methods in Predicting Stability of Homogenous Road-Cut Slopes. Sustainability 2022, 14, 3872. https://doi.org/10.3390/su14073872

Sengani, F.; Allopi, D. Numerical study on the evolution process of slope failure triggered by extreme rainfall along a road-cut in mountainous terrain. Scientific Report-Nature. https://doi.org/10.1038/s41598-022-10655-5

Sengani, F., Mashao, F, M., Allopi, D. 2022. An integrated approach to develop a slope susceptibility map based on a GIS-based approach, soft computing technique and finite element formulation of the bound theorems. Transportation Geotechnics, Volume 36, 2022 ,100818 ,ISSN 2214-3912. https://doi.org/10.1016/j.trgeo.2022.100818.

Dedication

Khakhamela, Vele, Silwane, Lutiti lu ambara dzhasi, tshau fuka na tshau adza, tshitaka tshitwu, marunga dzindevhelaho, dambatshekwa lina segere, tshiulu tshamandini. Avha a tshi sendela Sengani, mudulu wa Mmbulaheni, Radukununu, Nyamulambilu wa ha Nethathe na vhanwe, ene ene wa ha Nefundudzi, nya nkodolela wa sa kodolela u do wela, hayani havho nwali. Ha pfala kwatha itshi tavha mukosi u fhandula ho mbilu, mukosi wa u luvha vho Nwali na Nwali muhulu ene Ragole. Dungudzi u rotisa mutodzi, mutodzi wa tshilolo, a tshi vhidzelela vho Nwali na Ragoli ari "vho Nwali na Ragolo, vho Nwali na Ragolo, Vho Nwali na Ragolo, vho na ni ha mudi Mulilangoma ngei pfamoni ya manwalo, vhadziya tshingwindingwindi nda vheka vho difha maanda vha tshilingedza ukweta Tombo la vho Nwali na Ragolo uri li lile madi nga u viela lofha la vho Nwali na Ragolo Bakoni vhana vha edza Pfuko vha Musuku, vha tshiri Mahunguvhu hanga ivhoni". Dungudzi ahuwelela vho Nwali and Ragolo ari zwila zwithu zwo iteya, hari hwiiiiii, mifhululu yee ngindi ngindi, vhari na ngoho hutungula Pfene ha vho-Ravhembalani fhasi ha dzaula la muvhula, Dungudzi ari vho Nwali na vho Nwali vha Thavhani dzaha Molepo na Mamabolo na Ragolo, murorwane a u tungulwe ri divhe uri ri sendama nga lufhio lurumbu. He duuuu a khunyeledza nga uri "zwila zwithu zwo iteya". Ambo lavhelese vhudzula vho Nwali and Ragolo, ndi hone a tshi kuda Magota na u vusa vhane vha zwi Ingamo nga Thakula, ha pfala muungo u tshi vhidza vho the vhala vha daka la Ha-Nethathe na Nefundudzi, vhazwala na ma Khotsi-muhulu. Vha swika vho Nwali and Ragole vhari ngwana ya vhakololo ene ene mukololo "tshi kwilikwili tshi tula tshi nau nau" vhari vhalitshe fhedzi "Dzhiedzhie lola mutanga mutanga wa li la vho" vho Nwali na Ragolo vhari mahunguvhu ayo o vheya lwayo kha vhuredzi ha Zwifhoni husa vheiwi lwalo, vho Nwali na Ragolo vhe mirumba khai tambale tshanga rido tanga migadoni hune Ragole a thuka hone. Ha unga mukosi wa tshitameye tshi tshi vhidzelela mavhudzi a vho kwashaho khali ya vho Nwali and Ragolo, ha pfala khuwa ya zwililo. Wa salipfa uvhuzwani u doli pfela vhulaloni, ya lila Ngomalungundu yone yone ya vho Nwali na Ragolo, Khakhamela, Silwane, iwe mula Mundandane, Ndaa.

Acknowledgments

Firstly, I would like to thank Almighty GOD who made it possible for me to pursue a DEng research study. I appreciate the work, guidance, and encouragement He provided to my supervisor and myself.

I would like to gratefully acknowledge that the work reported in this research study was made possible by funding provided by Durban University of Technology. I acknowledge the guidance and assistance I got from my supervisor, Professor Dhiren Allopi. His knowledge and experience in the field of study is highly appreciated.

I also wish to acknowledge the contribution of Mr Nndanduleni Muavhi; his assistance in the creation of locality map is well appreciated. Mr Mashao is also acknowledged for his contribution with regards to maps generation for the GIS part of the study. All Civil Engineering Labs used for rocks and soil properties analyses are much appreciated.

Finally, it is crucial to appreciate the support I received from my son (Nkhumbudzeni Sengani) and his mother (my wife) Tebogo Millicent Mohlahlo. The support given by my parents (Khwathelani Sandra Nesengani and Ntuweleni Deon Sengani) and other relatives is well appreciated.

In the memory of my late grandfather, grandmother, uncle, and aunt

Chief Vho-Mmbulaheni Sengani, Vho-Mukumela Nekokwane, Vho-Simon Mmbulaheni Mudalahothe and Vho-Julia Ntshengedzeni Mudalahothe
(vha edele nga mulalo ndaa!!!)

Table of contents

List of Figures

List of Tables

List of Abbreviations

BSM	Bishop's Simplified Method
CEM	Corps of Engineers Method
DEMs	Digital Elevation Models
FE	Finite Element
FED	Finite Difference Method
FEM	Finite Element Method
FoS	Factor of Safety
GIS	Geographic Information System
JA	Joint Aperture
JI	Joint Infilling
JP	Joint Persistence
JRC	Joint Roughness Coefficient
JGM	Janbu's Generalized Method
Jn	Joint Set
JS	Joint Spacing
JSM	Janbu's Simplified Approach
JW	Joint Weathering
LE	Limit Equilibrium
LEM	Limit Equilibrium Method
LKM	Lowe-Karafiath’s Method
MPA	Morgenstern-Price Approach

N1	National Road
SM	Spencer's Method
SRF	Strength Reduction Factor
SRM	Strength Reduction Method
R71	Regional Road
RES	Rock Engineering System
RMR	Rock Mass Rating
RQD	Rock Quality Designation
USCS	Unified Soil Classification System
UCS	Uniaxial Compressive Strength

List of Symbols

b	Gradient of the relation
b^e	Elastic left Cauchy Green tensor
C	Cohesion of slope
c	Value of the element at risk
F_f	Factor of Safety
Φ	Angle of internal friction of slope
w	Weight of the block
ψ	Slope angle
b	Base length
h	Block height
R	Resistance
S	Load stress
s	Number of joints per metre
S	Discontinuity spacing
γ	Unit weight of rock mass

Chapter 1 Introduction

1.1 Context of the research

The stability of road-slope embankments is one of the common subjects of study in geotechnical engineering with its application in both civil and mining engineering projects (Renani and Martin, 2020). The stability of these slopes has been based on two common techniques which include the factor of safety (FoS) and the Strength Reduction Factor (SRF). Hoek and Bray (1981), among other scholars (Morgenstern and Price, 1965; Fredlund and Krahn, 1977; Varnes 1978; Zhou and Cheng, 2013; Renani and Martin, 2020) define FOS as “the value by which the shear strength of the slope material must be divided in order to bring the slope to the point of failure”. Nevertheless, the so-called Limit Equilibrium Methods (LEMs) are widely used by engineers and scientists when establishing the stability of the slope based on the FoS method. It has been evidenced that LEM is preferred over other techniques when evaluating the FoS of the slope due to its simplicity. Such evidence can be dated back to studies such as those of Bailey (1967), Fredlund and Krahn (1977), Duncan and Wright (1980), as well as Nash (1982).

There is no doubt that several scholars (Chen and Chameau, 1982; Lam and Fredlund, 1993; Yin, 2012; Zhou and Cheng, 2013; Jiang et al., 2016; Jiang et al., 2017 and Jiang et al., 2018) have strived to improve the shortcomings of the 2D LEMs by introducing 3D LEMs for slope stability analysis that was based on extensions of the 2D LEMs. However, the improved 3D LEMs are very relevant to complex failure surfaces, though most slope stability problems do not involve such complicity. However, the 2D LEM simplifies the problem based on plane strain conditions that do not consider the true 3D properties of the given slope (soil or rock slope) (Jiang and Zhou, 2018), in other words, the displacements are not incorporated in the analysis and it is also assumed that the driving and resisting forces are independent of deformation. Owing to the previous statements, 2D and 3D LEMs still present some critical limitations when performing slope stability analysis. Some of the limitations have been documented in several studies, such as those of Lu et al. (2020) and Renani and Martin (2020) and include the exclusion of stress and

deformation of rock slopes. Secondly, the failure surface of the slope is predefined by engineers. Thirdly, there are many assumptions on the internal forces' distributions used to simplify the governing equations in order to solve the FoS, and lastly, the evolution process of the failure surface may not be simulated using LEMs (Lu et al., 2020).

Based on the previous discussion, concern is often voiced on how accurate the LEMs 2D solutions are. The Strength Reduction Method (SRM)/Strength Reduction Factor (SRF) is normally used to avoid the concern. The SRM/SRF is based on the Finite Element Method (FEM) or Finite Difference Method (FED) to encounter the limitations presented by the LEMs in analyzing slope stability. The concern mentioned above is very critical, especially in those situations wherein the only method or technique available (in terms of resources) to deal with the problem of slope stability are LEMs.

In this research study, Finite Element Methods, Finite Difference Methods, Machine Learning, and GIS-based tools are used to conduct and develop new ways for reliability analysis of slope stability. Limit Analysis are firstly used to benchmark the limit equilibrium method to develop the accuracy chart, while FDM was used to develop a new method for stability analysis in a faulted slope and slope stability mechanisms were therefore predicted using an integrated approach of machine learning, GIS-based tool and FEM. The N1 national highway and its tributaries were used to perform the experiment and validate the results. As such, results concerning reliability analysis of slope stability are expected to be presented in this research study.

1.2 Statement of the problem

Slope instability is a global concern, and although its occurrence may not be frequent, its consequences often result in loss of lives, destruction of properties and road closures, among others (Sjöberg and Norstrom, 2001; Ansari et al., 2014; Göktepe and Keskin, 2018; Sengani and Mulenga, 2020a, 2020b). Most of the national, regional, and local roads in Limpopo Province have been developed through a rugged topography and artificial slopes have been created with loose rocks scattered across the slopes. These

unstable slopes pose a threat to communities and individuals who travel from one point to another through these roads.

The stability analysis of earth slopes is one of the fundamental calculations in civil engineering specifically in geotechnical engineering. It has been noticed in the past that slope stability is one of the major concerns in construction projects involving excavation, embankments, earth dams, and road construction among others. The commonly used slope stability analysis method is the deterministic (Khajehzadeh et al., 2009; Khajehzadeh et al., 2010a, 2010b; Sun et al., 2008; Wang et al., 2010; Maji, 2017). This method is governed by identification of the critical slip surface as well as the associated minimum factor of safety (FoS), and a single factor of safety is then determined (Maji, 2017; Wang et al., 2010; Sun et al., 2008) to classify the stability of the slope. A single deterministic safety factor of a slope is often not enough to analyze the slope stability due to uncertainty of the input parameters among others. Therefore, probabilistic methods are suggested to be the most appropriate approach despite the methods being rarely used in practice due to their complex process and length of analysis.

According to Wang et al. (2010), probabilistic methods are utilized to calculate the probability of slope failure. In contrast to the deterministic approach, probabilistic methods such as the kinetic approach aim to calculate the slope failure probability by taking into account the orientations, physical characters, and shear strength of joints (Wyllie and Mah, 2004; Cao, 2012). Several scholars (Al-naqshabandy, 2012; Huang et al., 2010; Chen, 2007; Cheng et al., 2008a, 2008b) emphasize that probabilistic methods are useful in analyzing slopes with uncertainties or measurement errors such that numerical models provide a poor reflection of the actual state of the slope condition. Cho (2007) states that probabilistic methods combined with risk assessment are better to assess slope design in engineered or artificial slopes such as road cuts than deterministic methods.

Furthermore, Cho (2007) and Turner and Jayaprakash (2012) documented that probabilistic analyses require more computer power than deterministic analyses. As such, probabilistic methods such as the Monte Carlo simulations (MC) may require numerous (thousands) analyses depending on the number of variables considered by the model to

calculate accurate output variables (Gavin, and Xue, 2010). Monte Carlo is envisaged to repeatedly calculate the factor of safety with input parameters that are randomly generated, resulting in obtaining a distribution of values which represent the uncertainty of the input parameters, instead of obtaining a single value of the factor of safety (Ishii et al., 2012). However, the computational efforts for incorporating a large number of possible slip surfaces into a slope system reliability might be very expensive (Mineo et al., 2017; Mineo et al., 2018; Göktepe, and Keskin, 2018). Subsequently, it is equally important to consider increasing the computational efficiency of MC simulations by combining or coupling them with other probabilistic models, such as the surrogate model (Göktepe, and Keskin, 2018).

One may argue that probabilistic analyses are paving the way for stability analysis due to their accuracy yet by engineers and scientists are partially preferred. In light of the above, the need to perform an advanced reliability analysis of the slope stability is significant to address several aspects of the accuracy of the Limit Equilibrium analysis. The development of a new method for analyzing slope stability governed by multi-faults is expected to be developed.

Similarly, the reproduction of the slope failure process based on numerical simulations is also investigated in the present research study. Lastly, the use of an integrated approach (machine learning, GIS tool, and geotechnical technique) in predicting the recurrence of slope instability is demonstrated in the research study. Nevertheless, all mentioned experiments are expected to be tested along the N1 highway with its tributaries.

1.3 Research objectives

The analysis of rock slope stability is generally performed to assess how safe and functional excavated and natural slopes are. Eberhardt (2003) argues that the analysis is aimed to assess slope conditions, potential failure mechanisms, and slope response to external factors that can trigger failure. Moreover, the analysis can be used not only to determine the most effective options for support stabilization but also to optimally design safe, reliable and economical excavation slopes. Limit-equilibrium methods are widely

used by engineers and scientists in predicting the stability of homogenous slopes; their use has been demonstrated to present significant errors due to the violation of kinematic and static admissibility. Limit analysis, machine learning and GIS tools are used to bridge the gap regarding the accuracy of LEM techniques.

Based on the above discussion, the aim of this study was set to conduct an advanced reliability analysis of road-slope stability in soft rocks geological terrain. In order to achieve the aim of the study, the following research objectives are set out as part of the research study:

- To develop a predictive chart on the accuracy of the Two-Dimensional Limit Equilibrium Methods in Predicting Stability of Homogenous Road Cut Slopes;
- To develop a new method for stability analysis in a multi-faulted rock slope and perform the numerical study on the flow evolution process of slope failure;
- To conduct a reliability analysis of slope stability using probabilistic analyses compared with deterministic analysis, and
- To apply the GIS-based approach, machine learning and finite element formulation of the bound theorems in developing reliable slope susceptibility along the R71 road in Limpopo.

It is anticipated that cases of slope stability in civil engineering or mining engineering content may be analyzed in the future based on reliability analysis, machine learning, GIS tools, Finite Element, as well as the Finite Difference paradigm suggested in this research study. As such, problems associated with slope stability along the road embankments may be addressed in detail, and remedial actions may be suggested effectively.

1.4 Contribution to the body of knowledge

The research study is anticipated to contribute to a better description of the reliability analysis of slope stability along the road cut slopes. The national road (N1) and its

tributary (R71) has been used as case studies to unfold and develop a new concept concerning reliability analysis of slope stability.

The reliability analysis of slope stability has been avoided for decades due to its complex process. Yet simplistic processes such as Limit Equilibrium have been implemented to analyze slope stability problems. As such, there is room enough to explore the reliability analysis of slope stability through understanding the accuracy of the limit equilibrium method, developing a new method for slope stability analysis in multi-faulted slopes, simulating the process of slope failure in a faulted slope, and performing reliability analysis of slopes based on probabilistic analysis and integrating machine learning, GIS tools and geotechnical techniques in analyzing the stability of the slopes.

The contribution added by the research study lies in various aspects, for example, in studies such as those of Chen and Chameau,(1982); Lam and Fredlund (1993); Yin, (2012); Zhou and Cheng, (2013); Jiang et al. (2016); Jiang et al. (2017); Jiang et al. (2018); Lu et al.; (2020) and Renani and Martin (2020). The concern regarding the accuracy of Limit Equilibrium Methods (LEMs) solutions in predicting the stability of homogenous slopes was often voiced. Yet, no exact limit equilibrium solutions or charts available against which to check the LEM solutions. The present research study used the rigorous upper and lower bounds solutions of limit analysis based on finite element formulations of the bound theorems to benchmark and develop an accuracy classification chart of limit equilibrium methods in predicting the stability of the homogenous slope. Furthermore, it is well established that the accuracy of the stability number simulated in a multiple-faulted slope has been one of the complex analyses of instability problems, as pointed out by Azarfar et al. (2018). The interaction of lithology with multiple geological features across one slope has been demonstrated to present a challenge in most road cut slopes, yet there is no simple method to follow that captures all sensitivity properties of the geological features. Accordingly, the present research study focuses on developing a new method for stability analysis in a multi-faulted slope using the ubiquitous joint model.

Based on previous studies such as those of Zhang (2014), Zhang, et al. (2018) and Zhang et al. (2019), modelling the flow evolution of a slope governed by solid mass has been recognized as a challenge, yet most stability analyses are only based on stability number or factors of safety (FoS). As such, the stability number, in most cases does not incorporate the deformation characteristics of the material and the change in solid mass phases such as from solid-like to fluid-like phases. Therefore, the present research study also contributes toward developing a numerical simulation of reproducing the failure evolution of a slope with a fault along a road cut. A finite element method associated with an elastoplastic model with strain softening was adopted to provide the failure evolution of R71 road cut slope instabilities.

Lastly, the N1 highway road and its tributaries (R71) in Limpopo Province, South Africa have reported multiple slope instabilities along the road slope cut. Yet, few studies have been conducted to understand the mechanism and classify the slope based on stability number. However, these studies were more concerned about the overall FoS of the slope using deterministic methods; regardless of these studies, slope instabilities along road cuts have been continuously reported. Therefore, the present research study has shown that an alternative way of conducting detailed stability analysis based on probabilistic analysis and using an integrated approach of machine learning, GIS tools and geotechnical techniques.

1.5 Location of the study area

The case study used for this research study is located in Limpopo Province, South Africa, along the N1 highway. The identified area is in the upper Rooiberg group, where shale dominates the slope (see Figure 1.1). It was observed that a highly fissile and brown shale with a purple hue was identified along the slope (Figure 1.1). Previous studies such as those of Armitage et al. (2007) argue that the shale in the study area exhibits a very planar and well-defined lamination which is characterized by green colour fracture or joint surfaces with small ripples on some bedding, and all those have been observed.

Furthermore, it was also observed that the orientation of these bedding planes in the shale and Rooiberg lithology are similar. It was also observed that the slope had been cut

across by three faults, the first fault with quartz as an infill (Figure 1.1), while the rest are filled with dolerite dyke (Figure 1.1). The observed dolerite dykes appeared to be undeformed, medium to coarse-grained dolerite with minor supplied as pointed out by Armitage et al. (2007). The dolerite dykes appear to have an irregular shape across the slope where it is exposed. While the bedding strike is general along NE-SW but varies between N-S and E-W, with gentle to moderate dips (Figure 1.1). The spread of dip angles between 7º to 65º has an uncertain cause in terms of reducing the stability of the slope.

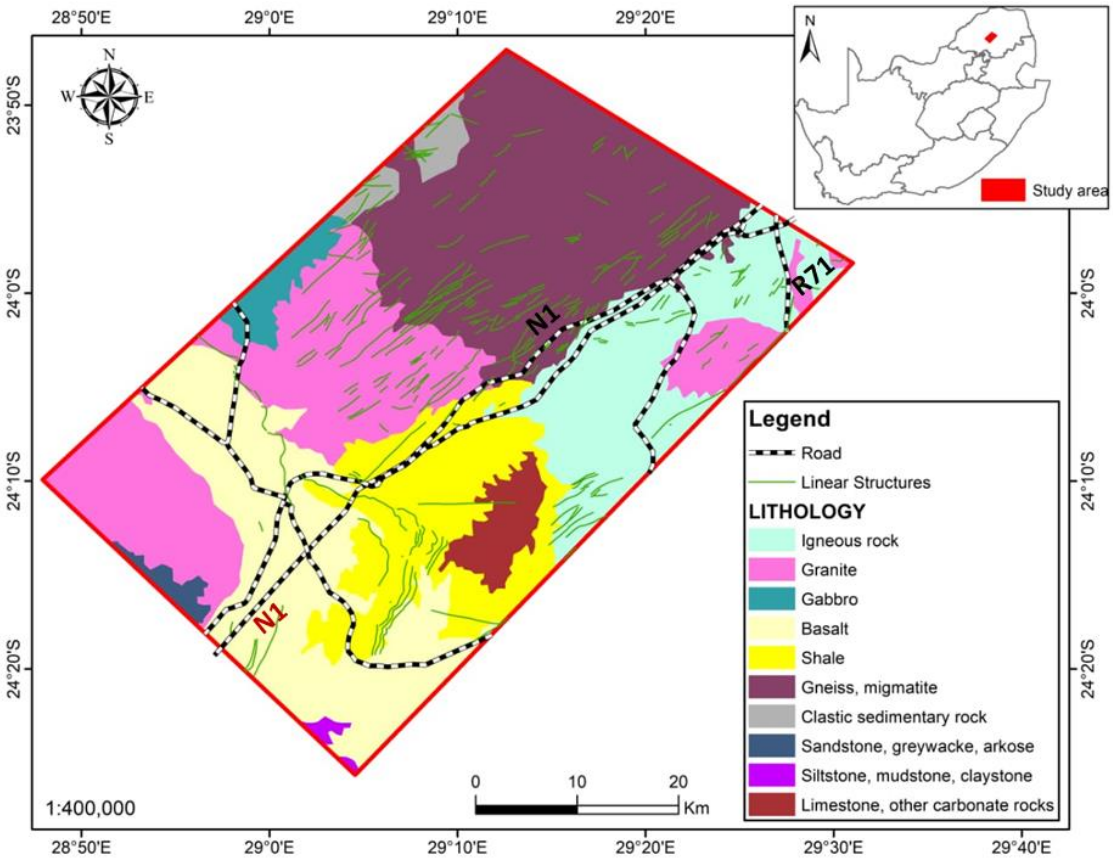

Figure 1.1 Locality map of the study area

R71, a regional road located in the steep and mountainous terrain of Limpopo Province, South Africa (Figure 1.2), was selected as one of the study sites for the N1 tributaries.. R71 connects Polokwane with Kruger National Park through major towns such as Tzaneen and Phalaborwa. The regional road can be found along the two coordinate points starting from 23°53'54.7"S, 29°30'39.9"E and ending at 23°56'44.5"S, 31°09'54.0"E. Although the length of the road extends 201 kilometres (km) from East to

West of Limpopo Province, this study is going to focus mainly on the steep and mountainous terrain of Makgoebaskloof mountains (23°56'53.3"S, 29°57'11.1"E and 23°54'32.7"S, 30°03'45.2"E).

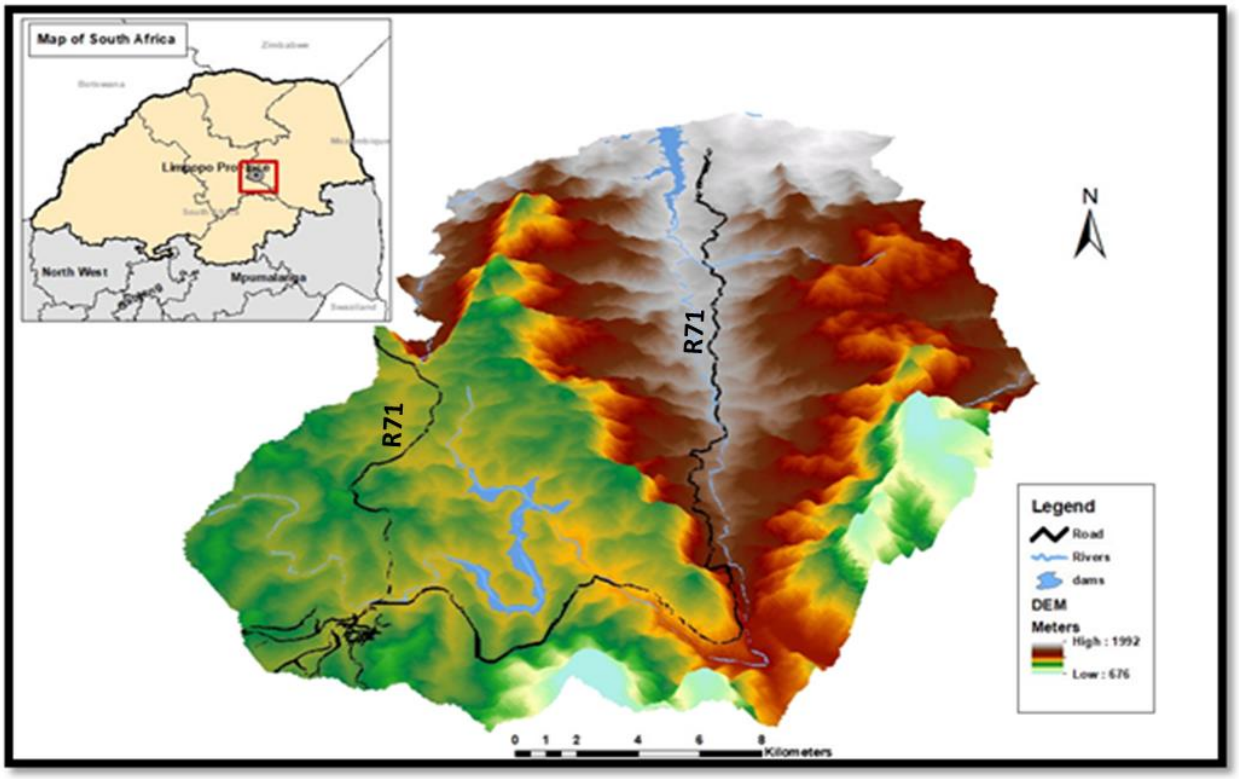

Figure 1.2 Location of Regional Road (R71) Networks.

Note that the map was developed using the DEM tool in ArcGIS 10.2.2, the software package is available at the institution.

The selected study area within R71 contains various rock types, which include granite, gneiss, shale, quartzite and sandstone. Nevertheless, a large portion of the area is dominated by granite. The R71 has been well known to experience slope instabilities along the road cut. This problem has been there for several decades, yet the mechanism behind this failure is still not clear. Similarly, the flow evolution of the failed slope is still not understood, yet the present short technical note on striving to provide an explanation of the failure evolution has been suggested.

1.6 Layout of the research study

Besides the introductory chapter, a detailed literature review on rock-slope stability is discussed in Chapter 2. The chapter commences with an overview of rock-slope stability and the common terms used are outlined. Analysis methods for rock-slope stability such as conventional method, limit equilibrium, and kinematic analysis, are then discussed. A detailed review of the literature on finite element methods is documented while their shortcomings in geotechnical applications are identified. Probabilistic methods are also documented, with a few case studies on the application in geotechnical engineering.

Detailed methodologies are documented in Chapter 3. The chapter commences with a description of the sections incorporated within the chapter. Data collections and experimental procedures are outlined, followed by a description of mathematical formulations of the numerical methods used. In this regard, governing equations of finite element methods are documented, followed by the steps followed when building a block of a model and how the results were acquired.

The first part of the results is documented in Chapter 4. The chapter documents how the accuracy error predictive chart of LEMs was developed. This chart emphasizes that there is way of finding the accuracy of the LEMs when predicting the stability of the slope, although these methods are used more often by engineers and scientists. The chapter also outlines, the rigorous upper and lower bound solutions of the limit analysis were used to benchmark the LEMs while predicting their accuracy in solving the problem. It is outlined that the developed chart is very useful and easy to use.

Following the first results chapter, the second results chapter (Chapter 5) documents some interesting results regarding the development of a new method for analyzing slope stability in a multi-faulted slope. The chapter has used the finite difference method and other geotechnical approaches to develop this new method. The chapter commences with a sensitivity analysis of fault properties, followed by incorporating sensitivity analysis results into the geotechnical analysis of the slope. In this regard, kinematic and stability analyses were therefore combined to develop this new method. The method incorporates the zone of influence within the stability analysis. Supporting Chapter 5, a flow evolution

of slope failure in which the slope is composed of faults has been studied. This study (Chapter 6) has proven that the used numerical model has the ability to present a reproduction of slope failure in a faulted slope.

A detailed, reliable analysis of slope stability is described in Chapter 7, both deterministic and probabilistic methods were implemented in order to conduct the reliability analysis. It is well documented (examples, Mineo et al., 2017; Mineo et al., 2018; Göktepe, and Keskin, 2018) that Monte Carlo simulation has proven that probabilistic analysis is more reliable than deterministic analysis. Probabilistic analyses were demonstrated to produce reliable results, unlike deterministic analyses. Following this chapter, a chapter on an integrated approach to developing slope susceptibility along the R71 road was presented. The chapter commences with a description of the methods used for the purpose, in this regard, machine learning, GIS-based approach and geotechnical methods were implemented to address the given problem. A successful slope susceptibility map of the R71 was developed and the final chapter demonstrates the summary, conclusions, overall conclusions and recommendations of the study.

Following the introduction is the literature review, which is documented below.

Chapter 2 Literature review

This chapter commences by introducing and documenting various definitions of slope stability. Following the definitions, the concept of safety factor was introduced and discussed. It was therefore found significant to state the common parameters influencing slope instability, from internal to external factors.

Slope stability analysis methods from traditional methods such as kinematic analysis, stability charts and limit equilibrium are also documented. A detailed description of advanced methods of slope stability such as numerical simulations which include finite difference methods and finite element methods among others are also stated and discussed. Being said that the probabilistic analysis methods are also incorporated and a few selected case studies on the use of the above-mentioned methods are discussed as well.

2.1 Introduction

The definition of road embankment instability or slope instability has been stressed by various authors such as Varnes (1978), Hoek and Bray (1981), and Irigaray et al. (2012). Nevertheless, the common agreement among the definitions is to state that slope instability is the detachment of the rock mass or soil mass from a slope cut/road cut or steep slope with no shear displacement occurring, and the falling rock mass or soil mass descends most of its distance through the air. Similarly, Guzzetti et al. (2004) and Hasanipanah et al. (2016) support the definition by further outlining that slope instability can be a form of rockfall or soil mass that falls or slide along a vertical cliff proceeding downslope by bouncing, flying, or sliding. Lastly, these events can occur rapidly or slowly depending on the triggering factor within the solid mass, however, in most cases, the slope instability usually presents a rapid moving of solid material along road slopes.

Slope instability has been established as the rapid movement of solid material from a

slope that poses a great threat or hazard to the roads as well as the surrounding environment (Guzzetti et al., 2004; Calamak and Yanmaz, 2014; Gordan et. al., 2015). Therefore, the safety of the slope or stability of the road cuts is important, as a result, the stability of the slope or road cuts is continuously assessed by the determination of the so-called factor of safety.

The originators of some of these concepts (FoS) must be acknowledged, however, Mah and Wyllie (2005) concur that the concepts of FoS can be summarized as "*how much stronger the system is than required*". The FoS is more concerned about how stable the slope is compared to the required stability standard of the slope. Though the stability of the slope is generally controlled by internal factors (mechanical properties of the solid material, rocks and soil, and the surrounding environment where the slope is), external factors also play an important role in terms of the stability of the slope. Compared to the previous concept of FoS, which revolved around the actual conditions of the slope and compared them to expected conditions to cause instability or accidents, there has been a deformation in the recent concept of FoS.

Authors such as Li et al. (2013) scrutinized the previous and recent concepts and discovered that the two concepts are almost similar though the recent one has a specific value when comparing the conditions. Therefore, these two approaches are closely related and as such, they should complement each other rather than compete with each other.

Owing to the previous discussion, the precise analysis of the slope stability is considered an important task in construction and various civil engineering structures such as highways, dams, and open pits (Yilmaz, 2009; Samui and Kothari, 2011; Erzin and Cetin, 2013; Armaghani et. al., 2016). Therefore, the ratio of shear strength to driving stress generated due to gravitational force along the weak plane or failure plane is then considered a factor of safety. In terms of evaluation FoS <1 and FoS>1 signify the slope to be unstable and stable respectively (Hoek and Bray, 1981; Davis et al., 1993; Helmstetter et al., 2004; Wang et al., 2005; De Blasio, 2010). Several key parameters are used in the slope stability evaluations, which are grouped into internal and external factors. In the field of slope instability, a clear distinction between these factors (internal

and external factors) influencing slope stability has been documented by several scholars (Hoek and Bray, 1981; Raghuvanshi, 2017); therefore, the section below outlines both internal and external factors which promote slope instability.

2.2 Factors Influencing Slope Instability

There are several governing factors of slope instability as noted in the introductory section, however, some of these factors are considered to act as a driving force meanwhile others are considered resistive forces. To simplify these factors, they can be grouped into internal and external factors (Hoek and Bray, 1981; Raghuvanshi, 2017; Lamessa, 2019), where internal factors incorporate those of potential failure planes, the geometry of the slope, surface drainage system, groundwater conditions, mineral composition, shear strength parameters of the material, on the other hand, the external factors are governed by seismicity, rainfall, and human activities.

2.2.1 Internal Factors

The internal factors of slope instability are mostly associated with the mechanical properties of the solid mass. In most cases, these are naturally occurring factors and are related to the composition of the solid mass and the surrounding environment. In this regard potential failure planes, slope geometry, surface, and groundwater drainage, and shear strength of the material are discussed in this section.

2.2.1.1 Potential Failing Planes

Some of the previous studies such as those of Hoek and Bray (1981) and Willy and Mah (2004) among others have concluded that among other internal factors that contribute to the occurrence of slope instability, the potential failure plane plays a vital role. However, these do not necessarily mean this factor is the most critical one, however, it is among the factors contributing to the occurrence of slope instability in rock and soil mass slope. In this regard, the so-called persistence of discontinuities that incorporate joint, fault as well as the shear plane present failure of plane within a slope. It has been well established

that the abovementioned geological features generate a plane of weakness within the rock slope. As such, a slight movement within the rock mass may create a failure along the plane of weakness. For example, the intersection of two joints presents a wedge that can slide depending on the driving and resisting forces acting along the plane of failure. However, the prediction of this failure may not be generalized since it depends entirely on the strength of the rock mass and slope angle. Hoek and Bray (1981) believe that hard strata may take time to fail while soft strata may easily fail provided certain conditions are met. Owing to that it has been well established that for a rock slope failure to occur, the *"dip of the potential failure plane should be less than dip of the slope face but greater than friction angle along failure plane"* (Hoek and Bray, 1981; Willy and Mah, 2004). This discussion on potential failure planes necessitates; discussion on how slope geometry contributes to slope failure as outlined below.

2.2.1.2 Slope Geometry

As already documented above the geometry contributes to slope failure, one may need to understand how this geometry contributes to slope failure. It has been documented in several previous studies including Raghuvanshi (2017) that slope geometry is governed by several parameters which contribute to slope failure.

Some governing parameters incorporate dip and dip direction of the slope and failure plane, slope height, upper slope dip and tension crack. The above-mentioned parameters have their effects on the stability of the slope, with slope steepness and height being considered the most sensitive factors towards the occurrence of slope instability. For argument's sake, Hoek and Bray (1981) have demonstrated that steeper slopes result in higher chances of instability; this suggestion has been validated by several authors such as Willy and Mah (2004); Raghuvanshi (2017); Lamessa (2019); Sengani and Mulenga (2020a; 2020b) and Sengani and Mulenga (2021). Nevertheless, slope geometry alone cannot initiate slope failure but other internal factors, such as surface and groundwater conditions, contribute to the movement of slope material. A detailed discussion on the effect of water bodies on slope instability is presented below.

2.2.1.3 Surface Water Drainage and Groundwater Conditions

The conditions of both surface and groundwater play a vital role in reducing and increasing the resistance of solid material along the plane of weakness. However, it has been demonstrated from several studies that the presence of surface water due to rainfall increases the volume of the material while changing the phase (solid to liquid) of the solid mass (Sengani and Mulenga, 2020a; 2020b), as such slope instability is therefore generated. In supporting the previous statement, scholars such as Hoek and Bray (1981) Robert (2002), as well as Raghuvanshi (2017), concur that the increase in water drainage reduces the resistance of solid particles while becoming a motivation for shear stress increase and decreasing shear strength of the material, which leads to the failure of the slope. Several studies including those of Sengani and Zvarivadza (2018) and Sengani and Mulenga (2020a) have looked into the influence of water drainage on the stability of the slope. Studies have documented that as rainfall increases the Drago forces increase while changing the phases of the solid mass and eventually a failure can occur as the sliding of solid mass and rock falls among others. Similarly, advanced numerical simulation has been conducted by Zhang and his co-authors (2014 to 2019) who reached similar conclusions to Sengani and his co-authors (2018 to 2021). These results demonstrate that water drainage has a vital effect on the stability of the slope, as such this has to be incorporated in slope stability assessments. As a result of this discussion some cardinal points associated with the shear strength of the solid mass are outlined.

2.2.1.4 Shear Strength Parameter of Materials Composing the Slope

The shear strength parameter of the material composing the slope is a major factor in determining the resistive force acting perpendicular to the plane of failure. (Barton and Bandis, 1990; Raghuvanshi, 2017). Roughness, continuity, aperture and filling are all conditions of discontinuities that affect these parameters (Johnson and Degraff, 1991). Barton and Bandis (1990) use the empirical law of the fundamental friction angle first proposed by Barton (1973) for the non-linear equation to predict shear strength along failure planes or natural joints expressed as follows:

$$\tau = \sigma_n \tan [JRC \log_{10} (JCS / \sigma_n) + \phi_b] \quad (2.1)$$

Where τ = is peak shear strength (kPa), σn = is effective normal stress (kPa), JRC = is joint roughness coefficient, JCS = is joint wall compressive strength (kPa) and ϕb = is basic friction angle. Definitions of each parameter are given below.

The anticipated coefficient of joint surface roughness, which varies from 0 to 20, is known as the joint roughness coefficient (JRC) (smoothest to roughest). Morelli (2014) connotes that JRC can be determined using a variety of approaches, the most frequent of which is based on a visual comparison of discontinuity surface roughness with a conventional joint roughness profile developed by (Barton and Choubey, 1977). The appearance of the discontinuity surface is visually compared to the profiles provided, and the best JRC value corresponding to the profile that matches the discontinuity surface is chosen. It can also be determined using the relationship between profile length and maximum amplitude (Barton and Bandis, 1982) or by back analyzing and tilt testing.

Joint wall compressive strength (JCS) is the strength of the layer of rock near the joint that controls the rock mass' strength and deformation (Barton, 1973). When the joint is unweathered, the joint wall compressive strength (JCS) is equal to the unconfined compressive strength (σc) of the unweathered rock (Barton, 1976; Barton and Choubey, 1977; Barton and Bandis, 1990). The joint wall compressive strength (JCS) of the rock will be represented by the suitable value of uniaxial compressive strength (σc) obtained from Schmidt rebound value (R) applied on an un-weathered rock surface with unit weight (γ). For worn rock surfaces or in the absence of a Schmidt hammer reading, JCS will become a fraction of the rock's uniaxial compressive strength (about 1/4σc) (Barton, 1976).

The basic friction angle (ϕb) is an angle formed by a flat, planar, and unweathered rock surface with a value ranging from 21º to 40º for the majority of the rock (Goodman, 1989). Barton (1973) also found that the value ranges from 25º to 35º for most smooth, flat, and undamaged rock surfaces. Tilt tests on smooth, flat, and unweathered joints cut from the rock surface with a saw can be used to determine the basic friction angle, or it can be adopted from the fundamental friction angle determined by (Coulson, 1972; Barton and

Choubey, 1977). For joints exposed to various weather conditions, the default friction angle can be related to the residual friction angle (ϕr) as shown below (Barton and Choubey, 1977).

$$\phi r = (\phi b - 20) + 20\,(r/R) \qquad (2.2)$$

where r is the Schmitt repulsion number of the wet and weathered fracture surface and R is the Schmitt repulsion number of the dry, unweathered sawing surface.

The Rocdata program (Rocdata 3.0 Rocscience, 2004) has the ability to calculate cohesion and friction angle along the failure plane, joint roughness coefficient profile, joint wall compressive strength range, and basic friction angle table. In addition, the Rocdata software imports the rock's slope height and unit weight. Finally, using Rocdata software non-linear failure criteria, cohesion and friction angle along failure planes or discontinuities will be assessed. Similarly, the cohesion and friction angle of a rock mass can be estimated using either rear analysis of failed or failing slope failures or front analysis of successful or failing slope failures (Hoek-Brown, 1980; Sharma et al., 1999). Furthermore, the shear strength parameter can be determined experimentally depending on the classification of the rock mass (Bieniawski, 1989).

2.2.2 External Factors

External factors that influence the occurrence of slope instability encompass human activity, seismicity, rainfall among other factors. Several authors have attempted to explain the above-mentioned components and their impact on slope stability; some of the comments on each factor are discussed below.

2.2.2.1 Human activities

The development of infrastructure/civil engineering structures has grown more widespread as a result of population growth, and inappropriate alterations and excavations, resulting in unstable slopes in rugged topography (Sengani and Mulenga, 2020a). Cutting the slope for road building, steepening the slope gradient, and adding more load to the slope are only a few examples of common human activities that cause slope instability (Raghuvanshi, 2017).

2.2.2.2 Seismicity

Slope instability is triggered by ground movement caused by earthquakes and human activities such as mining, particularly in places where the rock mass is dominated by seismically active geological features (Hoek and Bray, 1981). The minimal earthquake magnitude required to trigger slope failure is around 4-5 MM (Pantelidis, 2009). It is advised that seismicity be considered for crucial structures such as steep slopes from a safety standpoint (Dahle et al., 1992). Planar mode rock slope failures will be easily destabilized under seismic loading circumstances because horizontal seismic acceleration contributes to the driving force along the failure plane (Raghuvanshi, 2017).

2.2.2.3 Rainfall

The influence of rainfall, which is one of the external and triggering elements of slope instability, is usually the primary cause of slope failure (Ayalew et al., 2004; Pantelidis, 2009; Woldearegay, 2013). Rainfall infiltrating the slope reduces shear strength, increasing the instability of the probable plane failure (Pantelidis, 2009; Raghuvanshi, 2017). Rainfall has the effect of raising the elevation of groundwater levels. Groundwater, in turn, impacts on the rock slope's stability for the following reasons: (Wyllie and Mah, 2004).

- Water pressure impacts the rock slope's stability by lowering the resistive force along the failure plane.
- Weathering is accelerated by changes in the rock's moisture content, which reduces the rock's shear strength.
- The freezing of groundwater and surface water in tension cracks result in an increase in water pressure, which reduces the slope's stability.
- Increased weathering of the rock, put the slope's toe in jeopardy.
- Groundwater seeps into the slope face.

2.3 Rock Slope Stability Analysis Techniques

Different academics categorize the methods used to assess rock slope stability in various ways. According to Eberhart (2003), these methods can be divided into two categories: traditional methods, which include kinematic analysis, limit equilibrium analysis, and rockfall simulators, and numerical methods, which include the continuum approach, discontinuum approach (distinct-element method, discontinuous deformation analysis, and particle flow codes), and hybrid approach. In examining the rock slope stability, the author failed to consider the usage of rock mass categorization.

The rock slope stability can be separated into two classes, according to Gao (2015). The first category includes quantitative analytical methods such as the limit equilibrium method (LEM), limit state method, and numerical simulation approach. The calculation of the LEM based on force and momentum equilibrium (or the existence of a failure in the rock mass such as sliding and toppling) is straightforward and yields the safety factor. However, some reasonable assumptions are required, and the accuracy of the assumptions has a substantial impact on the results' credibility.

Experience is the primary criterion for determining stability, therefore, it is highly subjective (Gao, 2015). Determining the stability of a rock slope requires some experience because some subjective considerations are involved (Gao, 2015).The safety factor is often determined using the shear strength reduction methodology or numerical models that relate existing strength to limit equilibrium strength in the numerical simulation method. Although the computation is intuitive and straightforward, several computing parameters needed in the numerical analysis should be provided ahead of time, and determining these values is complex.

The second group is known as the qualitative analysis method and includes soft computing techniques such as the fuzzy evaluation method, multi-criteria decision-making approach, support vector machine method, genetic algorithm method, artificial neural network method, and colony clustering algorithm, as well as qualitative analysis methods such as rock engineering system (RES), rock mass classification, and engineering analogy methods. The stability of the rock slope is described by the stability

status rather than the safety factor in the qualitative analysis approach (Gao, 2015). This technique, on the other hand, takes into account the complex geological processes that affect rock slope stability. Some ambiguous elements of the rock slope's stability can be reflected in many ways, and the application is extremely useful.

2.3.1 Kinematic Analysis

Kinematic analysis is a technique for determining the likelihood of various forms of rock slope failure caused by discontinuities and their spatial orientation. The analysis, according to Allen and Huggel (2013), recognizes the movement that happens during slope deformation. The strength of the rock mass is mostly determined by the existence of discontinuities. Wilson and Cunningham (2003) differentiated between failure mechanisms that are mostly structurally regulated and failure mechanisms that are primarily stress controlled. Some failure mechanisms, however, are a combination of the aforementioned criteria and might occur as a result of time and weathering of excavation stability. Planar failure, wedge failure, circular failure, and toppling failure are the four typical mechanisms of slope failure used in slope stability analysis (Norrish and Wyllie, 1992).

2.3.1.1 Planar Failure

This occurs when a block or rock mass slides along a single continuous plane that protrudes from the slope (Surujbally, 2016). The angle of inclination of the plane in the excavation must be greater than the angle of friction and the sliding plane must lie on the inclined plane for plane failure to occur.

In addition, for plane failure to occur, several geometrical conditions must be met, including the strike of the sliding plane must be parallel or nearly parallel (approximately 120°) to the face of the slope, the slope of the plane must be greater than the slope of the sliding plane, the inclination of the sliding plane must be greater than the angle of friction, and the upper end of the sliding surface must intersect the upper slope or the end of the tension crack (Mah and Wyllie, 2005).

The following circumstances must be met for this type of failure to occur (Wyllie and Mah, 2004):

- The sliding plane must be parallel or nearly parallel to the slope face (about +/- 20°).
- The sliding plane must be able to see the slope face in the daylight.
- As a result, the plane's dip must be smaller than the slope face's dip, while the sliding plane's dip must be more than the plane's angle of friction.
- The presence of release surfaces that define the slide's lateral bounds should provide minimal sliding resistance.

This leads us to the second type of kinematic analysis failure mechanism, referred known as wedge failure. The next subsection contains a detailed description of wedge failure.

2.3.1.2 Wedge Failure

When a rock mass slides along two discontinuities on the slope, the line joining the two discontinuities (see Figure 2.1) appears on the slope, and this type of failure occurs (Surujbally, 2016). If the angle of inclination of the wedge is greater than the angle of friction, the piece of rock at the intersection of these continuums will slide down along the tangent line (Figure 2.1).

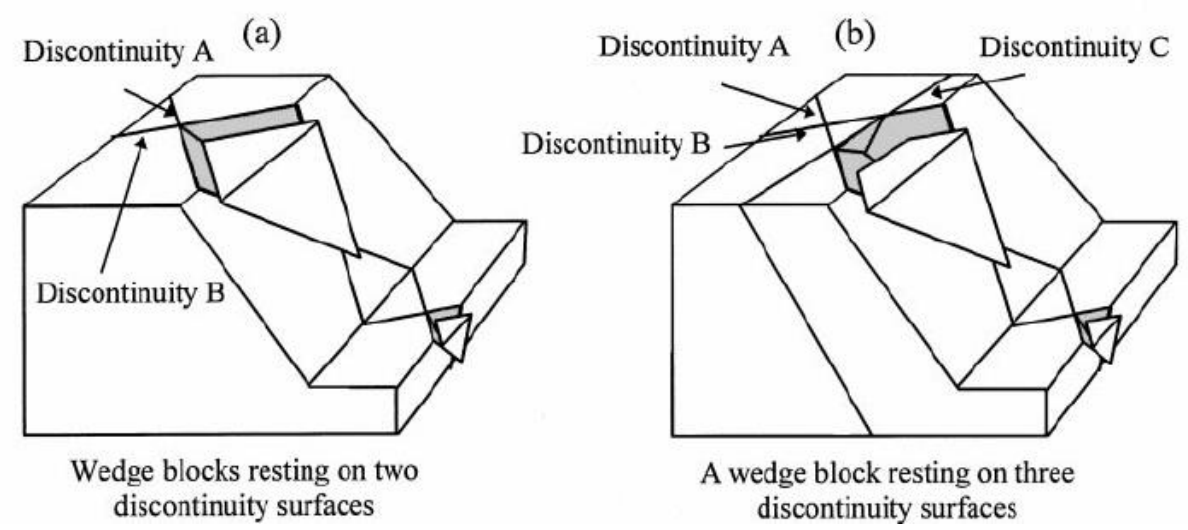

Figure 2.1. Types of wedge failure (Kumsar et al., 2000)

Due to its prevalence across a wider range of geology and geometric settings, wedge stability studies are an important part of rock-slope engineering (Mah and Wyllie, 2005). Stereonets are utilized to specify the wedge shape, line of intersection orientation, and overall sliding direction. Stereonet data is used to determine the likelihood of a wedge sliding off a slope cut (Hoek and Bray, 1981). Kinematic analysis is a technique that identifies possible imbalanced wedges but does not provide extensive information on their factor of safety (Mah and Wyllie, 2005). Face dip and line of intersection trends are generally comparable with plunge line intersection spanning from 50-55º and joint friction between 35-40º. As a result, the line of intersection dips steeper than the angle of friction, which is the kinematic condition that causes wedge failure (Mah and Wyllie, 2005). The following criteria must be met for this type of failure to occur (McMillan et al., 2000: 13):

- The dip of the slope must be greater than the dip of the intersecting line between the two discontinuity planes.
- The sloping plane must have the line of intersection of the two discontinuity planes.
- The dip of the line of intersection between the two discontinuity planes must be greater than the plane's friction angle.

Meanwhile, this type of failure is closely related to other kinematic failure mechanisms; for example, circular failure and wedge failure are commonly confused. Furthermore, the way in which the failure is caused determines the differentiation between the two. In summary, the section below provides a brief overview of circular failure.

2.3.1.3 Circular Failure

It occurs in loosely bound (low intact strength) and heavily fractured (no discernible structural pattern) rock masses or materials, where rock masses or materials collapse rather than individual rock blocks (see Figure 2.2). When compared to the slope size, the collapsing material is quite small. This form of collapse is also frequent in rock masses with closely spaced, randomly oriented discontinuities, such as rapidly cooled basalts (Hoek and Bray, 1981). The limit equilibrium approach is used for a stability study, in which the available shear strength along the sliding surface is compared to the force

required to keep the slope in equilibrium (Mah and Wyllie, 2005). The slope is divided into vertical slices during the limit equilibrium technique.

In the absence of a clear failure mechanism, Avery (2012) proposed the term "raveling failure" or "rockfall failure" (Figure 2.2). Small-scale rockfall occurrences occur when rock blocks fall freely from a rocky slope or slope cut (Avery, 2012).

Figure 2.2. Circular failure of the slope in highways (Google images, 2022)

2.3.1.4. Toppling Failure

Columnar bedding planes and joints characterize a form of failure that is widespread in rock masses. It happens when two forces induce rock blocks to rotate, with discontinuities slanting steeply towards the slope face (see Figure 2.3).

To detect likely toppling situations, a kinematic study of the structural geology is used to determine the stability of toppling failure (Mah and Wyllie, 2005). According to Godman and Bray (1976), there are two types of toppling: Block toppling and Flexural toppling.

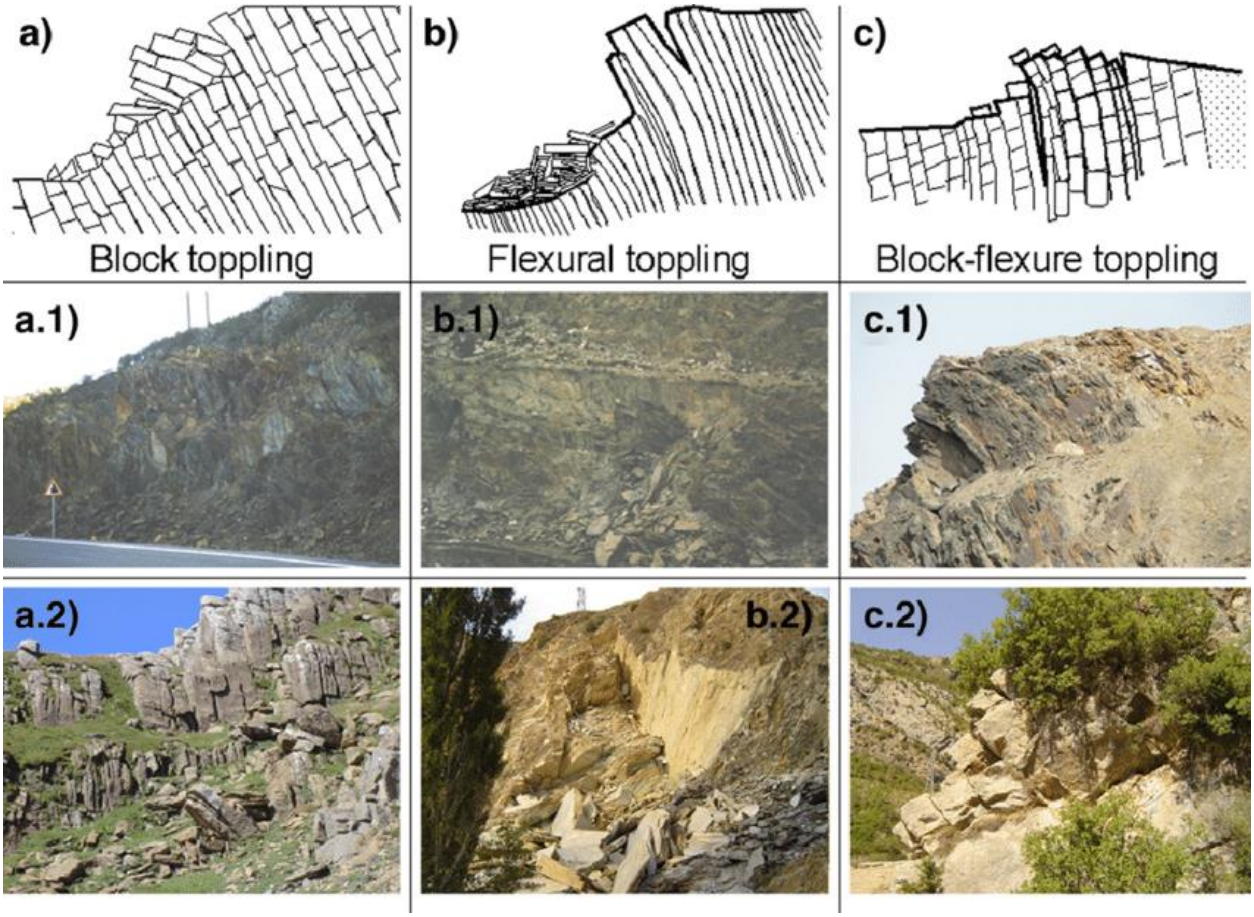

Figure 2.3. Common toppling failures as described by Willie and Mah (2004).

a) Block toppling of slabs of rock with widely spaced normal joints; a. 1) block toppling on the road in Salamanca (Spain); a. 2) block toppling in the Pyrenees (Spain).

b) Flexural toppling of slabs of rock dipping steeply into the face; b. 1) flexural toppling in a bench of the Tharsis copper open pit mine in Huelva (Spain); b. 2) flexural toppling near a riverbank in Sort near the Pyrenees (Spain).

c) Block flexural toppling is characterized by pseudo-continuous flexure of long slabs through accumulated motions along various cross joints; c. 1) block flexural toppling in a

slate quarry in La Cabrera in León (Spain); c.2) block flexural toppling in a riverbank near Gerri de la Sal in Lleida (Spain) (Alejano et al 2010).

Block toppling

This is most common in bedded sandstones and columnar basalts with well-developed orthogonal jointing. Individual columns form in strong rocks as a result of a series of discontinuities plunging steeply into the face.

Flexural toppling

This is frequent in thinly bedded shale and slates that lack well-developed orthogonal jointing. When continuous columns of rock are split by well-developed, sharply dipping discontinuities that break in flexure as they bend forward, this type of fracture occurs. The conditions necessary for toppling failure to occur are:

- The joints must dip sharply into the slope and be able to slip relative to each other for toppling to occur.
- The rock must be able to deform extensively for toppling to occur.
- Tensile bending failure at the base of the tumbling columns requires a low rock-mass tensile strength.

2.3.2 Limit Equilibrium Analysis

These approaches are used to generate a factor of safety (FoS) or a complete back-analysis (Eberhardt, 2003) and are used in a variety of slope-stability analyses due to their simplicity and precision (Arup et al., 2014). According to Eberhardt (2003), all limit equilibrium procedures employ the same method of comparing disturbing and resisting forces acting on a rock mass. Limit equilibrium approaches include slicing the slope under investigation into fine slices and then applying suitable equations (moments or force equilibrium) (Arup et al., 2014). The slicing method is the most widely utilized limit equilibrium approach. This methodology employs various analysis approaches depending on the type of problem and the level of precision required.

2.3.2.1 The Ordinary method

The Ordinary Method (OM) is widely known for satisfying the moment equilibrium for circular slip surfaces while omitting both the interslice normal (E) and the shear forces (T) (Abramson et al., 2002). Because its equation does not involve interaction processes, one of the most common advantages of this method is its simplicity in determining the factor of safety (FoS). Furthermore, for flat slopes with high pore pressure, the approach is regarded as inaccurate (Figure 2.4). As previously stated, the method's FoS is based on moment equilibrium, hence the FoS equations are as follows (Abramson et al., 2002; Nash, 1987):

$$F_m = \frac{\sum(C'l + N' \tan \emptyset')}{\sum W \sin \alpha} \quad (2.3)$$

$$N' = (W \cos \alpha - ul) \quad (2.4)$$

Where: α, c', φ', u, l and F are the inclination of slip surface at the middle of slice, cohesion, friction angle, pore pressure and slice base length respectively

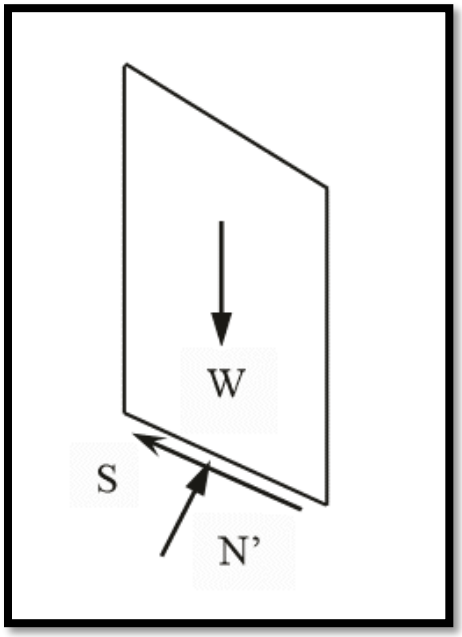

Figure 2.4. Forces considered in OM

2.3.2.2 Bishop's methods

In geotechnical engineering, Bishop's Simplified Method (BSM) is widely used; it is deemed accurate for only circular slip surfaces (Duncan 1996, Abramson et al., 2002). However, the approach also achieves vertical equilibrium and overall moment equilibrium (Figure 2.5). Furthermore, the approach implies horizontal side stresses on slices. The equation for the method is as follows:

$$N' = \frac{1}{m_\alpha} \sum \left(W - \frac{c' l \sin \alpha}{F} - ul \cos \alpha \right) \quad (2.5)$$

Where

$$m_\alpha = \cos \alpha \left(1 + \tan \alpha \frac{\tan \phi'}{F} \right) \quad (2.6)$$

Finally, the FoS is determined by iterative methods (Duncan, 1996). The forces that are taken into account in BSM are depicted in the diagram.

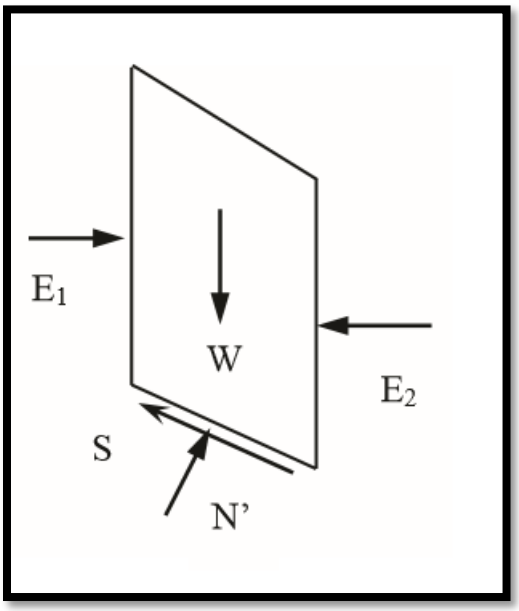

Figure 2.5. Forces considered in BSM

2.3.2.3 Janbu's simplified method

Janbu's Simplified Approach (JSM) is a force equilibrium method that may be applied to any shape of the slip surface. Compared to other methods that computed the safety factor by satisfying all conditions of equilibrium, this method assumes that side forces are horizontal (same for all slices and Figure 2.6) and the safety factor is usually smaller. This approach is governed by the Safety Factor equation, which is illustrated below (Duncan, 1996).

$$F_O = \frac{\sum\left\{\frac{b\left(C' + (p-u)\tan\emptyset'\right)}{n_\alpha}\right\}}{\sum p.b\tan\alpha} \quad (2.7)$$

Where

$$n_\alpha = cos^2\alpha\left(1 + \tan\alpha\frac{\tan\emptyset'}{F}\right) \quad (2.8)$$

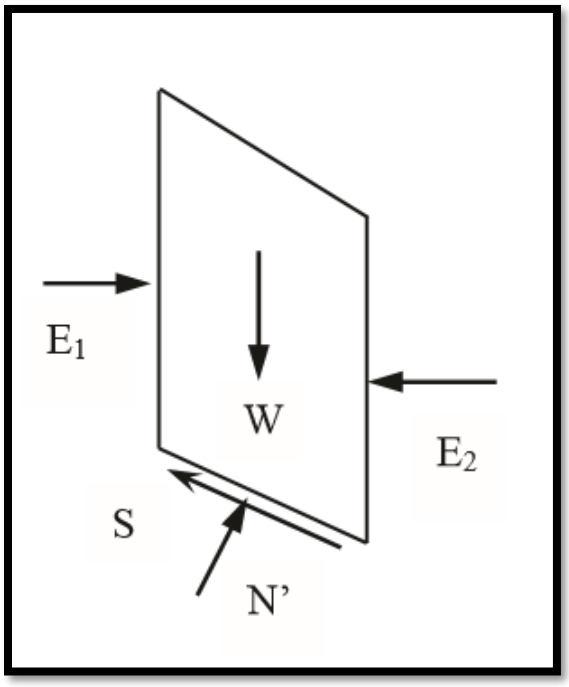

Figure 2.6.Forces considered in JSM

2.3.2.4 Janbu's generalised method

Janbu's Generalized Method (JGM) satisfies all equilibrium conditions and can be applied to any slip surface shape. The method is based on the heights of side forces above the slice's base (usually varied from slice to slice). It is also regarded as an accurate method that is widely used in numerical convergence difficulties. Figure 2.7 shows the FoS equation that governs this technique (Duncan, 1996), while Figure 2.7 shows the forces included in JGM

$$F_f = \frac{\sum[\{c'l+(N-ul)\tan\emptyset'\}\sec\alpha]}{\sum\{W-(T_2-T_1)\}\tan\alpha+\sum(E_2-E_1)} \quad (2.9)$$

Where, F_f is FoS E, T, W are forces

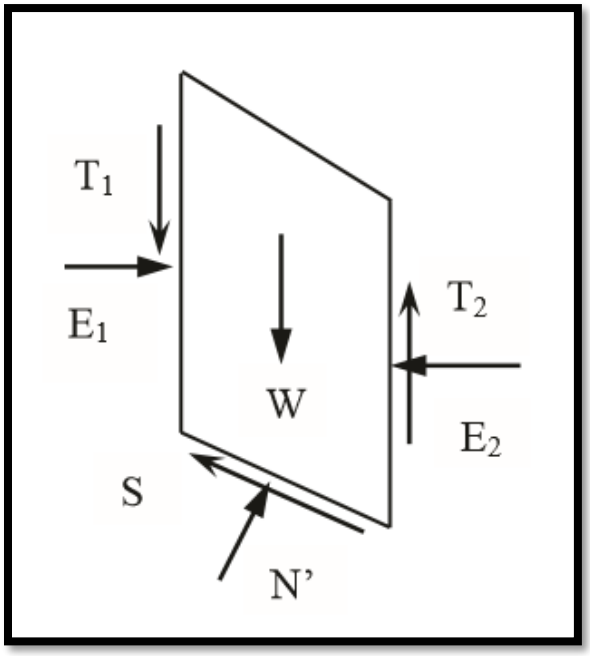

Figure 2.7.Forces considered in JGM

2.3.2.5 Lowe - Karafiath's method

Lowe-Karafiath's Method (LKM) is the most precise method of force equilibrium and may be applied to any slip surface shape. The force inclination is assumed to be the average of the slope surface and the slip surface in this method (varied from slice to slice). Vertical

and horizontal force equilibrium is achieved by using this method. Below is the FoS equation that governs this approach (Duncan, 1996).

$$T = E \tan \theta \quad (2.10)$$

Where, λ is the scale factor of the assumed function, E is the interslice forces, and T is the FoS.

2.3.2.6 Corps of Engineers method

The Corps of Engineers Method (CEM) is a precise method of force equilibrium that may be applied to any slip surface shape. The method presupposes that the side force inclination is equal to the shape's inclination (same from slice to slice). The safety factor is frequently thought to be higher than that determined by other methods that satisfy all equilibrium criteria. Below is the FoS equation that governs this approach (Duncan, 1996).

$$T = E \tan \theta \quad (2.11)$$

Where, λ is scale factor of the assumed function, E is the interslice forces, and T is the FoS.

2.3.2.7 Morgenstern-Price method

The Morgenstern-Price Approach (MPM) is a precise force equilibrium method that may be applied to any slip surface shape. The method assumes that the side force inclination follows a predetermined pattern called f(x), that the side force inclination can be the same or different for each slice, and that the side force inclination is calculated during the solution process to ensure that the equilibrium conditions are met. This method's FoS equation is depicted below (Duncan, 1996). Figure 2.8 depicts the forces that are evaluated in MPM.

$$T = f(x).\lambda.E \quad (2.12)$$

Where f(x) is the continuous interslice force function along the slip surface, s is the scale factor of the assumed function, E is the interslice forces, and T is the FoS.

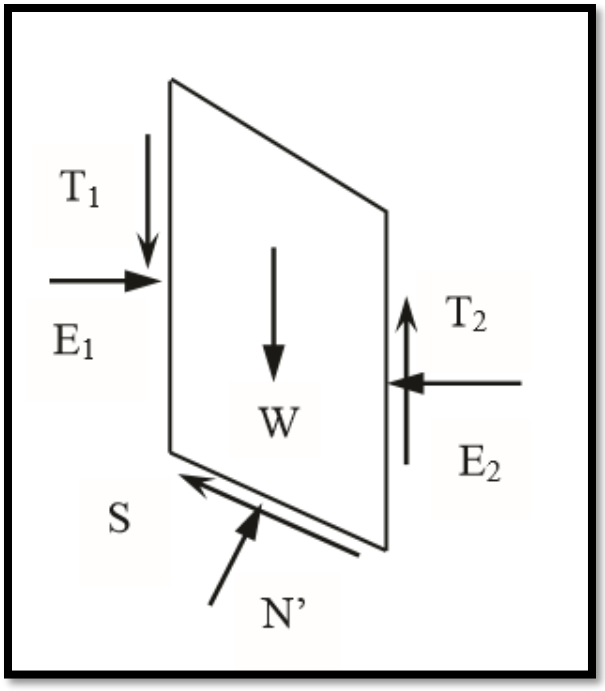

Figure 2.8. Forces considered in MPM

2.3.2.8 Spencer's method

Spencer's Method (SM) is a precise method of force equilibrium that may be applied to any slip surface shape. The approach presumes that the side force inclination is the same for each slice and that the side force inclination is determined during the solution process to ensure that the equilibrium criteria are met. Below is the FoS equation that governs this approach (Duncan, 1996). Figure 2.9 depicts the forces that are taken into account in SM.

$$T = E \tan \theta \qquad (2.13)$$

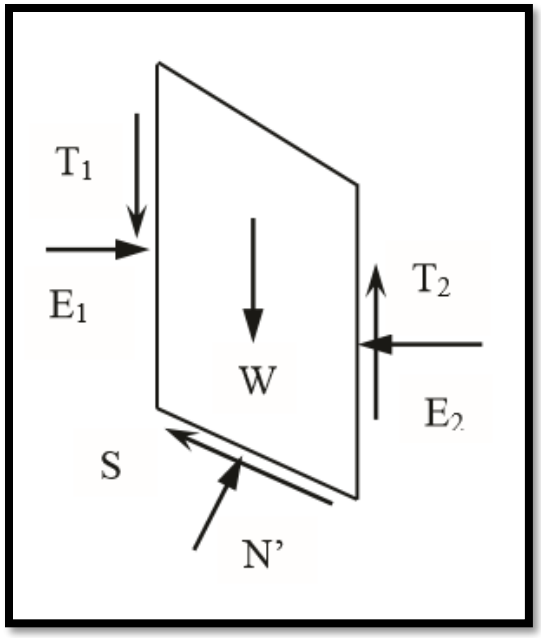

Figure 2.9.Forces considered in SM

2.4 Limit Equilibrium Methods

Due to the limitations of the standard slice method, it was upgraded to the Modified Bishop's method in 1955. Then, throughout time, other limit equilibrium approaches such as Lorimar's (Gerhardt, 1930s), Spencer's (Spencer, 1967), and Sarma's (Sarma, 1970) methods were introduced. These limit equilibrium approaches have a number of drawbacks, including the inability to compute displacement and the inability to describe increasing failure (Bartakke et al., 2017). Rock slope analysis is done using limit equilibrium methods such as Toppling, Rotational, and Transitional.

2.4.1 Toppling Analysis

Toppling analysis is used to investigate both direct toppling and flexural toppling modes of failure, but because flexural toppling involves interior deformations, limit equilibrium techniques are ineffective (Eberhardt, 2003). The likelihood of toppling and sliding is factored into a limit equilibrium study of toppling failure. The solution methodologies of Hoek and Bray (1981) are extended to take into account the entire system's equilibrium circumstances. Furthermore, Hoek and Bray (1981) stated that "a series of sliding blocks in the region, with sturdy blocks at the top and toppling blocks in the middle" is frequent.

This makes the equations simple to program, allowing for computer-assisted calculations and visualizations of sliding and toppling potential (Figure 2.10). (Eberhardt, 2003).

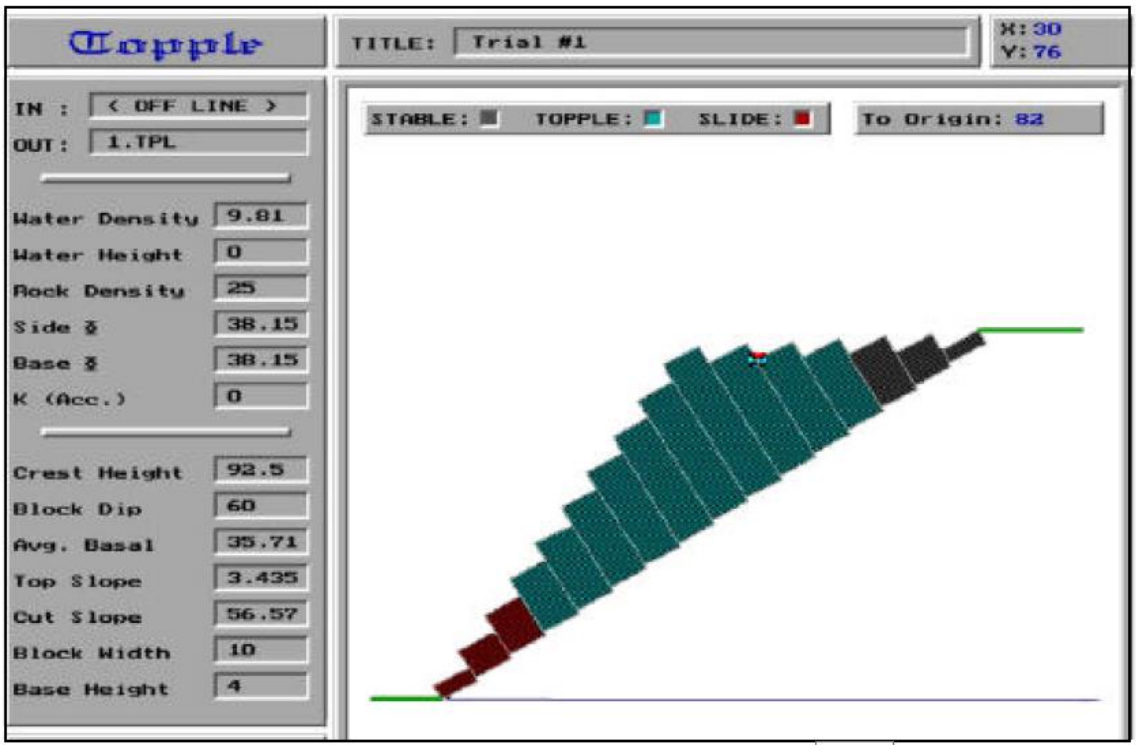

Figure 2.10. An example of a computer-based limit equilibrium analysis of toppling and sliding potential in rock slopes (After Eberhardt, 2003).

2.4.2 Rotational Analysis

Rotational failures, also known as curvilinear slips or circular failures, occur in extremely weak rocks where the material's strength is equal to man-made forces (Avery, 2012). Stability and failure modes, such as soil failure, may not be regulated by structural geology (Eberhardt, 2003). According to Eberhardt (2003), this study consider the "placement of the crucial slip surface and the determination of the factor of safety along it". Eberhardt (2003) further explains that Iterative techniques are applied, each including the selection of a potentially unstable slide mass, subdivisions of the mass into slices, and calculations of the force, and moment equilibrium acting on each slide. The Slide model is the most appropriate model to utilize for rotational analysis (see Figure 2.11). However, alternative

DEM-DEN models (see Figure 2.11) have been shown to successfully predict the rotational behaviour of the slope.

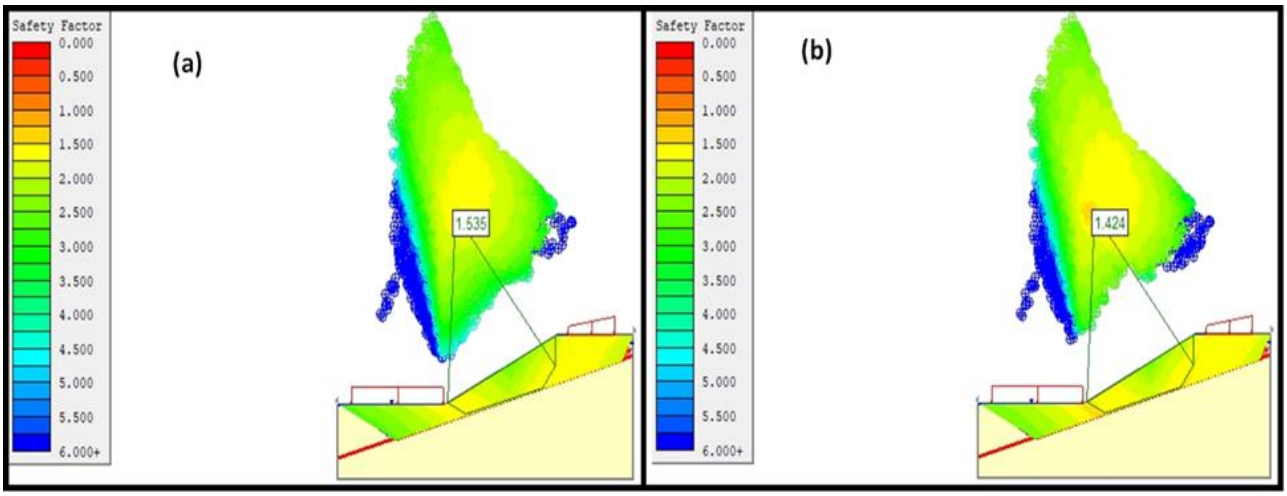

Figure 2.11. Simulated slope FoS using Slide model.

2.4.3 Transitional Analysis

These are limit equilibrium solutions for planar and wedge failure mechanisms required to evaluate discontinuity-controlled rock slope instabilities (Eberhardt, 2003). They are based on Hoek and Bray's (1991) solutions, which assume stiff body translation sliding along a plane or the intersection of two planes in the case of a wedge. All forces pass through the block's centroid because there are no rigid body rotations in the sliding block (Eberhardt, 2003).

Eberhardt (2003) remarked that "In all equilibrium solutions, it is assumed that all points along the sliding planes are on the verge of failure." The previous author went on to connote that these assumptions allow the problem to be solved statistically by allowing Safety Factor estimations (ratio of resisting forces and driving forces). Over time, computer programs/numerical simulations based on these solutions have been developed, such as SWEDGE (Rocscience 2001b), to determine the geometry and stability of a surface wedge defined by two intersecting discontinuity planes and a slope

surface, and ROCPLANE (Rocscience 2001c), which is a related program for planar analysis (Eberhardt, 2003).

2.5 Numerical Simulation

The numerical approach includes static and dynamic evaluations. These approaches are now preferred for slope stability assessments because they can simulate complicated behaviours such as geometry, material anisotropy, non-linear behaviour, in situ loads, and the presence of numerous processes such as pore pressures and seismic loading that occur in slopes (Chiwaye, 2010). As a result, they allow material deformation and movement inside the fault zone.

Numerical methods, according to Chiwaye (2010), can be divided into three categories: continuum, discontinuum, and hybrid modelling. Finite Difference Method (FDM), Finite Element Methods (FEM), Discrete Element Methods (DEM), Boundary Element Methods (BEM), and Discrete Fracture Network Methods (DFN) are some of the most common numerical methods. The material is assumed to be continuous throughout the body in continuum modelling. This model can be used to analyse slopes made from huge rock, intact rock, weak rock, soil-like material, or highly broken rock masses Itasca (in Chiwaye, 2010). FDM, FEM, and BEM are examples of continuum analysis methodologies (Jing, 2003). Discrete fractures, such as faults and bedding planes, are included in continuum modelling but are treated as special cases. Discontinuum modelling is best suited for slopes with discontinuities that are structurally controlled. The methods include DEM and DFN (Itasca, 2004). Cundall and Damjanac (2009) proposed a 3D numerical model called the synthetic rock mass (SRM), which allows fractures to initiate and grow dynamically according to the imposed stress and strain level. FEM and FDM are the most commonly used numerical methods in slope stability analyses. In numerical modelling, the slope is initially divided into a finite number of elements or zones. Subsequently, the forces and strains are calculated for each element in the slope.

According to Cundull (2002), the following advantages of continuum mechanics-based methods exist: no pre-defined surface is required, the failure plane can be of any shape, multiple failure surfaces are possible, no statistical assumptions are required, kinematics

is satisfied, and structural elements and/or interfaces can be included without concern for compatibility. When multiple failure mechanisms exist concurrently or when failure mechanisms occur progressively, numerical models can be used to calculate the slope's factor of safety (Hoek et al., 2000).

Similarly, to the LE methods, numerical methods have limitations and drawbacks of their own. Compared to the LE models, the numerical models take longer to compute. They are generally difficult to use and must be used by an experienced analyst. According to Hoek et al. (2000), the most difficult aspects of numerical modelling when modelling large-scale slopes are obtaining realistic input parameters for these models and interpreting the results produced. Dight and Baczynski (2009) concluded that numerical methods are the only way to evaluate deformation in slopes and that if enough simulations are performed and the results are validated, numerical methods will always provide valid results.

2.5.1 Finite Element and Finite Difference Methods

The slope is divided into a finite number of elements or zones in both the FDM and the FEM (Ryder and Jager, 2002). At each element, the FDM approximates the partial differential equations (PDEs), converting the original PDEs into a system of algebraic equations (Itasca, 2005). Polynomial functions are employed in the FEM to estimate the behaviour of PDEs at the element level and construct local algebraic equations that represent the elements' behaviour (Chimanye, 2010).

FEM and FDM are used in applications like Phase 2 and FLAC. Both the FDM and the FEM generate a set of algebraic equations; the methods used to obtain the equations differ, but the equations themselves are the same (Itasca Consulting Group, 2005). By applying appropriately defined initial and boundary conditions, the solution of the resulting equation is found. The factor of safety is defined as the ratio of the rock's real strength to the reduced shear strength at failure in finite element or finite difference methods. The name of this technique is the shear strength reduction method (Chiwaye, 2010).

2.5.2 Boundary Element Method

According to Crouch and Starfield (1983), boundary element methods are named after the fact that only the boundaries of the problem geometry are divided into elements. For multi-material problems, Hoek (2006) provides a simple explanation by pointing out that "only the excavation surfaces, the free surface for shallow problems, joint surfaces where joints are explicitly considered, and material interfaces" are divided into elements. For argument's sake, the boundary element approaches are a collection of several sorts of boundary element models that may be categorized using the following criteria (Hoek, 2006):

- In the indirect (fictitious stress) method, "*the first step in the solution is to find a set of fictitious stresses that satisfy prescribed boundary conditions. These stresses are then used in the calculation of actual stresses and displacements in the rock mass*";
- In the direct method, *"the displacements are solved directly for the specified boundary conditions*", and
- In the displacement discontinuity method, *"the result of an elongated slit in an elastic continuum being pulled apart*".

One may argue that the first two approaches are similar, but the difference may not be obvious to the user. Direct methods, on the other hand, have greater advantages in terms of program development than indirect methods. The following numerical methods are the so-called distinct element methods, which are discussed briefly below.

2.5.3 Distinct Element Method

The DEM is a numerical method for analysing rock stability that Ebherhardt (2003) and Lisjak et al. (2010) describe as a continuum analysis approach that is the most direct method for discretizing partial differential equations. The preceding statement implies that the method divides the problem domain into sets of subdomains and provides solutions through numerical approximations of governing equations. Pourkhosravani and Kalantari (2011) agree that DEM is based on governing differential equations of elasticity theory, which Finite Element methods can effectively use. The method accounts for rock

deformability, fracturing, and fragmentation in order to simulate complex failure behaviour and mechanics in rock masses (Fredj et al., 2019). According to Eberhardt (2003), the computational algorithm in DEM is based on the force-displacement law, which then specifies the interaction between the deformable intact rock units and the displacement triggered on the block by out of balance forces. Although continuum approaches differ from discontinuum methods in rock slope analysis, continuum programs now include distinguishing features such as bedding planes and faults, which are discontinuum parameters, according to Singh et al. (2017). The authors further argued that continuum codes can represent time-independent slope stability behaviour using multiple models (elasticity, elastoplasticity, elasto-viscoplasticity, and strain softening) (Brummer, 2003; Singh et al. 2017). Differential equations of equilibrium, strain displacement relations, and stress-strain equations are examples of governing equations (FLAC, 2003).

2.5.4 Hybrid approaches

The hybrid models are a combination of the methods mentioned above, and they are intended to eliminate undesirable characteristics while retaining as many benefits as possible (Hoek, 2006; Eberhardt 2008). The codes' advantages include the ability to simulate intact rock fracturing propagation as well as the fragmentation of jointed and bedded rock mass under certain stress and strain conditions. The model can simulate the propagation of intact fractures as well as the fragmentation of jointed and bedded rock. The difficulties encountered when using this code are that complex problems necessitate a large amount of memory and continuous calibration of the model is required to improve the model's accuracy.

According to Hungry (2016), the numerical model should always be based on enough data, or else the model will produce misleading results. However, other approaches use mostly empirical methods rather than numerical methods; these methods are listed under Frequency Analysis, and a brief review of the analysis is provided below.

2.6 Slope Stability Optimization Methods

Depending on how uncertainty is incorporated and evaluated, slope stability analysis can be classified as deterministic or probabilistic. A deterministic analysis requires a set of

fixed-value parameters as input (usually at the mean values of the data obtained from site investigations). These analyses are based on the calculation of a safety factor, defined as the ratio of the forces resisting a rock block's slide to the driving forces causing the slide. A deterministic analysis is a one-time process that is carried out using either limit equilibrium analysis or the numerical method. Because of the various sources of uncertainty involved in such stability problems, the deterministic approach, despite being simple and straightforward, cannot explicitly and sufficiently reflect quantified uncertainties. In recent years, the probabilistic approach, which calculates the probability of failure rather than an Fs against failure, has become more popular (Nilsen, 2000). The probabilistic method accounts for the inherent variability and uncertainty in the analysis parameters. Constant parameters in probabilistic analysis refer to common geometry and unit weight parameters. Water pressure, active frictional angle, and seismic acceleration are all variables that can vary widely. They do not all have the same value. There is no way to know ahead of time what one of these factors will be at any given location. As a result, these variables are referred to as random variables.

2.6.1 Deterministic Approach

When dealing with deterministic slope stability analysis, both conventional and numerical methods are effective. The stability of the slope is also described by a single value for the stability factor in the deterministic approach. Thus, the uncertainty is not explicitly considered. An Fs >1 signifies that stabilizing forces are larger than driving forces, resulting in a stable slope, according to its definition. The partial factor approach is an alternate way of determining the stability of a rock slope. Instead of an overall safety factor, this method employs partial factors for action and materials (Nilsen, 2000). The partial factor method typically produces more conservative designs than approaches that use deterministic Fs (Nilsen, 2000). Deterministic analysis, which has a lengthy history and appropriate Fs for diverse conditions, is well established. For slope stability analysis, it has become a standard procedure. Deterministic analysis, on the other hand, uses fixed input parameters and can only deal with uncertainty by demanding a large Fs number (Qian, 2012; Read and Stacey, 2009). Furthermore, the identical Fs for distinct failure types may have a varied failure probability (Einstein and Baecher, 1982; Low, 2007). The

chance of failure is highly sensitive to the degree of uncertainty and intrinsic variability in the input parameters, for Fs between 1.2 and 1.8 (a stable slope) (Toba, 1984). The main disadvantages of deterministic analysis are that it ignores many sources of uncertainty, resulting in less reliable output. A sensitivity analysis, on the other hand, allows for the use of a deterministic approach. A sensitivity analysis can provide a good qualitative understanding of the most important factors for a specific rock slope, but it cannot quantify the susceptibility to failure.

2.6.2 Probabilistic Approach

Probabilistic methods have long been used successfully in engineering disciplines. In the probabilistic approach, each combination of the strength parameters, which can be chosen randomly or not randomly, results in a different realization of the slope while the geometry remains constant. A deterministic value for the Fs is obtained by analyzing each realization. Finally, the values of the factor of safety may be fitted to a probabilistic distribution, and the chance of failure can be determined as a result (Chiwaye and Stacey, 2010; Miller et al., 2004; Shamekhi, 2014).

To demonstrate the methodology, suppose the load and strength of a structure element, such as a slope, can be described by two PDFs (Calderon, 2000; Shen, 2012). The strength or resistance of the element is termed R, and the load is denoted S. The respective mean and standard deviations of each distribution are denoted mR and mS. The distance between the means of resistance force and load defines the mean value of Fs. The overlap of the PDFs of resistance force and load indicates the possibility (or probability) of slope failure Pf. The resulting Fs would be significantly larger in a purely deterministic approach using only the mean strength and load.

2.6.3 Case studies on probability analysis

Low and Tang (1997) proposed a practical spreadsheet technique for the deterministic slope stability analysis based on Janbu's generalized procedure of slices (Janbu, 1973). The method presented by Low and Tang (1997) computes the Hasofer-Lind (Hasofer and Lind, 1974) reliability index as the first-order reliability method (FORM) via constrained optimization. The optimization method used by Low and Tang (1997) was the generalized

reduced gradient algorithm, which is one of the most robust nonlinear programming methods to solve optimization problems. Despite the fact that the factor of safety expressions and the performance function are not explicit, Low and Tang (1997) automated a search for the critical deterministic slip surface and the critical probabilistic slip in their proposed method.

In another paper, Low and Tang (1997) proposed the same methodology for the reliability assessment of embankments on soft ground. In this study, they used Spencer's method of slices (Spencer, 1967) to evaluate the factor of safety and performance function. As mentioned by Low and Tang (1997), the advantages of the new method were simplicity, transparency, versatility, accuracy, and the ease of implementing stochastic reliability analysis in the ubiquitous spreadsheet platform, notwithstanding the implicit and iterative nature of the limit state functions.

Bhattacharya et al. (2003) presented an optimization-based search algorithm for locating the critical probabilistic surface of the minimum reliability index for earth slopes. Their procedure uses a formulation similar to that used to search for the surface of the minimum factor of safety in conventional slope stability analysis. Bhattacharya et al. (2003) developed a computer program based on Spencer's method of analysis (Spencer, 1967) for deterministic slope stability and extended the program with an efficient Monte-Carlo technique (Greco, 1996) for probabilistic slope stability analysis. Their proposed algorithm does not make any a priori assumptions regarding the shape of the slip surface. The advantage of the formulation lies in enabling a direct search for the critical probabilistic surface by utilizing an existing deterministic slope stability algorithm with the addition of a simple module for the calculation of the reliability index. Applications to several cases verified the success of the procedure.

The application of the genetic algorithm (Holland, 1975) for reliability-based slope stability analysis was proposed by Xue and Gavin (2007). In their study, the soil properties were considered to be random variables, and the factor of safety was found using Bishop's simplified method for noncircular slip surfaces to evaluate the limit state function. By considering the variability of the soil properties, Xue and Gavin (2007) determined the probability of failure from the reliability index. To overcome the complexities associated

with defining the limit state function, Xue and Gavin (2007) transformed the variables, such as the soil strength parameters, into polar coordinates. In their study, the determination of the reliability index and associated slip surface was solved by utilizing a powerful and efficient genetic algorithm environment. The results indicated that the new approach provides reasonable and consistent estimates of the reliability index and the critical slip surface.

Cho (2007) proposed a numerical procedure for a probabilistic slope stability analysis based on a Monte Carlo simulation that considers the spatial variability of the soil properties. The approach adopts the first-order reliability method to determine the critical failure surface and to conduct preliminary sensitivity analyses. Cho (2007) formulated the factor of safety using Spencer's limit equilibrium method to evaluate the performance function and calculate the reliability index. The problem of locating the critical surface is formulated as a constrained optimization problem, and the feasible direction method is used to solve the problem. For example, Cho (2007) formulated the probabilistic stability assessments to study the effects of uncertainty due to the variability of soil properties on the slope stability in layered slopes. The examples provided insight into the application of uncertainty treatment to slope stability and showed the importance of the spatial variability of soil properties concerning the outcome of a probabilistic assessment.

Hong and Roh (2008) considered the first-order reliability method for estimating the probability of failure or reliability index of earth slopes. The system aspect of the slope in the reliability analysis is handled by defining a limit state of the system as a function of the minimum of the ratio of the shear strength to the mobilized shear strength for each potential slip surface. Hong and Roh (2008) evaluated ratios for a given slip surface using the extended generalized method of slices given by Chen and Morgenstern (1983), which is an extension of the well-accepted Morgenstern and Price method (Morgenstern and Price, 1965). In their study, the sequential quadratic programming (SQP) method presented by Schittkowski (1986) was implemented to compute the minimum factor of safety, reliability index, and associated critical deterministic and probabilistic slip surfaces. The numerical results suggested that the reliability of a slope might be sensitive to the assumed or adopted probability distribution types for the input parameters. Moreover, the

results suggested that a decrease in the positive spatial correlation of soil properties leads to a decrease in the probability of failure.

Recently, Khajehzadeh et al. (2010a, 2010b) applied the harmony search algorithm (Geem et al., 2001) and particle swarm optimization (Kennedy and Eberhart, 1995) to calculate the minimum reliability index and corresponding critical probabilistic slip surface of earth slopes. In their studies, the performance function formulated by Spencer's method (Spencer, 1967) of slices for the general shape of slip surface and the reliability index defined by Hasofer and Lind (1974) was employed to estimate the reliability index. Khajehzadeh et al. (2010a, 2010b) demonstrated the effectiveness and robustness of their proposed algorithm by considering a number of published cases, and the results showed that both HS and PSO algorithms might be successfully applied for probabilistic slope stability analysis. Moreover, the obtained results showed that the searched critical probabilistic surfaces have different locations than the critical deterministic surface, especially for layered soil.

Gavin and Xue (2010) proposed a hybrid method of assessing the stability of unsaturated soil slopes. The method utilized the benefits of the rational treatment of the variability of input parameters provided by the reliability-based design and the simplicity afforded by deterministic approaches. Fourie et al. (1999) noted that in most slope failures caused by infiltration, the failure plane forms parallel to the existing slope surface. Therefore, Gavin and Xue (2010) considered an infinite slope model to formulate the factor of safety and performance function. They considered the soil properties as random variables, transferred them to polar coordinates, and applied the genetic algorithm to calculate the Hasofer and Lind reliability index. Gavin and Xue (2010) presented the results in design charts from which a designer could choose the safety factor value required to ensure a given target reliability index for a slope.

2.6.4 Uncertainty in the Estimating Rock Slope Stability

Identifying the sources of uncertainty that affect the reliability of the output results is an important factor that is frequently overlooked in conventional rock slope stability assessments (Duncan, 2000). Many types of uncertainties are involved in the estimation

of rock slope stability, such as input parameter uncertainty, calculation uncertainty, and procedure uncertainty in which the input parameters are transferred into the numerical model. In general, they can be divided into the following three categories (Shen, 2012):

The first one is physic uncertainty. This type of uncertainty is a natural occurrence. This uncertainty is acquainted with natural variability or randomness of some properties, such as site topography, stratigraphy and variability, groundwater level, in situ soil and/or rock characteristics, engineering properties of rock mass, and rock behaviour, in slope stability. Natural variability, on the other hand, is one of the most significant sources of uncertainty, particularly when dealing with rock mass and discontinuity networks (Baecher and Christian, 2003). Natural or inherent variability is related to either different characteristics of geological structures at different locations (spatial) or different characteristics of geological structures at the same location but at different times (temporal) (Shamekhi, 2014). In numerical simulations, the spatial variability of a common source of uncertainty that is typically encountered in geometric parameters that define discontinuities like direction and size should be considered (Shamekhi, 2014). Measurements and statistical calculations can quantify this type of uncertainty, but it is unpredictable and thus nonreducible by collecting more experimental data or using more precise models (Shen, 2012).

The second one is knowledge (or statistical) uncertainty. The friction angle of a discontinuity, the uniaxial compressive strength and elasticity modulus of rock materials, the inclination and orientation of discontinuities in a rock mass, and the measured in situ stresses in the rock surrounding an opening are examples of parameters that do not have a single fixed value. There is no way to know ahead of time what each of these factors will be at any location. As a result, these variables are referred to as random variables. The development of the probability distribution of each random variable in slope probabilistic analysis is a fitting process based on limited data from measurements or tests (Shen, 2012). As a result, three key subcategories: site characterization uncertainty, model uncertainty, and parameter uncertainty have been introduced.

(1) The lack of knowledge of the governing geometric parameters,

(2) the simplifying assumptions in the modelling methods (model uncertainty), and

(3) the low level of accuracy in the acquired data (Baecher and Christian, 2003).

Knowledge uncertainty can be defined as human errors in data collection, such as field measurements, or a lack of data due to the inaccessibility of specific geological features. It should be noted that even if the input parameters have a low level of knowledge uncertainty, the output results may still suffer from this disadvantage. This is primarily due to the simplifying assumptions used in numerical simulations, such as those used in LEMs (Shamekhi, 2014).

Simulation uncertainty is the final type of uncertainty. Uncertainty in simulation is attributed to a lack of understanding of physical laws, which limits our ability to model the real world (Shen, 2012). Identifying the sources of uncertainty that affect the reliability of the output results is an important factor that is frequently overlooked in conventional rock slope stability assessments (Duncan, 2000). Slope stability analysis and design is a process that simulates the relationship between a set of random input data and output data (e.g., safety factor, reliability index and failure probability) using mathematical models (e.g., equations, functions, algorithms and calculation simulation programs). These models are built using mathematical, mechanical abstracts about the real process (Shen, 2012). There may be uncertainty in the input parameters, calculations, and the technique for transferring the input parameters into the numerical model. By adopting field study approaches capable of gathering sufficient and representative field data with an acceptable level of precision, both natural variability and knowledge uncertainty can be significantly decreased. However, the model uncertainty may not be completely resolved by relying on complex numerical simulations, which are often computationally expensive (Shamekhi, 2014).

2.7 Concluding remarks

Based on the literature review, it is well established that various methods are used for slope stability, yet many engineers and scientists prefer the using of LEMs, despite their inaccuracy. Following that, various cases of slope stability methods have been documented yet, there is no clear direction on analysing or conducting slope stability in

slopes dominated by faults. Owing to that, the reproduction of slope failure or failure evolution of slopes has been documented in large displacement cases, yet there is limited information regarding shallow slopes. The simplicity of deterministic methods, compared to probabilistic methods, has been cited by scholars as the primary reason for their preference over probabilistic approaches. Consequently, the above concerns provided a space to explore possible solutions for each case and those concerns motivated the current research study.

Chapter 3 Collection of experimental, field, simulation and remote sensing data

This chapter outlines the methodologies implemented in this research study. Although this research study focuses more on numerical simulations; simulations were conducted based on case studies observed along the National Highway (N1) and its tributaries. Therefore, it is imperative to follow data collection and experimental procedures when acquiring material properties of the slope and rock/soil mass. The chapter commences with a detailed description of data collection, followed by laboratory testing and concludes with numerical simulation formulations and procedures as well as the remote sensing processes.

3.1 Introduction

The data collection methods followed in this research study entailed desktop study, field observation, field measurements, experimental tests, and numerical simulation. In the desktop study, relevant materials were collected and reviewed to gain an understanding of slope stability and their methods of analysis. This data collection technique was used to lay the foundation for field and laboratory work. Owing to that, the desktop study served the purpose of devising an efficient and meaningful program for the acquisition of field and laboratory data.

The second stage of data collection was to perform field observations and measurements. Here, geological mapping and field measurements of the rock mass structures were conducted within the selected study areas. Both soil and rock samples were collected for the characterization of the mechanical properties and geotechnical parameters of the sites. Laboratory tests were the third stage; rock samples were tested for rock properties.

After acquiring the required material properties of the rock and soil mass as well as slope parameters, the third stage was considered. In the third stage, the accuracy of the two-

dimensional limit equilibrium analysis was performed. The purpose of the study was to use the rigorous upper and lower bounds solutions of limit analysis based on finite element formulations of the bound theorems to benchmark and develop an accuracy classification chart of limit equilibrium methods in predicting the stability of the homogenous slope. Nevertheless, two numerical programs were used for the analysis: SLIDES and Optimum 2G.

In the fourth stage, the Finite Difference Method was performed to develop a new method for stability analysis in a multi-faulted rock slope using the ubiquitous joint model. The investigation commences by analyzing the sensitivity factors of fault properties and their effect on the safety factor of the slope, in which fault geometry, thickness, shear strength properties, mesh densities, and change in joint orientation were evaluated. Therefore new method that strives to capture all these sensitivity factors into a single analysis was proposed. The method also captures the zone of influence generated by each fault and each fault is treated separately. The following numerical programs were used for the analysis: FLACslope, DIPS and ROCLAB.

In the fifth stage, an integrated approach to developing a reliable slope susceptibility map using on a GIS-based approach, machine learning and finite element formulation of the bound theorems was undertaken. The purpose of this chapter was to bridge the gap on how robust slope susceptibility estimates are, by introducing advanced geotechnical modelling using lower and upper bound solutions of limit analysis as benchmarking or validation techniques. The research was motivated by the fifth stage to explore the evolution process of slope failure triggered by extreme rainfall along a road cut in mountainous terrain using numerical simulation. In this regard, Optimum 2G and Rocdata were utilized. The purpose was to reproduce the slope failure process that occurred along a faulted slope based on numerical modelling. The final stage incorporates limit equilibrium analysis to perform reliability analysis of slope stability using probabilistic analyses compared to deterministic analyses. To accomplish this two case studies were analyzed, and Monte Carlo simulations and deterministic methods were applied.

3.2 Visual observation and field measurements

Visual observation was conducted along the national road in Limpopo Province to identify slope instabilities. Several slopes where soft rock is the country-rock denoted slope instability. Furthermore, the observations were also focused on identifying the mechanism or the failure mode in relation to each slope instability. As such, various images were taken for further analysis.

In terms of field measurements, geological or structural mapping was taken as a primary activity (see Table 3.1). In this regard, mapping was conducted in order to map structural geometrics (dip, dip direction, infill, among others). Geological mapping followed the standard procedure required to rate the quality of the rock mass such as those of Bieniawski between 1972 and 1973. The key parameters that were measured are listed in Table 3.1.

Table 3.1 Geological or geotechnical mapping parameters

	Symbol	Units
Sites	S	
Joint Set	Jn	
Joint Spacing	JS	mm
Joint Persistence	JP	m
Joint Aperture	JA	mm
Joint Roughness Coefficient	JRC	
Joint Infilling	JI	kPa
Joint Weathering	JW	
Rock Mass Rating class	RMR	

The identification of the parameters in Table 3.1 was aimed at compiling input data for later numerical simulation work. The information was also to be used in the classification of the rock mass of the study areas. The parameters capture the mechanical behaviour of the rock mass and assist in designing an appropriate support system for the area. The

parameters in Table 3.1 included the documentation of the set of joints, their spacing, and their persistence among others.

3.3 Mathematical Formulations applied in the research study

Numerical simulations are tools used to explain scientific problems which cannot be explained well using synonyms methods, yet the tools are believed to provide meaningful solutions. Various numerical tools were used in this research study, but their methodologies differ greatly based on their mathematical formulations or the governing equations used. To be too specific, limit equilibrium simulations and limit analysis were used. The governing equations of each simulation are documented below in chronological order showing how the simulation building was conducted.

3.3.1 Limit Equilibrium

The limit equilibrium approach assumes that a slope is stable when any free body inside the soil medium is at rest, this implies that the static equilibrium conditions are satisfied. Based on this assumption, LEMs cannot yield a direct measure of system reliability; instead, they analyze multiple paths within the soil/rock profile to determine the critical slip surface. For the given soil slope surfaces, the stability level was quantified using a constant name called factor of safety (FoS), which is the ratio between the available soil/rock shear strength and the equilibrium shear stress at the slip surface. In this regard, the FoS of the soil/rock slopes was expressed by equations 3.1 and 3.2. Equations 3.1 and 3.2 were formulated considering the generic slip surface, as shown in Figure 3.1, the mobilized shear strength was determined based on the inertial forces and external loads as well as base reactions. Depending on the type of problem and the accuracy of results required, this approach uses different analysis methods such as Ordinary Method, Bishop simplified, Gle/Morgenstern Price, Janbu Simplified, and Janbu Corrected, Spencer and Corp of Engineer number one, and Corp of Engineer Number two. Each method uses its own governing equation in order to simulate the stability number of the slope. Detailed descriptions of the formulation of the methods are documented below since all these methods were used in this research study.

$$F_S = \frac{\tau}{S} = \frac{C+\sigma_n \tan \emptyset}{C_m+\sigma_n \tan \emptyset_m} \quad (3.1)$$

$$F_S = \frac{c}{c_m} = \frac{\emptyset}{\emptyset_m} \quad (3.2)$$

Where τ: peak shear stress, s: equilibrium shear stress, σ_n: normal stress, c and ϕ: soil cohesion and friction angle (i.e., subscript "m" denotes the mobilized parameters).

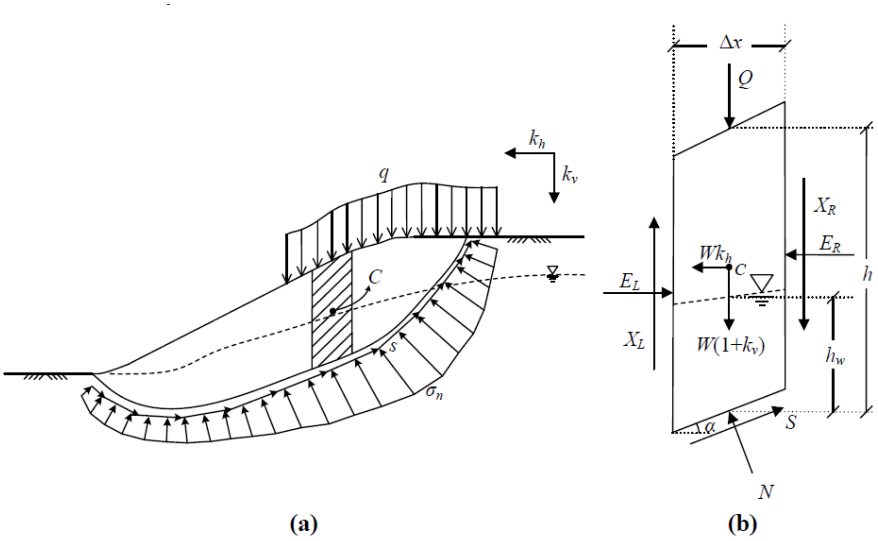

Figure 3.1 Free-body diagram of a generic slip surface (a) overall diagram (b) vertical slice diagram (Yalçin, 2018)

The governing equations of the limit equilibrium methods mentioned above were applied in a Rocscience code called SLIDEs 2D to simulate the stability number of the slope. The procedure for the computer code is documented below.

3.3.2 Limit Analysis

The limit analysis of this research study was performed using the so-called strength reduction factor (SRF) or strength reduction method (SRM). The SRM is mostly based on the Finite Element Method (FEM) or Finite Difference Method (FDM) to overcome the limitations presented by Limit Equilibrium Methods. The SRM method was first proposed by Zienkiewicz et al. (1975) with the purpose of analyzing slope stability; however, the

method has gained interest from many scholars (Matsui and San, 1992; Griffiths and Lane, 1999; Dawson et al., 1999; Zheng, Liu and Li et al., 2005; Griffiths and Marquez, 2007) who strive to improve the method. It has been observed that several scholars (Cheng et al., 2007; Tschuchnigg et al., 2015; Jiang et al., 2015; Zhang et al. 2015; Schneider-Muntau et al. 2018) have confirmed that SRM solutions are more accurate and can be closely related to the LEM solutions. This suggests that the SRM could be used as a benchmark method to evaluate the accuracy of the LEM.

In the strength reduction method, the factor of safety (FoS) is defined as the ratio between the actual shear strength and the reduced shear strength for the fault, joints, and intact rock when the slope arrives at a critical state. When implementing the strength reduction procedure, the reduced shear strength parameters, cohesive force c_r, and the fiction angle φ_r are obtained by the following (see equation 3.3):

$$C_r = \frac{C}{SRF} \tag{3.3}$$

$$\varphi_r = \tan^{-1}\left(\frac{\tan\varphi}{SRF}\right)$$

As already stated, the SRMs are based on FEM or built within the FEM framework, therefore, these methods have governing equations followed by their mathematical formulations in terms of the bound solutions (lower and upper) as well as the duality and bounds equations of the model. A detailed description of the mathematical formulation of the used SRM is documented below.

3.3.2.1 Governing equations

Governing equations defining the mathematical implementation of the FEM model of a solid system are encapsulated in Equations 3.4 to 3.9. Assuming an infinitesimal deformation is to be simulated, the equations can be expressed as follows (Zienkiewicz et al., 2005)

Equilibrium and static boundary conditions of the model:

$\nabla^T \sigma + b = 0$, in V (3.4)

Where $\sigma = [\sigma_x \quad \sigma_y \quad \sigma_z \quad \sigma_{xy} \quad \sigma_{yz} \quad \sigma_{zx}]^T$ are the stresses, $b = [b_x \quad b_y \quad b_z]^T$ are the body forces stemming for example from self-weight, and V is the domain under consideration.

$$\mathrm{P}^T\sigma = \alpha t \quad \text{on } S_\sigma \tag{3.5}$$

Meanwhile, the yield conditions of the model are as follows:

$$F^T\sigma - k + s = 0 \tag{3.6}$$

Since the current situation is dealing with strain problems, therefore associate flow rules or strain-displacement compatibility has to be incorporated as follows:

$$\nabla\dot{u} = F\dot{\lambda} \tag{3.7}$$

where $\dot{\lambda}$ is the plastic multiplier that satisfies the complementarity conditions.

Therefore, the scaling is applied with respect to the rate of work done by the reference tractions t as indicated above, in short, the scaling equation is denoted as follows:

$$\int_{S_\sigma} t^T \dot{u} dS = 1 \tag{3.8}$$

where $\dot{u}$ is taken as the exact velocity, *t* is *the* traction vector

And lastly, the complementarity conditions of the model are therefore incorporated as follows:

$$S^T\dot{\lambda} = 0, S \geq 0, \dot{\lambda} \geq 0 \tag{3.9}$$

Nevertheless, a detailed description of the model in terms of lower bound principles, upper bound principles and bounds is documented below.

3.3.2.2 Lower bound principle

In terms of the lower bound principles, the principle ensures that the strain-softening aligns with the governing equation of the limit analysis of the Finite element. However, the kinematic quantities, absent from the governing equations, appear as Lagrange multipliers when solving the problem. The main strength of the lower bound principle is

that it allows for a lower bound on the exact collapse multiplier to be computed, through constructing a stress field that satisfies the constraints without necessarily being optimal (Optum G2, 2019) (see Eq 3.10).

Maximize α

Subjected to $\nabla^T \sigma + b = 0$, in V

$$\mathrm{P}^T \sigma = \alpha t \quad \text{on } S_\sigma \tag{3.10}$$

$$F^T \sigma - k + s = 0$$

3.3.2.3 Upper bound principle

As already stated, the problem at hand incorporates kinematic quantities for which the LEMs do not have the ability. Therefore, the upper bound is intended to incorporate the compatible velocity field that satisfies the flow rule. A similar flow rule cannot be activated using the LEMs therefore this upper bound is critical. In order to achieve that, the rate of work done by the reference tractions is scaled to unity and the objective function, which comprises the internal rate of work minus the contribution from the constant body forces, then the collapse multiplier issought. The upper bound principles are denoted in equation 3.11.

Minimize $\int_V^{\cdot} k^T \lambda \cdot dV - \int_V^{\cdot} b^T u \cdot dV$

Subjected to $\nabla \dot{u} = F\dot{\lambda}, \lambda \geq 0$ (3.11)

$$\int_{S_\sigma} \boldsymbol{t^T \dot{u} dS} = \mathbf{1}$$

3.3.2.4 Bounds

The bounds are a critical part of the numerical simulation because this stage is used to verify the lower and upper bound principles to ensure that the bounds furnish with a collapse multiplier. Therefore, the stress field is considered first, to ensure that they satisfy the yield condition, equilibrium conditions and boundary conditions. Such expression on how the bound is performed is documented by equation 3.12.

$$\alpha_{ab} = \int_V^{\cdot} k\,\lambda_b dV - \int_V^{\cdot} b^T\,u\cdot dV$$

$$= \int_V^{\cdot} (F^T\,\sigma_b)^T \lambda_b dV - \int_V^{\cdot} b^T\,u\cdot dV \qquad (3.12)$$

$$= \int_V^{\cdot} \sigma_b^T F \lambda_b - \int_V^{\cdot} b^T\,u\cdot dV$$

3.4 Geotechnical testing programs applied in addressing objectives of the research study

The aim of field observations and measurements was to collect important data for the validation of simulation results. The field data was to give room for realistic simplifications of mathematical equations descriptive of the behaviour of the in-situ rock mass.

Fieldwork entailed visual observations, field measurements, and rainfall statistics of the selected study area. Further details are provided in this section.

3.4.1 SLIDES 2D

The computational procedures for SLIDEs are well explained in several studies such as those of Sengani and Mulenga (2020a; 2020b). The SLIDEs were utilized to estimate the FoS of the slopes in six scenarios; however, the code can use various LEMs at a time. In terms of model building, it starts with the creation of a new project. Similar to other modelling platforms, the new project required the delimitation of the model limitation in XY coordinates. For that, various X and Y coordinates defining the region were entered. The ultimate goal of this step was to draw the model of the region. Upon generating the boundaries of the model, the actual initial conditions of the simulation are defined next for the project. Inputs such as the statistics associated with groundwater conditions, the computational methods, and the failure directions are captured.

3.4.1.1 SLIDES for deterministic analysis

The traditional deterministic approach to slope stability relies on the simulation of the factor of safety (FoS) which is the ratio of resisting force over driving force in a specific block. Owing to that the methods use single-valued parameters to analyze the characteristics of a slope. As a result, the output from methods yields single-valued estimates of the factor of safety of the stability of a slope. Nevertheless, the stability number varies considerably based on the method applied and the slope properties. However, the parameters governing the stability of a slope vary considerably throughout the extent of the slope. In this study, four common deterministic methods (Ordinary method, Bishop's method, Janbu method and Morgenstern Price method) were implemented, the methods yield the factor of safety as follows (Eq 3.13 and 3.14):

$$F_S = \frac{\tau}{S} = \frac{C+\sigma_n \tan \emptyset}{C_m+\sigma_n \tan \emptyset_m} \quad (3.13)$$

$$F_S = \frac{c}{c_m} = \frac{\emptyset}{\emptyset_m} \quad (3.14)$$

Where τ: peak shear stress, s: equilibrium shear stress, σ_n: normal stress, c and ϕ: soil cohesion and friction angle (i.e., subscript "m" denotes the mobilized parameters).

Four different slopes in two locations were analyzed using the SLIDE model, as indicated the safety factors were calculated with the help of four deterministic models listed above; the results were also compared. However, the interest was to identify the stability number of the slope and describe what it yielded.

3.4.1.2 SLIDES for probabilistic analysis

Probabilistic methods are well established to provide solutions to address the fluctuation slope stability variables. In this regard, different scenarios are recreated using different random values to produce unique FoS values. Despite the fact that deterministic methods provide a single-valued stability number, probabilistic analysis incorporates the generation of random data using the Monte Carlo Simulation method.

Monte Carlo simulation is a powerful tool for slope stability risk analysis. An iterative process using deterministic methods of slope stability analysis is applied in this technique. Monte Carlo simulation is a popular method of slope stability risk analysis among engineers because of its simplicity and there is no need for comprehensive mathematical and statistical knowledge. This method consists of four steps (see Figure 3.2) below, as documented by Eckharedt (1987), Bureau of Indian Standards (1972), Fishman (1995), Hammond et al. (1991) and Chandler (1996):

(a) choosing a random value for each input variable according to the assigned probability density function,

(b) calculating factor of safety by using a proper deterministic slope stability analysis method (such as Janbu, Bishop, Spencer) based on selected values in step 1,

(c) repeating steps 1 and 2 for many times as necessary and

(d) determining distribution function of factors of safety and probability of failure.

For the above-mentioned sections, probabilistic analysis was performed using Monte Carlo simulations. According to the Monte Carlo simulation method, a random value has been selected for each input parameter based on the assigned probability density function and its amplitude. The literature (Chandler, 1996) reveals that Monte Carlo trials are more accurate however, the accuracy of the solution is controlled by the number of required Monte Carlo trials and the number of variables being considered. Nevertheless, the following equation has been recommended (Chandler, 1996) to be used for Monte Carlo Simulation, yet this study also implements a similar equation (see Eq 3.15):

$$N = (\frac{d^2}{4(1-e)^2})^{\wedge m} \quad (3.15)$$

Where: N = number of Monte Carlo trials, d = the normal standard deviation corresponding to the level of confidence, e = desired level of confidence, and m = number of variables.

The probability density functions of unit weight, cohesion and angle of internal friction, φ adopted in the analysis are shown in Table 1. Based on equation (3.15) for three variables (unit weight, cohesion and phi) and for a 90% confidence level 1000 trials have been done with respect to the average standard deviation of 1.5.

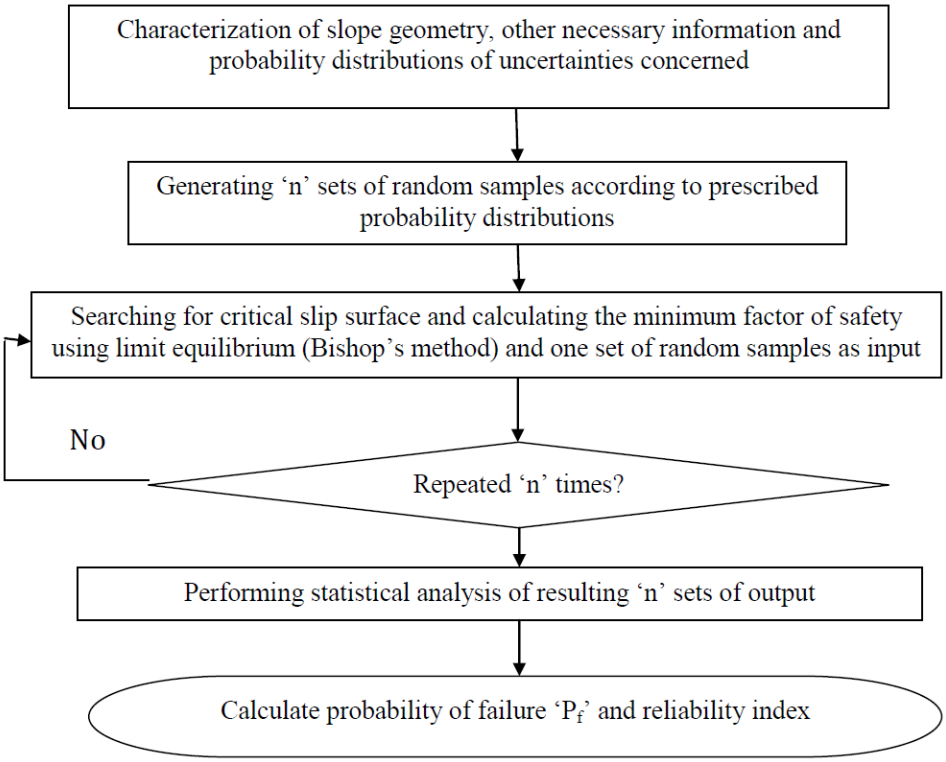

Figure 3.2. Steps followed in the Monte Carlo simulation method (Chandler, 1996)

3.4.2 Roclab/Racdata procedure

Further analysis was to identify the mechanical properties of the rock mass as well as the three faults. The so-called Rocdata computer code was used to estimate the mechanical properties of each feature mentioned. However, the estimation depends on the field observation, therefore the Hoek and Brown classification criterion was implemented to estimate the values as shown in Table 3.2. In terms of the strength of the rock mass and faults, the so-called Geological Strength Index (GSI) was used to predict rock mass and fault strength. The GSI criterion was introduced by Hoek (1994), Hoek, et al. (1995), and

Hoek et al. (1998) provided a number that, when combined with the intact rock properties, can be used for estimating the reduction in rock mass strength for different geological conditions. The GSI has been extended to cater to blocky rock masses, heterogeneous rock masses such as flysch and molassic rocks (Hoek et al 2006) and Ophiolites (Hoek et al., 2005). Similarly, the degree of disturbance (D factor) on the rock mass and the uniaxial compressive strength of the rock mass have been estimated based on developed charts by Hoek and Brown (1997) (see Figure 3.3 a-d).

Table 3.2 Mechanical properties of the rock mass and faults used for the case study

Parameters	
Hoek and Brown Classification parameters	UCS (sigci) (MPa)
	GSI
	D
	Mi
Mohr-Coulomb	Cohesion (MPa)
	Friction angle (phi) (degrees)

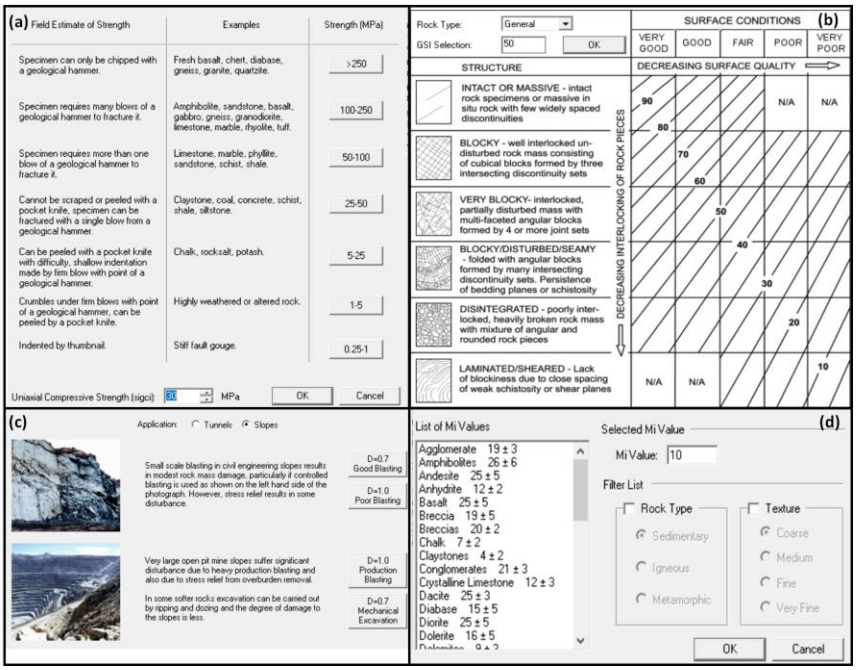

Figure 3.3 Rock mass properties estimator charts within the RoClab (a) the UCS (sigci) of the rock mass (b) GSI chart for rock mass (c) Disturbance factor (D) of slope (d) Constant rock mass value (Mi).

3.4.3 DIPS procedure for failure mechanism

Kinematic analysis is one of the common tools utilized to conduct slope stability analysis in rock slopes consisting of discontinuities. However, such analysis could be classified into one of the four categories in which the categories are controlled by the type and degree of structural control. As a result, the categories are planar failures, circular failure, toppling and wedge failures. Similar, to other previous studies (Basahel and Mitri, 2017; Gurocak et al. 2008; Lee and Wang, 2011; Pantelidis, 2009; Rusydy et al. 2017; Siddique et al. 2015) which have performed kinematic analysis, this dissertation also incorporated the kinematic analysis to predict the slope failure mode which could be expected within the study area.

A detailed scan line survey was conducted at two different slope sites which stretched to a maximum of 50 meters. One may argue that kinematic analysis is a purely geometric technique; it examines which mode of failure is possible in a jointed rock mass, therefore, angular relationships between discontinuities and slope surfaces were applied to determine the potential and mode of failure (plane, wedge and toppling) as stated by Kim et al. (2002). Furthermore, the Markland test (Markland, 1972) is one of the kinematic analysis methods designated to evaluate the possibility of wedge failure, in which a wedge-shaped mass slides along the line of intersection of two planes. Owing to that a refinement of Markland's test denoted by Hocking (1976), the refined Markland's test was implemented. Field observations include a natural slope condition, types and description of materials involved (see Figure 3.4); the information is crucial to perform accurate kinematic analysis and support the estimated slope failure by the model (DIPS). The measurements taken in the field were slope angle, dip and dip direction, spacing and persistence of discontinuities. As already mentioned, the data were graphically analyzed using DIPS software.

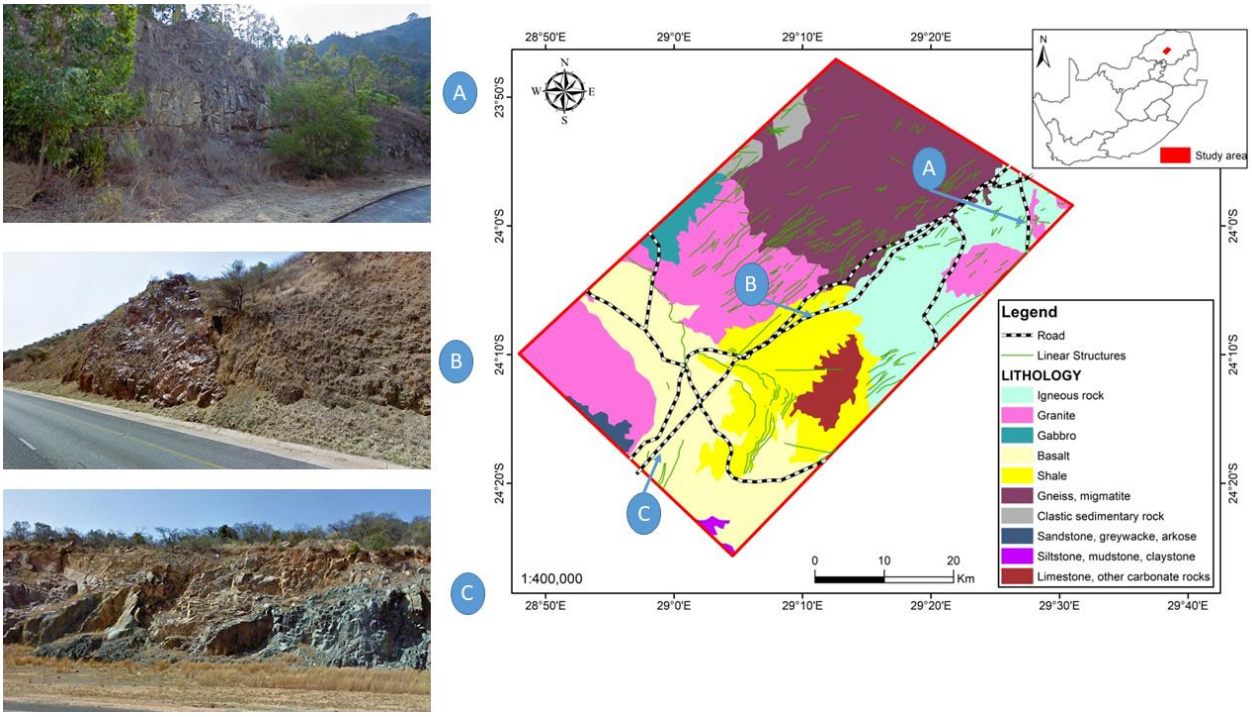

Figure 3.4 Field observations across sections of the study area, (a) Slope observed along R71, (b) slope observed along N1 within the sandstones, and (c) slope observed along the N1 within the shale and dolerite dykes.

3.4.4 Flacslope procedure

The methodology followed in this study is divided into four sections, the first section outlines the model construction, in this regard, the model construction of the FLACslope is documented. The construction incorporates four stages which are

(1) defining a project,

(2) building the slope conditions of the model,

(3) calculating the factor of safety of the model, and

(4) viewing the results.

The second section denotes the procedure followed when performing sensitivity analysis of the fault, this includes analyzing the effect of fault geometry, thickness, shear strength material, mesh density, and various methods of the ubiquitous joint model on the FoS of

the slope. The third section documents the material properties used for the model and it is followed by the last section of the methodology which gives a brief description of the practical example used to implement the developed reliability evaluation process of the multi-faulted slope.

3.4.4.1 Model Construction

The modelling begins with the creation of the project which involved checking that the setting of the project is appropriate, in this regard the setting was made to allow conditions (structural elements, water table, interface, and nonstandard gravity) but exclude regions from FoS, the SI units to be used and the project title can then be stated. Following that, the model build commences which involves defining the bounds of the model such as the slope dimensions (depth, rise and slope angle) (see Figure 3.5). After carefully defining the slope geometry, then layering the slope commence, in this regard materials with a variety of properties are defined per zones of slope (see Figure 3.6).

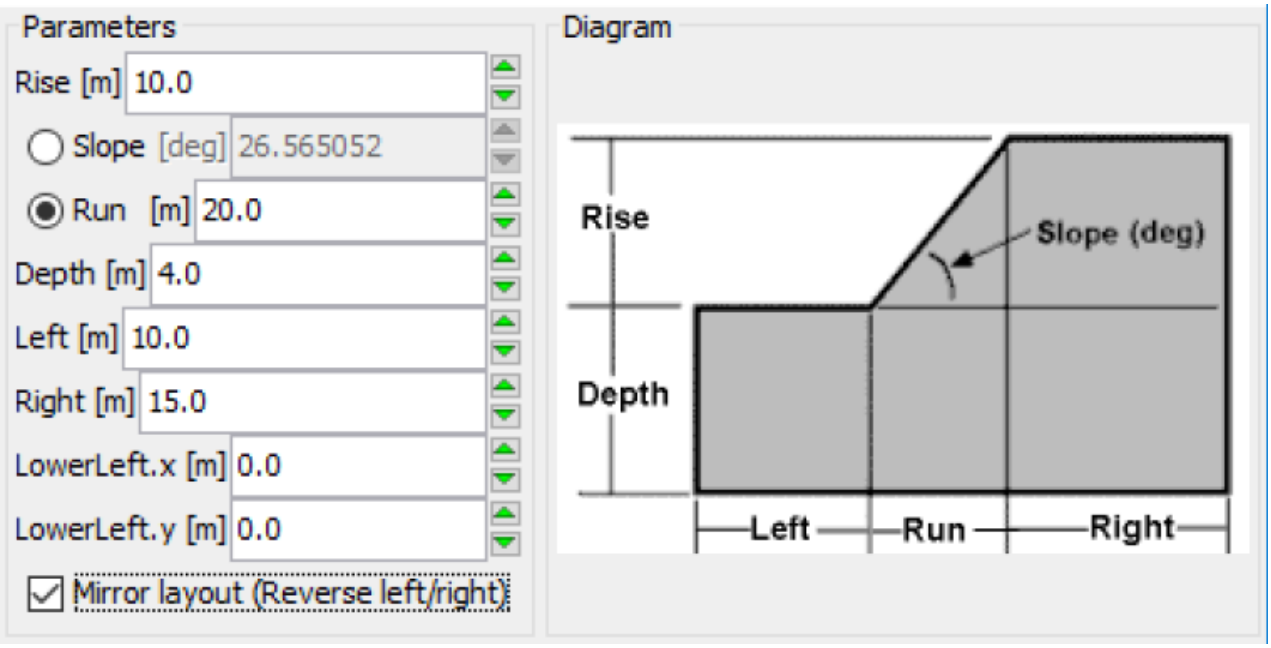

Figure 3.5. Slope dimensions allocation

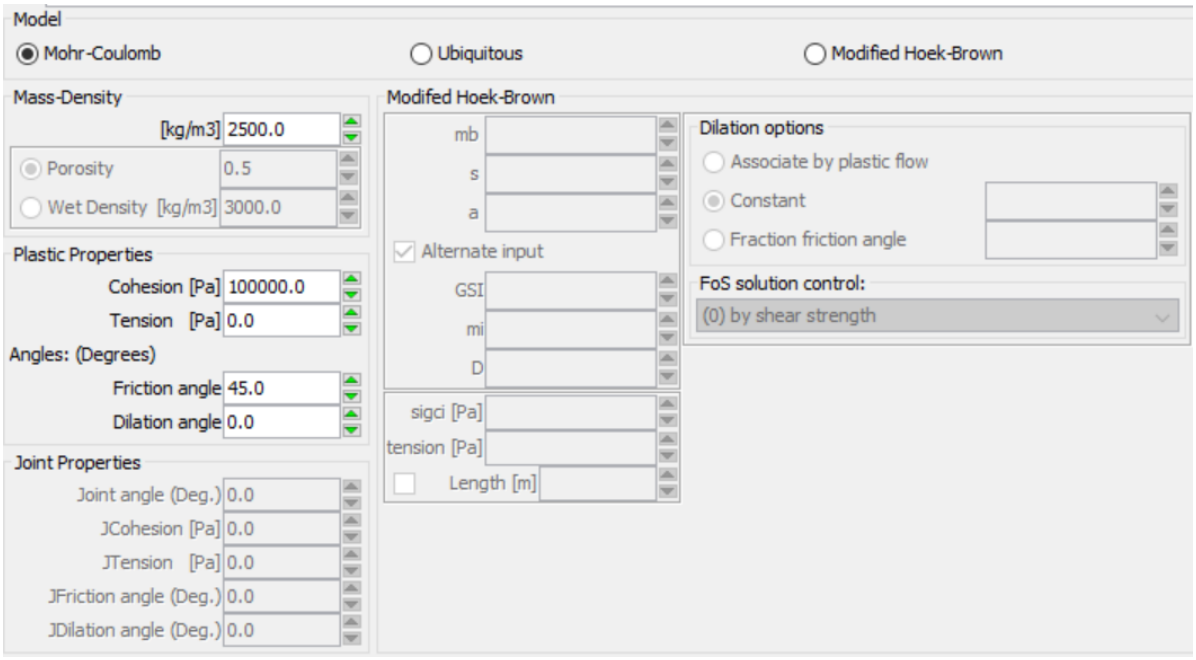

Figure 3.6. Material properties dialog

After materials are well created, they are assigned across the slope based on which layer they should be assigned. To achieve that, the material is firstly highlighted, then clicked on the model view inside the layer that one wishes to assign the material. As a result, the material will be assigned to the layer and the name of the material will be shown (see Figure 3.7).

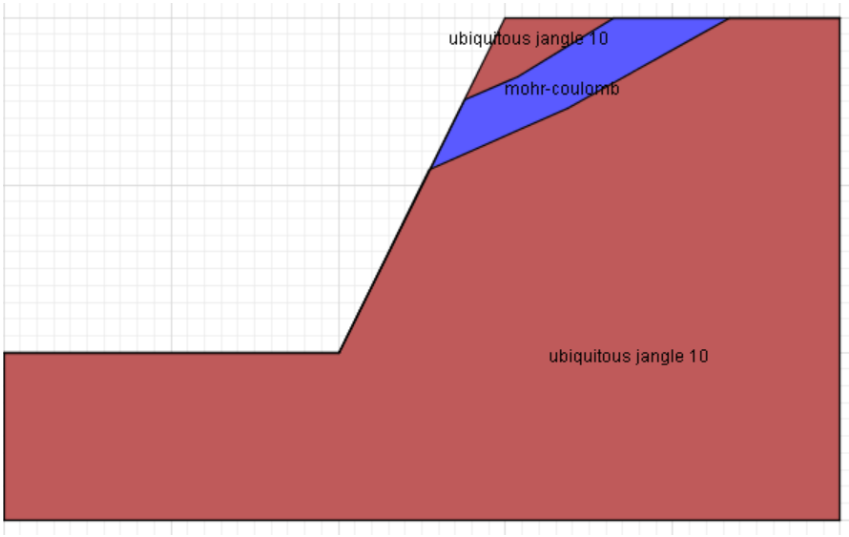

Figure 3.7. Materials assigned to the two layers in the

Following that, the model will be ready for FoS calculation, the solving tool is then used to begin the analysis. Immediately after utilizing the solving tool, the selection of mesh type comes up, and in this regard, there are four options (coarse, medium, fine and user specifications) (see Figure 3.8). The coarse grid mesh model is most used for preliminary analyses, but the solution for the model is rapid. While the medium grid is normally recommended for detailed studies, it is believed that the medium grid solutions are closely related to those of the lower and upper bound solutions of limit analysis, and the fine model is recommended for comprehensive analyses, though the model may be very slow. In this study, all types of mesh models were utilized to see the sensitivity analysis. After selecting the mesh, the model runs to estimate the FoS and displacement concurrently and the results are displayed at the end (see Figure 3.9).

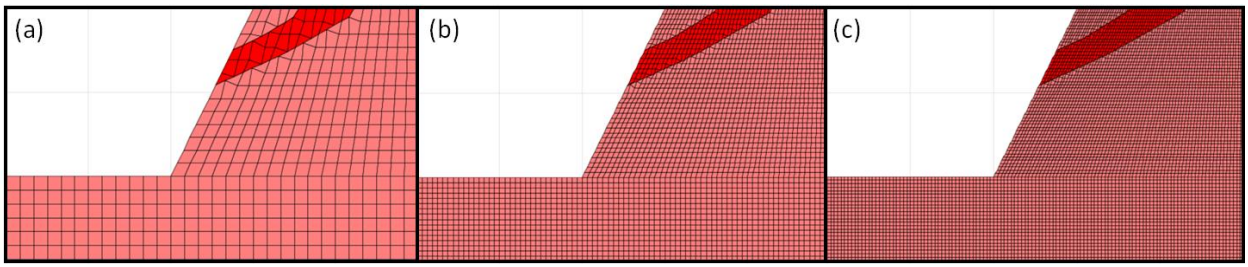

Figure 3.8. Various grids of the model (a) course mesh, (b) medium mesh and (c) Fine mesh.

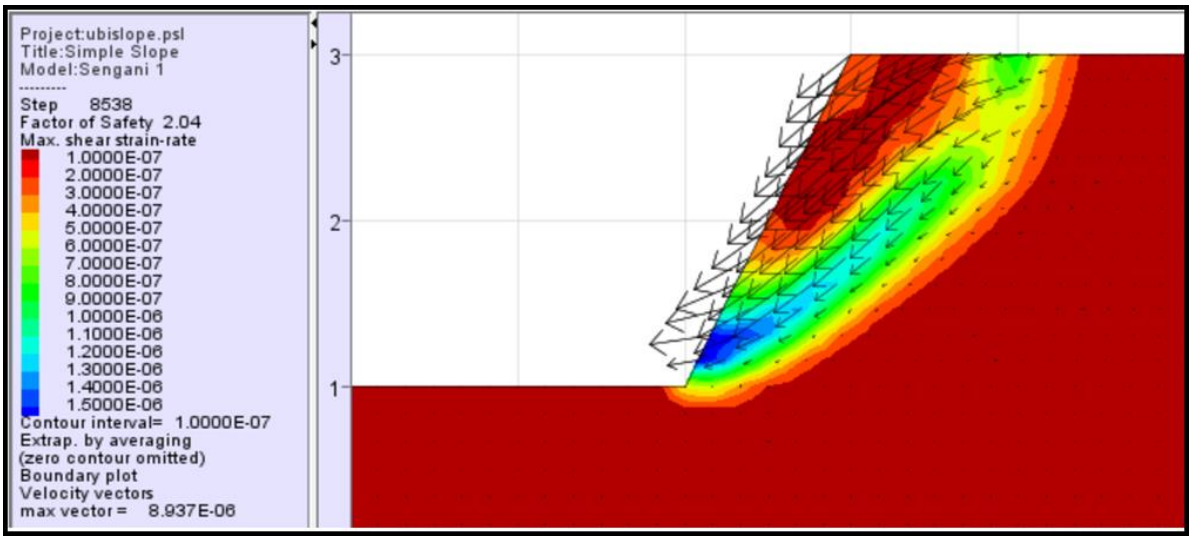

Figure 3.9. Factor-of-safety and maximum shear strain-sate plot for course-grid/mesh.

3.4.4.2 Sensitivity parameters of fault modelled

This section documents the procedure followed when performing sensitivity analysis of the fault, and it includes the procedure used when analyzing the effect of fault geometry, thickness, shear strength material, mesh density, and various methods of the ubiquitous joint model on the FoS of the slope.

Fault geometry

The effect of shape in fault geometry on the FoS of the jointed slope was investigated, and both planar and undulated planar faults (see Figure 3.10) were used to achieve the objectives. In this case study, material properties and other numerical settings remained constant.

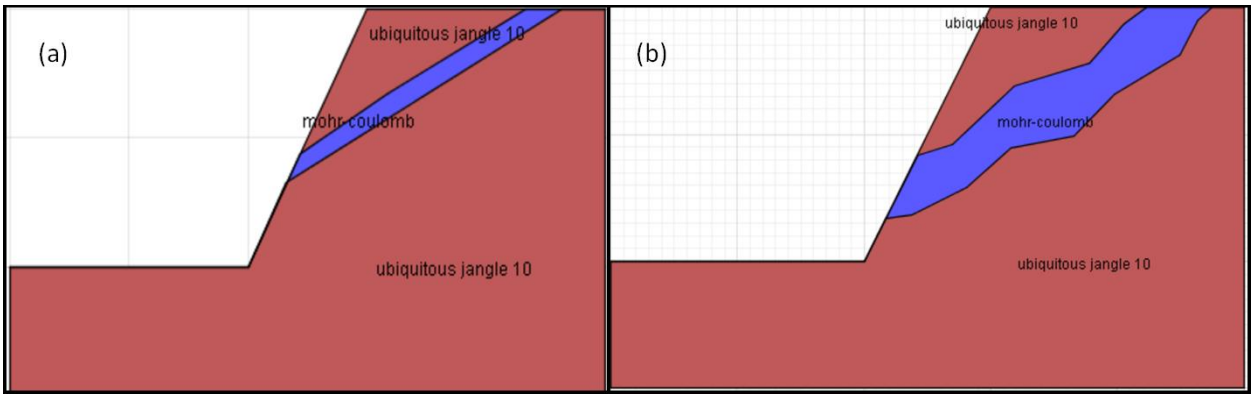

Figure 3.10. Fault geometries used for the study (a) planar fault (b) undulating planar fault

Fault thickness

The effect of fault thickness on the FoS of the slope was also investigated using various ubiquitous joint models (models differ with the joint properties as shown in Table 3.3). The fault thickness of the fault ranged from 2m to a maximum of 8m (see Figure 3.11). Considering that the previous studies, such as that of Azarfar et al. (2018), mentioned that the estimation of an accurate fault thickness is always not practical, especially in cases where there is no daylight for the fault zone, introducing the accurate fault zone in the model is always a challenge. Secondly, a change in fault thickness was documented

(Azarfar et al., 2018) to influence the increase in the number of elements within the model, therefore, such simulation of fault thickness is critical.

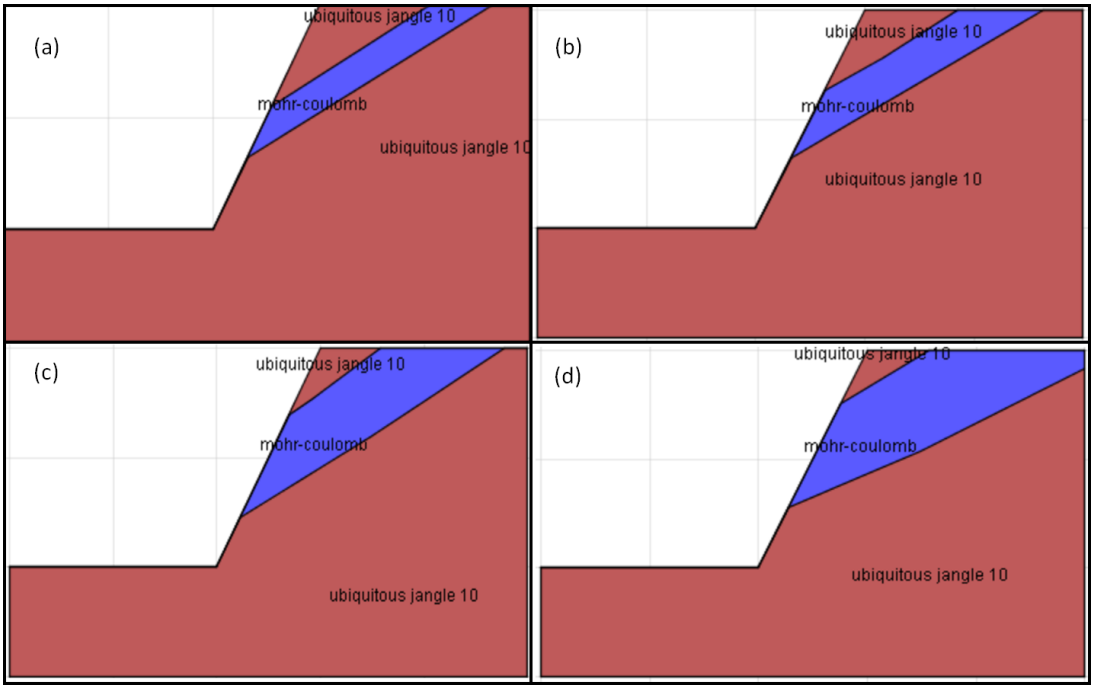

Figure 3.11. Fault thickness used for the study (a) 2m thick fault (b) 4m thick fault (c) 6m thick fault and (d) 8m thick fault

Shear Strength properties of the fault

The effect of shear strength properties of fault on FoS of the slope was also investigated using three types of ubiquitous joint methods. In this regard both cohesion and the friction angle were considered separately, cohesion used ranged from 100000 Pa to 400000 Pa, while the friction angle used ranged from 0^0 to 18^0. The results of both cohesion and friction angle were compared with the FoS of the slope.

Mesh density

It is well established that the element type, mesh discretization and convergence toleration significant impact the estimated FoS (Ghavidel, et al., 2017; Lu et al., 2020). In this study, change in mesh density was also considered, the first mesh to consider was the course mess, followed by medium and then fine mesh in all methods.

Varying ubiquitous joint angle

The effect of the ubiquitous joint angle used per method was also investigated; in this regard the joints used varied from 10^0 to 135^0. This analysis was conducted simultaneously with the change in the cohesion of the joints while the rest of the material properties including fault remained constant.

3.4.5 Optimum 2G

The model procedure followed in Optum G2 is readily available on the Optum Computational Engineering website under Optum G2 analysis and examples. In summary, the procedure followed includes the project definition (Project File dialog, slope parameters dialog, Model layout), building the model in terms of model layers, input properties of the material, and model setting. After processing the provided information in the model, the results of the model are then presented in terms of SRF and gravity multiplier though the current study is interested in SRF analysis only, furthermore, the model can also provide results on displacement, stress, the strain among other aspects such as yielding function and dissipation. As already stated, the model build was varied based on the material properties the case is interested in and the material properties of each case are given in Table 3.3 below.

Table 3.3 Material properties used for Optimum 2G

	Material Type
Stiffness	E (MPa)
	v (-)
	c (kPa)
	ϕ (º)
Strength	kt (kPa)
	ϕt (º)
	γdry (kN/m³)
Tension cut-off	γsat (kN/m³)
	K0 (-)
	σ0 (kPa)
Unit Weights	Kx (m/day)
	Ky (m/day)
	h* (m)

3.5 GIS-based tools and Machine learning

The methodology of this study is divided into three sections, the first section documents how susceptibility factors were designed followed by procedures for both AHP and fuzzy logic, and lastly, the detailed procedure in the validation method is documented.

3.5.1 Preparation of susceptibility of Slope

The preparation for slope susceptibility commences with the development of an inventory map of the study area (R528 regional road) from the field observation along the road cut slope and thereafter the interpretation of Google Earth images. A similar procedure followed by Pradhan et al. (2010) in terms of landslide inventory development and arrangement has been followed. Ten landslide affecting factors such as slope angle, distance to road, and distance to the river, lithology/lithosphere, land use, slope aspect, distance to lineaments (faults), soil type, annual rainfall, and elevation were used for

landslide analysis in the present study. The factors selected were mostly based on the field observation across the exposed slopes and benchmarking with other previous studies of this form (e.g., Sengani et al., 2020). Furthermore, the various thematic layers in relation to the above-mentioned factors were used to generate the landslide susceptibility hazard scheme of the R528 regional road. The AHP and fuzzy logic were used to develop the landslide susceptibility. In terms of verification, both field observation images were used and a detailed numerical simulation of the stability of each slope was also performed using the finite element method of the upper and lower bound solutions. The details on the preparation of different landslide factor layers are documented below.

3.5.1.1 Preparing landslide factor layers

As already stated, ten landslide factors were considered in this study, the details of each factor incorporate the buffering zones among others. Such details are documented below.

Distance to roads

Distance to roads has been well established as one of the major anthropogenic factors contributing to slope instability (Nourani et al., 2014; Yilmaz, 2010). One may argue that the development of a road usually creates slope cut with unstable solid mass (rock or soil) as such this factor is very crucial. Furthermore, during the field observation, some pre-existing landslides appeared to due to those unstable road slopes generated during road construction. In order to capture all those small aspects that may contribute to the occurrence of landslides. In the current study, six different buffer zones were generated with an interval of 500 m (Figure 3.12a).

Distance to River

Hydrological networks across the study area were also incorporated, studies such as those of Dai and Lee (2002), Bui et al. (2011), and Park et al. (2013) have validated the significance of the hydrological network in landslide development. Historical studies (Dai and Lee, 2002; Bui et al., 2011) have documented that the hydrological network influences the stability of the slope, especially in areas prone to erosion and weathering processes. In the present study the river network is produced from 30-m DEM by

hydrology tools in ArcGIS 10.2.2. Six different buffers were generated using the Euclidean distance method to determine the degree to which the streams could affect the bank slopes (Figure 3.12b).

Distance to lineaments

Geological fault areas are, in general, highly susceptible to landslides because the surrounding rock strength decreases due to tectonic breaks (Chen et al., 2017). In this study, the fault buffers were reclassified into six categories to produce the distance to fault map at a 500 m interval using Euclidean distance (Fig. 3.12c), based on the geological map of the Limpopo mobile belt.

Land-use change

Land-use change is influenced by factors relating to population needs, such as converting the agricultural and forest land to the urban areas, converting of forest to farmland, and reducing of the involuntary or unethical slope for infrastructure developments. Land use is a major factor in mapping landslide susceptibility. In this study, land use was generated using Landsat 8 Oli image applying a supervised classification Likelihood with ArcGIS 10.2.2 and Envi 5.0 software and reclassified into six classes, namely forest, agriculture, uncultivated land, bare land, urban, and water body (Figure 3.12d).

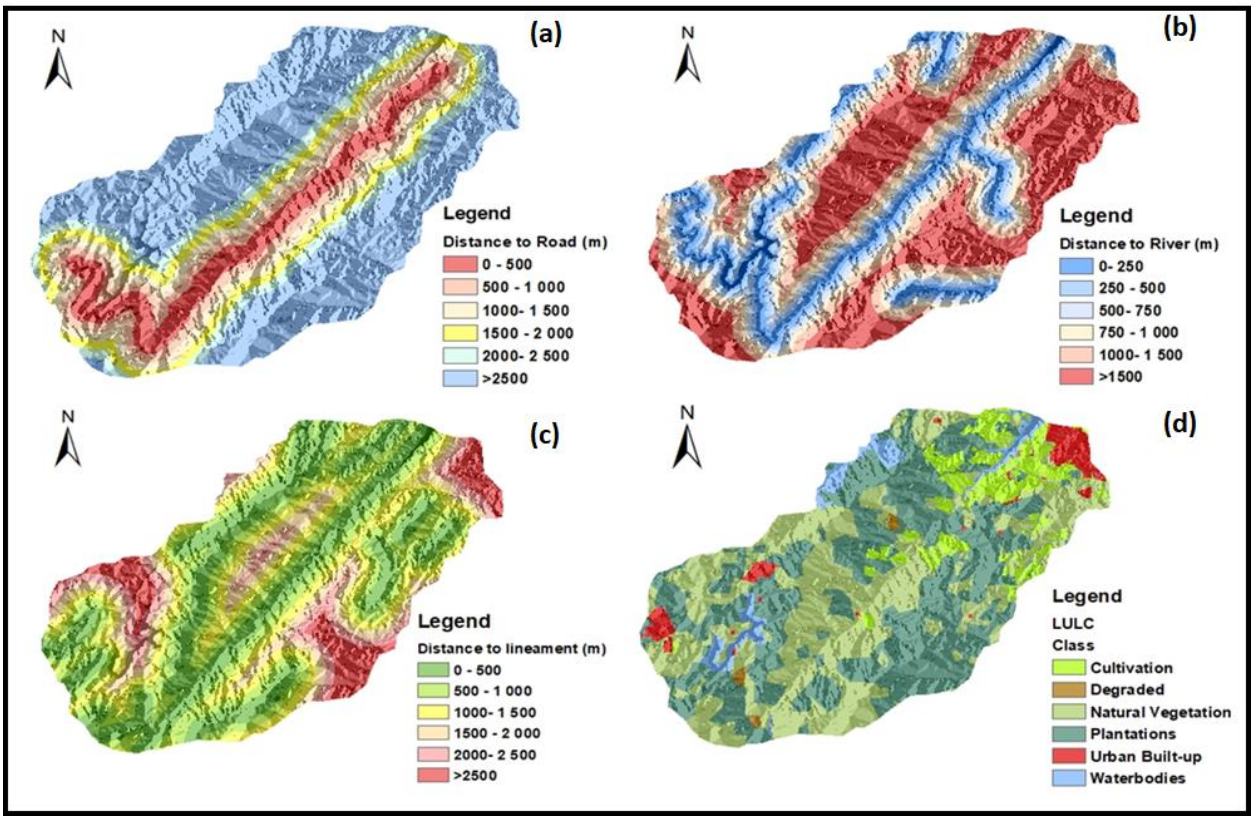

Figure 3.12 Slope susceptibility factor layers (a) distance to road (b) distance to the river (c) distance to lineament (d) LULC

Slope or Topographic factors

In the present study, topographic factor data was extracted from the 30-m DEM. The slope aspect referring to the direction of the slope face (Poudyal et al., 2010; Pourghasemi et al. 2012) is frequently used as a landslide-conditioning factor. This factor was reclassified into nine directional classes (Figure 3.13a). Slope angle, considered a main causal factor, is frequently used to map the susceptibility to landslides (Wei Chen et al., 2017; Nourani et al., 2014). In the current study, the slope angle map was reclassified into seven classes with an interval of 5° (Figure 3.13b).

Elevation and Lithology

An elevation thematic map was extracted and generated from 30-m DEM using ArcGIS software; ranging between 676m and 1992m, it was reclassified into five classes (Figure 3.13c). Lithology is a frequently used factor in landslide susceptibility analyses (Althuwaynee and Pradhan, 2016). The lithology map extracted from the 1:500000-scale geology map of Rabat showed that the study area is covered with various types of lithological units. These units were classified into four classes as illustrated in Figure 3.13d. Other factors such as aspects, soil type, and annual rainfall are also denoted in Figures 3.14a-b respectively.

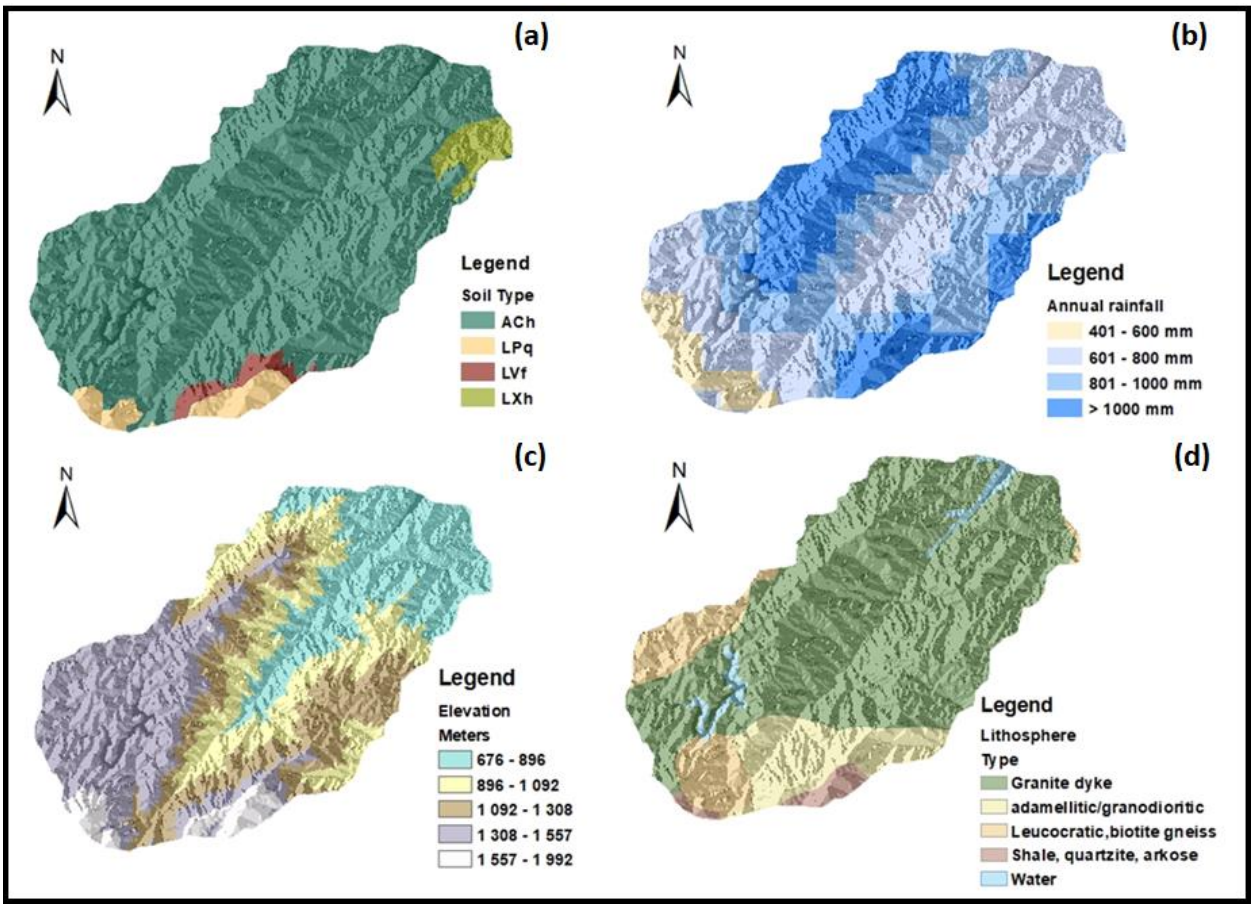

Figure 3.13 Slope susceptibility factor layers (a) soil type (b) annual rainfall (c) elevation (d) Lithology

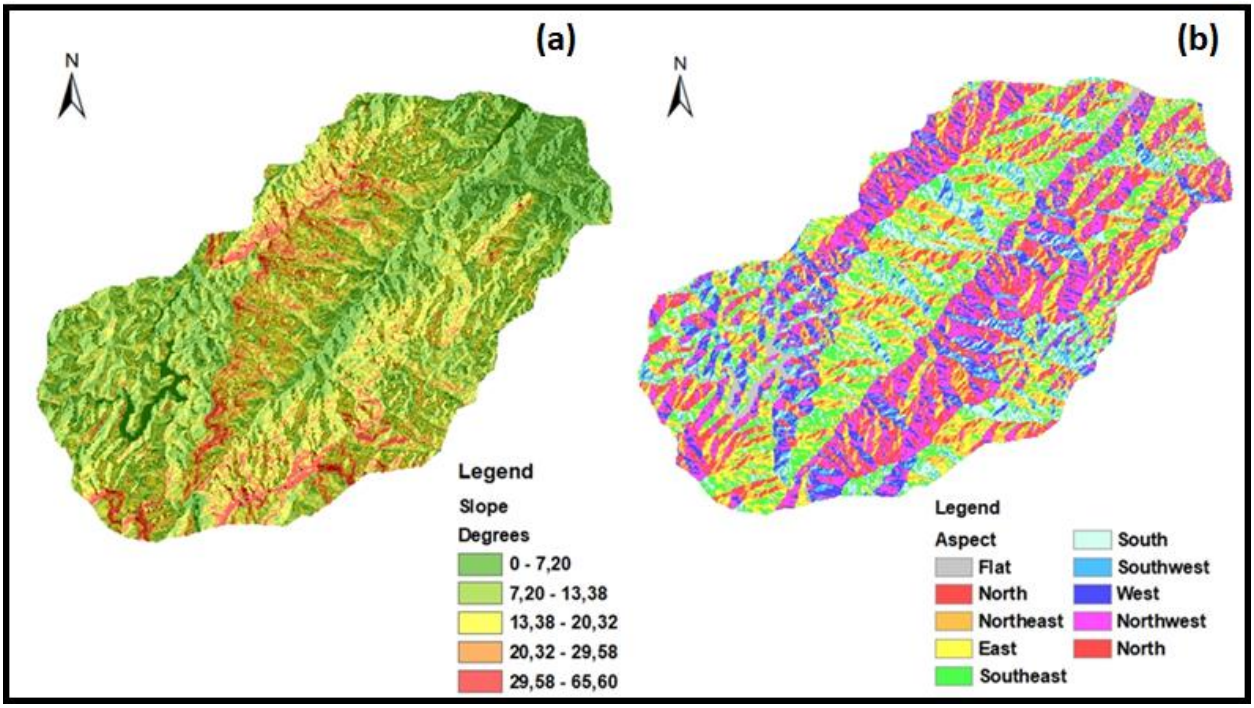

Figure 3.14 Slope susceptibility factor layers (a) slope and (b) aspect

3.5.1.2 Susceptibility mapping

The susceptibility mapping of this study was based on two approaches, as stated above, nevertheless, both AHP and fuzzy logic were used for the purpose. The detailed description of the methods is documented in the subsections below.

Fuzzy Logic

For the present study, the fuzzy method was assembled with AHP methods. The fuzzy maps of selected parameters have been prepared with the help of the membership function (MF) tool in the GIS environment. The membership function (MF) values range between 0 and 1 (Roy and Saha, 2019). The value 0 means that x is not a member of the fuzzy set, while the value 1 means that x is a full member of the fuzzy set. A sample of a fuzzy set is shown in the following equation (Eq 3.16) (Mcbratney and Odeh 1997).

$A = \{x, \mu_A(x)\}$ for each $x \varepsilon X$ (3.16)

Where μ_A is the MF (membership of x in fuzzy set A) so that:

If x does not belong to A, then $\mu_A = 0$.

If x belongs completely to A, then $\mu_A = 1$.

If x belongs in a certain degree to A, then

$0 < \mu_A (x) < 1$

According to equation 3.17 MF was used for rainfall, elevation, aspect, and slope.

$$\mu_A (x) = f (x) = \begin{cases} 0 & x \leq 0 \\ x \text{ - a} = \text{b- a} & a > x < b \\ 1 & a \geq b \end{cases} \quad (3.17)$$

Where x is the input data and a, b are the limit values. For geology, soil texture, distance from the river, distance from lineament, LULC, and distance from the road, the following MF has been used equation 3.18.

$$\mu_A (x) = f (x) = \begin{cases} 0 & x \leq 0 \\ b \text{ - x/b- a} & a > x < b \\ 1 & a \geq b \end{cases} \quad (3.18)$$

Fuzzy gamma operators

Several fuzzy operators exist for combining membership functions such as AND, OR, SUM, PRODUCT and GAMMA. The current study uses the gamma operator which combines membership functions automatically. Similarly, to other previous studies (Roy et al., 2019), the fuzzy gamma operation has been calculated using equation (3.19).

$$\mu_\gamma = (\mu_{sum}) k^\gamma . \left(\mu_{product}\right).^{1-\gamma} \quad (3.19)$$

The exponent γ, a number from < 0, 1 > interval, allows optimization of the membership combination. Setting it to the extremes of the interval gives either a fuzzy algebraic sum (γ = 1) or a fuzzy algebraic product (γ = 0). To perform fuzzy gamma operation, several gamma operator (k) values, i.e., 0.50, 0.70, 0.80, 0.90, 0.95, and 0.975 are there. In the present study, a fuzzy gamma operator (k) value of 0.90 has been applied to produce the landslide susceptibility map.

3.5.2 Analytic Hierarchy Process (AHP)

The analytic hierarchy process is a multi-criteria decision analysis method that distributes the elements related to the decision into the target layer, criterion layer, and scheme layer, and qualitative and quantitative analyses are conducted on this basis (Mersha and Meten, 2020). The AHP method has been widely used in landslide susceptibility mapping. When using the AHP method to evaluate landslide susceptibility, the corresponding hierarchy model should be established first. Similar to other previous studies, both causative factors and pairwise comparison matrix and weights of landslide causative factors were developed shown in Tables 3.4 and 3.5 respectively.

Table 3.4 Causative factors reclassified and ranked from 1 to 5.

Variables	Class	Reclassified Ranks	Variables	Class	Reclassified Ranks
Road	0–500 m	5	Rainfall	400 - 600mm	2
	500–1000 m	4		600 - 800mm	3
	1000–1500 m	3		800 - 1000mm	4
	1500–2000 m	2		>1000mm	5
	>2000 m	1			
River	0–250m	5	Landcover	Cultivation	2
	250–500m	4		Degraded/bareland	5
	500–750m	3		Natural Vegetation	3
	750–1000m	2		Plantations	1
	>1000m	1		Urban Built-up,	4
				Water bodies	3
Leanment	0–500m	5	Lithology	Granite dyke	2
	500–1000m	4		adamellitic/granodioritic biotite	3
	1000–1500m	3		granite	4
	1500–2000m	2		Leucocratic/ leucogneiss	5
	>2000m	1		Shale, quartzite, arkose, basalt	

Elevation	676 - 896m	1		Aspect	Flat, E	1
	896 - 1 092m	2			N, NE, NW	2
	1 092 - 1 308m	3			SE	3
	1 308 - 1 557m	4			SW, W	4
	>1 557m	5			S	5
Slope	0 - 7,20	1		soil	Haplic ACRISOLS -ACh	4
	7,20 - 13,38	2			Lithic LEPTOSOLS -LPq	5
	13,38 - 20,32	3			Ferric LUVISOLS - LVf	2
	20,32 - 29,58	4			Haplic LIXISOLS - LXh	3
	>29,58	5				

Table 3.5 Pairwise comparison matrix and weights of landslide causative factors.

Factor	Road	Lineament	Stream	Slope	Geology	LULC	Elevation	Aspect	Soil	Rainfall	Weight
Road	1	3	4	2	3	3	4	5	3	2	21,05%
Lineament	1/3	1	3	1/3	2	3	3	4	3	1/2	11,48%
Stream	1/4	1/3	1	1/3	1/3	1/2	1/3	2	1/3	2	5,22%
Slope	1/2	3	3	1	3	3	3	5	3	2	17,15%
Lithology	1/3	1/2	3	1/3	1	3	3	4	1/3	1/3	8,72%
LULC	1/3	1/3	2	1/3	1/3	1	3	4	3	1/2	8,20%
Elevation	1/4	1/3	3	1/3	1/3	1/3	1	2	1/3	2	6,51%
Aspect	1/5	1/4	1/2	1/5	1/4	1/4	1/2	1	1/3	1/3	2,63%
Soil	1/3	1/3	3	1/3	3	1/3	3	3	1	1/3	8,26%
Rainfall	1/2	2	1/2	1/2	3	2	1/2	3	3	1	10,99%

3.6 Limitations and challenges encountered

One of the limitations of the experimental program presented in this chapter is that the study did not contemplate a three-dimensional analysis of the slopes. Although the development of such a numerical simulation tool would have been a viable option, this was beyond the scope and the timeframe of the research study.

Second, field stresses were estimated (with the use of Roclab software) and not measured in any way. This is because field stress measurements require expensive equipment that cannot be covered by the budget allocated for the study.

Third, access to some target locations of the study area was impossible as part of the fieldwork. The main reason is that the said locations were very steep or covered with a large and wild forest. In other instances, some areas were considered unstable to walk over for observation and surveying.

Fourth, a detailed laboratory test on rock strength using core samples was not performed. The core logs and supporting hardware equipment failed when only four samples were collected for testing. The other rock strength tests were performed using a Swedish hammer. In view of the small size of the core samples, it was decided not to perform any laboratory testing of rock strength. Estimates from past work done in the great Limpopo province were sorted for a reasonable substitute to be used in the area.

Chapter 4 Accuracy of two-dimensional limit equilibrium methods in predicting the stability of homogenous road cut slopes

The departure of this chapter is to argue that although limit-equilibrium methods are widely used by engineers and scientists in predicting the stability of homogenous slopes, their use has been demonstrated to present significant errors due to the violation of kinematic and static admissibility. The concern is often voiced regarding the accuracy of Limit Equilibrium Methods (LEMs) solutions in predicting the stability of homogenous slopes. There are no exact limit equilibrium solutions or charts available against which to check the LEM solutions.

The present chapter has used the rigorous upper and lower bounds solutions of limit analysis based on finite element formulations of the bound theorems to benchmark and develop an accuracy classification chart of limit equilibrium methods in predicting the stability of the homogenous slope. Six case studies of homogenous road cut slopes, which vary with material properties were used and the effect of the increase in material strength with depth was considered.

The results of LEMs and limit analysis solutions have shown that Janbu Simplified limit-equilibrium solutions are closely related to rigorous upper bound solutions with an accuracy error ranging from 1 to 7% in various slope materials. Meanwhile, the Corp of Engineer 2 limit equilibrium solutions were found to overestimate among other methods, with an accuracy error ranging from 12 to 17% in various cases. Based on the results of the study an accuracy error classification chart of LEMs was developed.

4.1 Introduction

Since many years, the limit equilibrium method has been used to assess the stability of slopes, assuming that the soil material obeys the perfectly plastic Mohr-Coulomb criteria (example of some of the studies as documented by Fellenius, (1926) and Terzaghi (1943)). The improvement in these methods has been demonstrated for decades with well-known contributions by Bishop (1995), Janbu (1954), Morgenstern and Price (1965)

and Spencer (1967), among others. Though critical improvement has been demonstrated in the literature, the methods tend to apply a global equilibrium condition. As such, the approach is purely static since it neglects the plastic flow rule of soil. Owing to that, the static admissibility of the stress field is also not satisfied due to arbitrary assumptions made to remove the static indeterminacy. In summary, the methods only satisfied the global equilibrium conditions. To overcome the limitations of LEMs, the Finite Element Limit Analysis is used in slope stability problems. The Finite Element Limit Analysis uses the lower and upper bound rigorous solutions in simulating the stability of the slope, the lower bound limit analysis was firstly introduced by Lysmer (1970). Nevertheless, the lower bound method has been improved by several scholars (Anderheggen and Knopfel, 1972; Bottero et al., 1980; Sloan, 1988; Sloan, 1991a, 1991b) in order to meet all requirements for the stability analysis, the method uses three types of the element under the conditions of plane strain as shown in Figure 4.1. It has been documented that the stress field for each of these elements is assumed to vary linearly.

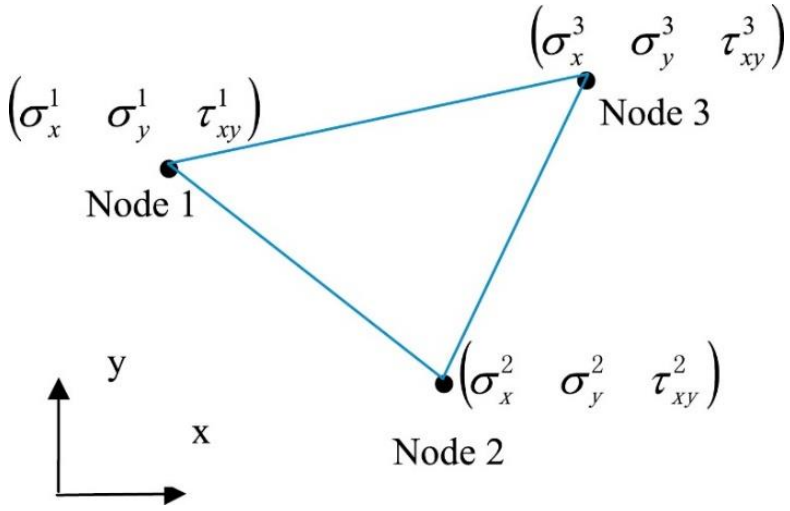

Figure 4.1. Elements used for lower bound limit analysis (Li et al 2017)

On the other hand, the literature (Anderheggen and Knopfel, 1972) reveals that the first formulation for the upper bound theorem was developed in 1972, with the purpose of analyzing the plate problems, further modifications were then introduced thereafter by scholars such as those of Bottero et al. (1980), Sloan (1989), Yu et al. (1992), to incorporate velocity discontinuities in a plane strain of limit analysis. Although there has

been some improvement, the upper bound formulations did not have a large number of discontinuities in the velocity field, therefore, Sloan and Kleeman (1995) strived to address the problem in the formulation of the upper bounds, which is the recent bound used in the current study. An example of the constant-strain triangular element used in the upper bound analysis is shown in Figure 4.2.

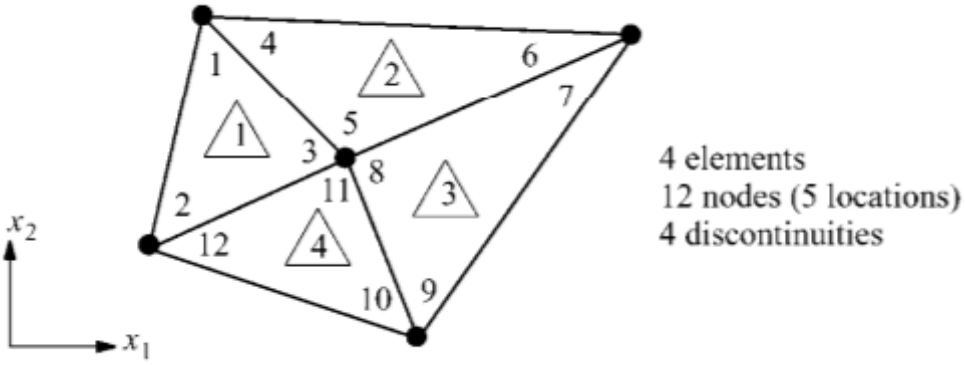

Figure 4.2 Elements used for Upper bound limit analysis (Lyaminz and Sloan, 2002)

Although there have been several improvements in the LEMs in predicting the stability of the slope, the method still presents some limitations as stated within the introduction section. Furthermore, the use of LEMs has gained momentum despite their accuracy error. One may say their simplicity increases their use in the industry, yet there is no accurate prediction chart to benchmark the LEM solutions, though the SRF method is preferred by few engineers due to its complexity. The recent study is intended to identify the error accuracy of LEMs benchmarked with lower and upper bound limit analysis methods. It is anticipated that the error accuracy chart will give freedom to those engineers who still prefer LEMs over any other method and the authors will be able to benchmark their solutions. Six common types of soil slope material were chosen to identify the accuracy per material of the slope, however, several case studies also increased the confidence of the outcome of the study.

The previous sections led to the discussion of methodology in terms of the numerical formulations of both LEMs and lower and upper bound of limit analysis using Finite

elements. The study results are thereafter documented with six case studies and concluding remarks.

The practical examples are implemented in homogenous slope materials with the Mohr-Coulomb model based on the case study. The limit analysis computer software so-called Optimum 2G is used in conjunction with limit equilibrium computer software called SLIDEs 2D in order to answer the above-mentioned objectives. The Optimum 2G is based on finite element formulations of the bound theorems of limit analysis, as such the best lower and upper bound solutions are obtained through the optimization of the admissible stress fields and kinematically admissible velocity field using linear programming techniques. On the other hand, the SLIDEs numerical model uses Limit Equilibrium formulations by locating the critical surface failure. Many methods have been developed; however, this study uses Bishop Simplified (Bishop, 1955), Lowe Karafiath (Lowe and Karafiath, 1960), Gle/ Morgenstern Price (Morgenstern and Price, 1965), Janbu Simplified and Janbu Corrected (Janbu, 1968), Spencer (Spencer, 1967), and Corp of Engineer number one, and Corp of Engineer Number two (U.S. Army Corps of Engineers, 1970) formulations.

4.2 Approach to data collection and analysis

The material and methods' section of the chapter is divided into two sections. The first section documents the limit equilibrium method applied in this research study, and the second section documents the mathematical formulation of each method, followed by the description of the procedures adopted when simulating LEM solutions using a computer code called SLIDEs 2D as documented in Chapter 3. The procedure for a computer code called Optum G2 is briefly documented in Chapter 3 and applied in this chapter and the input parameters for the model are shown in Table 4.1. Nevertheless, the section following the research approach is the result and discussion of the chapter and details of the section are documented below.

Table 4.1 Material properties used for case studies

	Material Type	Loose Sand	Medium Sand	Dense Sand	Soft Clay	Firm Clay	Stiff Clay	Dimensions of the model	
Stiffness	E (MPa)	30	30	30	30	30	30	Rise (m)	10
	v (-)	0.25	0.25	0.25	0.25	0.25	0.25	Depth (m)	4
Strength	c (kPa)	03	04	06	09	12	20	Left (m)	10
	ϕ (º)	13	15	17	18	20	22	Run (m)	20
Tension cut-off	kt (kPa)	0	0	0	0	0	0	Right (m)	15
	ϕt (º)	90	90	90	90	90	90	Slope degree	27º
Unit Weights	γdry (kN/m³)	14	16	18	19	20	21		
	γsat (kN/m³)	19	20	21	19	20	21		
Initial Conditions	K0 (-)	0.5	0.43	0.36	0.69	0.66	0.63		
	σ0 (kPa)	0	0	0	0	0	0		
Hydraulic Model	Kx (m/day)	1E-05	1E-05	1E-05	1E-05	1E-05	1E-05		
	Ky (m/day)	1E-05	1E-05	1E-05	1E-05	1E-05	1E-05		
	h* (m)	0.5	0.5	0.5	0.5	0.5	0.5		

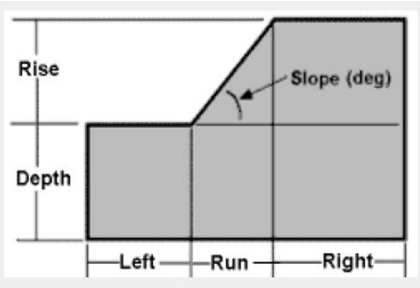

4.3 Results and discussion of the simulations

The results of this chapter are divided into two sections, the first section presents numerical simulation results in a homogenous road slope using the Mohr-Coulomb model. In this section, several examples of the prediction of the factor of safety or Strength Reduction Factor using both limit equilibrium (SLIDEs) and Limit Analysis (Optum G2) are presented. A detail comparing the accuracy of the LEMs in predicting the stability of the slope is well presented. The presentation of these results also incorporates the overestimation of FoS by several LEMs compared with the SRF stability number predicted. As already stated, several examples were used to quantify the accuracy prediction of slope stability using LEMs benchmarking with the Limit Analysis approach. A homogenous road slope with loose sand, medium sand, dense sand, soft clay, firm clay and stiff clay mechanical properties was used to conduct the investigations. However, the slope solid material properties differ in terms of stiffness, strength, flow rule, unit weight and hydraulic conditions. As such a clear distinction of the accurate slope stability prediction of the road slope in strain-softening has been documented.

The second section of the results documents a classification chart in terms of accurate prediction of slope stability among the LEMs; the chart classifies LEM's accuracy in terms of their rate of overestimating the stability of the slope, with the most accurate methods considered to be the lowest percentage of overestimating the stability of the slope. The chart was based on the previous section and benchmarked with the Limit Analysis results.

4.3.1 Stability analysis of a Homogenous Road Embankment Slope

The results of homogenous slope stability calculations using the rigorous upper and lower bound methods of limit analysis and the limit equilibrium method (Ordinary, Bishop, Gle/ Morgenstern Price, Janbu Simplified, and Janbu corrected, Spencer, and Corp of Engineer number one, and Corp of Engineer Number two) are presented in Figures 4.21, for slopes with homogenous loose sand, medium sand, dense sand, soft clay, firm clay and stiff clay respectively. The limit analysis results are plotted in terms of a strength reduction factor for both lower and the upper bounds, however, the simulation also included the total slope displacement though it is not of interest in the study. The solutions

from limit equilibrium computer code SLIDEs 2D are presented in terms of factor of safety for all stated methods. In both computer codes, it is assumed that the material gain strength with depth. Similar to other studies such as Yu et al. (1998), to account for the effect of increasing strength with depth, the results are always presented in terms of stability number (SRF or FoS) against the dimensionless parameters. For each homogenous slope, the stiffness, strength (cohesion, friction angles) unit weight (dry and saturated soil) and hydraulic conditions differ greatly. Furthermore, the geometry of the slope was kept constant throughout different case studies given, details of each case study are outlined below.

4.3.1.1 Road Embankment slope with loose sand

A soil slope with a slope angle of 45^0 is selected as a case study shown in Figures 4 to 6. In the slope, loose sand with a friction angle of 13^0, the cohesion of 3 kPa and unit weight of 14 kN/m³ and other input parameters as shown in Table 4.1 were taken into consideration. Both rigorous lower and upper bounds limit analysis and limit equilibrium methods were used to perform the analysis through separate numerical codes implemented as stated in the methodology section. The limit analysis results have shown that the slope is expected to be unstable considering the effect of an increase in the strength of material with a depth of slope. Furthermore, the lower bound solution estimated the SRF of 0.6588, while the upper bound solution was about 0.666 SRF. On the other hand, the limit equilibrium method solutions ranged from 0.718 FoS to 0.776 FoS. For all the cases considered, (see Figures 4.3, 4.4 and 4.5) it has been denoted that the exact solutions are bracketed within 8 to 17% of error accuracy. This implies among the limit equilibrium method, none of them was able to provide the exact solutions as compared to the rigorous lower or upper bound solutions, however, the LEM solutions were denoted to be closely related to those of the upper bound solutions. This type of result has been demonstrated by previous scholars such as Yu et al. (1998). Meanwhile, the Corp of Engineer number two was found to produce the highest accuracy error in predicting the stability number. Though several scholars assumed that the LEMs produce similar results to the Limit Analysis based on the predicted SRF and FoS number without considering the calculation of error accuracy or benchmarking the two methods, as such

the outcome of this analysis demonstrated different views within those studies such as Renani and Martin (2020). One may note that previous studies such as those of Renani and Martin (2020) did not consider exact solutions but closely related solutions and by so doing the author concludes that the solutions of LEMs and rigorous upper bound solutions are similar.

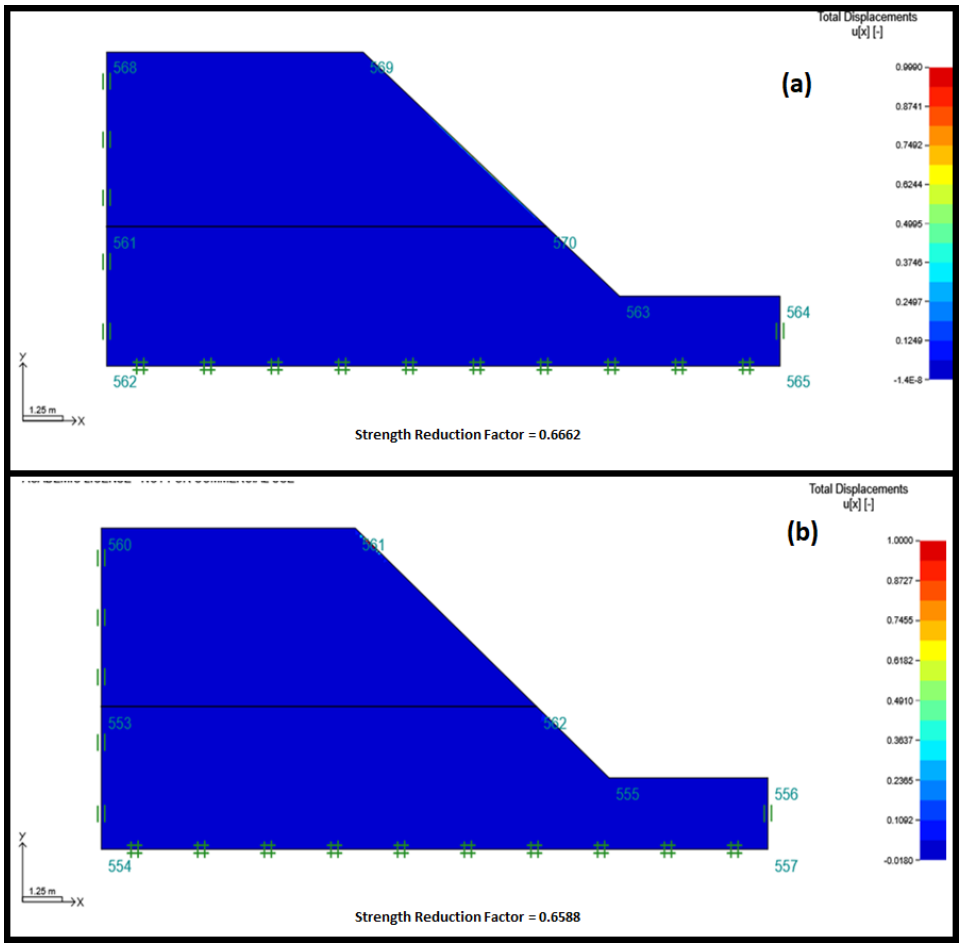

Figure 4.3. Predicted stability number using limit analysis method of strength reduction factor in loose sand (a) the SRF of the upper bound solutions of limit analysis (b) the SRF of the lower bound solutions of the limit analysis.

It was also observed that the Bishop Simplified of limit equilibrium also produces a stability number that agrees well with the upper bound solutions of the limit analysis. The method has produced a stability number with an accuracy error of about 9%, which is acceptable in the industry. It is said that the Bishop Simplified method accuracy error solution was

closely related to that of the Janbu Simplified method with just a 1% difference. Furthermore, another method, including Spencer, Morgenstern and Price, and Corp of engineering had produced an accuracy error above 10% but less than 20%. In summary, all the LEMs (see Figures 4.4 to 4.5) produce a stability number closely related to that of upper bound solutions, however, the stability numbers are not the same. Further case studies are discussed below to solidify the outcome.

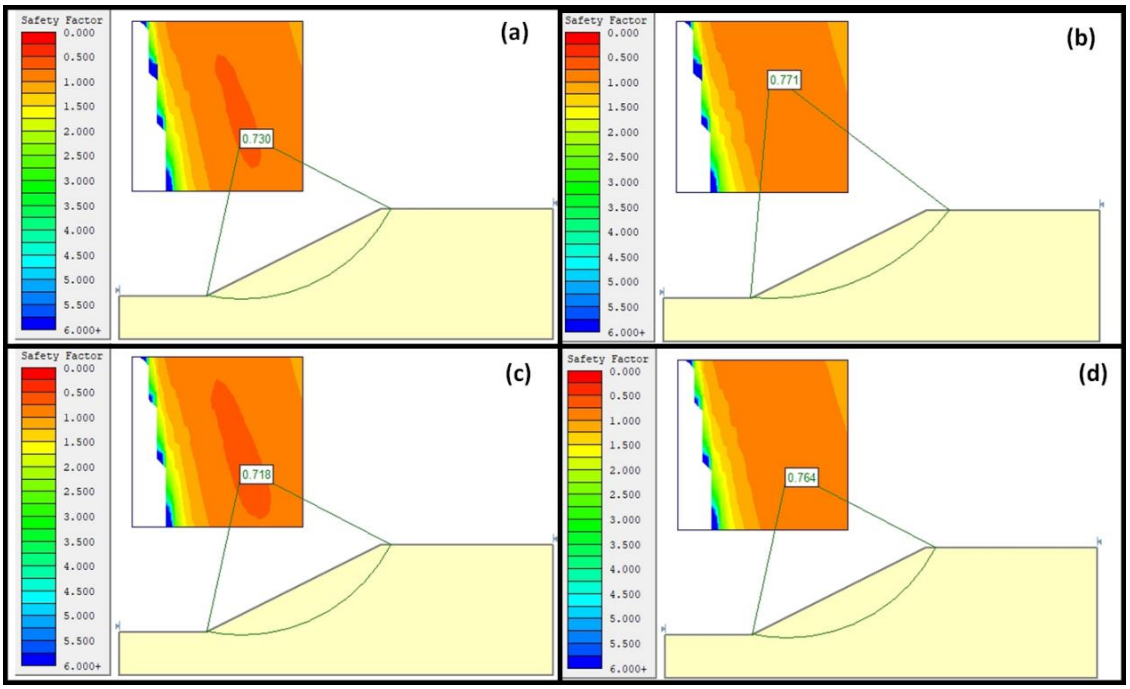

Figure 4.4. Limit Equilibrium stability number of loose sand slope produced using (a) Ordinary method, (b) Bishop simplified method (c) Janbu Simplified method (d) Janbu Corrected Method.

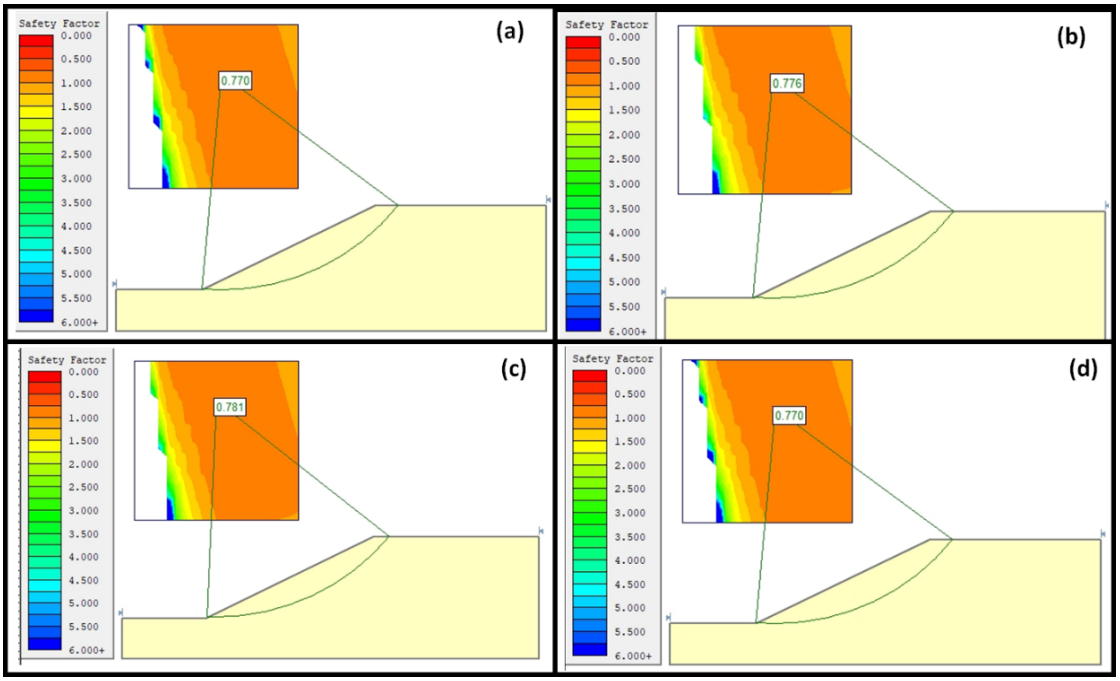

Figure 4.5. Limit Equilibrium stability number of loose sand slope produced using (a) Spencer method, (b) Corp of Engineering one (c) Corp of Engineering two (d) Morgenstern and Price Method.

4.3.1.2 Road Embankment slope with Medium Sand

Similar soil slope profiles were considered in this case as well as it is shown in Figures 4.6 to 4.8. In the slope, medium sand with a friction angle of 15^0, the cohesion of 4 kPa and unit weight of 16 kN/m³ and other input parameters as shown in Table 4.1 were taken into consideration. Both rigorous lower and upper bounds limit analysis and limit equilibrium methods were used to perform the analysis. The limit analysis results have shown that the slope is expected to be unstable. The lower bound solution estimated the SRF of 0.7782, while the upper bound solution was about O.8068 SRF. On the other hand, the limit equilibrium method solutions (FoS) ranged from 0.834 to 0.908. For all the cases considered, (see Figures 4.6, 4.7 and 4.8) it has been denoted that the exact solutions are bracketed within 3 to 13% of error accuracy. This implies the limit equilibrium method has still been considered to produce reasonable solutions in medium sand, however, Janbu and Ordinary methods were found to produce very small accuracy errors ranging from 3 to 5%, which is still within the acceptable error accuracy.

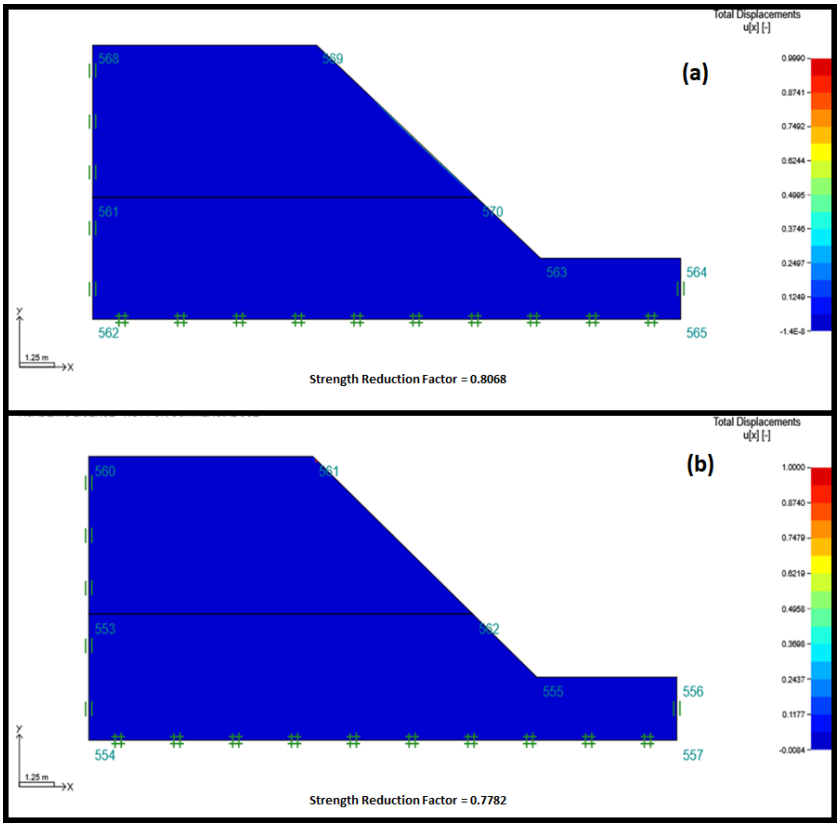

Figure 4.6. Predicted stability number using limit analysis method of strength reduction factor in medium sand (a) the SRF of the upper bound solutions of limit analysis (b) the SRF of the lower bound solutions of the limit analysis.

On the other hand, Corp Engineering two was also observed to produce the highest error of accuracy but in this case, the error was just about 10%. This gives the impression that almost all Limit Equilibrium methods can produce solutions that are in good agreement with the upper solutions in medium sand. As in the previous case, the Spencer and Morgenstern and Price methods produced similar stability.

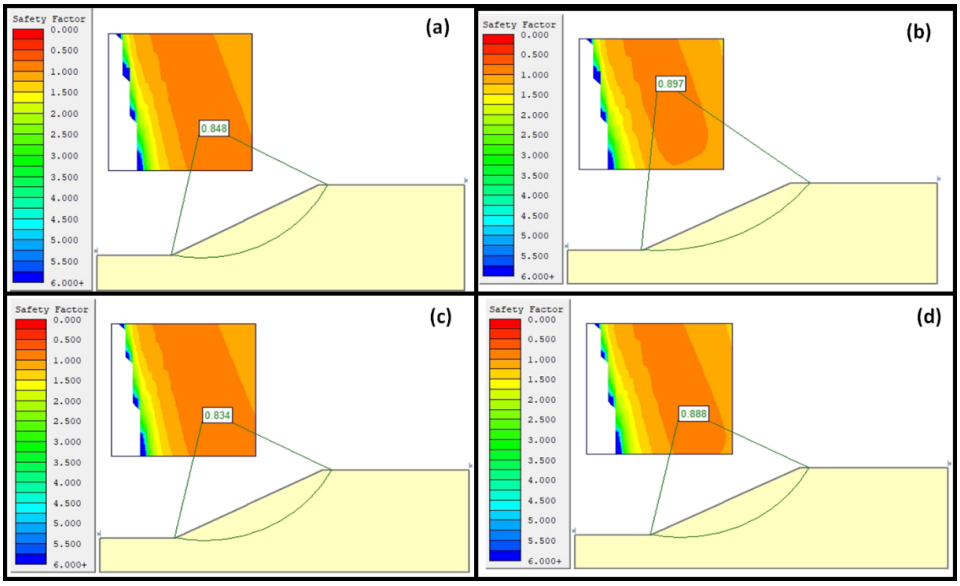

Figure 4.7. Limit Equilibrium stability number of medium sand slope produced using (a) Ordinary method, (b) Bishop simplified method (c) Janbu Simplified method (d) Janbu corrected method.

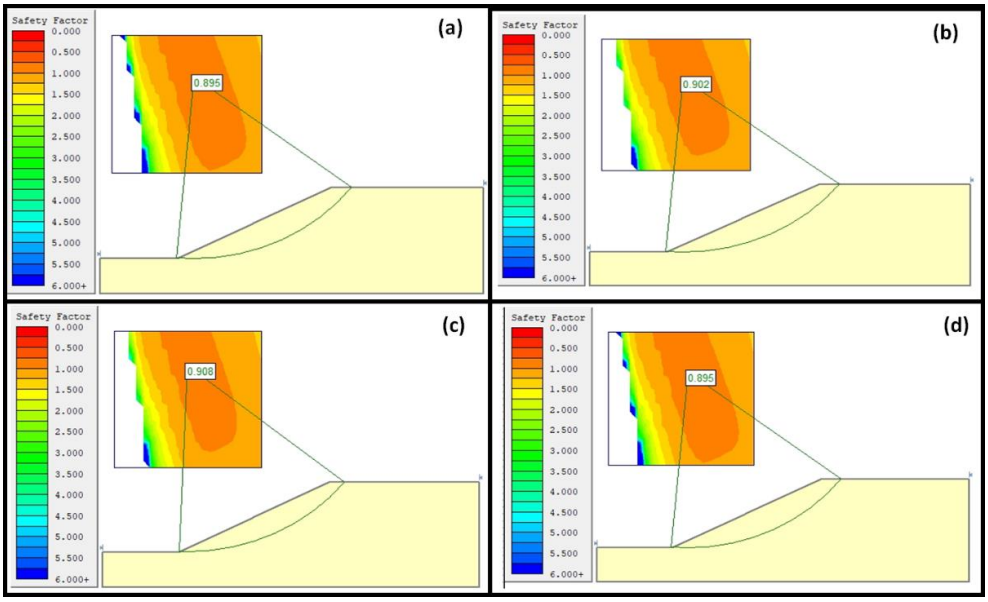

Figure 4.8. Limit Equilibrium stability number of medium sand slope produced using (a) Spencer method, (b) Corp of Engineering one (c) Corp of Engineering two (d) Morgenstern and Price Method.

4.3.1.3 Road Embankment slope with dense sand

A soil slope with a slope angle of 45^0 is selected as a case study shown in Figures 4.9, 4.10 and 4.11. In the slope, dense sand with a friction angle of 17^0, the cohesion of 4 kPa and unit weight of 16 kN/m³ and other input parameters as shown in Table 4.1 were taken into consideration. Both rigorous lower and upper bounds limit analysis and limit equilibrium methods were used to perform the analysis through separate numerical codes implemented as stated in the methodology section. The results of the limit analysis have shown that the slope is expected to be unstable considering the effect of the increase in strength of material with a depth of slope.

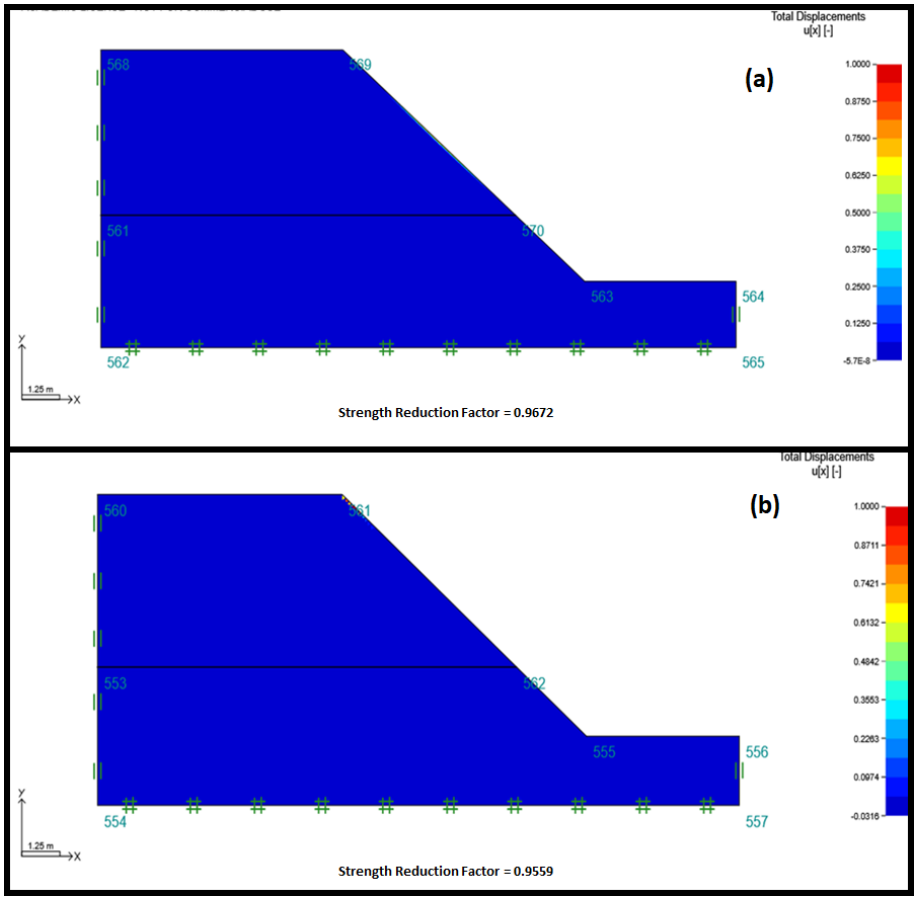

Figure 4.9. Predicted stability number using limit analysis method of strength reduction factor in dense sand (a) the SRF of the upper bound solutions of limit analysis (b) the SRF of the lower bound solutions of the limit analysis.

Furthermore, the lower bound solution estimated the SRF of 0.9559 while the upper bound solution was about 0.9672 SRF. On the other hand, the limit equilibrium method solutions ranged from 0.994 FoS to 1.085 FoS. For all the cases considered (see Figures 4.9 and 4.11) it has been denoted that the exact solutions are bracketed within 8 to 17% of error accuracy. In this case, the Limit Equilibrium method produces two scenarios wherein Janbu Simplified classifies the slope as unstable and the solutions are closely related to the upper solutions. In another scenario the rest of the method classified the slope as stable, this implies that most of the LEMs have overestimated the stability of the slope.

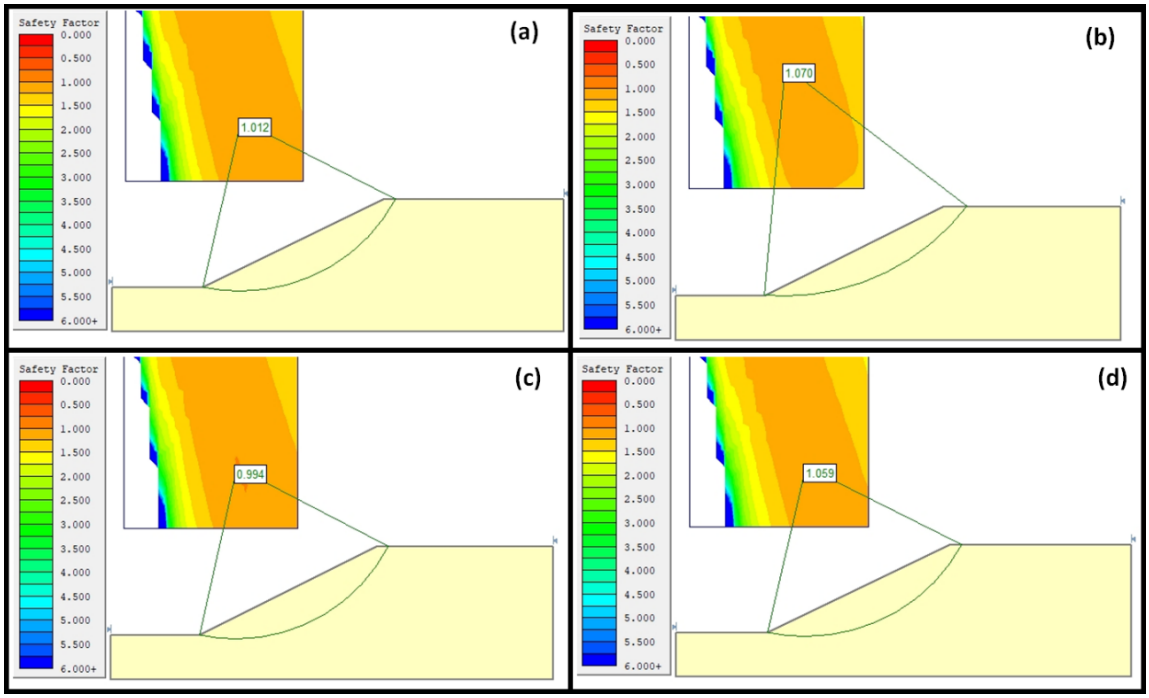

Figure 4.10. Limit Equilibrium stability number of dense sand slope produced using (a) Ordinary method, (b) Bishop simplified method (c) Janbu Simplified method (d) Janbu corrected Method.

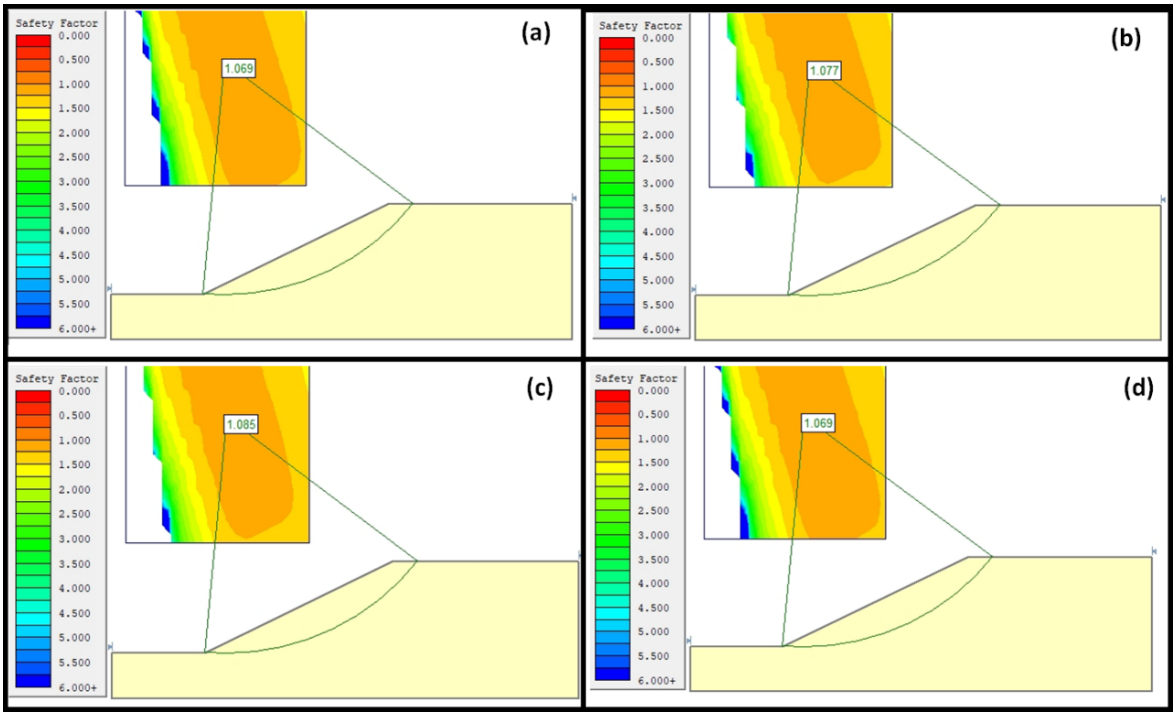

Figure 4.11. Limit Equilibrium stability number of dense sand slope produced using (a) Spencer method, (b) Corp of Engineering one (c) Corp of Engineering two (d) Morgenstern and Price Method.

4.3.1.4 Road Embankment slope with Soft clay

A soil slope with a slope angle of 45^0 was selected as a case study shown in Figures 4.12, 4.13 and 4.14. In the slope, soft clay with a friction angle of 18^0, the cohesion of 9 kPa and unit weight of 19 kN/m³ and other input parameters, as shown in Table 4.1 were taken into consideration. Both rigorous lower and upper bounds limit analysis and limit equilibrium methods were used to perform the analysis. The results of the limit analysis have shown that the slope is expected to be unstable using the rigorous lower and upper bound solutions with the SRF of 0.8257 and 0.8079 for upper and lower bounds respectively. Meanwhile, the limit equilibrium method solutions estimated a stable slope with FoS ranging from 1.155 to 1.274 (see the simulation results in Figures 4.12 to 4.14).

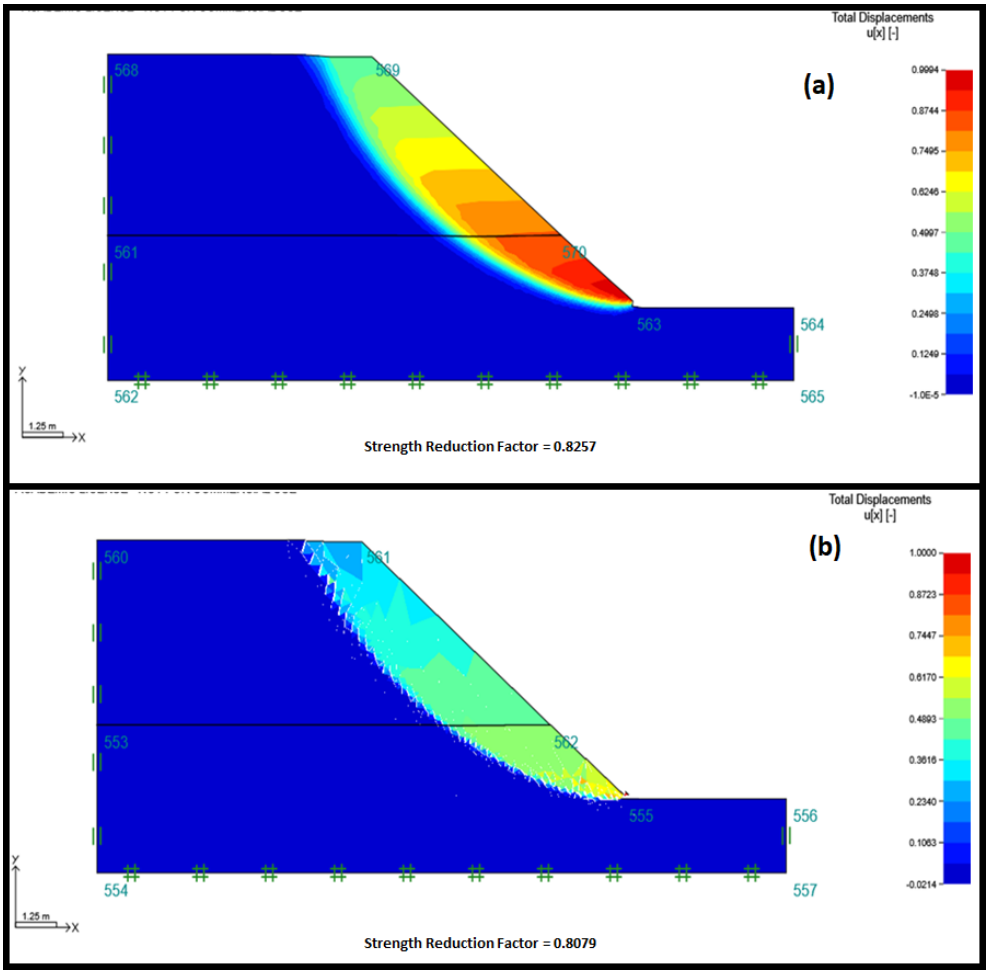

Figure 4.12. Predicted stability number using limit analysis method of strength reduction factor in soft clay (a) the SRF of the upper bound solutions of limit analysis (b) the SRF of the lower bound solutions of the limit analysis.

For all the cases considered (see Figures 4.12 to 4.14) it has been denoted that the exact solutions are bracketed within 40 to 54% of error accuracy. This implies among the limit equilibrium method, none of them was able to provide the exact solutions as compared to the rigorous lower or upper bound solutions. In this regard, all methods were found to overestimate the stability number of the slope. This implies that it is best not to use LEMs in soft clay soil slopes due to the high accuracy error produced by the methods.

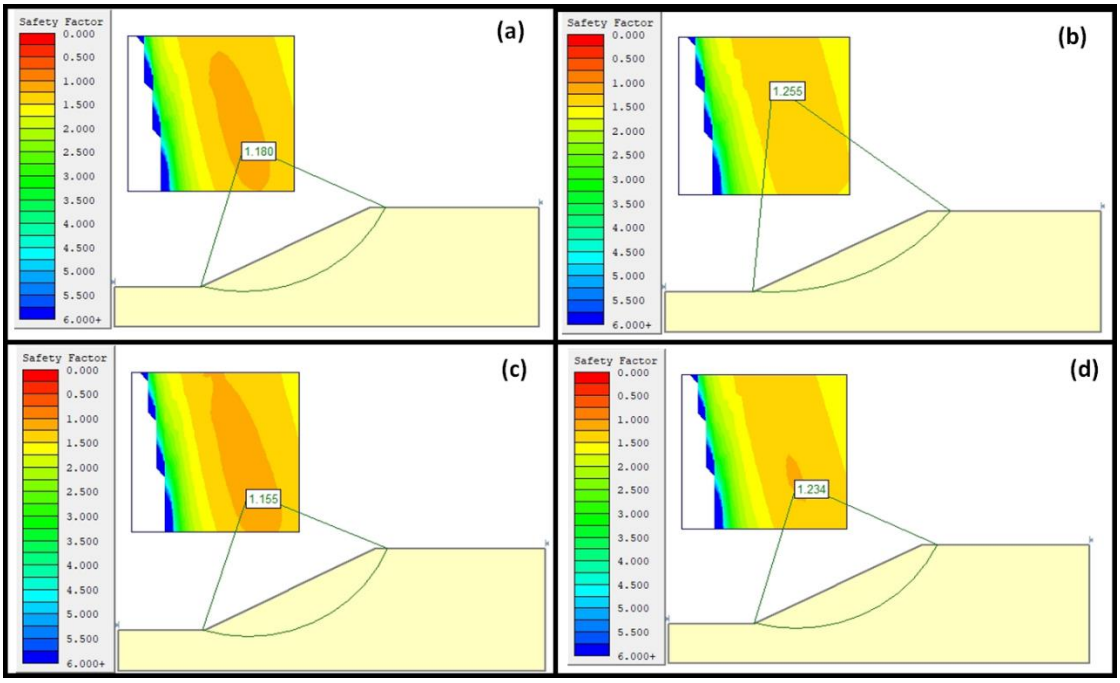

Figure 4.13. Limit Equilibrium stability number of soft clay slope produced using (a) Ordinary method, (b) Bishop simplified method (c) Janbu Simplified method (d) Janbu corrected method.

It was also observed that this material behaves differently from others, which demonstrates that though the slope may consist of soil, the properties of the soil matter in order to estimate the stability number accurately. One may argue that such abnormality observed could be due to the fact that the limit equilibrium formulations suffer from stress and deformation of the material (Renani and Martin, 2020), meanwhile, the failure surface is predefined by engineers, which results in predicting such a high stability number.

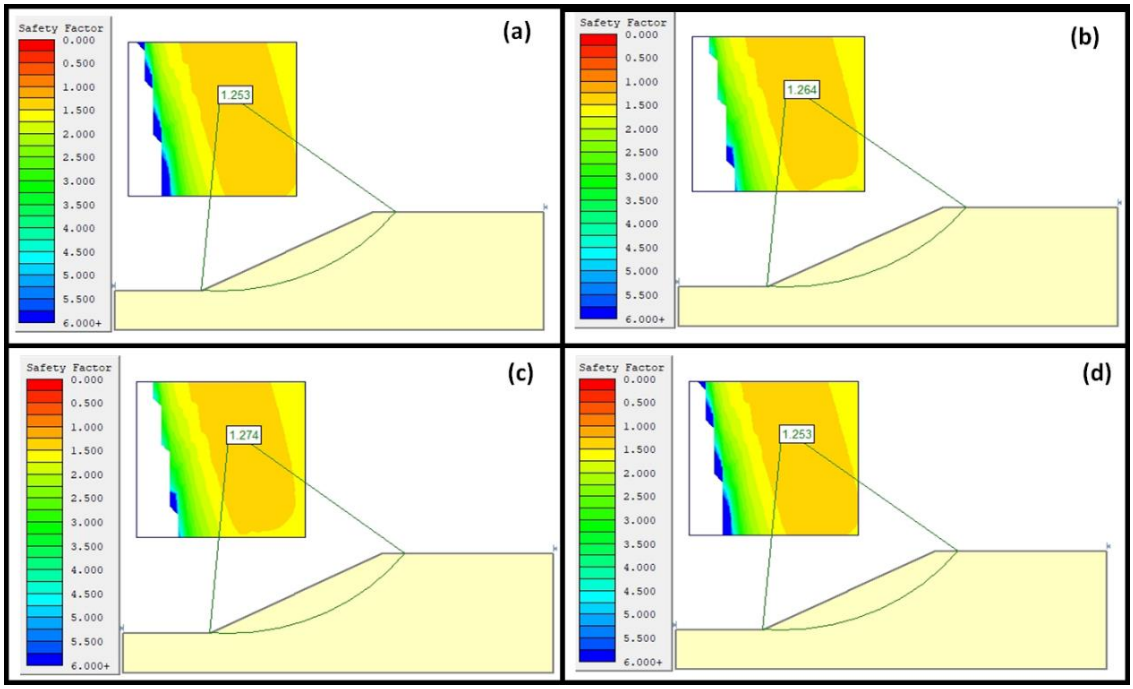

Figure 4.14. Limit Equilibrium stability number of soft clay slope produced using (a) Spencer method, (b) Corp of Engineering one (c) Corp of Engineering two (d) Morgenstern and Price Method.

4.3.1.5 Road Embankment slope with Firm Clay

A soil slope with a slope angle of 45^0 is selected as a case study shown in Figures 4.15 to4.17. In the slope, firm clay and with a friction angle of 13^0, the cohesion of 3 kPa and unit weight of 14 kN/m³ and other input parameters as shown in Table 4.1 were considered. Both rigorous lower and upper bounds limit analysis and limit equilibrium methods were used to perform the analysis through separate numerical codes implemented as stated in the methodology section. The results of the limit analysis have shown that the slope is expected to be unstable considering the effect of the increase in strength of material with a depth of slope. Furthermore, the lower bound solution estimated the SRF of 0.6588 while the upper bound solution was about 0.666 SRF. On the other hand, the limit equilibrium method solutions ranged from 1.350 to 1.497. For all the cases considered, (see Figures 4.15 to 4.17) it has been denoted that the exact solutions are bracketed within 17 to 29% of error accuracy. This implies unlike the limit

equilibrium method, none of them was able to provide the exact solutions as compared to the rigorous lower or upper bound solutions.

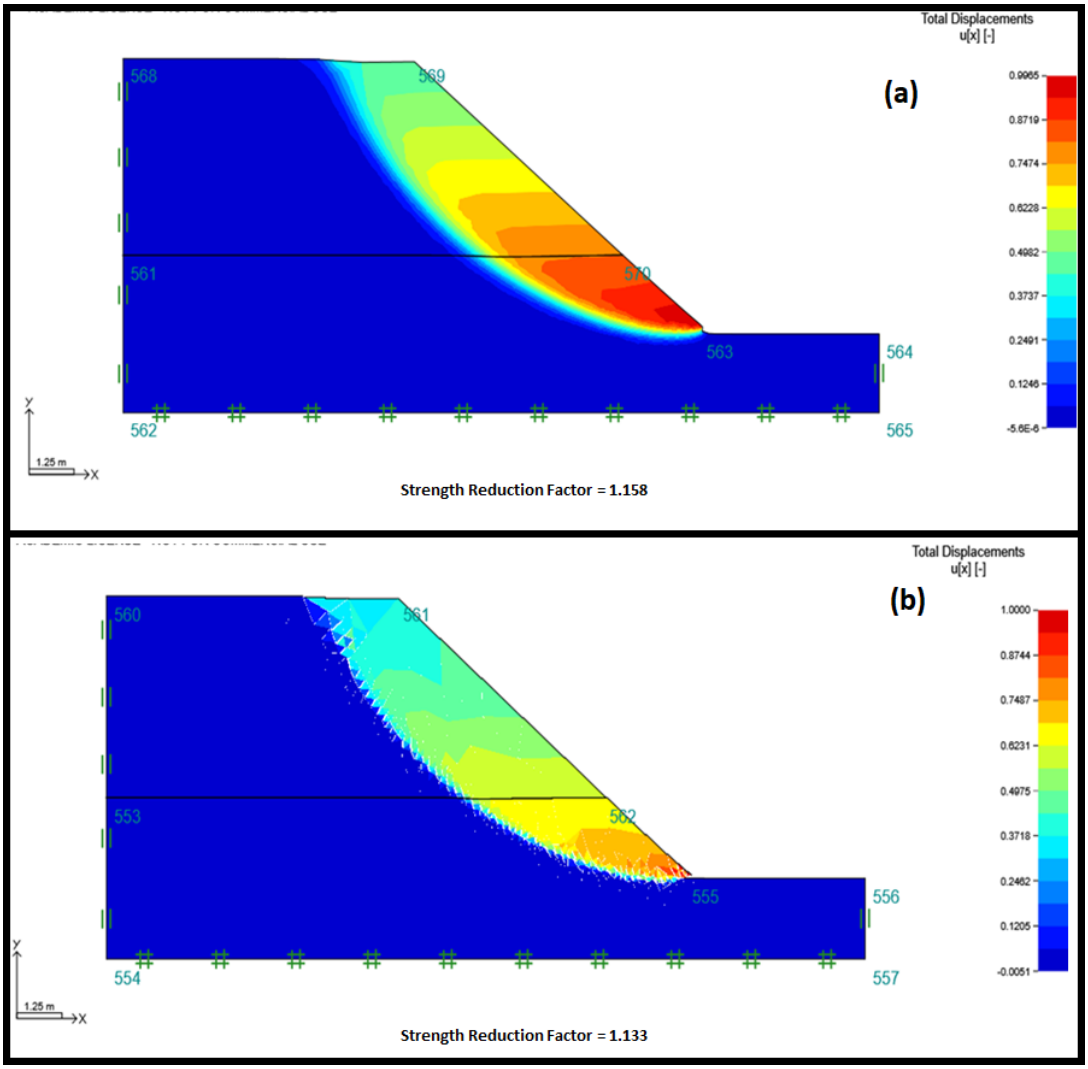

Figure 4.15. Predicted stability number using limit analysis method of strength reduction factor in firm clay (a) the SRF of the upper bound solutions of limit analysis (b) the SRF of the lower bound solutions of the limit analysis.

It was also observed that the result also shows that the Janbu Simplified limit equilibrium method had a more closely related solution to those of the upper bound solutions as compared to other LEMs. However, the method produces about a 17% error accuracy as compared to the benchmarking rigorous upper bound solutions of limit analysis. This implies that none of the limit equilibrium methods has an accuracy error below the

acceptable industry, therefore, LEMs are not recommended in analyzing soil slope with firm clay.

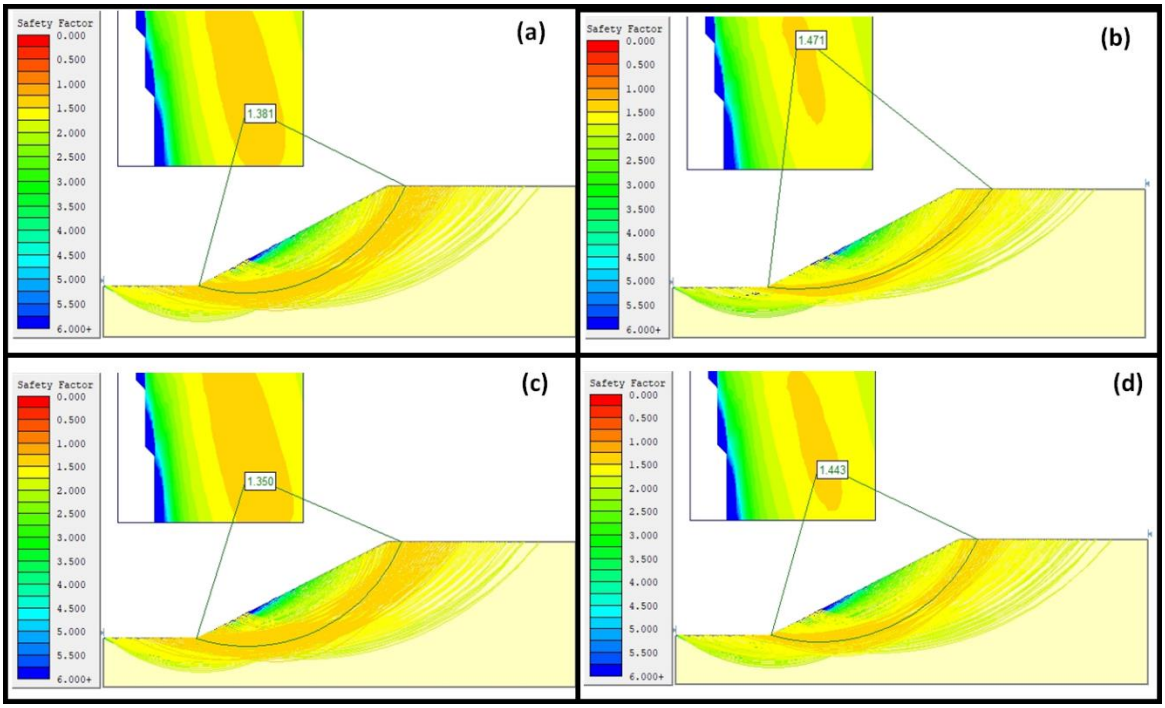

Figure 4.16. Limit Equilibrium stability number of firm clay slope produced using (a) Ordinary method, (b) Bishop simplified method (c) Janbu Simplified method (d) Janbu corrected method.

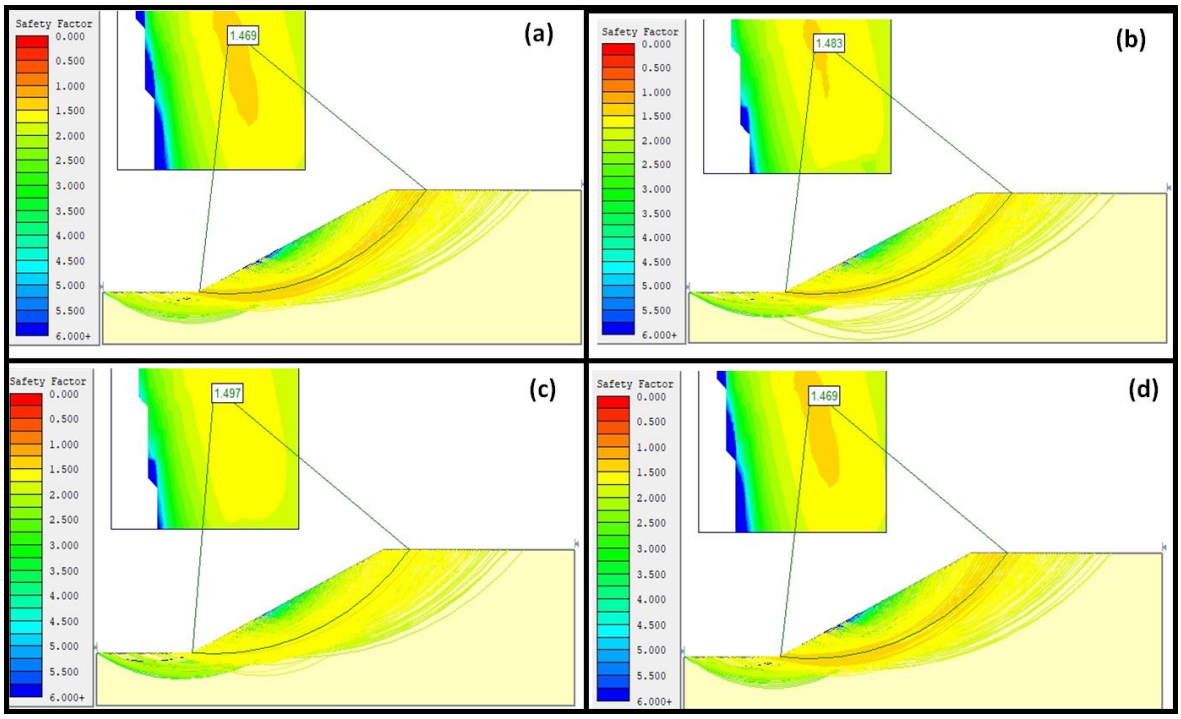

Figure 4.17. Limit Equilibrium stability number of firm clay slope produced using (a) Spencer method, (b) Corp of Engineering one (c) Corp of Engineering two (d) Morgenstern and Price Method.

4.3.1.6 Road Embankment slope with Stiff Clay

A soil slope with a slope angle of 45^0 is selected as well as demonstrated in Figures 4.18 to 4.20. In the slope, a stiff clay with a friction angle of 22^0, a cohesion of 20 kPa and unit weight of 21 kN/m³ and other input parameters as shown in Table 4.1 were taken into consideration. Both rigorous lower and upper bounds limit analysis and limit equilibrium methods were used to perform the analysis through separate numerical codes; (SLIDEs and Optum G2) were implemented. The limit analysis results have shown that the slope is expected to be stable. Furthermore, the lower bound solutions estimated the SRF at 1.655 while the upper bound solutions were about 1.689 SRF. While the limit equilibrium method solutions ranged from 1.717 FoS to 1.932 FoS. For all the cases considered, (see Figures 4.18 to 4.20), it has been denoted that the exact solutions are bracketed within 5 to 14% of error accuracy. This implies among the limit equilibrium method, none of them was able to provide the exact solutions as compared to the rigorous lower or upper bound

solutions, however, the LEM solutions were denoted to be closely related to those of the upper bound solutions.

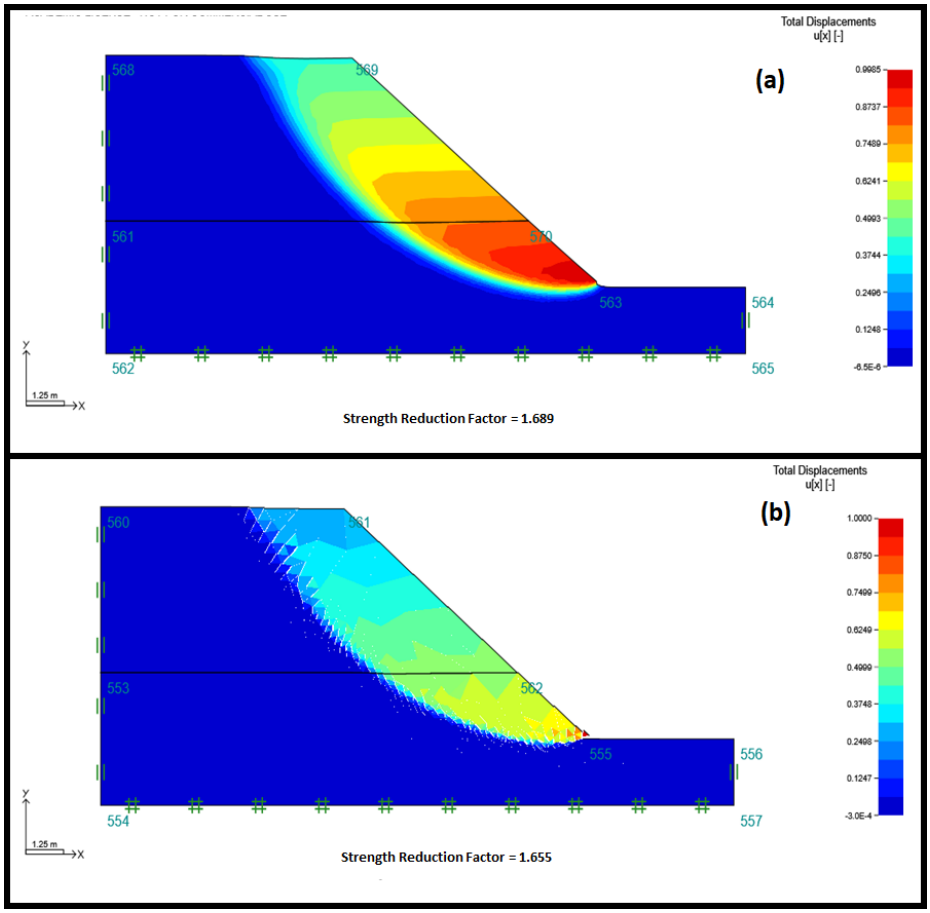

Figure 4.18. Predicted stability number using limit analysis method of strength reduction factor in stiff clay (a) the SRF of the upper bound solutions of limit analysis (b) the SRF of the lower bound solutions of the limit analysis.

It was observed that among other cases considered, limit equilibrium methods perform much better in stiff clay. In summary, the error accuracy produced by Janbu Simplified was about 2% which is almost the same as the exact solutions of the upper bound solutions. This implies that though LEMs are known to produce less accurate solutions, the method produces different accuracy errors based on the material being dealt with. In this study, one may deduce that almost all LEMs used for the study were within the required acceptable accuracy error of the industry. Furthermore, the Ordinary method was also found to be the second-best method in terms of producing low error accuracy;

as a result, Ordinary and Janbu Simplified can be recommended as the reasonable methods to use in order to acquire closely related solutions to those of upper bound solutions of limit analysis. On the other hand, the Corp Engineering Two method was still found to be the last method to produce closely related solutions to those of upper bounds, but their solutions were still less than 15%.

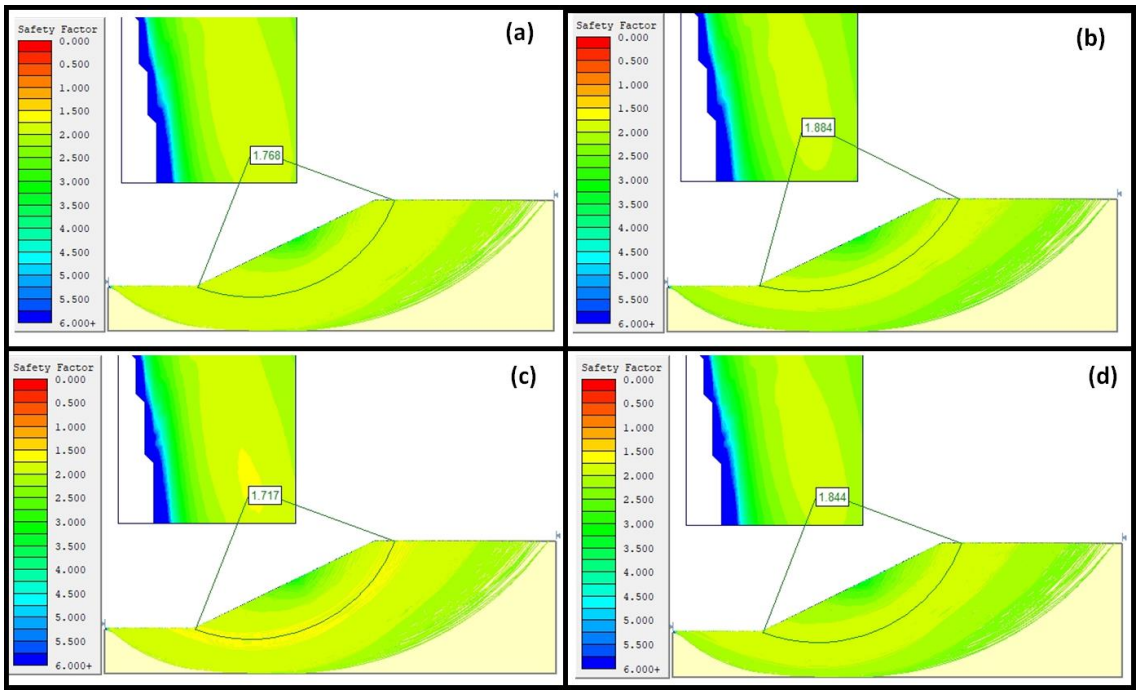

Figure 4.19. Limit Equilibrium stability number of stiff clay slope produced using (a) Ordinary method, (b) Bishop simplified method (c) Janbu Simplified method (d) Janbu corrected method.

These results bring a similar argument that it cannot be assumed that LEMs produce similar results though the solutions produced by the two methods are not exact. In simple terms, the results of this paper demonstrate some disagreement with previous studies such as those of Cheng et al. (2007) and Renani and Martin (2020), however, the disagreement lies along the lines of assuming that no exact solutions are similar without considering the error accuracy generated by very small differences in solutions. The behaviour of the material in terms of how they respond to each method may have been partially captured. Some of the studies that strived to capture the response of different soil material behaviour on the slope are those of Bjerrum (1954), Skemton (1964), Hettler

and Vardoulakis (1984), but still there is no specification of error accuracy of the LEMs. The section below is, therefore, intended to develop an accuracy classification chart of LEMs in predicting stability numbers based on the benchmarking discussed in this paper.

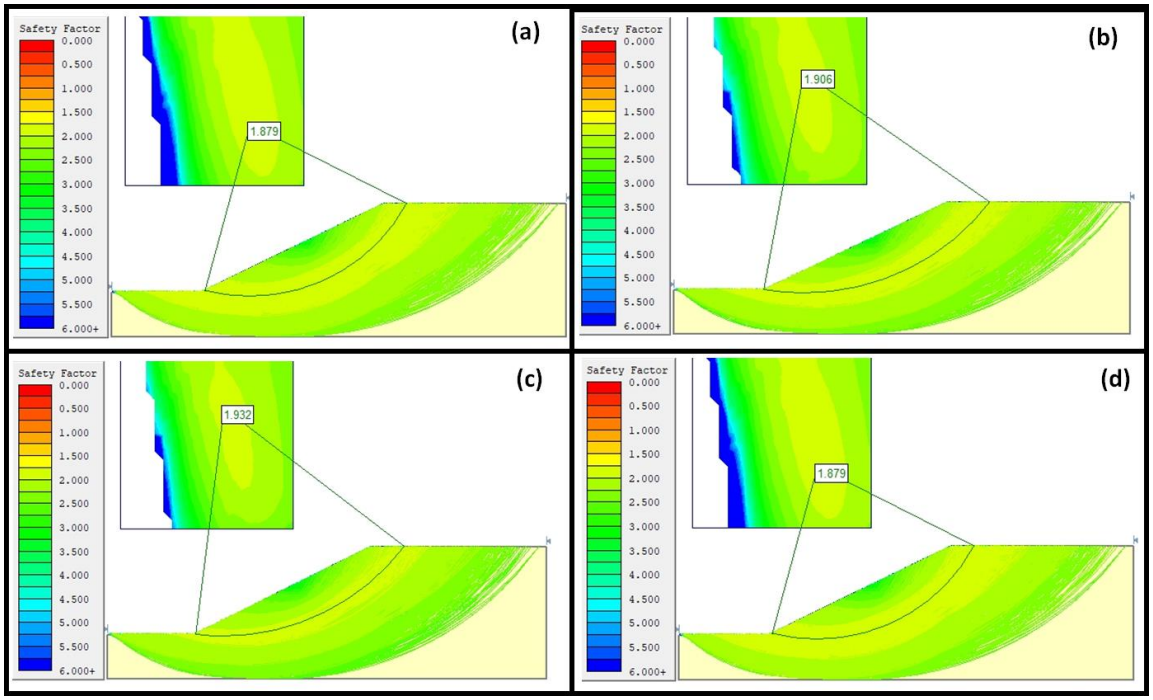

Figure 4.20. Limit Equilibrium stability number of stiff clay slope produced using (a) Spencer method, (b) Corp of Engineering one (c) Corp of Engineering two (d) Morgenstern and Price Method.

4.3.2 Accuracy Classification Chart of Limit Equilibrium Method in predicting the stability of the homogenous slope

For all the cases considered in the sections above, it has been observed that in almost all cases, Janbu's Simplified limit equilibrium solutions are in good agreement with the rigorous upper and lower bounds, but close to the limit analysis rigorous solutions of the upper bounds. In all cases, the limit equilibrium results were generally close to those of the upper bound solutions, while the lower bound solutions appeared to be underestimated compared to all the limit equilibrium solutions presented (see Figure 4.21).

In summary, the Janbu Simplified limit equilibrium method produces the most reasonable and accurate solutions for the stability of homogenous soil slopes whose strength increases with depth. Nevertheless, the Janbu Simplified limit equilibrium method was very accurate (1-7% of overestimated compared to the rigorous upper bound solutions) in a homogenous slope consisting of stiff clay, dense sand and medium sand. In fact, the Janbu Simplified method presented an accuracy error of about 1% when estimating the stability of the slope in stiff clay, these results imply that the method has the ability to produce similar or closely related results to those of the upper rigorous bound solutions of limit analysis. Furthermore, the reliability of the method (Janbu Simplified) was demonstrated when estimating about 2% accuracy error of slope stability in dense sand slopes; and 3% of accuracy error when estimating the stability of slopes with medium sand . It was also demonstrated that when estimating the stability of the slope with loose sand, the method produces a 7% error accuracy which is still below the acceptable error accuracy of 10%.

In other cases, the method was still denoted to be the most accurate as compared to other limit equilibrium methods, however, in firm clay, loose sand and soft clay, the predicted stability number was over the acceptable accuracy error percentage, in fact, it was more than 10%. Though the study focused on benchmarking the Limit Equilibrium solutions with the Limit Analysis solution since limit solutions are usually used to overcome the accuracy of predicting problems associated with the Limit Equilibrium solution, one may deduce the Janbu Simplified solutions in good agreement with the upper bound solution, although in soft clay, the method overestimates by about 40%. In the case of firm clay, the method is just after the acceptable accuracy error (10%) but less than 20%, these results can still be used in cases where rigorous upper and lower bound solutions are unavailable.

Fair enough, the Janbu Simplified method was not the only method found to produce stability numbers with very low error accuracy, the so-called ordinary limit equilibrium method was observed to produce very fair solutions or closely related to the rigorous upper bound solution, but the solutions produced were always greater than those of the Janbu Simplified limit equilibrium solutions by about 2-3%. Similar to the Janbu Simplified,

the Ordinary limit equilibrium method has produced stability numbers with acceptable error accuracy in almost all cases with the exception of the soft and firm clay. This implies that this method is not in good agreement with the upper bound solutions of limit analysis when predicting the stability of the homogenous slopes subjected to either soft clay or firm clay. Nevertheless, the method has shown its constant prediction throughout the case study given and it was always found to be the second-best in terms of stability number in relationship with the benchmark solutions produced by upper bound solutions.

On the other hand, the Corp of Engineer (2) limit equilibrium solutions were found to overestimate the stability of the homogenous slopes in all given case studies. The overestimation was be greater than the acceptable error accuracy in all cases. The accuracy error of this method was also found to be 10 to 13% more than those of Janbu Simplified limit equilibrium solutions. Similarly, the method was also denoted to overestimate the stability of the slope in soft clay though the overestimation was about 54%, this result provided a trend in all limit equilibrium solutions that soft clay cannot be accurately predicted despite the method being used in Limit Equilibrium.

Another interesting observation was that both Spencer limit equilibrium solutions and Gle/ Morgenstern Price limit equilibrium solutions were similar throughout. Similar results were observed in all cases, although the method provided reasonable accuracy in some cases and unreasonable accuracy in others.

As far as the limit equilibrium method is widely used by engineers and scientists in predicting the stability number of the slope, concern will always be voiced about the accuracy of these types of solutions. Therefore, a classification chart on accuracy predicting of the limit equilibrium method in homogenous slope is proposed (see Figure 4.22). The chart is based on the results discussed above, however, the chart is more concerned about the error accuracy of the limit equilibrium methods in different soil materials, considering the effect of the increase in material strength with depth. Furthermore, the chart can suggest the best limit equilibrium method to estimate the stability of the slope based on material properties. However, the chart is more applicable to those who prefer limit equilibrium solutions due to their simplicity.

The chart demonstrates that in the case of loose sand soil slope, Janbu Simplified and Ordinary methods are preferred to be used due to an acceptable error accuracy ranging between 6 and 10% compared to the upper bound solutions of limit analysis. Owing to that, the chart also denotes that the other six methods may be used, but the accuracy error will range between 11 and 20%, in which case such error accuracy is not recommended for industry use. In terms of medium sand soil slope, both Janbu Simplified and Ordinary are recommended due to their highly acceptable error accuracy which ranges from 1 to 5%, meanwhile, others can still be used with caution because of the present accuracy error above the acceptable stand. A similar situation has been observed in dense sand, though the Janbu Simplified method, is the most accurate method followed by the Ordinary method with error accuracy ranging from 6 to 10%. However, in the case of soft clay, none of the LEMs is recommended due to large error accuracy numbers ranging from 40 to 54%. In firm clay, no LEMs can be used within the acceptable accuracy error, while in stiff clay Janbu Simplifies and Ordinary methods are within the acceptable zone.

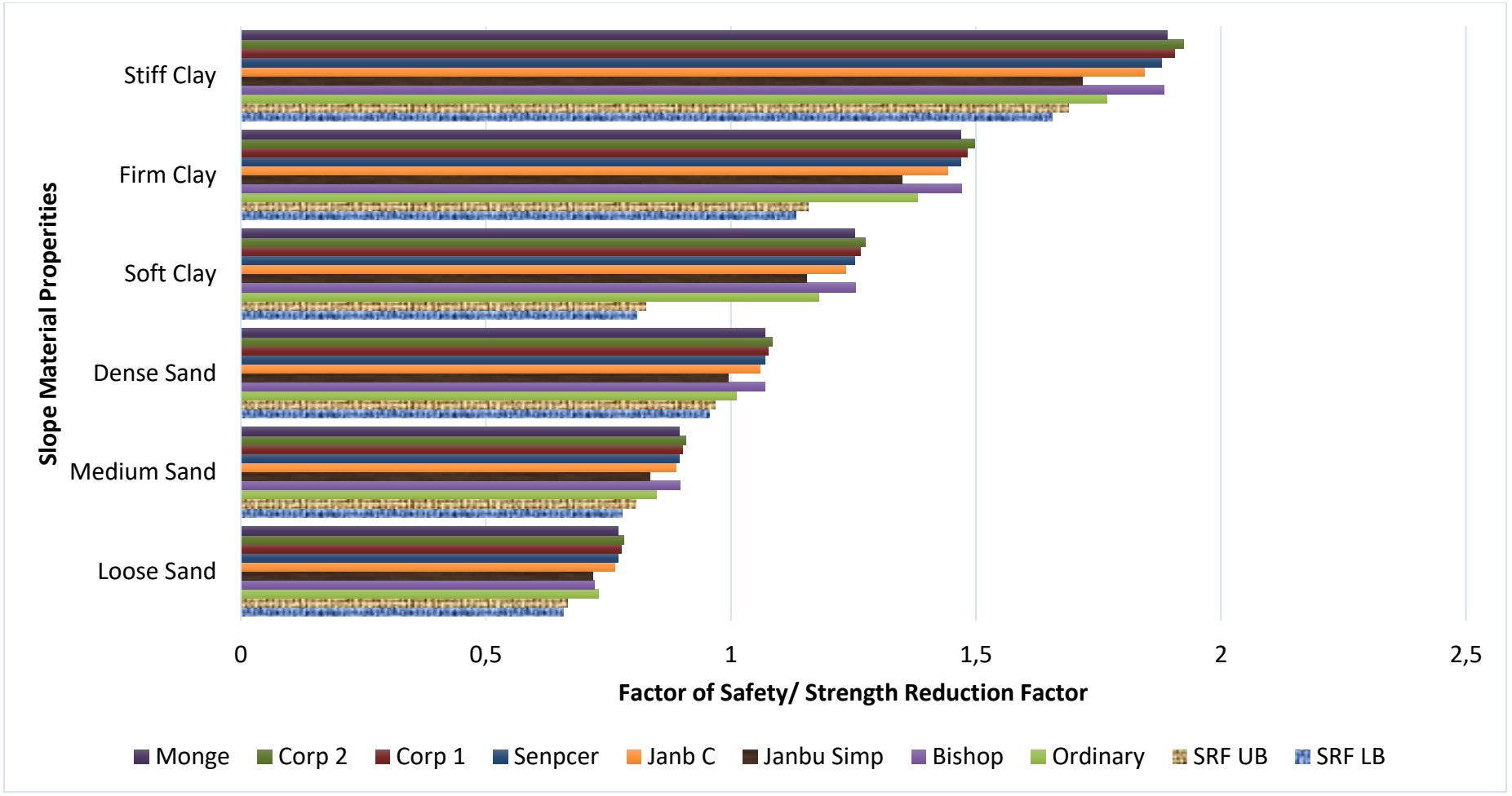

Figure 4.21. Distribution of Stability number (SRF and FoS) in various homogenous slope materials with Limit Equilibrium benchmarked with Limit Analysis.

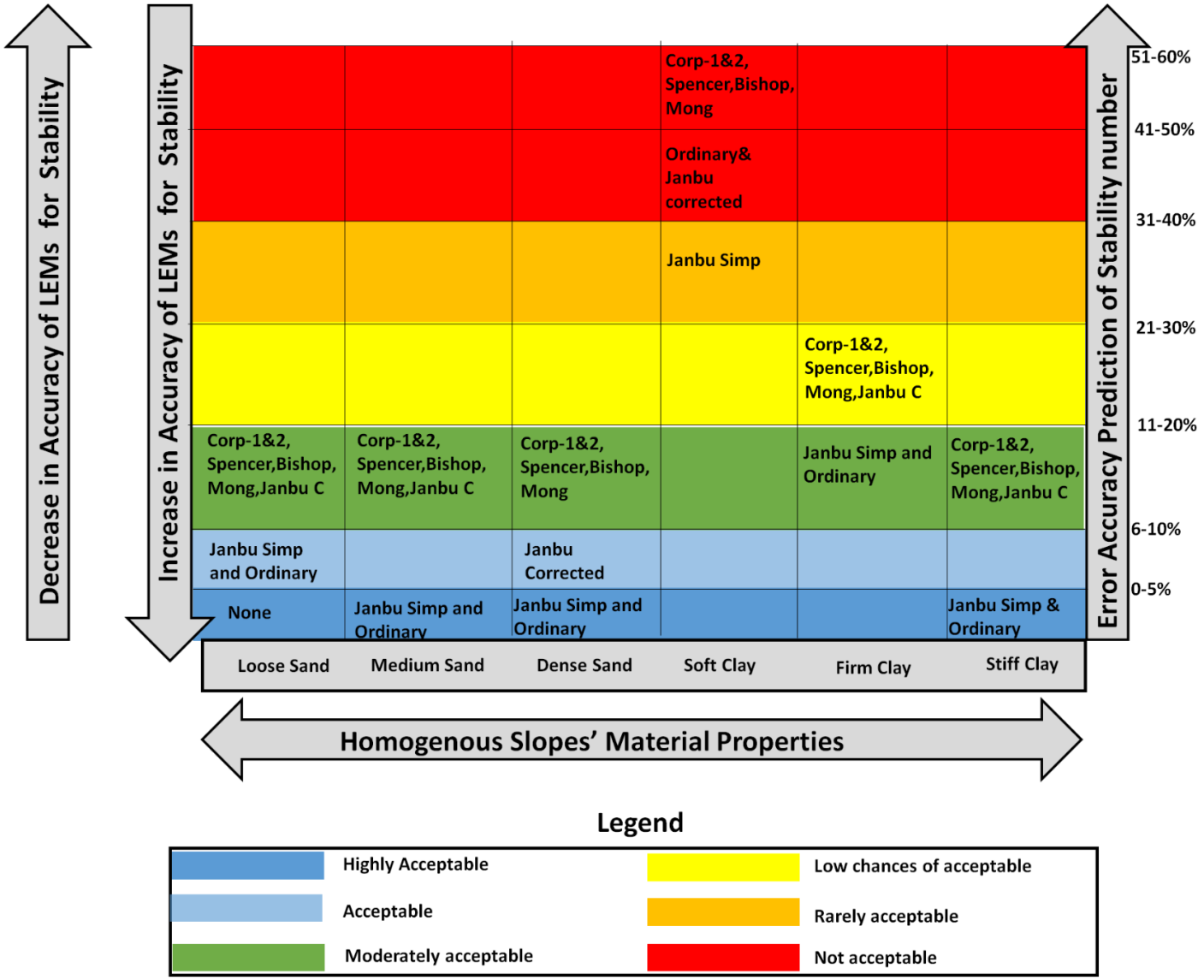

Figure 4.22. Classification chart of accurate prediction of LEMs on stability number

4.4. Concluding remarks

Based on the six case studies considered in this study, it was found that the exact stability solutions produced by Janbu Simplified and Ordinary Methods of limit equilibrium in most cases are bracketed within the 2-10% accuracy error range as compared to the rigorous upper bound solutions of the limit analysis. However, these conditions of lower accuracy error were noted in loose sand, medium sand, dense sand and stiff clay soil slope, with the consideration of the effect of the increase in strength of material with depth. It is, therefore, concluded that in cases of the above-mentioned soil slope material, Janbu Simplified and Ordinary methods of limit equilibrium are best to implement.

Furthermore, the detailed comparison of the bounding solutions with limit equilibrium methods has also demonstrated that the prediction of stability numbers by the Spencer and Morgenstern Price methods are similar throughout, though the methods were not producing closely related solutions to those of upper bound solutions. This implies that the use of these two methods simultaneously is not required since they give similar solutions.

It was also observed that the Corp Engineering number two method of limit equilibrium produced the highest accuracy error percentages throughout the case studies provided, however, its error accuracy was also found to differ from those of Janbu Simplified with a bracket within 10-12%. In simple terms, the method has been found to overestimate the stability number in all cases.

Though the focus was to benchmark the limit equilibrium solutions with the upper and lower bound solutions of limit analysis, all the lower bound solutions were found to be a bit smaller than those of limit equilibrium solutions in all cases. It is, therefore, concluded the lower bound solutions can be used for designing stable excavation, in order words the lower bound solutions are related more to the realistic stability number of the slope as stated by previous scholars such as Yu et al. (1988).

A simple accuracy classification chart was developed based on the results of the study. The chart shows various methods of LEMs and their accuracy error percentage per material or soil slope material. The chart is believed to be useful to engineers who prefer

to apply LEMs in classifying the stability of soil slope. Furthermore, the chart also provides room to explore other sophisticated methods that can improve the prediction of error accuracy of the LEMs in stability analysis.

Chapter 5 A new method for stability analysis of a multi-faulted rock slope using a ubiquitous joint model

The accuracy of the stability number simulated in a multiple-faulted slope has been one of the complex analyses in stability problems. The interaction of lithology with multiple geological features across one slope has been demonstrated to present a challenge in most road cut slopes, yet there is no simple method to follow that captures all sensitivity properties of the geological features. This chapter is intended to present a new method for stability analysis in a multi-faulted slope using the ubiquitous joint model. The investigation commences by analysing the sensitivity factors of fault properties and their effect on the safety factor of the slope, in which fault geometry, thickness, shear strength properties, mesh densities and change in joint orientation were evaluated. Therefore, a new method that strives to capture all these sensitivity factors into the analysis was proposed. The method also captures the zone of influence generated by each fault, and each fault is treated separately. Lastly, an overall stability number of the slope can be determined. A practice example using a road rock slope cut along the highway in South Africa was used to demonstrate the application of the method. However, a comparison with the common practice was made and it was discovered that the current practice overestimates the stability of the slope due to the failure to capture all sensitivity factors surrounding the slope. It is maintained that the proposed method can reduce design challenges and reduce large failures along the slope in both mining and civil engineering constructions.

5.1 Introduction

The definition of road embankments instability or slope instability has been stressed by various authors such as Varnes (1978), Hoek and Bray (1981), and Irigaray et al. (2012). Nevertheless, the common agreement among the definitions is to state that slope instability is the detachment of the rock mass or soil mass from a slope cut/road cut or

steep slope which has no shear displacement occurring, and the falling rock mass or soil mass descends most of its distance through the air. Similarly, Guzzetti et al. (2004) and Hasanipanah et al. (2016) supported the definition by further outlining that slope instability can be a form of rockfall or soil mass that falls or slides along a vertical cliff proceeding downslope by bouncing, flying, or sliding. Lastly, these events can occur rapidly or slowly depending on the triggering factor within the solid mass, but in most cases, the slope instability usually presents a rapid moving of solid material along road slopes.

According to this definition, slope instability is the rapid movement of solid material of the slope that poses a severe hazard to the roads and surrounding environment (Guzzetti et al., 2004; Calamak and Yanmaz, 2014; Gordan et. al., 2015). Therefore, the safety of the slope or stability of the road cuts is important, as a result, the stability of the slope or road cuts is continuously assessed by the determination of the so-called factor of safety.

The originator of some of these concepts (e.g., FoS), are acknowledged for their contribution, however, Mah and Wyllie (2005) concurred that the concept of FoS can be summarized as “how much stronger the system is than required”. FoS is more concerned about how stable the slope is as compared to the required stability standard of the slope. Though the stability of the slope is generally controlled by internal factors (mechanical properties of the solid material (rocks and soil) and the surrounding environment where the slope is external factors also play an important role in terms of the stability of the slope. One may argue that the recent concept of FoS has deformed a bit compared to the previous concept of FoS in which the concept revolves around the actual conditions of the slope and compare it with expected conditions to cause instability or accident. Authors such as Li et al. (2013) scrutinized the previous and recent concepts and discovered that the two concepts are almost similar though the recent one has specific value when comparing the conditions. Therefore, these two approaches are closely related and as such, they should complement each other rather than compete.

Owing to the previous discussion, the precise analysis of the slope stability is considered an important task in construction and various civil engineering structures such as highways, dams, and open pits (Yilmaz, 2009; Samui and Kothari, 2011; Erzin and Cetin, 2013; Jahed Armaghani et. al., 2016). Therefore, the ratio of shear strength to driving

stress generated due to gravitational force along the weak plane or failure plane is then considered a factor of safety. In terms of evaluation FoS <1 and FoS>1 signify the slope to be unstable and imminent stable respectively and FoS more than 1.5 is considered stable (Hoek and Bray, 1981; Davis et al., 1993; Helmstetter et al., 2004; Wang et al., 2005; De Blasio, 2010). Several key parameters are used in performing the slope stability evaluations and these parameters are grouped into internal and external factors. In the field of slope instability, a clear distinction between these factors (internal and external factors) influencing slope stability has been documented by several scholars (Hoek and Bray, 1981; Raghuvanshi, 2017).

However, despite knowing all these factors, the stability assessment of a multi-faulted rock slope has been a concern to many scholars (Azarfar et al., 2018). Due to the complexity of the situation, no simple method has been developed to carefully analyze the stability of the multi-faulted slope. Therefore, the main objective of this paper is to present a reliable and simple method for analysing the stability of the multi-faulted slope. Further, the objectives are to conduct sensitivity analysis in association with faults properties and be able to classify the most important factors to filter when analysing multi-faulted slopes using numerical simulation. A practical case study of a highway road cut-slope located in Limpopo Province, South Africa within the Rooiberg group geological terrain was used. The road cut-slope comprises of multi-faults (planar and undulating planar faults) with shale as a country-rock and dolerite dyke intrusions. Both field observations and numerical simulation were used to establish the objectives of the study. In terms of the modelling, the sensitivity analysis factors such as fault geometry, fault thickness, strength properties and mesh densities were evaluated with different ubiquitous joint models.

5.2 Research approach

The method followed in this study is divided into four sections, the first section outlines the model construction, in this regard, the model construction of the FLACslope is documented. The construction incorporates four stages.

(1) defining a project,

(2) building the slope conditions of the model,

(3) calculating the factor of safety of the model, and

(4) viewing the results.

The second section denotes the procedure followed when performing sensitivity analysis of the fault, this includes analysing the effect of fault geometry, thickness, shear strength material, mesh density, and various methods of the ubiquitous joint model on the FoS of the slope. The third section documents the material properties used for the model and it is followed by the last section of the method which gives a brief description of the practical example used to implement the developed reliability evaluation process of the multi-faulted slope.

In this study, the rock slope was modelled using elastic-plastic material which obeys the Mohr-Coulomb failure criterion. Furthermore, the geometry design was for a road cut slope since the example on the application of the simulation will be based on a road cut slope. Two types of faults were introduced to the model through the implementation of the ubiquitous model. The material properties used for initial simulations are shown in Table 5.1. One of the reasons why the ubiquitous joint model was chosen is that the model is closely related to the realistic situation of rock slopes in both mining and road construction. Owing to that, the ubiquitous joint model introduces fault material to the model block as a weak plane with its geometry (dip and dip direction). Following that, the Mohr-Coulomb model also considers the orientation of the fault, in which the criterion for the failure of such weakness consists of a composite Mohr-Coulomb envelope with tension cutoff. It is Qing's (2009) view that the Mohr-Coulomb model weaknesses or faults incorporate the non-associated flow rule for shear failure and an associated rule for tension failure. In summary, the ubiquitous joint model detects failure first; thereafter, plastic correction may be made.

Based on the sensitivity analysis of fault properties, a new method for stability analysis in multiple faulted slopes was developed. The method strived to capture all sensitivity parameters of the fault within the stability analysis.

The practical example of a highway road cut slope with multiple faults was used to evaluate the reliability of the developed method for the stability of a multi-faulted slope. A practical example is located within the N1 highway road in Limpopo Province, South Africa; a detailed description of the areas is documented in the results section.

Table 5.1. Material properties of the model

Categories	**Material properties**	**Case study material used**			
		Ubiquitous J1	Ubiquitous J1	Ubiquitous J1	Fault (Initial properties)
Mass-density	Density (kg/m^3)	2700.0	2700.0	2700.0	2500.0
Plastic properties	Cohesion (Pa)	200000.0	200000.0	200000.0	100000.0
	Tension (Pa)	0	0	0	0
Shear Strength properties	Friction angle (^{0})	45	45	45	0
	Dilation angle (^{0})	0	0	0	0
Joint properties	Joint angle (^{0})	10	45	135	N/A
	Cohesion (Pa)	10.0	1000.0	10000.0	N/A
	Tension (Pa)	0	0	0	N/A
	Friction angle (^{0})	40	40	40	N/A
	Dilation angle (^{0})	0	0	0	N/A

5.3 Results and discussion

The results of this study are divided into three sections, the first section investigates the sensitivity analysis of fault properties of the stability of the slope. The first section enables the second section to establish a new method on how a multi-faulted slope may be analyzed in terms of stability. The last section of results provides a practical example of to applying the proposed method compared with the common practice.

5.3.1 Sensitivity analysis of fault properties

Several scenarios that govern the sensitivity of the fault along the slope were modelled in order to identify their sensitivity and FoS calculation. The scenario commences with analyzing the effect of fault geometry on the stability of the slope, followed by the effect of fault thickness, shear strength properties of fault and mesh densities on the stability of the slope were fully investigated.

5.3.1.1 The geometry of the fault

The results from Figures 5.1, 5.2 and 5.3 show that both shallow and steep ubiquitous joint models exhibit high values of FoS when the shape or geometry of the fault changes from planar to an undulated planar fault. Meanwhile, the moderately steep ubiquitous joint model exhibits low values of FoS from planar to an undulated planar fault. These results indicate that all methods are very sensitive to fault irregularity in geometry. However, such results have been noted in previous studies such as those of Azarfar et al. (2018).

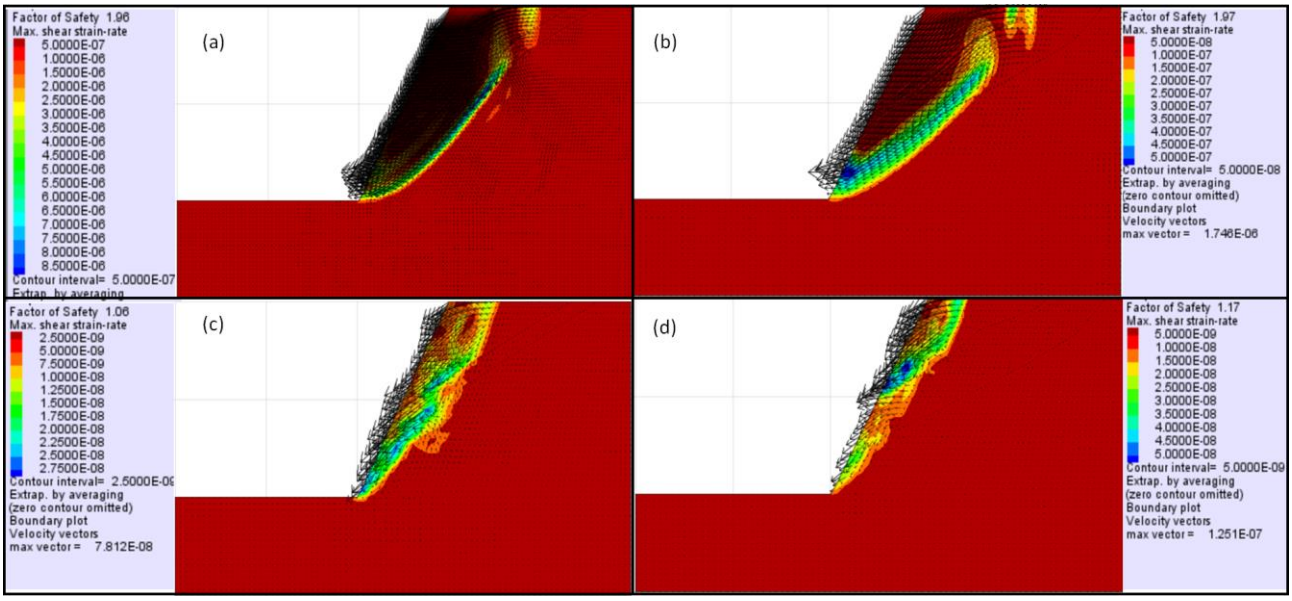

Figure 5.1. FoS of different geometry in (a) planar with shallow joint (b) undulated planar with shallow joint (c) planar with moderately steep joint (d) undulated planar with moderately steep joint

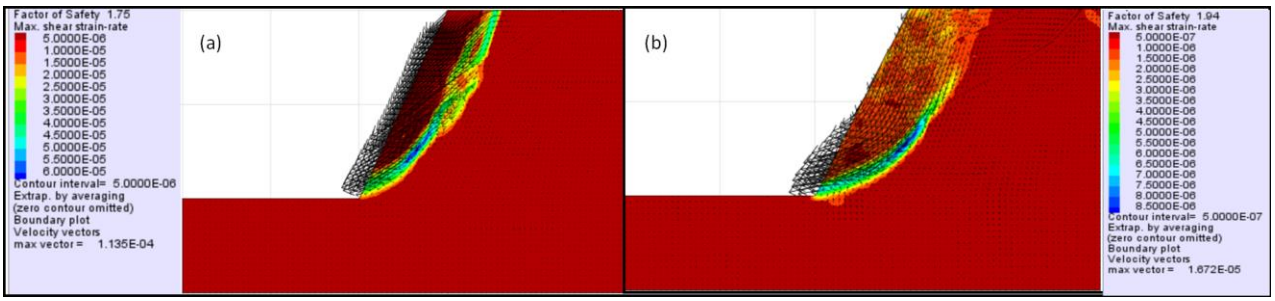

Figure 5.2. FoS of different geometry in (a) planar with steep joint and (b) undulated planar with steep joint

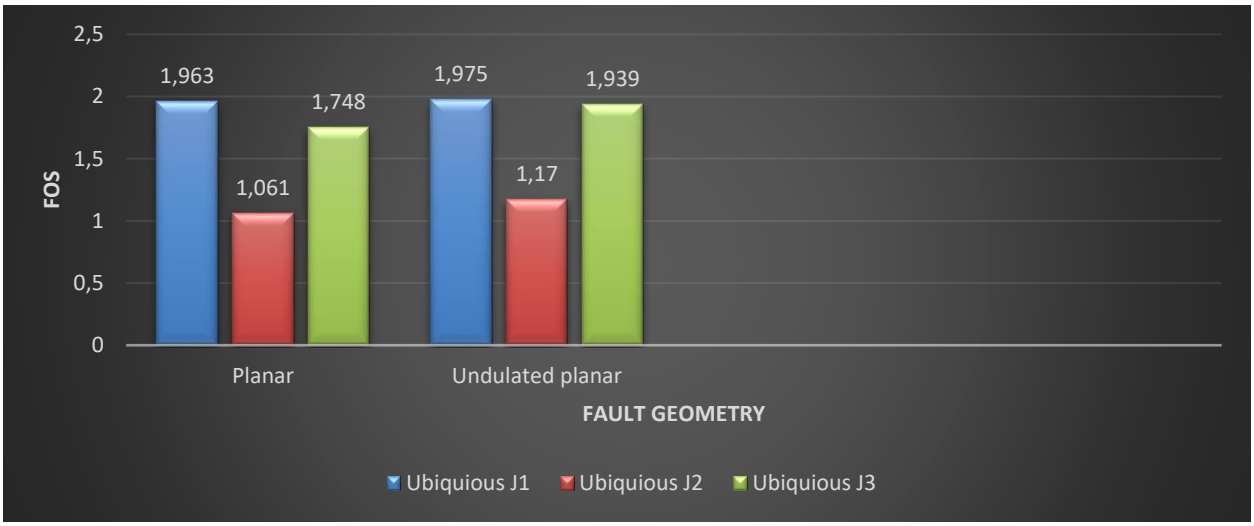

Figure 5.3. Distribution of FoS of different geometry in both planar undulated planar

5.3.1.2 Fault thickness

The results of the simulation have shown that various ubiquitous joint models are sensitive to fault thickness (see Figures 5.3 to 5.7). It was denoted that an increase in fault thickness from 2 to 8m has influenced the increase in FoS of the slope by approximately 10% to 17%. However, it has been noticed that shallow joints also influence the distribution of FoS in a negative distribution or a decrease in FoS by approximately 0.026%. Meanwhile, the moderately steep and steep joints have influenced the FoS with an increase of approximately 10% to 17 %. This distribution implies that the thickness of the fault is sensitive to the FoS of the slope, therefore, an accurate thickness of the fault is imperative in a model. It is documented in a study by Azarfar et al. (2018) that the number of zones along the faults thickness is the primary reason for variations in FoS results. Therefore, the fault thickness is sensitive to the FoS of the slope.

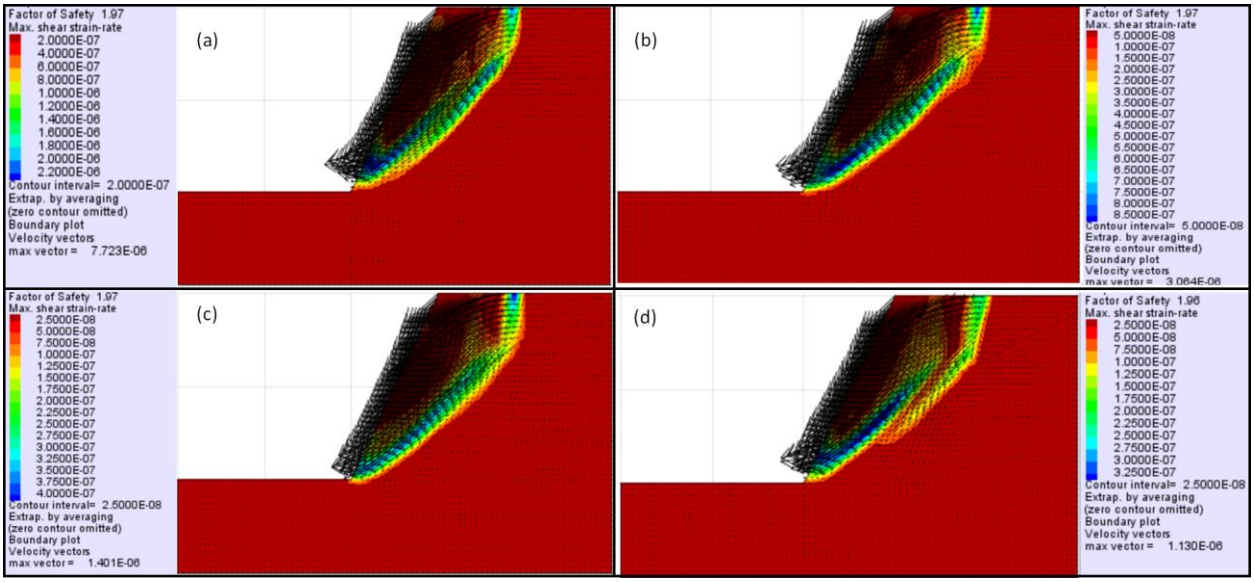

Figure 5.4. FoS for different fault thickness in a planar fault (a) 2m thick fault (b) 4m thick fault (c) 6m thick fault (d) 8m thick fault

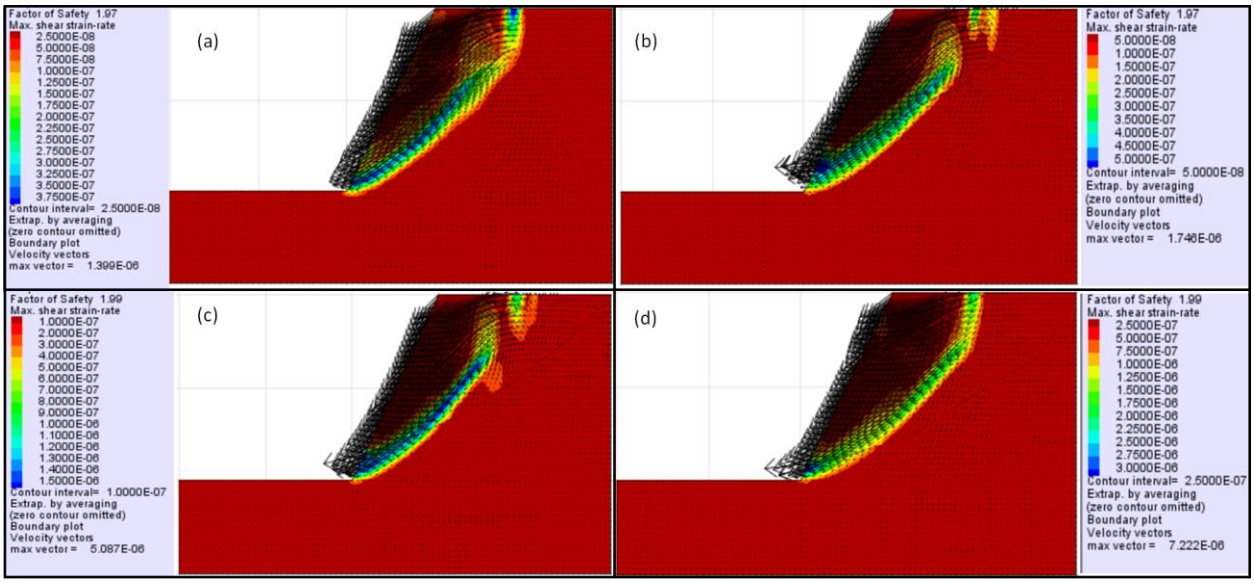

Figure 5.5. FoS for different fault thickness in an undulated planar fault (a) 2m thick fault (b) 4m thick fault (c) 6m thick fault (d) 8m thick fault

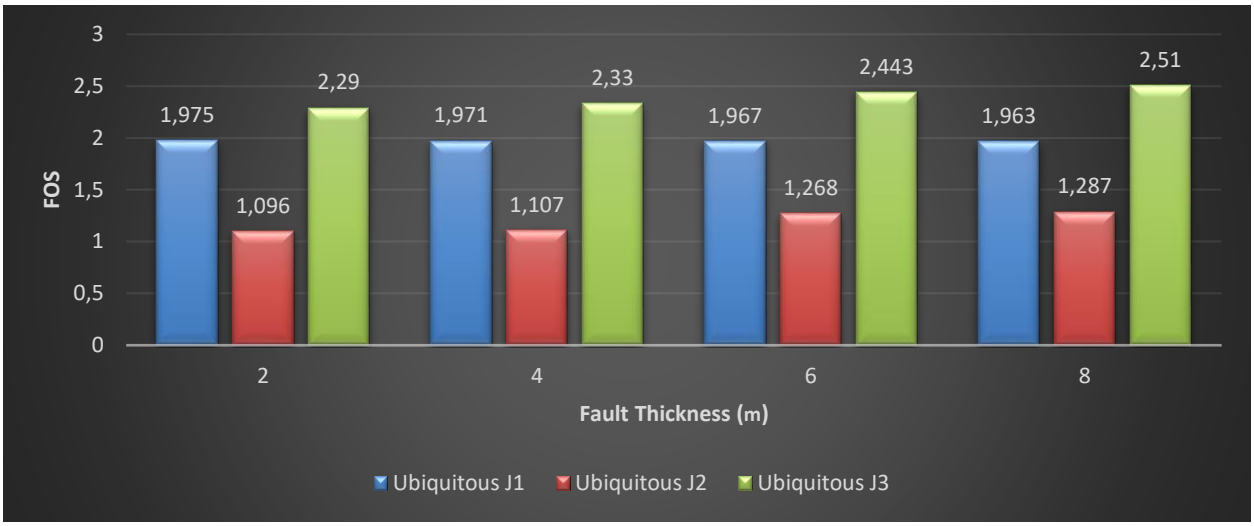

Figure 5.6. Distribution of FoS for different fault thickness in a planar fault with various ubiquitous joints (a) 2m thick fault (b) 4m thick fault (c) 6m thick fault (d) 8m thick fault

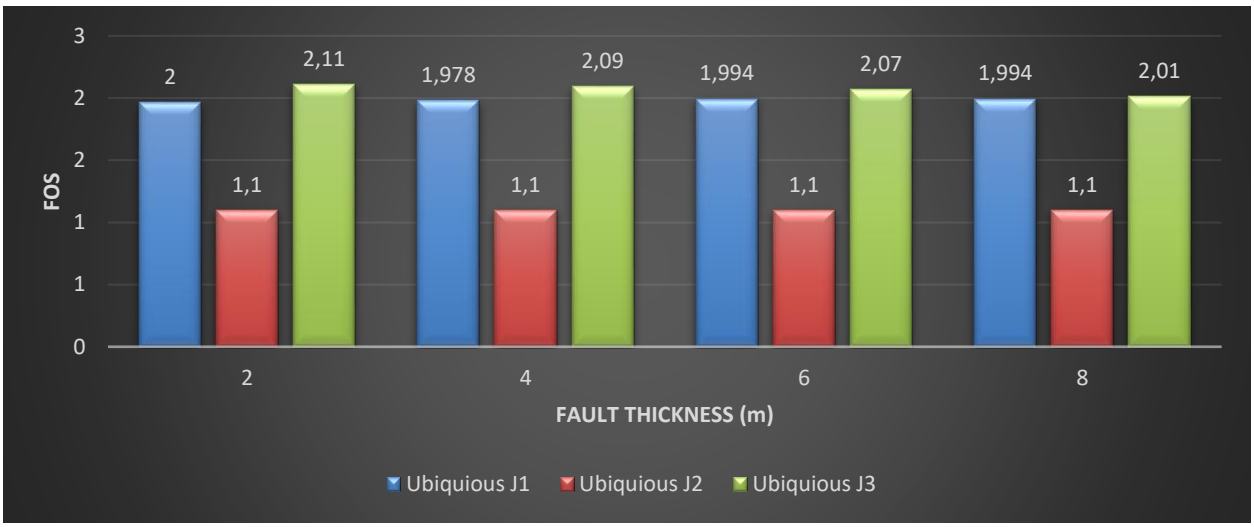

Figure 5.7. Distribution of FoS for different fault thickness in an undulated planar fault with various ubiquitous joints (a) 2m thick fault (b) 4m thick fault (c) 6m thick fault (d) 8m thick fault

5.3.1.3 Shear Strength properties of fault

The results of the modelling of the FoS values upon the different values of cohesion and friction angles are denoted in Figures 5.8 and 5.10 (for cohesion) and Figures 5.9 and 5.11 (for friction angle). The results show that the change in faults shear strength

properties influences the sensitivity of the slope in terms of FoS. It was observed that an increase in cohesion increase in FoS of the slope, similarly to friction angle. This implies that the shear faults strength must be taken care of when modelling a multi-faulted slope.

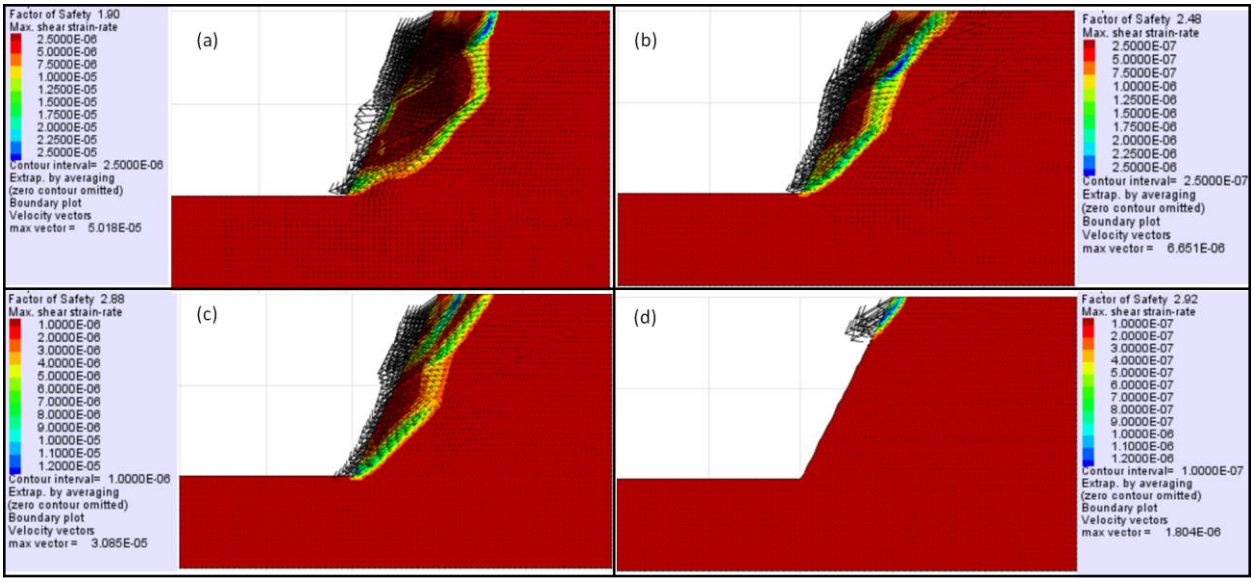

Figure 5.8. The FoS for different cohesion values in planar fault (a) 100000 Pa cohesion (b) 200000 Pa cohesion (c) 300000 Pa cohesion (d) 400000Pa cohesion

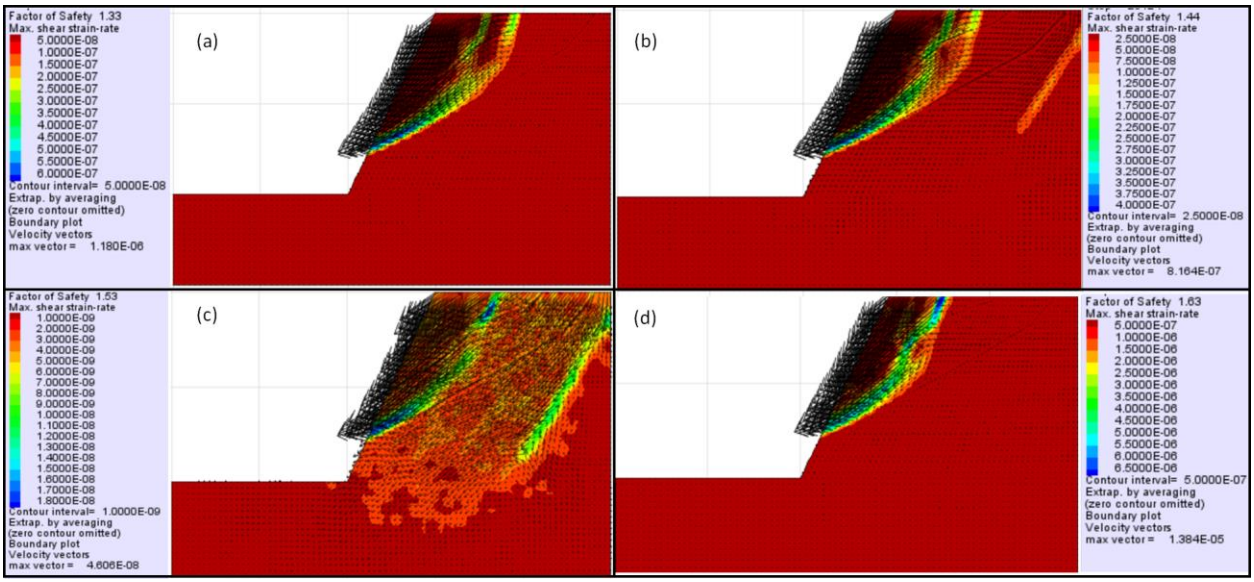

Figure 5.9. The FoS for different friction angle values in planar fault (a) 5 degrees (b) 10 degrees (c) 15 degrees (d) 20 degrees

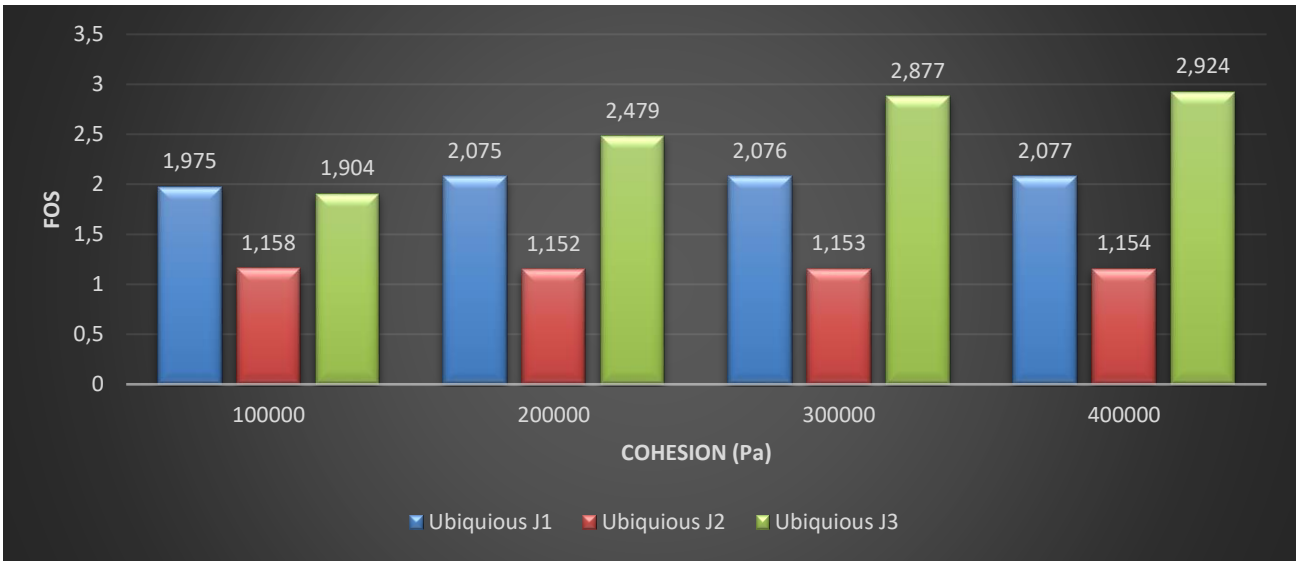

Figure 5.10. The distribution of FoS for different cohesion values in planar and undulated planar faults

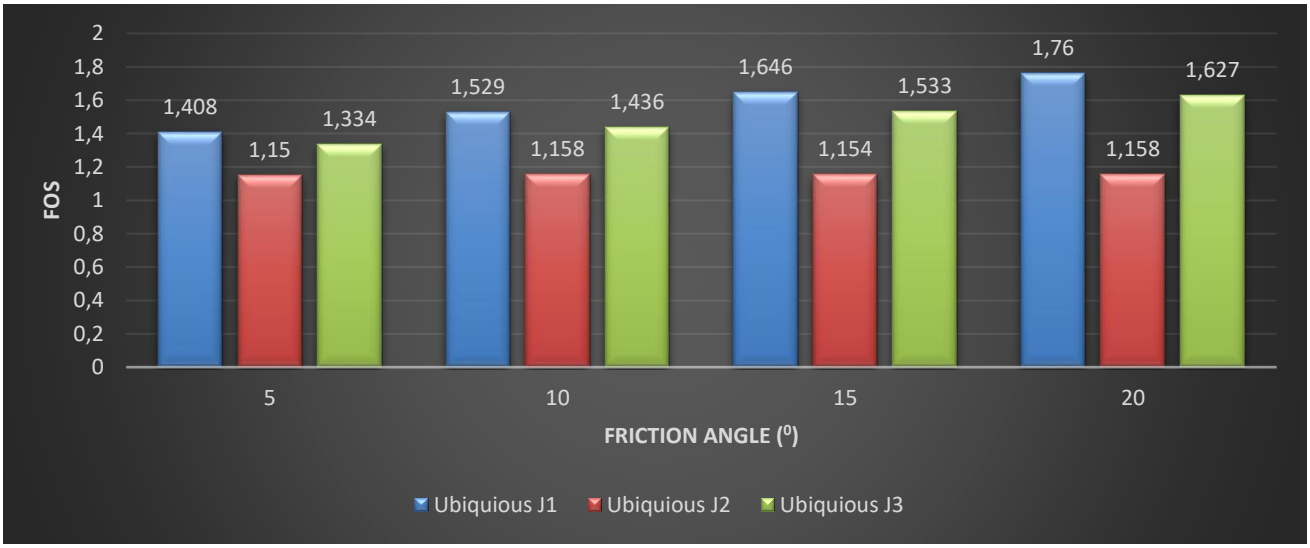

Figure 5.11. The distribution of FoS for different friction angle values in planar and undulated planar faults

5.3.1.4 Mesh density

The study results have shown that the mesh densities (coarse, medium and fine) influence the sensitivity of the stability number in both planar and undulated planarly. However, it has been noted that in shallow ubiquitous joints (10 degrees) the FoS of the

slope is much higher as compared to the moderately steep (45 degrees) and steep joints (153 degrees). This implies that though the mesh densities influence the estimated stability number of the slope in both planar and undulated planar faulted slopes, the orientation of the joints also played a major role in the estimated stability number (see Figures 5.12 and 5.13).

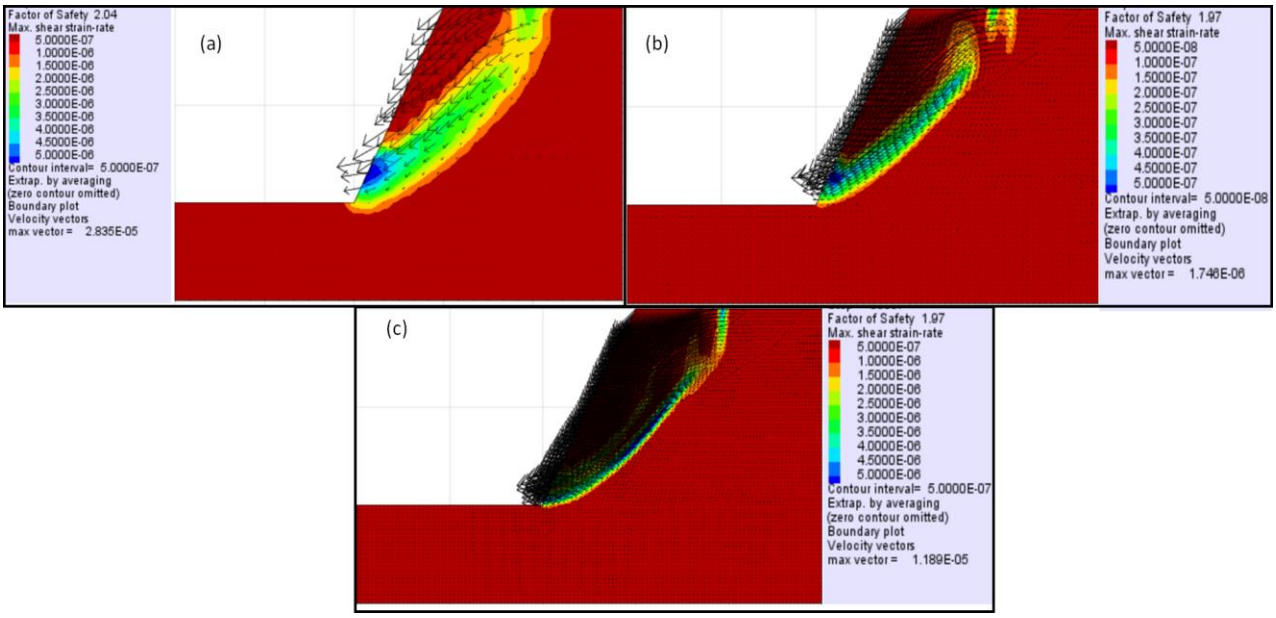

Figure 5.12. Simulated stability number in different mesh densities in planar faulted slope (a) course mesh (b) medium mesh (c) fine mesh.

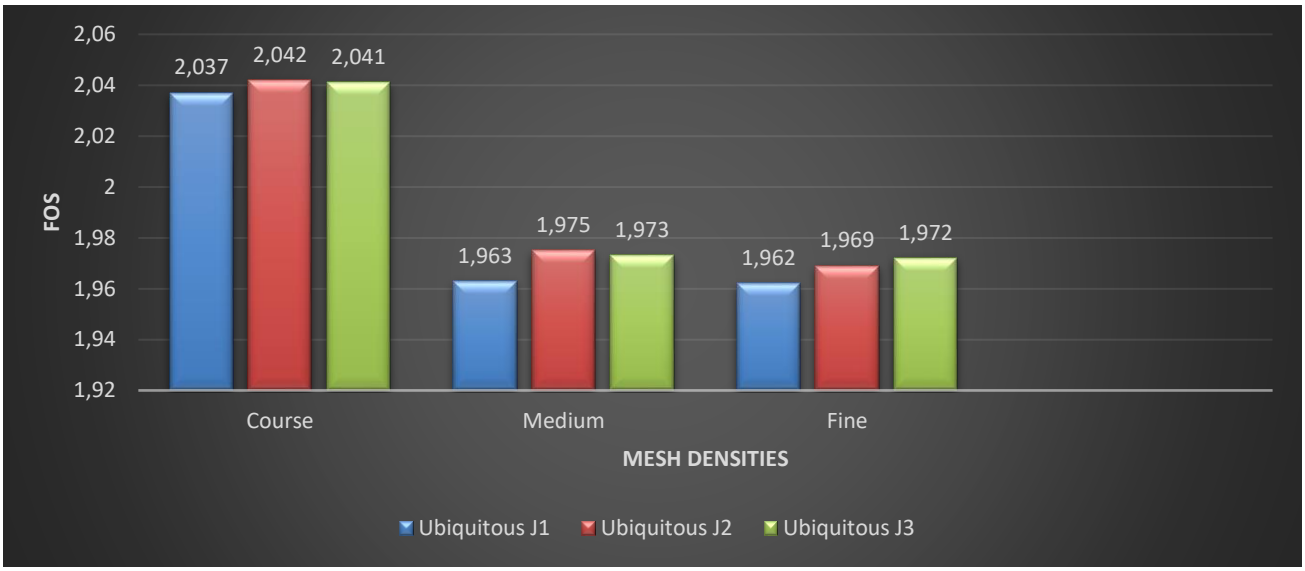

Figure 5.13. Distribution of FoS for different mesh densities in both planar and undulated planar faults with various ubiquitous joints

5.3.2. Developing a method of stability analysis in multi-faulted rock slope

The proposed new method of assessing slope stability in a multi-faulted rock slope does not exclude the previous method or the common practice. However, the new method tends to add a few aspects that have not been included in the common method. The new method introduces the so-called zone of influence principle. The concept of the zone of principle comes after the stability number of the slope has been determined. This concept then looks into the influence of each fault on the rock mass across the slope and it also looks into the influence of various ubiquitous joints on the stability of the slope. However, this method is described in terms of stages as documented below (see Figure 5.14).

5.3.2.1. Stage one: Geological background of the area

The first stage of stability analysis of a multi-faulted slope begins with the understanding of the geology of the study area (see Figure 5.14). This incorporates the structural mapping of the slope such as mapping the orientation of the outcrop, strike and dip of the geological structures (joints, faults and dykes). After all the structural details are known, the rock mass properties in terms of mechanical properties can be estimated or measured, these properties include rock strength and stress orientations among others.

The detailed geological information will allow us to commence with stability analysis using Hoek and Brown or Mohr coulomb criteria.

5.3.2.2 Stage two: Stability analysis criteria (Hoek and Brown, and Mohr-Coulomb)

Several parameters can easily be identified using the Hoek and Brown classification criteria (see Figure 5.14). For example, the geological strength index of the material can be identified based on field observation, this could range between 10 and 90 based on the composition of the rock mass. Furthermore, the uniaxial compressive strength (Sigci) can also be identified based on the field observations as well. Owing to that the so-called material factor (mi) and the disturbance factor (D) of the slope can also be estimated based on field observation. On the other hand, if all the above parameters are identified using Roclab or Rocdata, the Mohr-Coulomb parameters will be estimated automatically. After knowing all these parameters, a numerical simulation can commence.

5.3.2.3 Stage three: Numerical simulation

The numerical simulation can be done to estimate stability numbers in terms of the strength reduction factor (SRF) or safety factor (FoS). Both methods will require parameters documented in stage 2. For example, if the SRF method is chosen to estimate the stability number of the slope, the upper and lower bound solutions are normally used to determine the stability of the slope (see Figure 5.14). Meanwhile, if the FoS method is chosen Limit Equilibrium methods or other Finite Difference methods can be used to estimate the FoS. In our current practice after the identification of the stability number the stability assessment ended. This study, therefore, proposes that in a multi-faulted slope the common practice generalized the stability of the slope without looking into the influence of fault properties on the stability of the slope. Therefore, the study introduces a few steps to incorporate the influence of fault properties on the stability of the slope. A few stages are thereafter added to the common practice to incorporate the influence of fault properties based on the sensitivity analysis of fault properties documented in the above sections.

5.3.2.4 Stage four: Zone of influence principle

Based on the sensitivity analysis of the fault properties it has been denoted that fault geometry, thickness, shear strength properties, and joint orientation are very sensitive while influencing the stability of the slope surrounding the fault. It is therefore noted that the zone of influence surrounding the fault is important (see Figure 5.14). The study argues that the zone of influence per fault may be estimated based on the rule of thumb, wherein the zone of influence can be identified by half the width of the fault. Knowing the distance will enable one to estimate how far each fault can influence rock mass disintegration. For example, if the fault is 4m thick, the zone of influence is 2m from the fault boundaries toward the surrounding rock mass. However, it is assumed that stresses acting across the fault is very minimal and allow the deformation or disintegration of the rock mass to extend up to the half-width of the fault. However, in cases where two faults are closer to other, and their zones of influence overlap each other the mean of the FoS or SRF of the two faults is used as a FoS or SRF of that particular zone. Furthermore, it was also denoted that most multi-faulted slopes consist of various joint orientations, therefore, a mean of FoS or SRF with different joint orientations can be used to classify such slopes.

In order to create a meaningful procedure on how to incorporate the zone of influence in the stability analysis of a multi-faulted slope, it is proposed that each fault should be studied separately based on its thickness, orientation and shear strength properties. Therefore, if a slope has two faults which are planar and undulated planarly and the faults are surrounded by three types of ubiquitous joints, each fault should be studied separately. Three simulations of FoS or SRF with each joint orientation should be combined to acquire the mean FoS or SRF and the mean FoS can be considered as the stability number in the vicinity of the fault. Furthermore, the stability number identified per fault is effective to the maximum distance of the zone of influence which is based on the rule of thumb. Nevertheless, if the zone of influence among the faults overlaps each other, the two mean FoS or SRF are combined to get a mean FoS or SRF then the identified SRF will be used to classify the slope.

5.3.2.5 Stage five: Zoning stability of the multi-faulted slope

When the zones of influence fail to overlap, another concept called zoning of the slope is therefore implemented. This concept divides the slope into zones based on stability number. For example, if Fault A is planar and Fault B is undulated planar, Fault C is an undulated planar and fault D is planar and none of these faults has an overlap in terms of zone of influence (see Figure 5.14). The slope will therefore be divided into four zones with different stability numbers.

5.3.2.6 Stage six: Overall stability of the multi-faulted slope

If the slope has multiple stability numbers, an overall stability number has to be calculated based on the mean FoS or SRF per zone (see Figure 5.14). Therefore, the mean FoS or SRF will then represent the stability of the multi-faulted slope. However, in terms of the slope with an overlap zone of influence, stages 5 and 6 will not be incorporated into the calculation. This means that the SRF or FoS mean acquired using the stage four procedure will be used as an overall stability number of the slope.

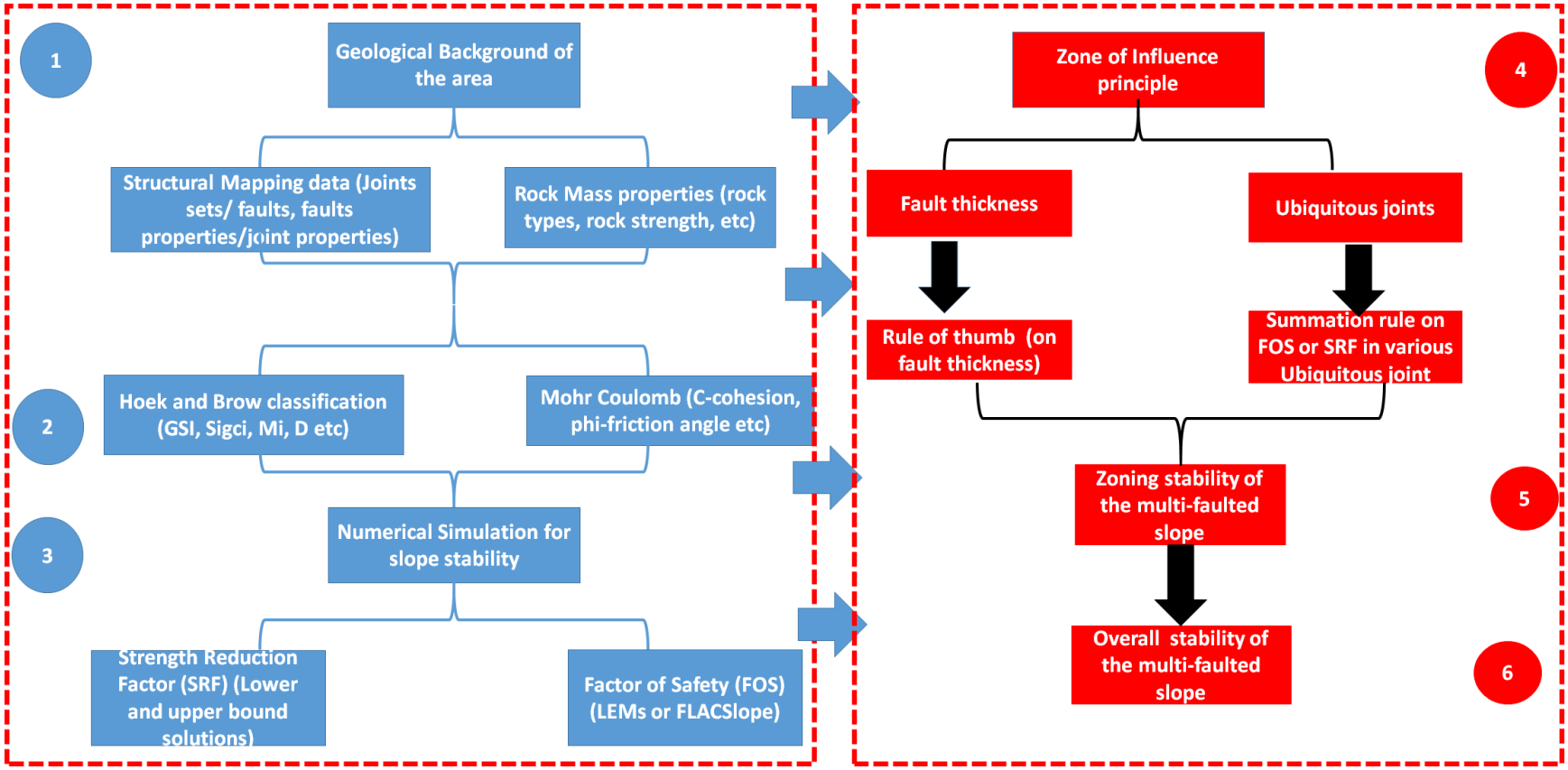

Figure 5.14. A new method for stability analysis in a multi-faulted rock-slope

5.3.3 Application of the method to a real case study

One practical example was used to demonstrate the application of the proposed method. The section commences with a geological description of the study area, followed by structural mapping and joint set description, estimation of mechanical properties of the rock mass and fault using field observation and a computer code called Rocdata. All of that led to the prediction of the stability number of the slope using common practice followed by the proposed method.

5.3.3.1 Descriptions of the study area

The case study used for this paper is located in South Africa in Limpopo province along the N1 national highway. Situated in the upper Rooiberg group, the area is dominated by shale (see Figure 5.15). It was observed that a highly fissile and brown shale with a purple hue was denoted along the slope (Figure 5.16). On previous studies, for example, Armitage et al. (2007) contend that the shale in the study area exhibits a very planar and well-defined lamination which is characterized by green colour fracture or joint surfaces with small ripples on some bedding, all those have been observed. Furthermore, it was also observed that the orientation of these bedding planes in both shales and Rooiberg lithologies are similar. It was also observed that the slope had been cut across by three faults, the first fault with quartz as an infill (Figure 24), while the rest are filled with dolerite dyke (Figure 5.17). The observed dolerite dykes appeared to be undeformed, medium to coarse-grained dolerite with minor supplied as pointed out by Armitage et al. (2007). The dolerite dykes appear to have an irregular shape across the slope where it is exposed. While the bedding strike is general along NE-SW, it varies between N-S and E-W, with gentle to moderate dips (Figure 25.18). The spread of dip angles between 7^{o} to 65^{o} has an uncertain cause in terms of reducing the stability of the slope.

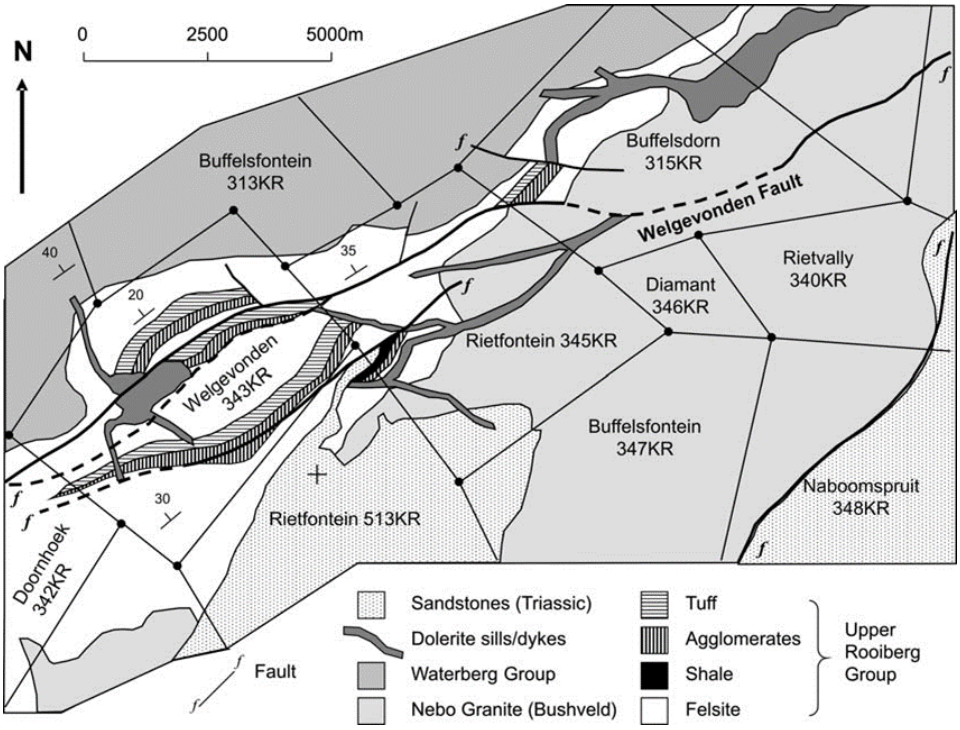

Figure 5.15. General Geology of the study area and the surrounding (Armitage et al., 2007)

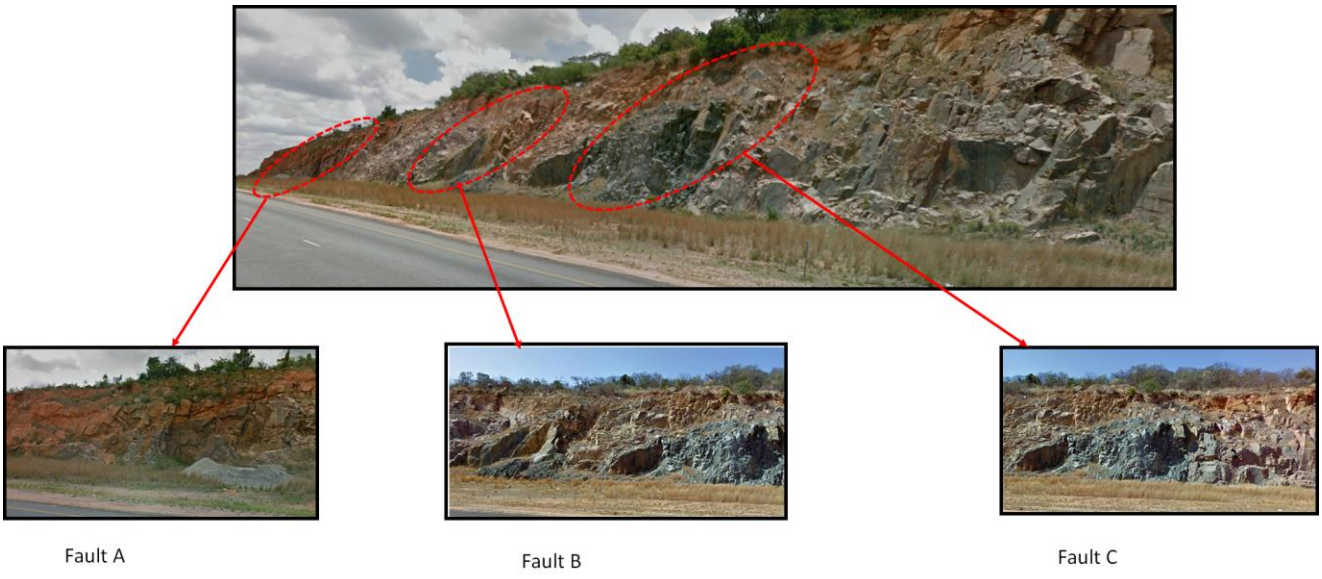

Figure 5.16. General overview of the selected slope with multiple faults

Figure 5.17. Planar fault cutting across shale outcrop

Figure 5.18. Undulated faults are filled with dolerite dykes that vary with thickness.

5.3.3.2 Structural mapping and joint set description

Structural mapping was also conducted across the slope in order to develop joint sets that are observed on the slope. To achieve this, the strike and dip of each joint on the slope were transferred to a Dips computer code to simulate the set, the fisher concertation distribution enables a group of the data into three sets. The first joint set was moderately shallow with 55 dips with a strike of 112, the second set was moderately steep with 67 dips and 223 strikes, and the last set was steep with 70 dips with 347 strikes. The sets

were, therefore, used to simulate the ubiquitous joint model with different fault geometry. Simulated joint sets are shown in Figure 5.19.

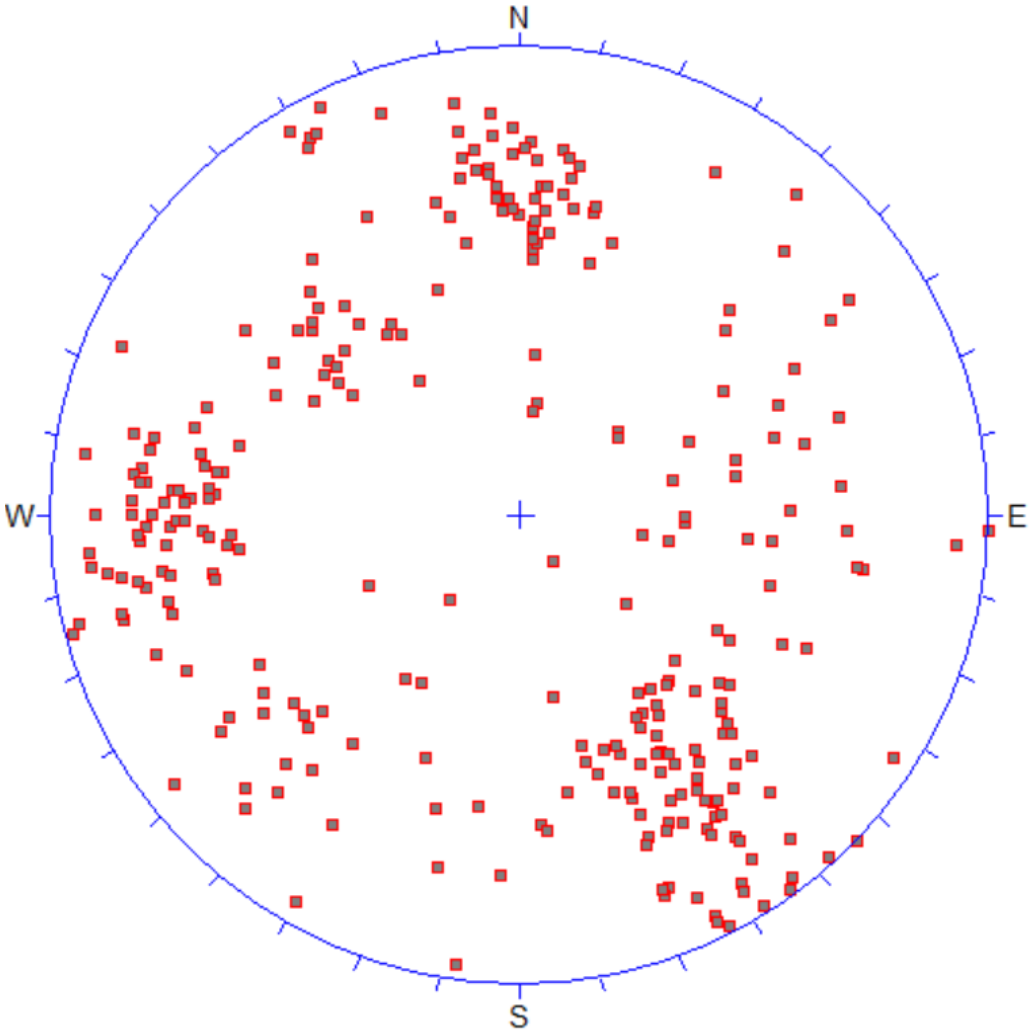

Figure 5.19. Structural mapping data (joints) distribution in terms of sterionet.

The data collected was distributed in an excel spreadsheet and exported to Digital Image Processing (DIPS) in order to generate sets. Seven sets were developed as documented in Table 5.2. However, the plots of the collected data are documented in Figure 5.20a while the contour plot along with the mean discontinuity planes and face plane for the selected study area is shown in Figure 5.20b.

Table 5.2. Joint sets developed based on mapping data

		Dip	Dip direction
1	Set (weighted)	14	246
2	Set (weighted)	71	328
3	Set (weighted)	74	90
4	Set (weighted)	85	153
5	Set (weighted)	69	180
6	Set (weighted)	55	132
7	Set (weighted)	70	51

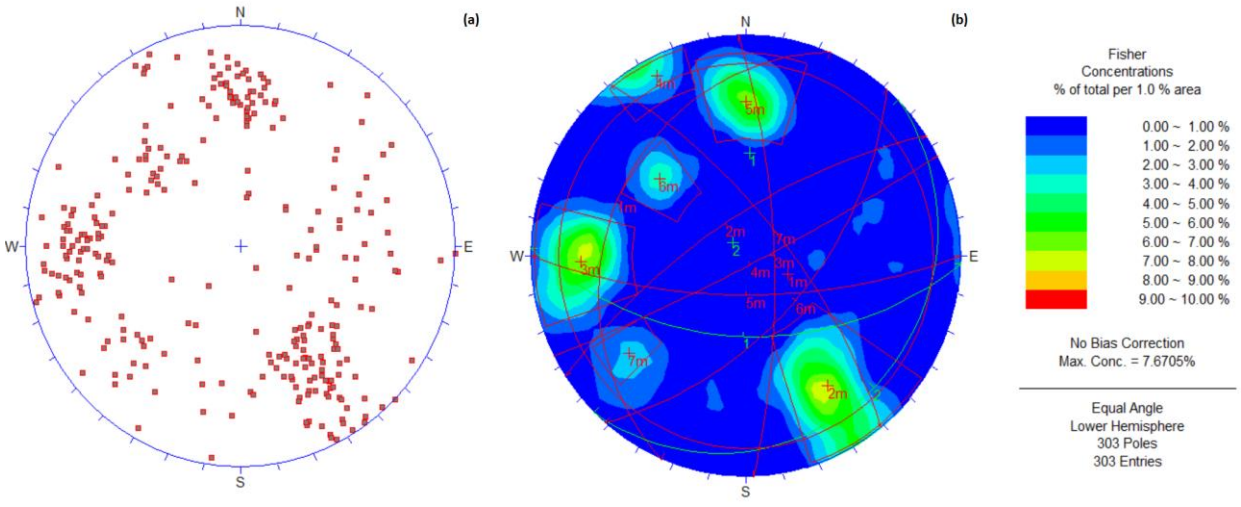

Figure 5.20. Distribution of kinematic data (a) Pole Plot, (b) Contour Plot along with Mean Discontinuity Planes and Face plane for the selected study area.

The results of the kinematic analysis demonstrated that several slope failures are expected to occur across the slope, in which planar, toppling and wedge failures have been identified. As can be seen in Figure 5.21, the zone bounded by a generated curve demonstrates the toppling region. Owing to that the toppling region shown in Figure 5.21 is governed by poles plotting within it, as such the poles plotting within it denote toppling risk. Furthermore, the visual estimate on risk indicated that 55% to 65% of the theoretical population of joint set 2 falls within the toppling zone. Arguably, one may point out that if the variability in friction angle is ignored, the toppling risk of 65% is possible across joint set 2.

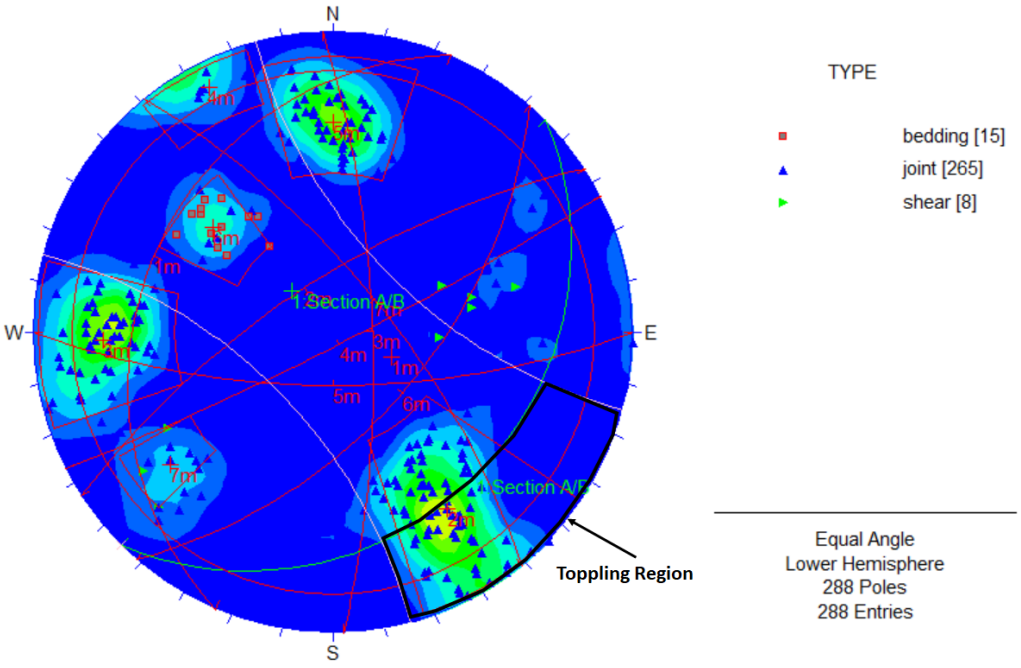

Figure 5.21. Toppling analysis was found across the study area.

Following the results stated above, it has been observed that the toppling slope failure interferes with the rotation of the blocks or columns of rock on the slope as pointed out by Wyllie and Mah (2004). A close look at the occurrence of the toppling failure across the slope was undertaken, and it has been revealed that the analysis has met the following conditions associated with toppling occurrence. The strike of the layers was approximately parallel to the slope face, as shown in Figure 5.21. Following that it is

observed from Figure 6.3 that the dip of the layers must be into the slope face. Lastly, as documented by Goodman (1980), for the interlayer slip to occur, the normal to the toppling plane must have a plunge less than the inclination of the slope face less than the friction angle of the surface. A similar situation has been observed and it is wise to conclude that toppling failure may be expected across the selected slope.

It is denoted in Figure 5.22 that the zone bounded by a generated curve shows a clear demonstration of the planar sliding zone. Owing to that the planar region shown in Figure 5.22 is governed by poles plotting within it as such the poles plotting within it denote planar risk. Furthermore, the visual estimate of risk indicated that 5% to 6% of the theoretical population of joint set 1 falls within the planar failure zone. Arguably, one may point out that if the variability in friction angle is ignored, the planar risk of 6% is possible to be achieved across joint set 1.

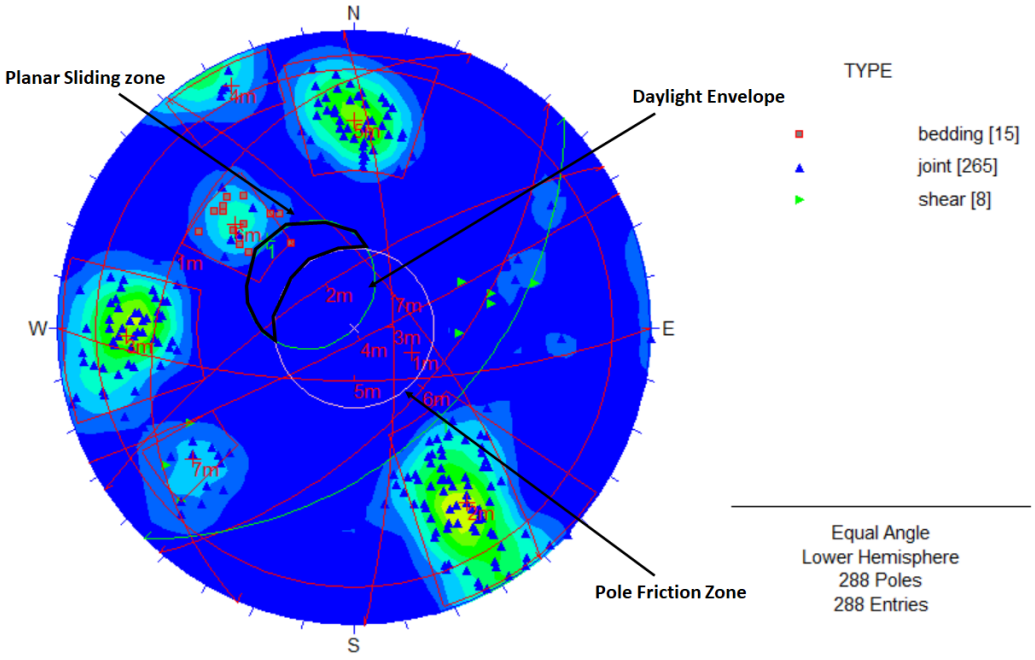

Figure 5.22. Planar failure

It is well established that a plane failure occurs in rock slopes when certain geometric circumstances are fulfilled. It is documented in Wyllie and Mah (2004) that plane failure develops under the following circumstances:

(a) "*the strike of the joint planes on the sliding has a strike orientation parallel within ± 20° to the slope strike*"

(b) *"the dip of the joint plane must be less than the slope angle"*

(c) "the dip of the joint should be greater than the friction angle" and

(d) "*the upper part of the sliding surface must either intersect the upper slope or terminate in a tension crack*" (see Figure 65.22)".

Yet, the results documented in Figure 5.22 support the suggestions governed by the planar failure, as such, it is concluded that planar failure may also be expected.

In Figure 5.23, the zone outside the selected slope which is enclosed by a friction cone, represents the zone of wedge sliding. Nevertheless, any plane which intersects other planes (see the black dots in Figure 5.23) shows unstable wedges which can occur. One may argue that the analysis demonstrates that few small wedges are expected across the study areas. Furthermore, it is well established (Wyllie and Mah, 2004) that wedge failure occurs when two intersection joints inside the slope and forms a wedge. Therefore, it is concluded that wedge failures are expected across the selected study area.

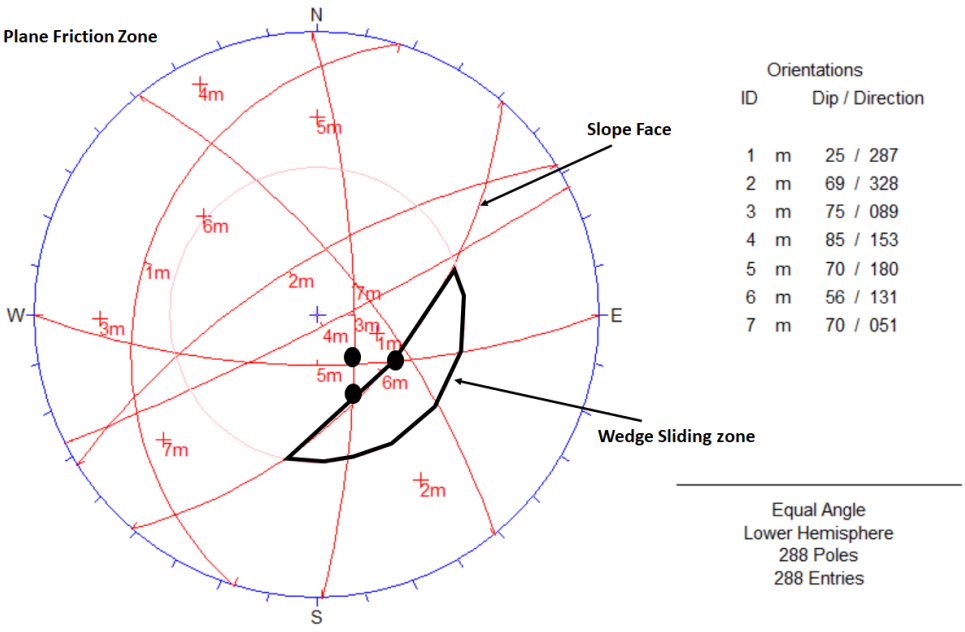

Figure 5.23. Wedge failure

5.3.3.3 Estimation of mechanical properties of the rock mass and faults

Further analysis was to identify the mechanical properties of the rock mass as well as the three faults. The so-called Rocdata computer code was used to estimate the mechanical properties of each feature mentioned. However, the estimation depends on the field observation, therefore the Hoek and Brown classification criterion was implemented to estimate the values as shown in Table 5.3. In terms of the strength of the rock mass and faults, the so-called Geological Strength Index (GSI) was used to predict both rock mass and fault strength. The GSI criterion was introduced by Hoek (1994), Hoek, et al. (1995) and Hoek et al. (1998) provided a number that, when combined with the intact rock properties, can be used for estimating the reduction in rock mass strength for different geological conditions. The GSI has been extended to cater to blocky rock masses, heterogeneous rock masses such as flysch and molassic rocks (Hoek et al 2006) and Ophiolites (Hoek et al., 2005). Similarly, the degree of disturbance (D factor) on the rock mass and the uniaxial compressive strength of the rock mass have been estimated based on developed charts by Hoek and Brown (1997).

Table 5.3. Mechanical properties of the rock mass and faults used for the case study

Parameters		Rock Mass	Fault A	Fault B	Fault C
Hoek and Brown Classification parameters	UCS (sigci) (MPa)	35	25	175	180
	GSI	61	61	61	61
	D	1	1	1	1
	Mi	6	6	16	16
Mohr Coulomb	Cohesion (MPa)	1.056	0,754	7.280	7.488

	Friction angle (phi) (degrees)	18.95	18.95	26.22	26.22

5.3.3.4 Stability analysis of the slope based on the common practice

In common practice, one section of the slope is usually selected, modelled and used as a representation of the entire slope stability number. Similarly, the practice has been exercised in this case, however, three sections of the slope were selected to identify the variation in stability number across the three faults. The simulation results show that all sections of the slope modelled are stable with safety factors ranging from 1.97 to 1.99 (see Figure 5.24). Nevertheless, with common practice, it is argued that a multi-faulted slope is stable.

One may argue that the overestimation presented by the current practices has imposed several design challenges in slope stability as well as increased the possibility of slope failure if a support system is not installed (Kalkani, 1975; Sjöberg and Norstrom, 2001; Franz, 2009; Tutluoglu et al., 2015). This implies that the currently common practice still needs some modification in order to capture all sensitivity properties of the fault and surrounding rock mass and how these features influence the stability of the slope. Many authors have used the LEMs (Fleurisson, 2012; Abderrahmane and Abdelmadjid, 2016; Sengani and Mulenga 2020a; 2020b) in sloping the stability problem in multi-faulted slopes but the concern is always voiced in terms of the accurate prediction of the method in the given situation. Therefore, the current method strives to explore the actual stability number considering of joint orientation across all three sets of faults.

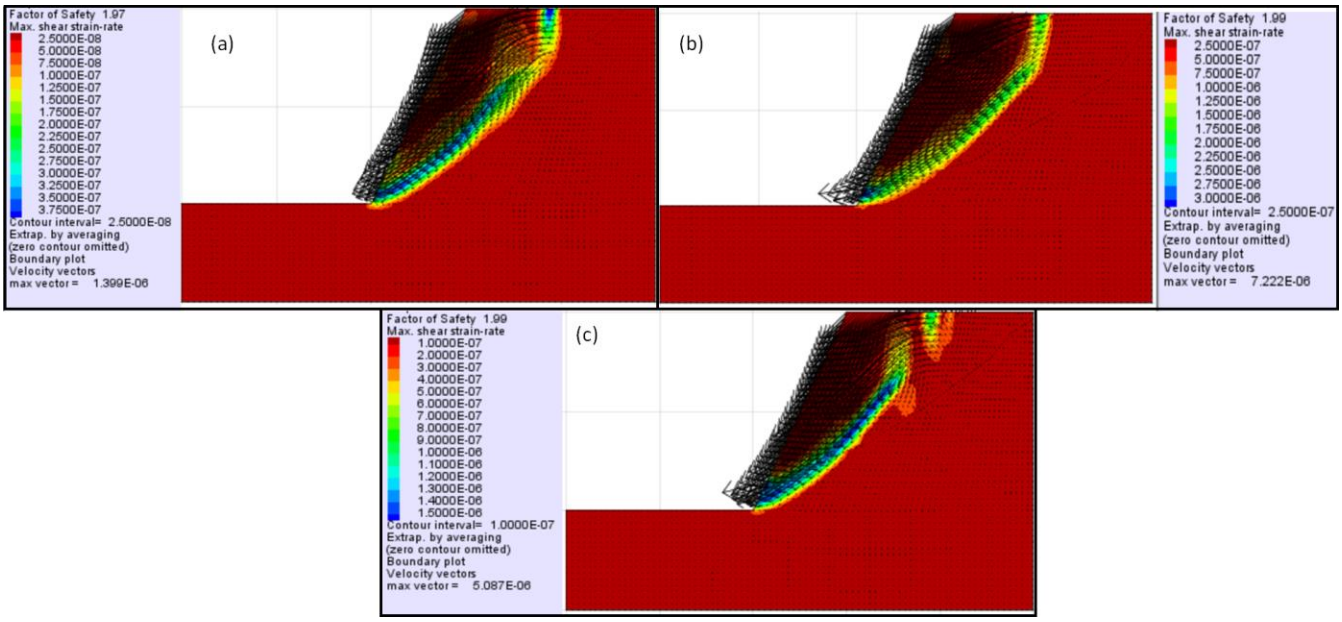

Figure 5. 24. FoS is different fault geometry (a) Planar fault (b) Undulated planar with the maximum thickness of 4m (c) Undulated fault with a maximum thickness of 9m

5.3.3.5 Stability analysis of the slope based on the proposed method

In terms of the proposed method, inside of analyzing the stability of the multi-faulted slope with only the fault zone included, the ubiquitous joints with various orientations across the three faults were also incorporated. The results of the simulation have shown that when joints are included within the model block the stability of the slope reduces gradually as compared to the common practices. Nevertheless, it has been observed that the FoS of the slope varied from 1.037 to 1.303 (see Figure 5.25). It was also noticed that when the block is modelled with steep joints, the FoS are higher as compared to those with moderately steep and intermediately steep joint angles. Similar to the sensitivity analysis of the fault when the rock mass is subjected to different joint orientations, it was noted that the joint orientation and shear strength properties of the fault influences the stability number of the slope. Therefore, if all scenarios are well captured the actual stability number of the slope can be obtained. Furthermore, the proposed method suggested that the FoS simulated across all various joint angles should be combined to acquire the mean FoS, the mean FoS was found to be 1.213. The mean FoS implies that the overall stability of the slope selected is unstable considering the standard set by Hoek and Brown (1981),

which pointed out that the minimum stability number for a slope showing stability is 1.5 FoS, while a FoS =1 represents an imminent failure.

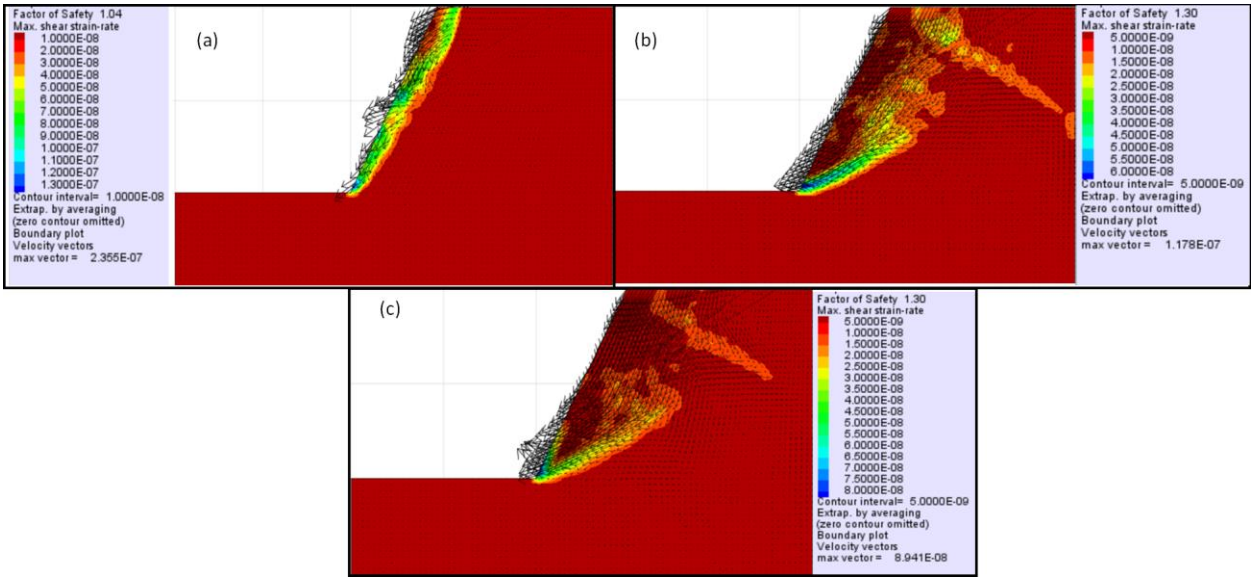

Figure 5.25. FoS of a planar fault with different ubiquitous joints (a) shallow angle (b) moderately steep joint (c) steep joints

On the other hand, the second and the third fault (undulated planar fault) (see Figures 5.26 and 5.27) were implemented with various joint angles. It has been observed that the FoS of the slopes varied from 1.244 to 1.412. It was also noticed that when the block is modelled with steep joints the FoS are higher compared to those with moderately steep and intermediately steep joint angles. In terms of the mean FoS of the slope, it was found that the second zone of the slope presented a FoS of 1.352. Unlike the common practice which does not incorporate joint orientations, the stability of the slope is still considered unstable in this case.

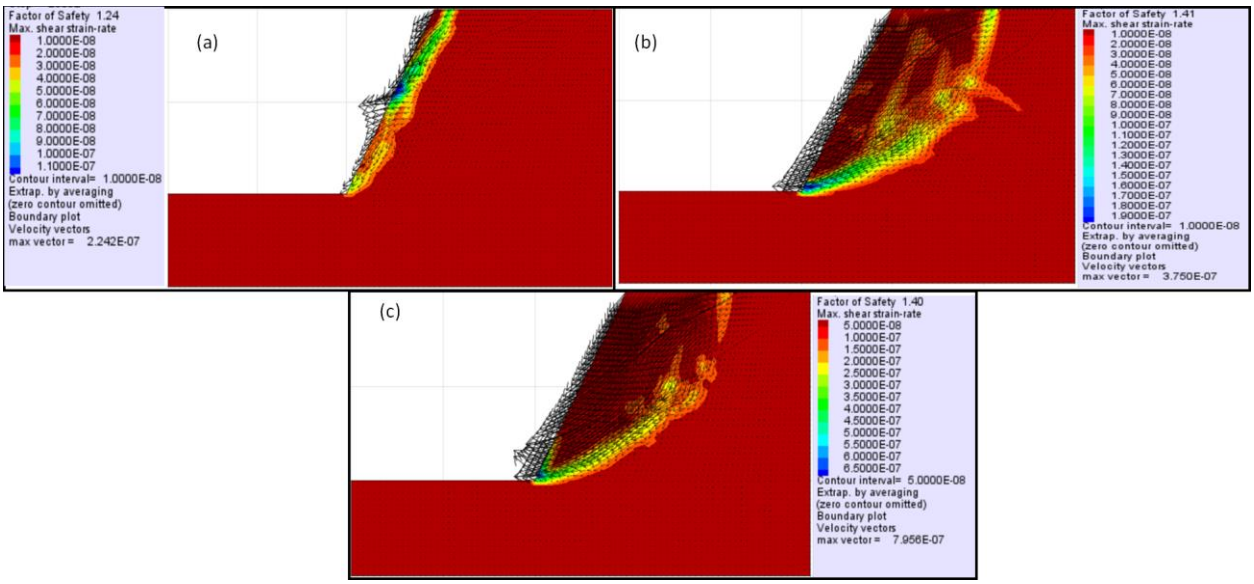

Figure 5.26. FoS of an undulated planar fault in zone 2 with different ubiquitous joints (a) shallow angle (b) moderately steep joint (c) steep joints

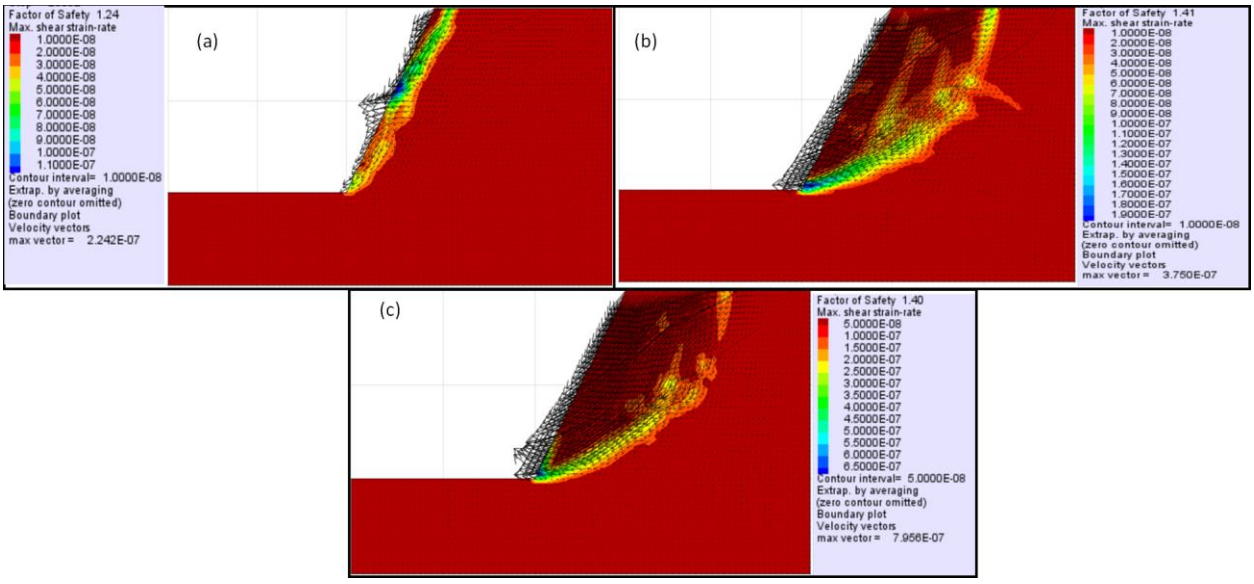

Figure 5.27. FoS of an undulated planar fault in zone 1 with different ubiquitous joints (a) shallow angle (b) moderately steep joint (c) steep joints

In terms of zoning the slope, the slope can be divided into two zones of stability number, however, the second zone will be the combination of zone 2 and 3. As already stated that the zone of influence plays a major role in classifying the zones of the slope. Fault 3 has a zone of influence of about 4.5m which overlaps with fault 2. On the other hand, the zone

of influence for both faults 1 and 2 could not overlap each other therefore, the two faults cannot be zoned together.

In terms of the actual stability of the entire slope, the method suggested that the overall stability of the slope can be determined by identifing of the overall mean FoS of the slopes. Therefore, the overall stability number of the slope is 1.2825. The overall stability number of the slope confirms that the slope is not stable, however, this implies that the fault properties play a major role in the stability of the slope considering the orientation of the joint set across the slope. Unlike the common practice which excludes some of the sensitivity analysis of the fault properties and its surrounding, the proposed method appears to capture the necessary features to classify the slope stability number.

5.4. Concluding remarks

The current chapter commences with evaluating of the sensitivity analysis of fault properties on the stability number of the slope (FoS). These sensitivity analyses incorporated fault geometry, thickness, shear strength properties and mesh densities with a comparison of several ubiquitous joints. After establishing the sensitivity of fault properties, a new method was proposed to capture all these sensitivity properties of faults and rock mass into the stability analysis. The new method introduced the so-called zone of influence, and it also studies each fault as a case study. Lastly, an overall stability number of the slope can be identified.

A practical application of both current practice and the proposed method was demonstrated based on a slope composed of three faults (planar and two undulated planar faults filled with dolerite dyke while the planar fault is filled with quartz). The results of the study have shown that the current practice tends to overestimate the stability number of the slope, furthermore, the current practice also generalizes the composition of the slope which jeopardized the accuracy of the estimated stability number. The proposed method was implemented, and it was discovered the current practice overestimates the stability number of a multi-faulted slope by 37%. This implies if all sensitivity properties of faults and joint orientation are well captured in the analysis the estimated stability number is reduced by 37% compared to the current practice. It is

maintained that if the proposed method can be implemented in jointed and multi-faulted rock slopes, an accurate stability number of the slope can be achieved. However, it is crucial to mention the proposed method requires extra inputs such as structural properties of the joints and faults properties to achieve the accurate stability number. One may argue that capturing the actual size of the fault in a model has been a concern to many authors, but the proposed method strives to look into the details of each fault in order to acquire the accurate stability number of the slope.

Chapter 6 Numerical study on the evolution process of slope failure triggered by extreme rainfall along a road cut in mountainous terrain

Modelling the flow evolution of a slope governed by solid mass has been recognized as a challenge, yet most stability analyses are only based on stability number or factor of safety (FoS). The stability number in most cases does not incorporate the deformation characteristics of the material and the change in solid mass phases such as from solid-like to fluid-like phases. Therefore, the purpose of this study is to present a numerical simulation that describes the failure evolution of a slope dominated by faults along with a road cut. A finite element method associated with an elastoplastic model with strain softening is adopted to provide a failure evolution of R71 road cut slope instabilities. The study results have demonstrated that the present computational framework is capable of quantitatively reproduce the failure evolution process and the final run-out distance of the slope material. The simulation has evidenced that the flow evolution of material during extreme rainfall is expected to extend to the final deposit of 4.5m, the field measurements and observations also confirm this. Furthermore, the simulations also demonstrated that the distance which material can reach is largely controlled by the composition and phases of the material during flow evolution. Owing to that, the material resistance has a major role in the run-out of the material; this resistance of the material is also controlled by shearing and absorbing kinetic energy during the process. The overall conclusion is that, for material to flow for a longer distance, high kinetic energy and more shearing of material are expected to take place during this process. It is recommended that other sophisticated methods could be utilized to further the results.

6.1 Introduction

A rockfall is the most common slope movement that makes rock cuts along transportation corridors in mountainous regions hazardous (Parise, 2002). It is essential to understand the deformation characteristics and failure mechanism driving the instability of slopes (Whalley, 1984; Read et al., 2003). Slope stability refers to the potential of the earth's surface material (soil and rocks) on inclined slopes to withstand or undergo movement.

The strength and cohesion of the slope material as well as the amount of internal friction between materials help in maintaining the stability of the slope. Stability is determined by the angle of the slope and the strength of the constitutive material. The steepest angle, at which a cohesionless slope can maintain the mass without losing its stability is referred to as its angle of repose. Slope stability also refers to the relationship between the driving and the resisting forces. The ratio of resisting forces to driving forces is known as the factor of safety of the slope. The gravitational force is evidently the main driving force acting on a slope. The gravity-induced driving force is directly proportional to the slope inclination. The existence of discontinuities in the rock leads to uneven distribution of strength and stress in all directions. Elastic properties of the rock mass are consequently altered, leading to the disrupted balance of rock mass strength as well as landslides. The orientation of discontinuities is another major factor affecting rock stability and rock failure alike (Read et al., 2003).

Rock slope failures can be classified depending on the type and degree of structural control. The most encountered rock slope failures include planar, wedge, toppling, and circular failures. The geometry of the slope, the characteristics of the potential planes of failure, surface drainage, and groundwater conditions are the main internal factors controlling rock slope stability. On the other hand, rainfall, seismicity, and man-made activities, hand, are external factors. The combination of these factors is responsible for the conditions of slope stability (Wyllie and Mah, 2004).

The analysis of rock slope stability is generally performed to assess how safe and functional excavated and natural slopes are. Eberhardt (2003) argues that the analysis is aimed at assessing slope conditions, potential failure mechanisms, and slope response to external factors that can trigger failure. Moreover, the analysis can be used not only to determine the most effective options for support stabilization but also to optimally design safe, reliable and economical excavation slopes. This analysis mostly revolves around the concept of the factor of safety.

The factor of safety (FoS) can be defined in three ways: limit equilibrium, force equilibrium and moment equilibrium (Abramson et al., 2002). It should be noted that factor of safety of a rock slope is usually assessed through a detailed comparison of the calculated FoS

against the acceptable FoS. Hoek (1981) argues that the acceptable standard threshold value of FoS is 1.5 for road rock slopes before failure occurs.

Limit equilibrium methods are known to suffer from the uncertainty associated with estimated input parameters among others. To overcome this, probability methods usually resort to Chen, (1995). Most of these methods replace FoS values with a probability of failure as a measure of slope stability (see Oka and Wu, 1990; Sarma, 1973; Krahn, 2004; Sengani and Mulenga, 2020a; 2020b; Sjöberg and Norstrom, 2001; Tutluoglu et al., 2015; Rabie, 2014). Yet most of the landslides, rockfalls, and slope stability analyses centred on limit equilibrium methods,

The analysis of the stability of rock slopes is performed primarily to assess their safety (Ansari et al., 2014; Rubio et al., 2016; Göktepe and Keskin, 2018; Duncan, 1996), the selection of the analysis tool depends on the conditions of the site and its expected mode of failure (Peric et al., 1996; Oliver et al., 2007). The challenge has been finding adequate tools to describe failure as a nonlinear phenomenon involving solid-like and liquid-like behaviours. The latter known as Fluid-Solid-Structure Interaction (FSSI), cannot be solved using, for example, the classical Arbitrary Lagrangian-Eulerian (ALE) formulation of the FEM framework (Wang et al., 2015; Aubry et al., 2005; Idelsohn et al., 2003). While most of these methods fail to provide a description of the flow evolution of the material, it is always emphasized on how the slope instability occurred..

Over the last two decades, a framework known as the Particle Finite Element Method (or PFEM) has been explored in geotechnical engineering. The numerical modelling paradigm is a combination of finite element and meshless finite element methods. It revolves around the numerical resolution of the Lagrangian formulation of particulate systems. The technique has gained popularity due to pioneering work by Aubry et al. (2005); Idelsohn et al. (2003 and 2004); Oñate et al. (2008 and 2004), and Larese et al. (2008). Originally, the PFEM was intended to solve solid particulate systems interacting with fluid (Zhang, 2014). It is widely used in fluid mechanics because it allows for mesh distortion while following the evolution of free surfaces (Zhang, 2014; Zhang et al., 2014, 2015, 2017, 2018, 2019a; 2019b; Zienkiewicz and Taylor, 2000). The PFEM has been well established in solving large deformation problems, yet shallow deformation problems

remain unsolved or still not well understood. The current technical note attempts to explain a failure evolution of a shallow deformation-using road cut slope (R71 road) as a case study. Nevertheless, a new framework called Optimum G2 (Optimum G2, 2019) was applied to establish the flow evolution of this slope.

6.2. Methodology of the study

The data collection was performed through field observations and measurements. Here, geological rock units' information and field measurements of the rock mass structures were conducted within the selected study areas. Observations focused on the rock conditions as well as evidence of slope instability across the selected study areas. Field measurements focused more on collecting the rock mass properties as shown in Table 6.1. In terms of observations, the rock mass of interest in this study was governed by granodiorite, with very limited joint sets and a fault cutting across the rock unit. Nevertheless, the fault was observed to present very limited infill material, in fact, the fault had no infill material. It was also observed that the rockfall across the selected slope occurred along the fault plane and broken rock units of granodiorite were observed at the bottom part of the slope. The majority of the broken rock is in boulders and some of the blocks are still intact (see Table 6.1). Yet, understanding how the failure occurred is significant.

Nevertheless, the observed and measured rock properties were applied in a Roclab model to estimate the rock mass classification, Hoek and Brown criterion properties, Mohr-coulomb fit, rock mass properties, failure envelope range of rock mass, fault properties and general properties of rock slope. In terms of rock mass classifications, the model was able to estimate the uniaxial compressive strength of the rock (sigci), the geological strength index and contact value of rock mass (mi) as well as the disturbance rate (D). The GSI was used to predict both rock mass and fault strength. The GSI criterion was introduced by Hoek (1994), Hoek, et al. (1995) and Hoek et al. (1998) provided a number that, when combined with the intact rock properties, can be used for estimating the reduction in rock mass strength for different geological conditions. The GSI has been extended to cater to blocky rock masses, heterogeneous rock masses such as flysch and molassic rocks (Hoek and Diederichs, 2006) and ophiolites (Hoek et al., 2005). Similarly,

the degree of disturbance (D factor) on the rock mass and the uniaxial compressive strength of the rock mass have been estimated based on developed charts by Hoek and Brown (1997). Similar to rock mass classification, other parameters were also identified as shown in Table 6.1. Furthermore, the model also simulated the relationship between major and minor stress acting on the rock mass, provided there is an increase in stress with time, following the relationship between shear stress and normal stress was also simulated by the model (see Figures 6.1 and 6.2).

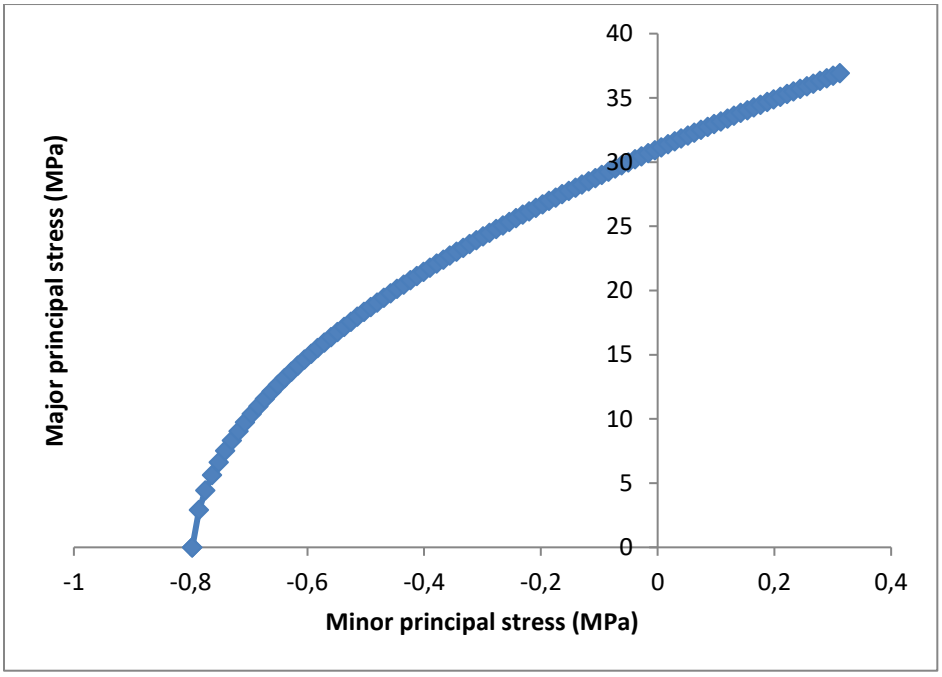

Figure 6.1. Plot on the relationship between major and minor principal stress of the rock mass provided there is a change in stress with time.

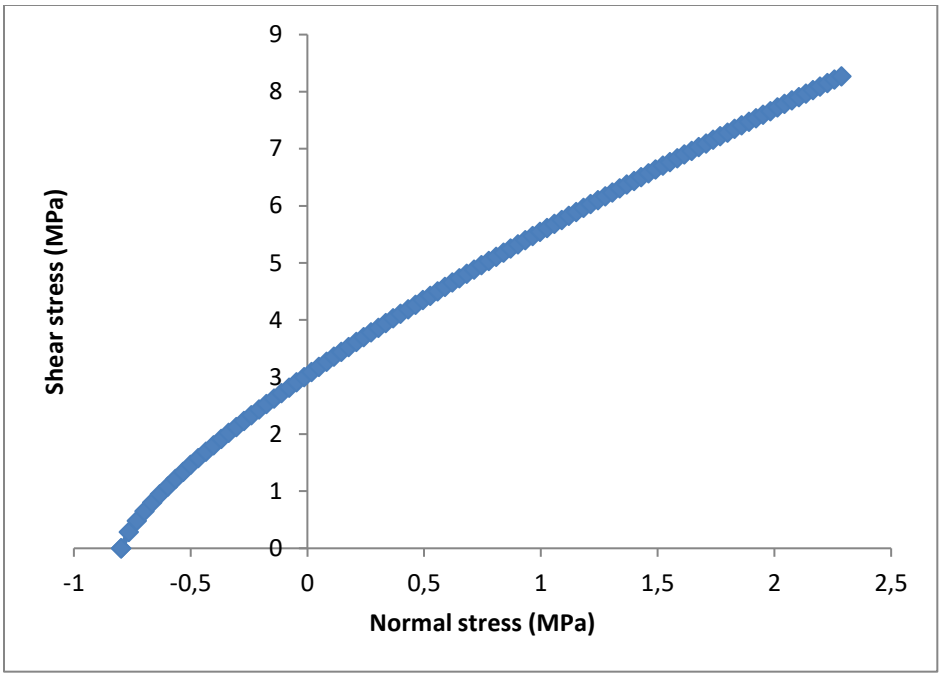

Figure 6.2. Plot on the relationship between shear and normal stress of the rock mass provided there is a change in stress with time.

.

Table 6.1. Material properties of the selected slope

	Parameters			Parameters		Overview of the Slope studied
Rock Mass Classification	Sigci (MPa)	250	Failure Envelope Range	Application	Slopes	 Image A
	GSI	75		sig3max (MPa)	0.312268	
	mi	29		Unit Weight (MN/m3)	0.026	 Image B
	D	1		Slope Height (m)	10	
Hoek Brown Criterion	mb	4.86264	Rock Mass Parameters	sigt (MPa)	-0.79709	
	s	0.0155039		sigc (MPa)	31.0107	
	a	0.500911		sigcm (MPa)	76.5769	
Mohr-Coulomb Fit	C (MPa)	2.93988		Em (MPa)	21084.8	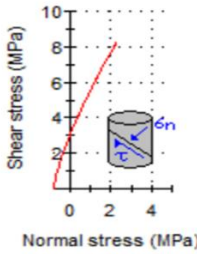 Shear and Normal stress plot of rock mass
	Phi (degrees)	68.3739	Fault Properties	Density (kg/m^3)	2500.0	
General properties of rock slope	Dip (^{0})	65^o		Cohesion (Pa)	100000.0	
	Dip Direction (^{0})	N 130^o E		Tension (Pa)	0	

	Height, (m)	7		Friction angle (^{0})	18	
	Nature of Slope	Man-made slope		Dilation angle (^{0})	0	
	Geology	A granodiorite with few joint sets cutting across the rock mass with minor weathering and a fault cutting cross (see Image A). A granite dyke is extremely weathered and blocky few several joint sets (see Image B). *Note the interest is on the granodiorite slope failure.*				

6.3. Results and Discussion

The Finite Element Method (FEM) called Optimum 2G was utilized to establish the failure evolution process and shear dissipation of a faulted road cut slope, and the extreme rainfall of the study area was incorporated (which is about 1000mm/hour). Detailed results of the simulation are documented in the sections below.

6.3.1 Failure Evolution process of the road cut slope

The results of the failure evolution are presented in Figures 6.3a to 6.3f with the distance of material/soil/tailing movement measured in metres. Furthermore, the results are presented at a relatively short time interval of approximately 5s per single computational cycle and it is assumed that the computational cycle is equal to the real lifetime. In Figure 3a, it has been observed that when the computational simulation is at the rest of 0s there is no movement of material at all, after an elapsed time of 5s, a sliding mass of solid material (soil and rocks) was observed (see Figure 6.3b). The initial sliding of material has been noted to begin at the toe part of the slope. In Figure 3b, it was also noted that there was a severe deformation of a material causing a total sliding distance of about 1.8m, in short, this deformation occurred at about 0.36m/s velocity. One may deduce that the initiation of this sliding has taken at high velocity, which correlates with the dis-locking of the material, wherein several stresses (shearing, tension and compressive) interacted. Further simulations have shown that from t (time) = 10s to 25s the sliding material already reached the flat area. To be specific at t =10s, almost 10% of the sliding mass has reached the flat surface. Surprisingly, the velocity of the material was noted to reduce as the duration of computational cycles increased (see Figures 6.3c to 6.3f), these results correlate very well with some of the previous studies such as those of Zhang and his co-authors (Zhang, 2014; Zhang et al., 2014; 2015; 2017; 2018; 2019a 2019b). Although the mentioned authors studied landslide flow-like structures, the implementation merges with the present study. Therefore, one may argue that as material flows/slides the speed at the material flows gradually reduces with distance.

Lastly, the run-out time of the simulation has shown that at about 25s of the computational cycle the maximum distance which the material can reach is approximately 5.2m. Despite

the fact that this is a numerical simulation, there have been several previous studies that conducted flow-like slides of landslides in steep terrain with similar properties as the present case studies, and it has been documented that the distance at which the material runs out is mostly influenced by the composition of the material as well as the smoothness of the ground flowing on. Arguably, the numerical simulation presented in this section has some commonality with several previous studies which give the simulation potential to present realistic results. It is crucial to indicate that the computational simulation of the rate-independent model is based on the average process of sliding of the material and the real flow-sliding of solid mass slopes is similar to those of landslides. These simulations of flow-slide may govern by a complicated mechanism that may require a more sophisticated numerical tool with a high format of algorithms. In short, the presented model still presents reasonable results for estimating the flow evolution of the slope and its run-out distance of the final deposit, which are more critical for hazard assessment of the road slope stability.

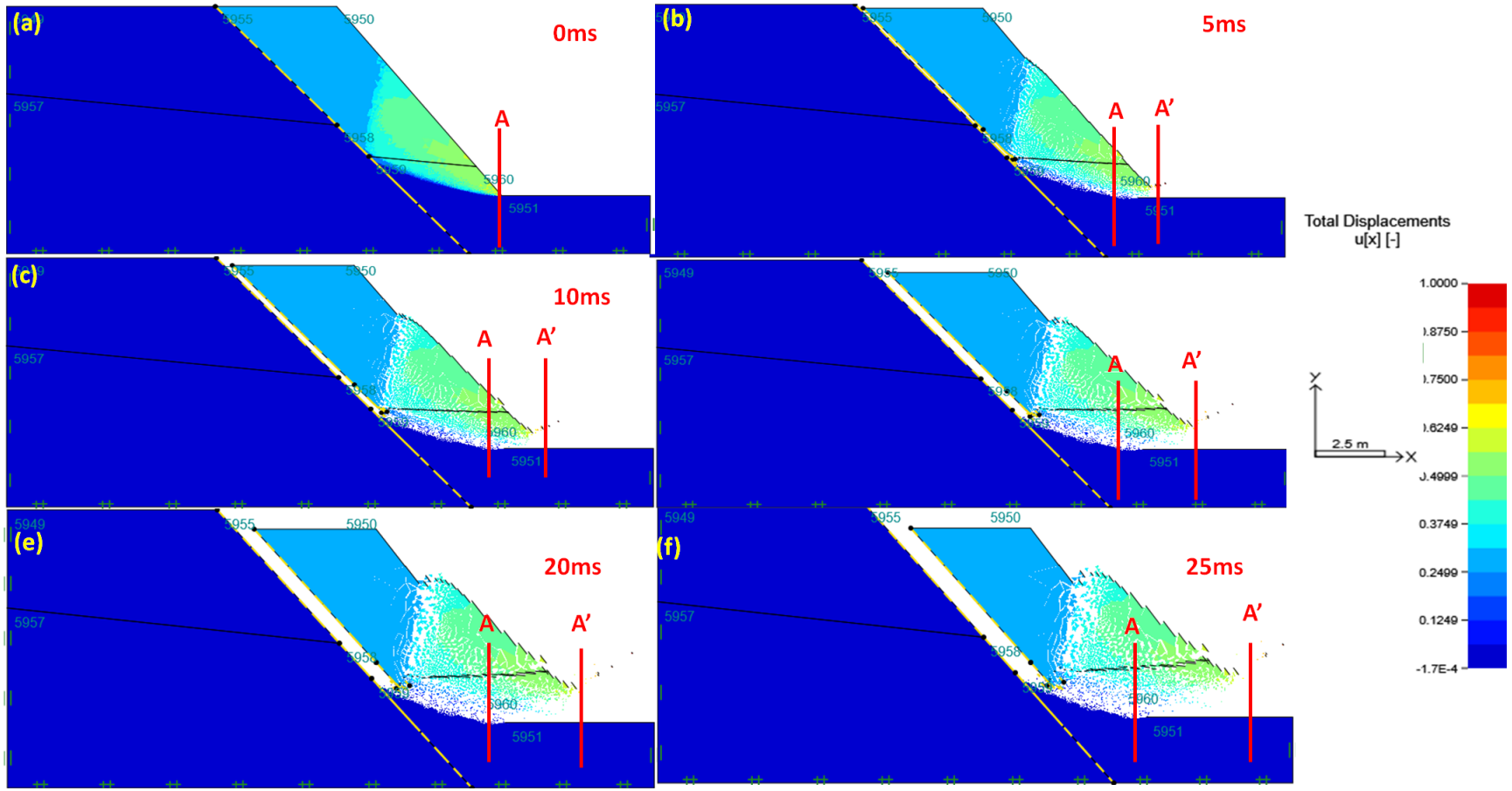

Figure 6.3. The total displacement of the slope in flow evolution process at (a) 0ms (b) 5ms (c) 10ms (d) 15ms (e) 20ms (f) 25ms

6.3.2 Shear dissipation of the material

The shear dissipation of the material is one of the critical concepts which integrates the turbulent kinetic energy and shear rate of material during flow-sliding of material. This fundamental principle allows verification of energy distribution relative to the resistance of the material.

In this regard, the road slope was divided into three sections (upper, middle, and lower); refer to Figure 6.4a to compare the section regarding shear dissipation and its relation to the flow sliding of the material. The results of the computational simulation in all cycles (from 0s to 25s) (see Figures 6.4a to 6.4f) have shown that the lower section of the slope experience extensive shear dissipation throughout the computational cycle. This result gives the impression that high kinetic energy and high shearing are expected at the toe of the slope during the initial stages of the evolution of flow until the last stage of the evolution flow of material. It makes sense that for the slope to collapse, the deformation starts at the bottom section of the slope, this process requires more energy, and more shearing of the material is expected. Therefore, the previous section on failure evolution is well supported by the shear dissipation of the material. This analysis also presents some form of the accuracy of the model. Zhang (2014) is believes that if there is a correlation between shear dissipation and flow evolution of sliding material exposed to extreme rainfall fall, the computational simulation may present a failure of a model rather than the failure of the slope.

It is crucial to indicate that the shear dissipation of the material appeared to correlate very well with the failure evolution of the slope simulated in section 6.3. Nevertheless, the shear dissipation analysis is mostly conducted to understand the fundamental principles governed by sliding taking kinetic energy into account together with the shearing of material. This simulation also involves the resistance of the material with time. From Figures 6.4a to 6.4f, one may argue that the resistance of material increases with time as well as distance. These observations were made wherein the speed of material gradually reduces with time. This implies that as material flows or slides, its phases change gradually from liquid-like to solid-like, which gives the material stability to resist the flow.

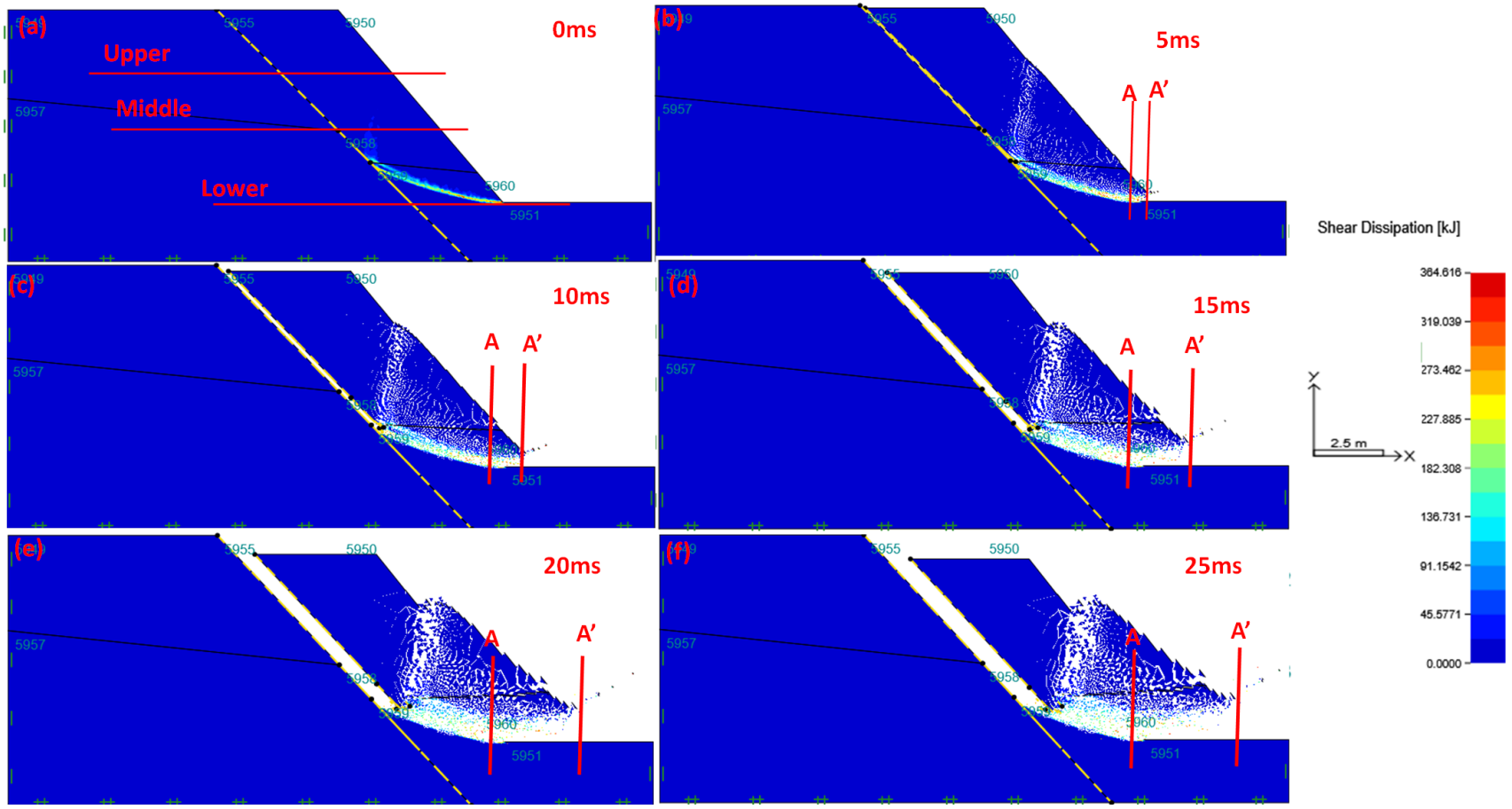

Figure 6.4.The shear dissipation of the slope in flow evolution process at (a) 0ms (b) 5ms (c) 10ms (d) 15ms (e) 20ms (f) 25ms

6.4. Concluding remarks

The study results o have demonstrated that the present computational framework can quantitatively reproduce the failure evolution process and the final run-out distance of the slope material. The simulation has evidenced that the flow evolution of material during extreme rainfall is expected to extend to the final deposit of 4.5m. Owing to that the field measurements and observations also confirm this. Furthermore, the simulations also demonstrated that the distance material can reach is largely controlled by the composition and phases the material undergoes during flow evolution. Owing to that, the resistance of material has a major role in the run-out of the material; this resistance of the material is also controlled by shearing and absorbing kinetic energy during the process. The overall conclusion is that, for material to flow for a longer distance, high kinetic energy and more shearing of material are expected to occur during this process. It is recommended that other sophisticated methods could be utilized to further the results such as establishing the failure mechanism and the kinematics of the slope instability.

Chapter 7 Reliability analysis of slope stability using probabilistic analyses compared deterministic analysis

Multiple slope instabilities have been reported along the N1 highway's slope cut in Limpopo Province, South Africa. Yet, few studies have been conducted to understand the mechanism and classify the slope based on stability number. However, these studies were more concerned about the overall FoS of the slope using deterministic methods, regardless of these studies, slope instabilities along road cuts have been reported continuously. Therefore, the proposed aim is to present a reliable approach to studying the stability of these slopes using a few case studies in the study area. A deterministic approach with different methods of stability analysis, namely the ordinary method, Bishop’s method, Janbu's method and Morgenstern Price method, using the iterative capabilities of software SLIDEs have been used to assess the stability of numbers. The deterministic analysis was followed by probabilistic analysis using Monte Carlo Simulation to simulate the mean safety factor, probability failure and reliability index of the slope. The deterministic approach yields conservative values of factor of safety due to input parameters being single-valued and the spatial variation of the input parameters not accounted for. The results from deterministic analysis denoted that slope in location one is stable and the slope in location two is unstable. Nevertheless, the results obtained from probabilistic analysis denoted that the mean safety factor of the slopes was closely related to deterministic solutions, furthermore, the probability of failure shows that 70% of the slope in location one is stable meanwhile, 9 to 13% of the slope in location two was declared stable. Furthermore, the results on the reliability index have shown that both slopes are not reliable though the slope in location one presents a reliable index closer to 1. It is therefore concluded that though deterministic analysis may declare that the slope is stable, a detailed analysis of the slope point has to be analyzed using probabilistic analysis in order to acquire a reliable stability number.

7.1 Introduction

Slope instability is a global concern, and although its occurrence may not be frequent, its consequences often result in loss of lives, destruction of properties and roadblocks, among others (Göktepe and Keskin, 2018). Most of the national, regional, and local roads in Limpopo Province have been developed through a rugged topography and artificial slopes have been created with loose rocks scattered across the slopes. These unstable slopes pose a threat to communities and individuals who travel from one point to another through these roads. The stability analysis of earth slopes is one of the fundamental calculations in civil engineering, specifically geotechnical engineering. It has been noticed in the past that slope stability is one of the major concerns in construction projects involving excavation, embankments, earth dams, and road construction among others. The commonly used slope stability analysis method is the deterministic method (Khajehzadeh et al., 2009; Khajehzadeh et al., 2010a, 2010b). This method is governed by the identification of the critical slip surface as well as the associated minimum factor of safety (FoS). In this regard, the shear strength, slope geometry, external load, and pore water pressures are assigned as specific unvarying values, and as a result, the single factor of safety is then determined (Maji, 2017; Wang et al., 2010; Sun et al., 2008). However, the single deterministic safety factor of a slope is often not enough to analyze the slope stability due to the uncertainty of the input parameters among others. Therefore, performing a simulation that produces a reliable analysis of the slope is significant.

Wang et al. (2010) described probabilistic methods as methods that are utilized to calculate the probability of slope failure. In contrast to the deterministic approach, probabilistic methods such as the kinetic approach aim to calculate the slope failure probability, taking into account the orientations, physical characters, and shear strength of joints (Wyllie and Mah, 2004; Cao, 2012). Several scholars (Al-naqshabandy, 2012; Huang et al., 2010; Chen, 2007; Cheng et al., 2008a and 2008b) emphasize that probabilistic methods are useful in analyzing slopes with uncertainties or measurement errors such that numerical models provide a poor reflection of the actual state of the slope condition. Cho (2007) states that probabilistic methods combined with risk assessment are better to assess slope design in engineered or artificial slopes such as road cuts than

deterministic methods. Furthermore, the previous author, Cho (2007) and Turner and Jayaprakash (2012), documented that probabilistic analyses require more computer power than deterministic analyses. As such, probabilistic methods such as the Monte Carlo simulations (MC) may require numerous (thousands) analyses depending on the number of variables considered by the model to calculate accurate output variables (Gavin, and Xue, 2010). Monte Carlo simulations are envisaged to repeatedly calculate the factor of safety with input parameters that are randomly generated, resulting in obtaining a distribution of values which represent the uncertainty of the input parameters, instead of obtaining a single value of the factor of safety (Ishii et al., 2012). However, the computational efforts for incorporating a large number of possible slip surfaces into a slope system reliability might be very expensive (Mineo et al., 2017; Mineo et al., 2018; Göktepe, and Keskin, 2018). Subsequently, it is equally important to consider increasing the computational efficiency of MC simulations by combining or coupling them with other probabilistic models, such as the surrogate model (Göktepe, and Keskin, 2018). Nevertheless, the reliability of slope stability is frequently measured based on the reliability index, which consists of the probability of failure as well as the means safety factor. This method appeared to provide reliable results, though many scholars do not prefer it because it's time-consuming.

To the best of our knowledge, there is very limited research on slope stability within Limpopo Province. However, these studies were more concerned about the overall FoS of the slope using deterministic methods, regardless of these studies, slope instabilities along road cuts located within soft rocks have been reported continuously. The objective of this research is to develop a probabilistic model for slope analysis through the understanding of the concept of reliability analysis and its application in slope stability analysis using the N1 road slope as a case study, and secondly, to perform the reliability analysis of slope stability using Monte Carlo simulations based on mean safety factor, probability failure and reliability index compared with deterministic analysis using various methods. The case study used for this paper is located in Limpopo Province, South Africa along the national road (highway-N1). The slope in the upper Rooiberg Group area was predominantly sandstone and siltstone..

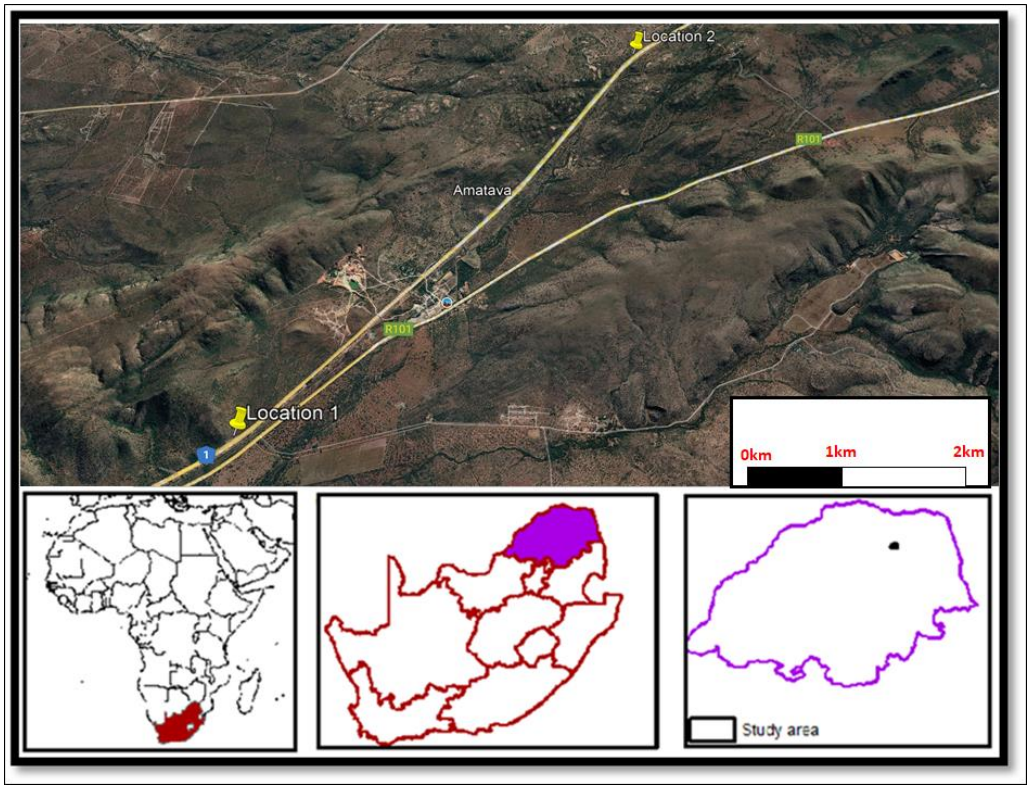

Figure 7.1. Location of Regional Road (R71) networks

7.2. Methodology of the study

The research approach followed in this chapter is well documented in Chapter 3, however, a brief of the methodology is documented here. The data collection was performed through field observations and measurements. Here, geological rock units' information and field measurements of the rock mass structures were conducted within the selected study areas. Observations focused on the rock conditions as well as evidence of slope instability across the selected study areas; the information was used to generate a database for Monte Carlo simulations as shown in Table 7.1. Field measurements were more focused on collecting the rock mass properties as shown in Table 7.2. Therefore, the collected rock mass properties were, used for simulation of the stability number based on deterministic and probabilistic analysis of the slopes.

Table 7.1 Rock mass properties used for the simulation of both deterministic and probabilistic simulation

Material Name	Property	Distribution	Mean	Std. Dev.	Rel. Min	Rel. Max
L1 Rock Unit	Cohesion	Normal	7.221	1	3	3
	Phi	Normal	26.25	3	9	9
	Unit Weight	Normal	21	0.5	1.5	1.5
L2 Rock Unit	Cohesion	Normal	5.5	1	3	3
	Phi	Normal	22.4	3	9	9
	Unit Weight	Normal	19	0.5	1.5	1.5

Note that *Rel.Min* means relative minimum values, *Rel.Max* means relative maximum value and *Std Dev* means standard deviation.

Table 7.2. Field measurements and observations across the locations

	Parameters	Location One	Overview of the location one	Location two	Overview of the location two
Rock Mass Classification	Sigci (MPa)	175		50	
	GSI	51		24	
	mi	17		7	
	D	0.7		0.7	
Hoek Brown Criterion	mb	1.15132		0.107538	
	s	0.000824		1.65E-05	
	a	0.50535		0.533437	
Mohr-Coulomb Fit	C (MPa)	7.50439		0.719214	
	Phi (degrees)	27.4596		11.1346	
General properties of rock slope	Dip (^{0})	65^o		75^o	
	Dip Direction (^{0})	N 130^o E		N335^{o}E	
	Height (m)	8		10	
	Nature of Slope	Man-made slope		Man-made slope	
	Geology	An interact sandstone rich with quartz arenite, Minor weathering taking place, few joint sets cutting across the rock mass		Weathered siltstone rich with hematite and another iron-rich mineral, with blocky loos rock. Evidence of weathering erosion across the slope. Rock slope with the recent failure	

7.3. Results and Discussion

The results and discussion section of this chapter are divided into various subsections, with deterministic analysis being the first to be discussed, followed by probabilistic analysis which is divided into several categories. The results and discussion are outlined below.

7.3.1 Deterministic approach

The results of the first location show that the factor of safety values simulated by the Ordinary and Janbu methods are in close proximity (FoS of 1.018 and 1.014, respectively, see Figures 7.2a and 7.2c), whereas the values indicated by Bishop's method and Morgenstern Price's method are closer (FoS of 1.052 and 1.047 respectively, see Figures 7.2b and 7.2d). Nevertheless, the factor of safety determined using all four methods for location on the slope are closely related, yet they all concluded that the slope is stable. According to Hoek and Brown (1981) and similar studies, one may argue that the factor of safety values is dependent upon slope geometry and characteristics, The previous statement correlates very well with other previous authors such as Farhan et al. (2019). Furthermore, the factor of safety also demonstrates that the slope for location is critically stable when the slope material is dry, whereas, in location two, different results were observed. The factor of safety simulated by all four methods shows that the slope is unstable (see Figures 7.3a, b, c and 7.3d). One may argue that the cohesion of material in location two is very small compared to the cohesion in location one, therefore materials are expected to be unstable. Furthermore, the visual observation has also provided some evidence of slope failure across all slopes in location two, the evidence was also supported by extreme erosion and weathering taking place across the slope. Nevertheless, the slope in location two is unstable in all loading conditions which shows that slope stabilization measures are required to maintain the stability of the slope.

Despite the above-mentioned results for both locations using deterministic analysis, several scholars always questioned the reliability of a single slope stability number. As such, the reliability of a single stability number has been considered a challenge since the deterministic factor of safety is the safety factor calculated for the global minimum slip

surface, from the regular slope stability analysis. In order to address the above-mentioned concern, the simulation was extended to probabilistic analysis, and the detailed results are outlined below.

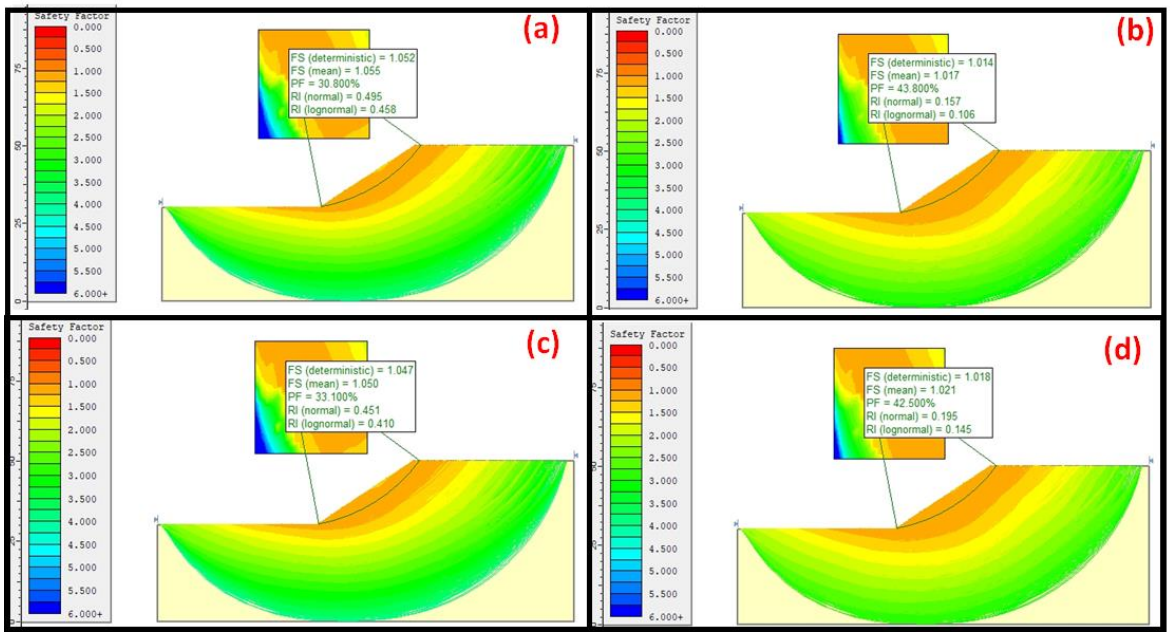

Figure 7.2. Deterministic and probabilistic analysis of the slope in location one (a) Ordinary method failure distribution (b) Bishop method failure distribution (c) Janbu Simplified failure distribution (d) Morgenstern-price failure distribution.

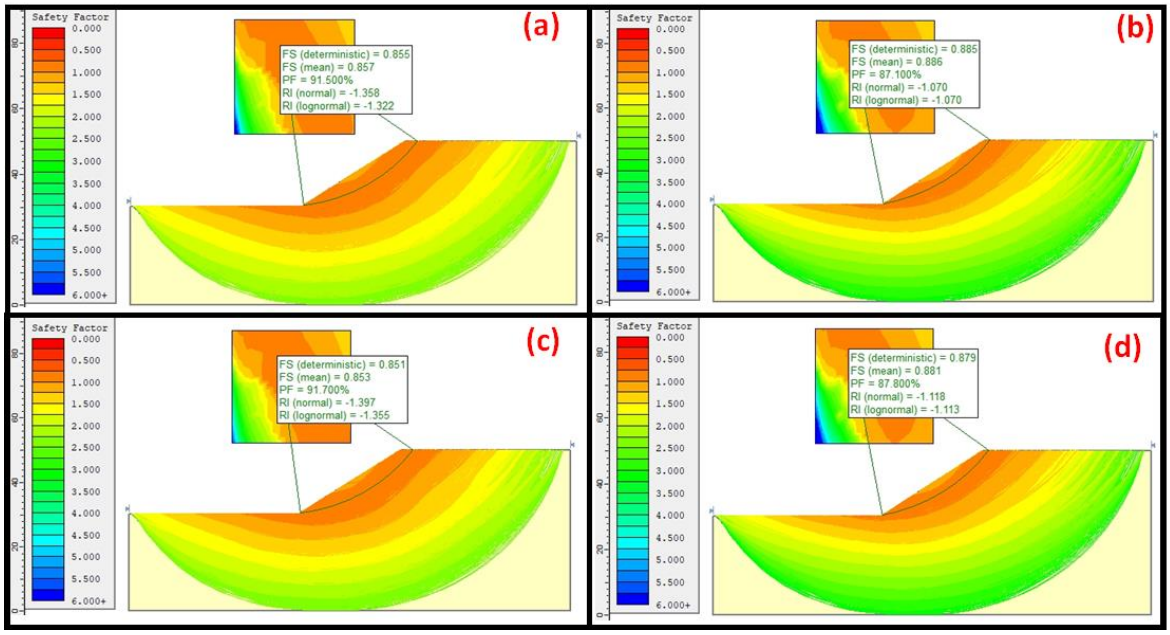

Figure 7.3. Deterministic and probabilistic analysis of the slope in location two (a) Ordinary method failure distribution (b) Bishop method failure distribution (c) Janbu Simplified failure distribution (d) Morgenstern-price failure distribution.

7.3.2 Probabilistic analysis

The probabilistic analysis of this study is based on three main analyses, which include the mean safety factor, the probability of failure and the reliability index of the slope. The mean safety factor is the mean (average) safety factor which is obtained from the probabilistic analysis. This safety factor is simply the average safety factor of all the safety factors calculated in the simulation across the slope, and it is usually closely related to the deterministic safety factor if a sufficient number of samples are used. Meanwhile, the probability of failure is simply equal to the number of analyses divided by the total number of samples used for analysis with a safety factor of less than one. In this regard, the analysis has the ability to outline the probability of failure across the slope, this analysis is more detailed as compared to a single stability number. Moreover, the reliability index is one and the last analysis of probability in terms of the stability of the slope. This analysis can be presented in terms of the normal or lognormal distribution, and a reliability index of three is usually recommended as a minimal assurance of a safe slope design. The probabilistic analysis of the study is therefore outlined below.

7.3.2.1 Mean Safety Factor

The results of probabilistic analysis for location one correlate very well with the deterministic safety factor as pointed out by the mean safety factor concept. Nevertheless, the results show that location one presents a stability number above one corresponding to the deterministic analysis. However, in location two, both deterministic and mean safety factors declared that the slope is unstable (see Figures 7.2a-d and 7.3a-d). These results indicate that the first analysis of probabilistic is closely related to the deterministic analysis solution, however, the first stage of analysis does not provide a concrete decision regarding the actual slope design number required. As a result, the second stage of probabilistic analysis is presented in the next section.

7.3.2.2 Probability Failure

The probability failure analysis is considered more specific and provides reasonable results regarding the stability of the slope per slope point. Nevertheless, the results of the analysis in location one have shown that the probability failure values simulated by the Ordinary and Janbu method are in close proximity (PF of 42.5% and 43.8% respectively, see Figures 7.4a and 7.4c), whereas the values indicated by Bishop's method and Morgenstern Price method are closer (PF of 30.8% and 33.10% respectively, see Figures 7.4b and 7.4d). Nevertheless, despite the fact that the factor of safety determined using all four methods for location on the slope (see Figures 7.2a-d) declared that the slope is stable, the probability failure revealed that the slope is not necessarily stable, but there is about 70% of the sampled points in the slope which are stable. However, it is important to note though the deterministic and mean safety factor declared that the slope is stable, in reality, not every part of the slope is stable. One may argue that it is expected that the rock mass does not have similar cohesion as well friction angle across the slope, therefore generalizing the stability of the slope may affect the determination of the slope design required. Following the previous discussion, further analysis on location two was conducted and it denoted that the probability of failure of the slope ranged from 87.1% to 91.7%. These results indicate that the slope in location two is unstable, and as such, the

failure of the slope is extremely likely, (see Figures 7.5a-d) with about 9.3% to 13.7% of the slope being stable. These analyses provide the most realistic results which were evidenced by visual observation demonstrated in Table 7.2. Besides that, it has been observed that the slope in location two had several broken rocks and soil at the bottom or slope toe, which confirms a gradual failure taking place across the slope. Unlike the slope observed in location one, wherein no broken rocks or soil were found at the bottom of the slope. One may also note that the stability analysis performed using deterministic analysis shows that the slope is close to one rated stable, meanwhile, the analysis is based on the global means safety factor value. Therefore, this analysis leads us to discuss the reliability index of the slopes.

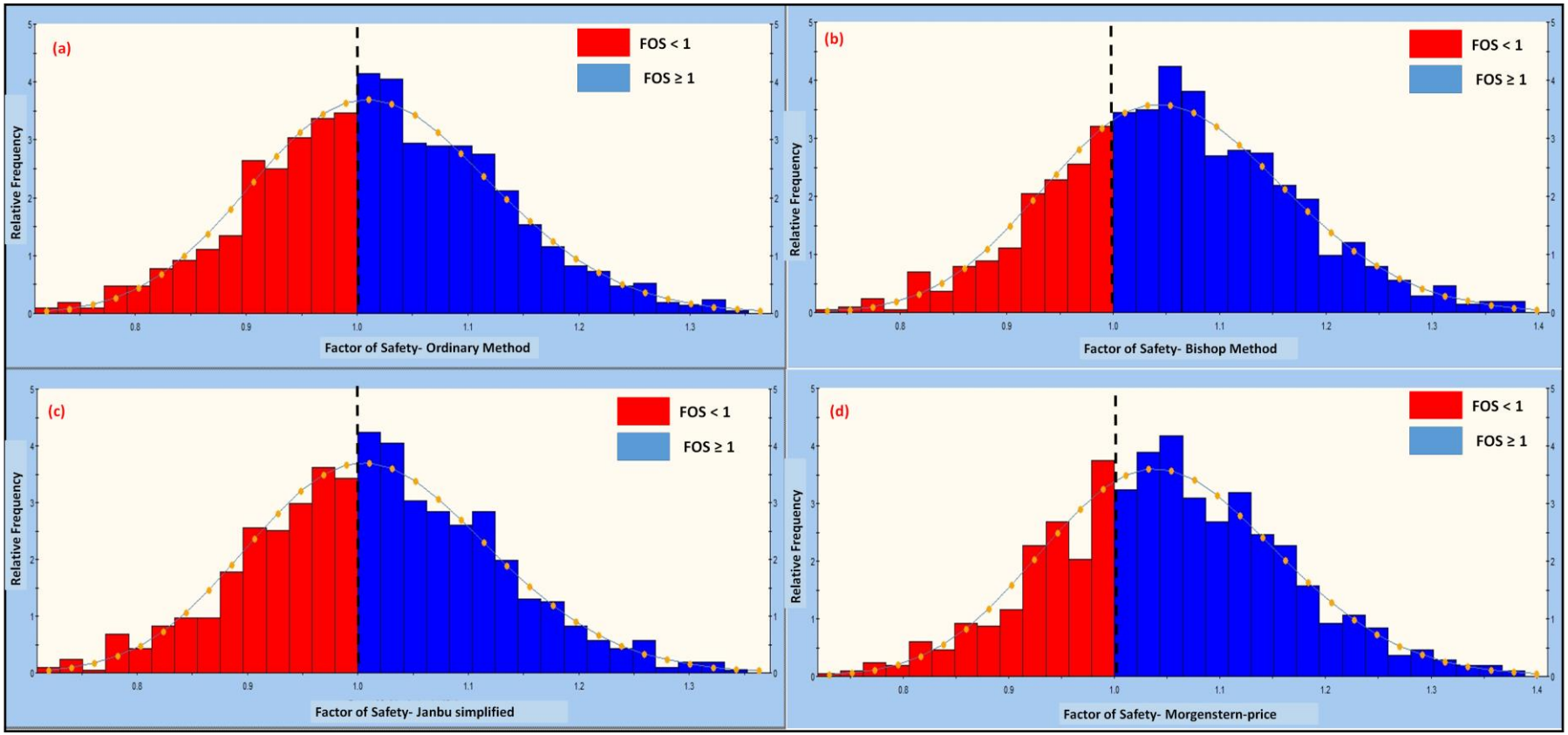

Figure 7.4. Probability Failure of the slope in location one (a) Ordinary method failure distribution (b) Bishop method failure distribution (c) Janbu Simplified failure distribution (d) Morgenstern-price failure distribution.

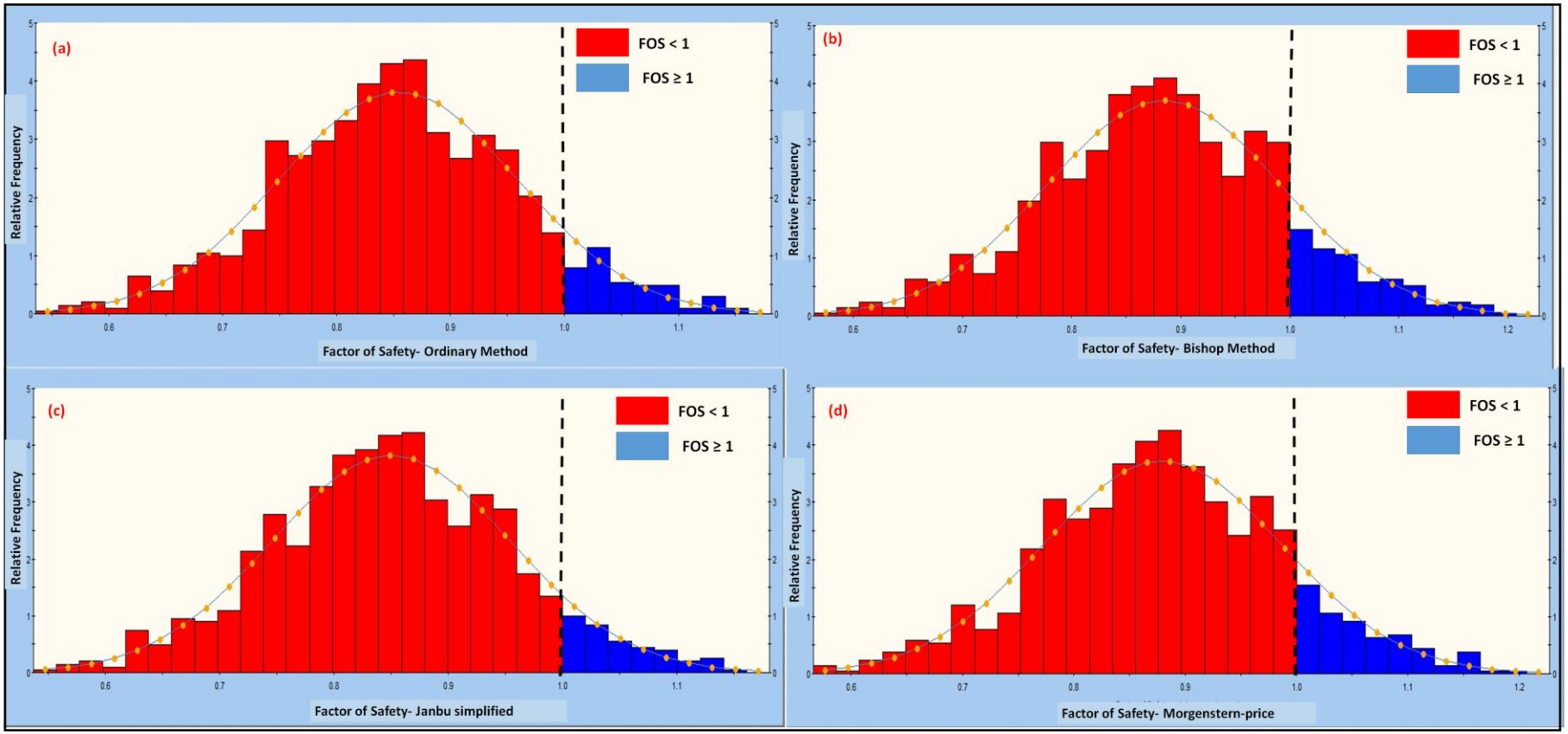

Figure 7.5. Probability Failure of the slope in location two (a) Ordinary method failure distribution (b) Bishop method failure distribution (c) Janbu Simplified failure distribution (d) Morgenstern-price failure distribution.

7.3.2.3 Reliability Index

The reliability index analysis in terms of normal and lognormal distribution (see Figures 7.2a-d and 7.3a-d) denoted that both slopes are reliable in terms of stability. However, the reliability index in location one is much better than to the slope in location two. This gives the impression that despite the fact that deterministic analysis declared that the slopes are stable, in the actual sense both slopes are not reliable; they require stabilization to maintain and improve the stability of the slope. It is, therefore, argued that the results of the probabilistic analysis are more realistic as compared to the results obtained from the deterministic analysis. Further, the results obtained from the probabilistic analysis can be used to determine the probability of failure corresponding to a particular factor of safety of the slope. Therefore, an allowable risk criterion can be classified and well established. However, the results also demonstrated that the factor of safety can be assessed, and the design stability number of the slope cut can be decided accordingly. The reliability of the proposed factor of safety could be assessed and the design of the cut slope can be decided accordingly. Similar to other reliability analyses verification of the results was conducted based on the correlation coefficient and convergence plots of the analysis. The results are discussed in the sections below.

7.3.2.4 Correlation Coefficient

It is well established that the relationship between friction angle and safety factor correlates very well if the parameters used are correct. Similarly, such tests were conducted in this study to verify if the analysis had enough samples and provide reliable results. Furthermore, it is also established that a coefficient close to one indicates a high degree of correlation, meanwhile, a correlation coefficient close to zero indicates little or no correlations. Nevertheless, the verification results have shown all analyses conducted have a high degree of correlation in both locations. This can be verified by the alpha and beta of the slope, wherein alpha represents the slope or gradient and beta represents the intercept. Figures 7.6a-d and 7.7a-d clearly demonstrated that the correlation was of a high degree. These results, therefore, verify that the samples used were enough for the analysis.

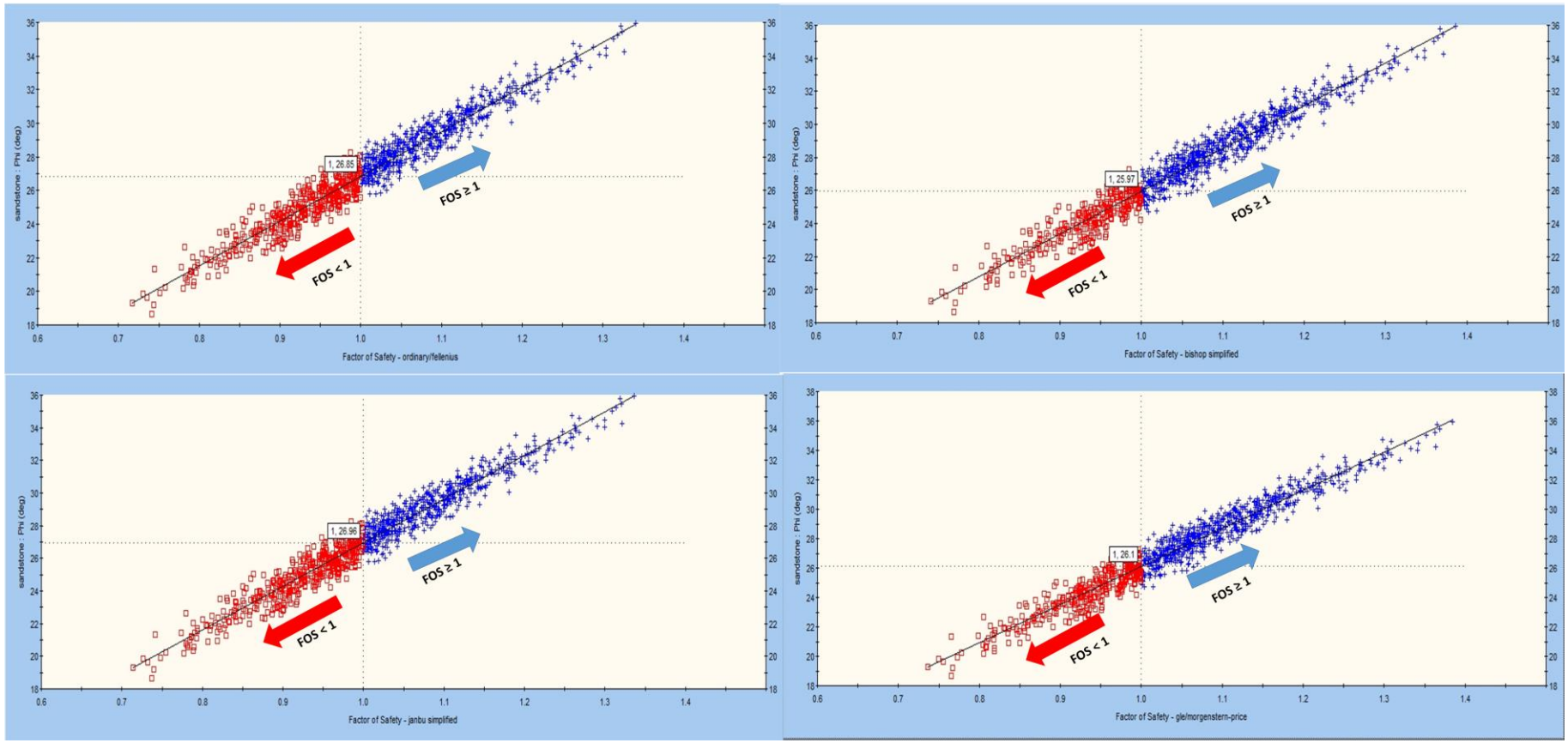

Figure 7.6. Correlation Coefficient of the slope in location one (a) Ordinary method failure distribution (b) Bishop method failure distribution (c) Janbu Simplified failure distribution (d) Morgenstern-price failure distribution.

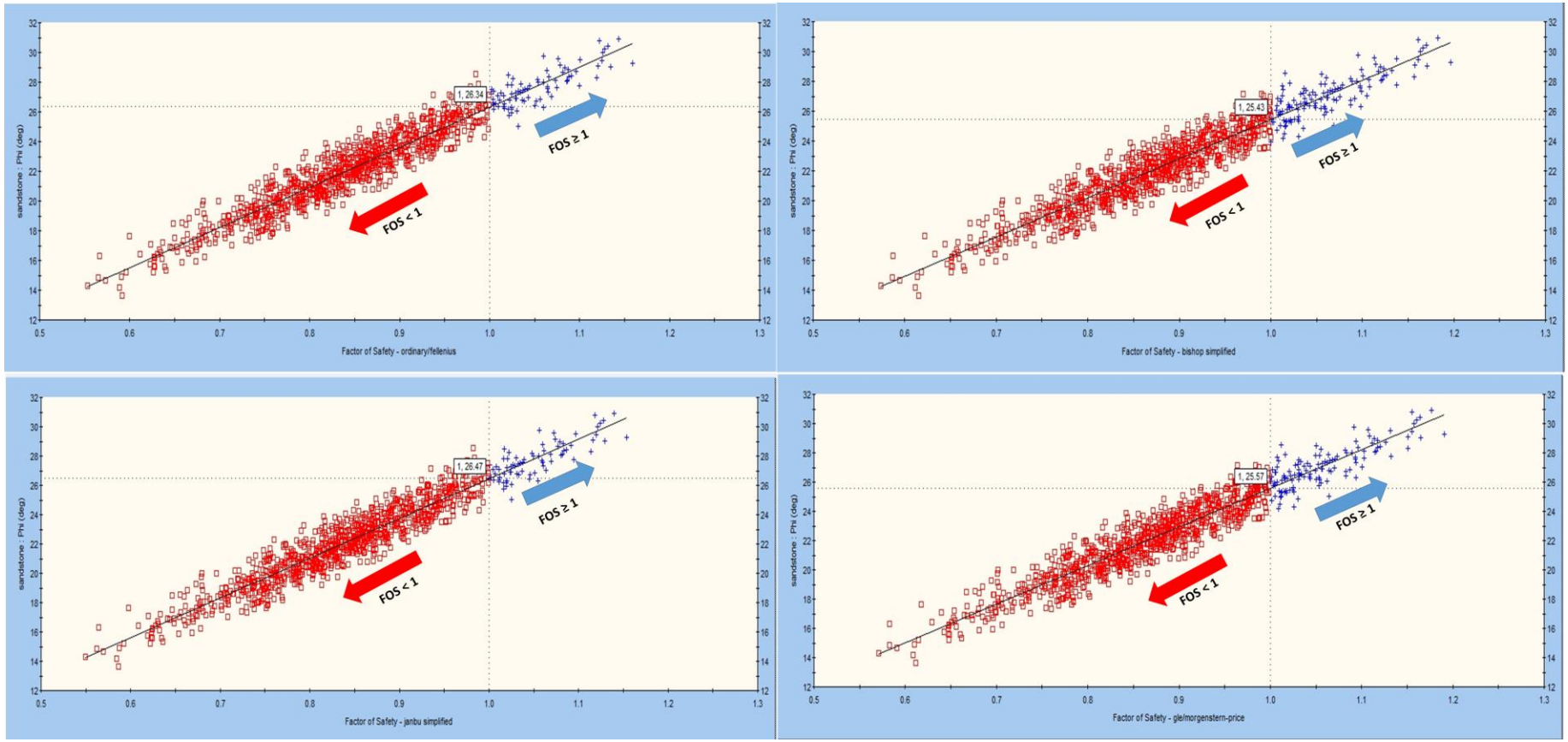

Figure 7.7. Correlation Coefficient of the slope in location one (a) Ordinary method failure distribution (b) Bishop method failure distribution (c) Janbu Simplified failure distribution (d) Morgenstern-price failure distribution.

7.3.2.5 Convergence Plot

Further verification was performed using convergence plot analysis and the results of the analysis also proved that the samples used were enough and the verification was exactly at the failure point (see Figures 7.8 to 7.11 as an example).

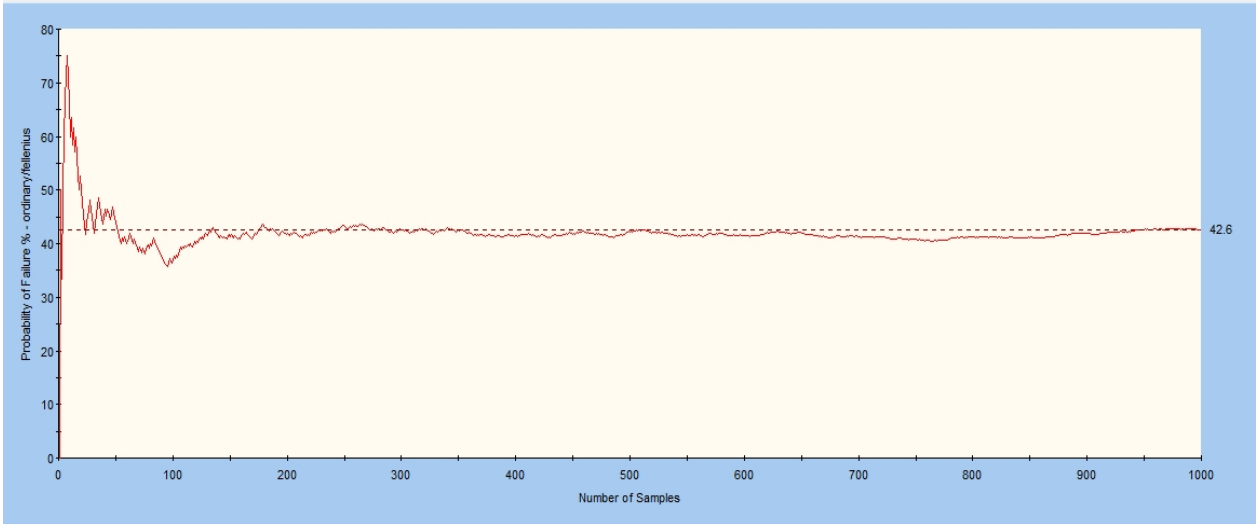

Figure 7.8. Convergence plot using Ordinary method.

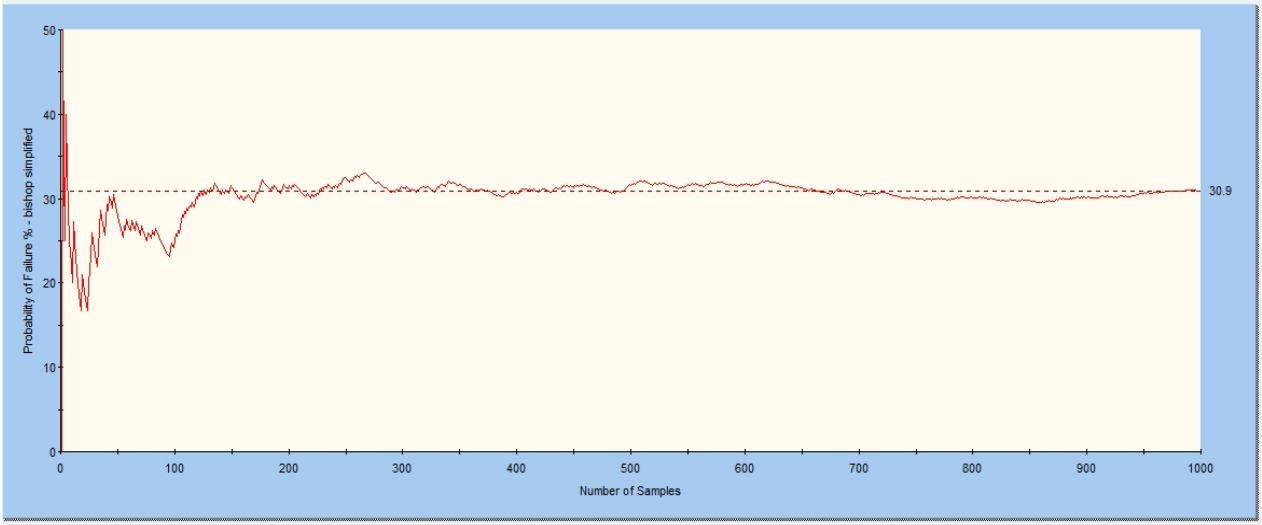

Figure 7.9. Convergence plot using bishop method.

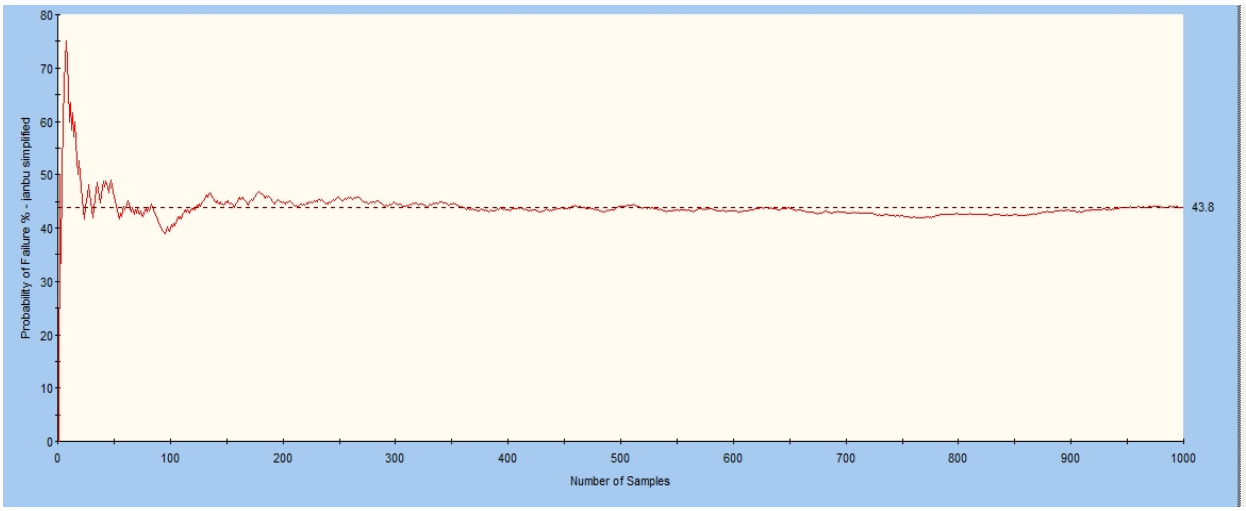

Figure 7.10. Convergence plot using bishop method.

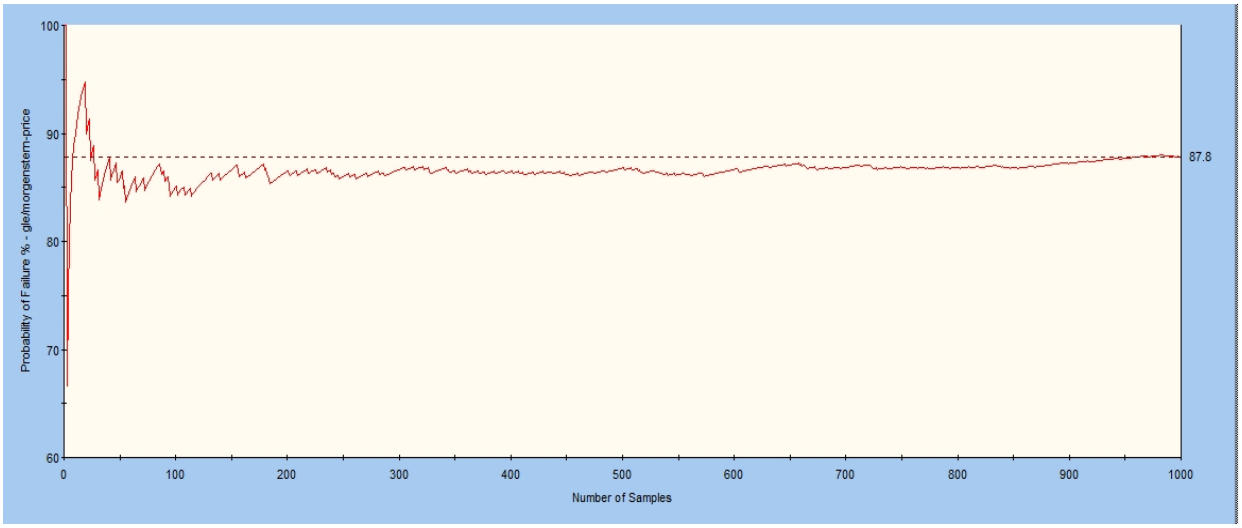

Figure 7.11. Convergence plot using bishop method.

7.4. Concluding remarks

The results from deterministic analysis denoted that slope in location one is stable and the slope in location two is unstable, these results were validated by all deterministic approach techniques. Nevertheless, the results obtained from the probabilistic analysis denoted that the mean safety factor of the slopes was closely related to deterministic solutions, furthermore, the probability failure shows that 70% of the slope in location one

is stable meanwhile, 9 to 13% of the slope in location two was declared stable. Furthermore, results on probability analysis using the reliability index have shown that both slopes are not reliable though the slope in location one presents a reliable index closer to one. The probability analysis approach declared that though deterministic analysis may declare the slope stable detailed analysis of the slope point must be analyzed to acquire a reliable stability number. One may argue that a single stability number that has been used in N1 highway roads could have been the main issue that contributed toward reoccurred slope stability since the slopes were declared stable meanwhile, they were not. It can, be concluded that the probability of failure corresponding to a particular factor of safety and an allowable risk criterion can be used to establish a consistent target for the design process of slopes along the N1 road. It can be recommended that the reliability analysis may be preferred as compared to deterministic analysis which is based on a global mean safety factor of the slope.

Chapter 8 Developing a reliable slope susceptibility map based on a GIS-based approach, machine learning and finite element formulation of the bound theorems

Although both the GIS-based approach and machine learning have been extensively explored in predicting and mapping the landscape in terms of slope failure based on landslide susceptibility, the question that is always raised is how robust landslide susceptibility estimates are. In this study, we strive to bridge the gap by introducing advanced geotechnical modelling using lower and upper bound solutions of limit analysis as benchmarking or validation techniques. Similar to other landslide or slope susceptibility mapping studies, this study commenced with developing the slope susceptibility map using analytic hierarchy process (AHP) and fuzzy logic (GIS-based approach and machine learning respectively) and later followed by validation using upper and lower bound solutions. The results of the simulations denoted both AHP and fuzzy logic present closely related results in highly susceptible areas while differing greatly in both low and moderate susceptible. Following that six sections of the study area divided into three categories low, moderate, and highly susceptible were used for validation using upper and lower bound solutions. The finite element solutions have confirmed that the areas classified as high, moderate, and low susceptible are benchmarked with upper bound solutions yet a bit far from the lower bound solution. It is argued that if correct mechanical and physical properties of the slopes are used, the AHP and fuzzy logic present reliable results in terms of slope susceptibility. Owing to that the sharp drop in the AHP and fuzzy logic is believed to be controlled by the algorithms among the models. Therefore, further studies may be conducted in understand a sharp distinction between the GIS-based approach and machine learning tools.

8.1 Introduction

Landslide susceptibility mapping (LSM) is considered one of the recent risk hazard analysis techniques that explores the use of ASTER imagery in management planning and risk mitigation measures of landslides (Arabameri et al., 2019; Fan et al. 2019). Numerous recent studies explore various LSM approaches worldwide (Refahi 2000; Bouma and Imeson 2000; Zhang et al., 2019). These approaches are summarized into two categories: heuristic deterministic and statistical techniques (Zhang et al., 2019). Based on the expert's knowledge, heuristic methods are used to classify landslide-prone areas into several groups, from high to low classes; although these methods or techniques are not completely accurate, they provide reasonable results. The above-mentioned is often used for susceptibility mapping in large areas, with the historical background of the landslide occurrence (Aleotti and Chowdhury 1999; Reichenbach et al., 2018). Meanwhile, the deterministic techniques fully depend on numerical simulation of the physical mechanism that controls slope failure (Zêzere et al., 2017; Budimir et al., 2015). However, this method is not appropriate for large-scale mapping due to the impracticality with which the model will be present.

On a large scale, the material could be heterogeneous, therefore the model has a greater chance of failing to capture all features. Another factor that made the technique unreliable for large scale is the huge array of data, rock mechanical properties, wetness and soil saturation, and soil depth. Lastly, the statistical and probabilistic techniques incorporate bivariate, multivariate statistical methods, certainty factors, and knowledge-based techniques such as artificial neural networks and fuzzy logic approaches (Dehnavi et al., 2015), this method appears to be most promising in detecting landslides (Dehnavi et al., 2015). Nonetheless, for all these methods to produce reliable results the input parameters such as causative factors have to be correctly filtered. The most common causative factors that define LSM are briefly discussed below.

The analysis of the conditions leading to landslide events is crucial when attempting to identify landslides causative parameters (Tyodo, 2013; Rawat et al., 2015; Ghosh et al., 2017; Ramesh et al., 2017; Gupta et al., 2018; Ramos-Bernal et al., 2018). The parameters controlling landslide occurrence can be generally grouped into three

categories: static, variable, and triggering factors (Tyoda, 2013). First, static factors are factors unlikely to change within a short period of time, such as geology, geomorphology, and vegetation type (Sarkar and Kanungo, 2004). These factors define the preparatory factors of the landslide. Second, variable factors vary as little as seasonally to as much as daily. They include vegetation health and productivity and soil water contents. A dry season may cause rapid deterioration and loss of vegetation cover thus increasing the likelihood of landslide occurrence. Last, triggering mechanisms such as heavy rainfall and earthquakes set off landslide occurrences provided that the static and/or variable factors characterizing the area are susceptible to slope failure (Tyoda, 2013).

Different techniques are used to weight the causative parameters of landslides and to model susceptibility maps (Quan and Lee, 2012; Rawat et al., 2015; Ghosh et al., 2017; Ramesh et al., 2017; Gupta et al., 2018; Ramos-Bernal et al., 2018; Bchari et al., 2019). The appropriate technique is selected based on the nature of a problem, observation scale, and the availability of data related to the causative factors (Sarkar and Kanungo, 2004). These techniques can be categorized into two groups i.e., quantitative and qualitative (Glade and Crozier, 2005). The quantitative technique, also known as the Weight of Evidence approach (Tyoda, 2013), focuses on developing ways of quantifying the relative importance of various factors to slope failure (Kanungo et al., 2009; Gupta et al., 2018); while the qualitative technique, also referred to as map combination approach (Tyoda, 2013), relies on the knowledge of the expert in assigning weights to the causative factors (Ghosh et al., 2017; Ramesh et al., 2017). The quantitative approach requires a large number of landslide points as an input dataset to weigh the significance of each causative factor characterizing the area (Singh et al., 2011; Tyoda, 2013; Gupta et al., 2018).

Geotechnical simulation as a validation model for both the GIS-based approach (AHP) and machine learning (fuzzy logic) solutions of slope susceptibility estimates is introduced in this study. Very limited studies have implemented this approach, yet this study found it significant. Owing to that, it has been documented that geotechnical properties of the solid mass contribute largely to the accuracy of the slope analysis, yet this study proposes to benchmark the GIS-based approach and machine learning tools with lower and upper

bound solutions of limit analysis using finite element formulations theorems. Furthermore, instead of relying on the accuracy of the two models (GIS-based approach and machine learning) different tools which are well established in the field of slope stability to accurately verify the performance of the two models will be implemented.

The usual landslide susceptibility analysis using a GIS-based approach and machine learning tools as stated above was performed. The results of the two methods were therefore subjected to accuracy analysis using the area under curve technique. Following that few sections of the study area denoted as highly, moderately and low landslide susceptible were used as cases to validate the accuracy of the two models using finite element formulations based on the stability number of the slope in both lower and upper bound solutions of limit analysis. Excluding the introduction, this section which is divided into various sections, documents a brief description of the study area followed by methods and materials, and then the results and discussion. The results and discussion incorporate the development of landslides susceptibility maps, followed by an accuracy analysis of the two models, and the last section is dedicated to validating the results documented by two methods using the geotechnical approach. Thereafter, the concluding remarks of the study follow.

8.2 Methods

The methodology of this study is divided into three sections, the first section documents how susceptibility factors were designed followed by procedures for both AHP and fuzzy logic, and lastly, the detailed procedure in the validation method is documented.

8.3 Results and Discussion

The section is divided into three subsections which incorporate results and discussion on AHP, fuzzy logic as well as the validation conducted using finite element formulations of lower and upper bound solutions. Detailed results and discussions of the study are documented below.

8.3.1 AHP and Fuzzy Logic results

The results simulated by AHP are shown in both Figure 8.1 and Table 8.1. Based on the results of the study low, moderate and high susceptibility occurrences are represented by

34%, 65%, and 1% of the study area respectively. According to Figures 8.2 and 8.3, the areas with high slope susceptibility are mostly those along with the road cuts with high slope height, discontinuities and weathered rock mass, cut across by several joint sets. However, these areas are not necessarily based on the direction but rather based on rock type and slope parameters. In fact, weathered granites and steep slopes were noticed to be the common factor associated with the instability. Furthermore, the field observations as shown in Figure 8.3 have documented that most of these areas rated highly susceptible are not far from major geological structures. These slopes were affected by improper road construction, which changed the morphology of the area.

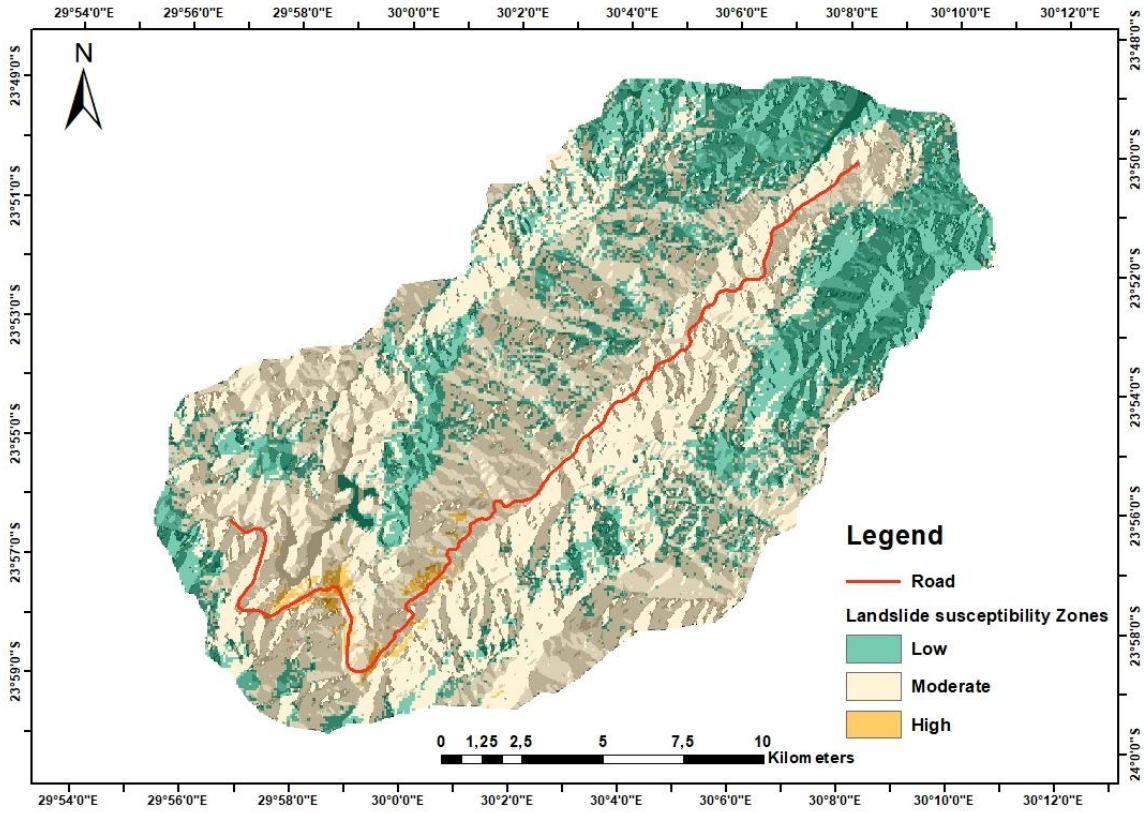

Figure 8.1. AHP results

According to the previous discussion, the areas considered highly susceptible covered about 3616 hectares of the entire study area. Furthermore, the areas were also found to be bounded by contact zones of various granites, and historically these granites are expected to be formed in a different age as such the formation of different rock units may

have contributed to the disintegration of the rock mass, while weakening the rock mass. Additionally, the effect of mechanical blasting may have catalysed the development of fractures across the slopes. Meanwhile, the heavy rainfall reported in the study area may have also contributed to reducing the resistance of the material to flow, as shown in Figure 8.3a.

Table 8.1. Different classes of landslide susceptibility maps obtained by the AHP method

Landslide susceptibility	Count of pixels	Area (Ha)	Area (%)
Low	116915	10522.35	34
Moderate	226637	20397.33	65
High	3616	325.44	1

The slope instability in the area may be attributed to both driving forces and resistive forces. To simplify these factors, based on the observation and previous studies (Hoek and Bray, 1981; Raghuvanshi, 2017; Lamessa, 2019), all highly susceptible areas were governed by both internal and external factors where internal factors incorporate those of the geometry of the slope, surface drainage system, groundwater conditions, mineral composition, shear strength parameters of the material, on the other hand, the external factors are governed by rainfall, and human activities. Therefore, the high susceptibility estimates by the model correlate with the observations.

Following the high susceptibility, a moderate susceptibility category of the slope was also noted (see Figures 8.2 and Figure 8.3b and e and Table 8.1) and the area with moderate susceptibility was found to take a high portion of the study area with about 65%. The areas covered about 20397.33 hectares, mostly dominated by stiff clay soil. It is expected that the soil material will gain strength with depth. It has been observed that most of these slopes were affected by soil erosion and some portions of these slopes had experienced

shallow slope sliding due to heavy rainfall, which changed the solid material from a solid phase to liquid-solid phase. One may also argue that most of this clay soil contained minerals such as muscovite or micas which are prone to low shear strength among other aspects.

Nevertheless, the moderate susceptibility areas also have some pre-existing slope failure, it was also noticed that most of these slopes were dominated by soil mass which appears to sit on top of the country-rock, and the thickness of the soil mass varied. Furthermore, the thickness of the layers at some point was very thin as such large deformation or movement of material is not expected. In terms of the very low and low susceptibility, the area was contained by about 34%, nevertheless, these areas were mostly dominated by vegetation with various soil types, however, the road slope cut height was very moderate or less than 3m and as such the possibility for such slopes to fail has been considered very low to low. Though some of the areas were dominated by granite which is not weathered. One important factor is that most of these slopes were located far from drainages and faults as well as jointing, which contribute to the low susceptibility of the slope. It was also evidenced that the slope does not even present some pre-existing slope failure.

In terms of fuzzy logic, three categories of slope susceptibility were developed, which are low, moderate, and high susceptibility. According to the study results, approximately 1, 3% of the study area with a total area of 394,7 hectares is in the high susceptibility areas.. Though the estimation was higher than those of AHP they are closely related, in fact, the two methods overlap each other by 0.3%. Furthermore, in terms of moderate, it appears that fuzzy logic considered most of the areas to be considered moderate susceptible to low susceptible. However, this gives the impression that though fuzzy logic is assembled within the ArcGIS its results are independent. Furthermore, it may be deduced that the sharp drop (from 35% to 1.1%, see Tables 8.2 and Figure 8.3) the percentage in moderately susceptible from AHP to fuzzy logic may be due to the algorithms per method. However, the sharp drop has also affected the total area considered moderate susceptible.

In terms of low susceptibility, fuzzy logic considered several portions of the study area as low susceptible; however, one may argue that the large drop in moderate susceptibility indicates that a large portion of the study area is low susceptible. These two techniques appear to give closely related results in terms of being highly susceptible but the low and moderate groups appear to differ greatly, and it is believed that the variation may be controlled by their algorithms.

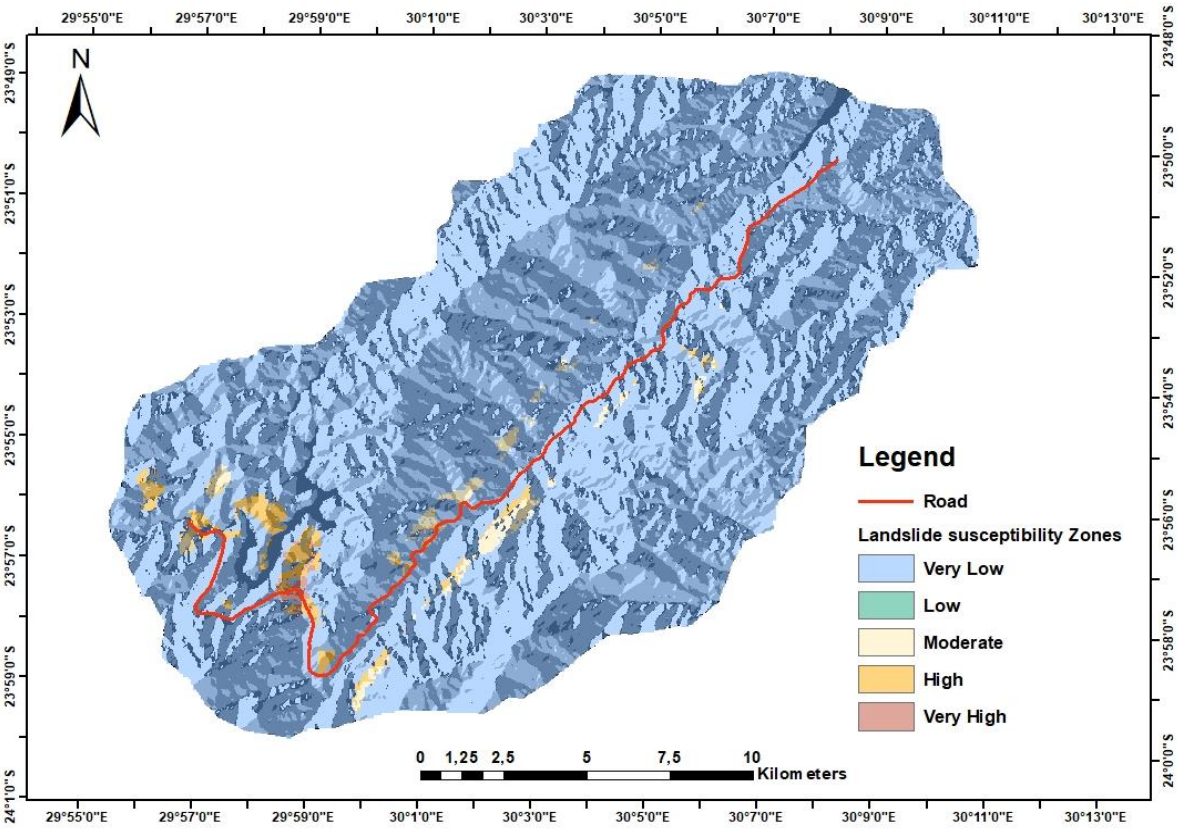

Figure 8.2. Fuzzy logic slope susceptibility

Table 8.2. Different classes of landslide susceptibility maps obtained by the fuzzy method

Landslide susceptibility	Count of pixels	Area (Ha)	Area (%)
Low	339050	30514,47	97,6
Moderate	3877	348,93	1,1
High	4383	394,47	1,3

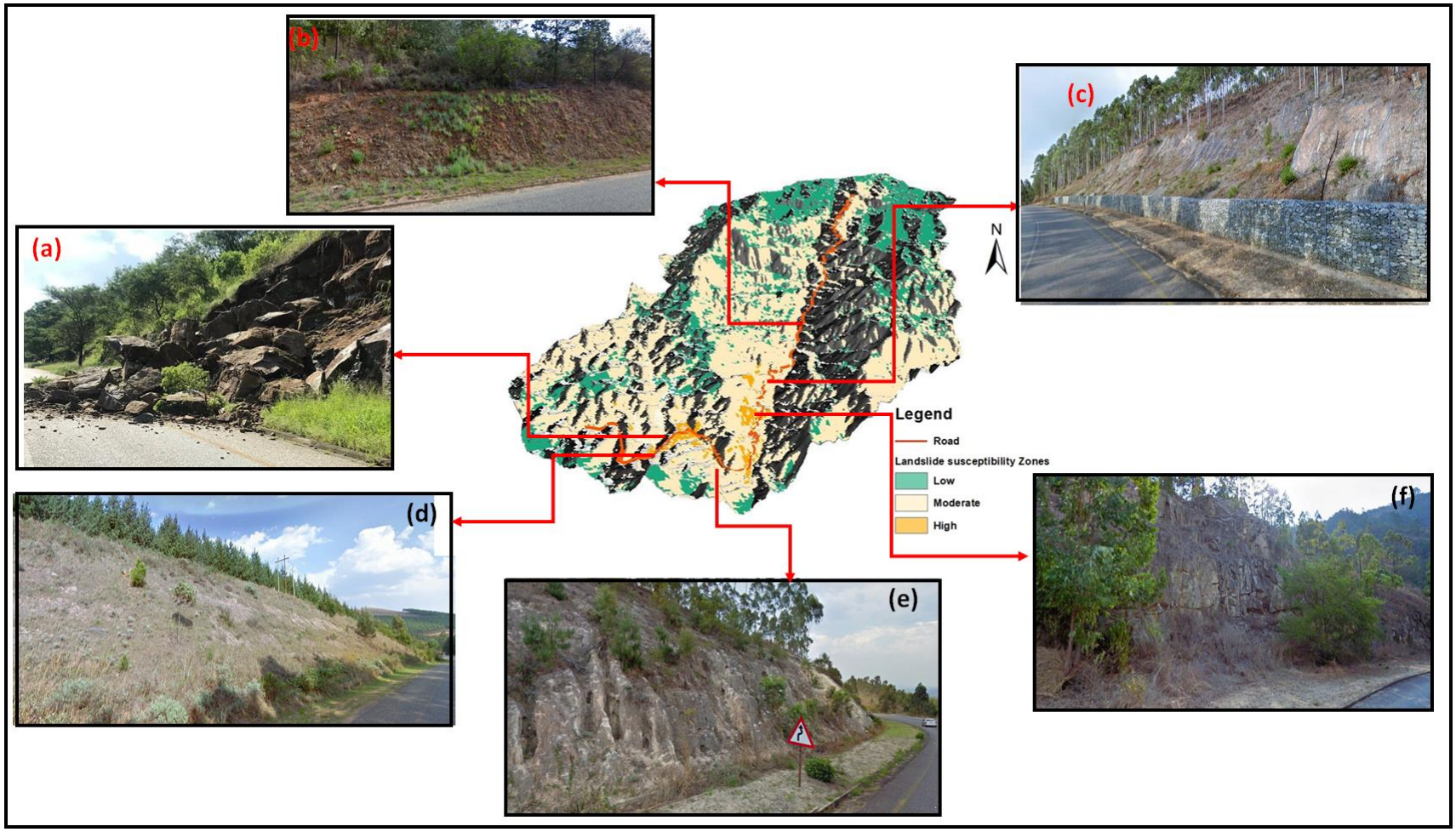

Figure 8.3. Observations on the conditions of the selected slope studied

8.3.2 Accuracy of the assessment

To validate the precision rate of landslide susceptibility models (maps) of the study, the area under curve (AUC) method was used. A total of pre-existing and existing 100 landslides (slope failure) observed at the field were used for training and validation of the models. The data were divided into two groups: one with 70 as training data (70%) and validation data (30%). Therefore, it was found possible to develop a success rate in both models as shown in Figures 8.5 and 8.6. AUC values of the accuracy curve were calculated by the simple trapezium method and the values were 0.712 and 0.88 for fuzzy logic and AHP respectively. One may argue that the high accuracy of 88% obtained for AHP may be influenced by the field observation which therefore helped in rating each slope susceptibility factor, while fuzzy logic uses a knowledge-based system.

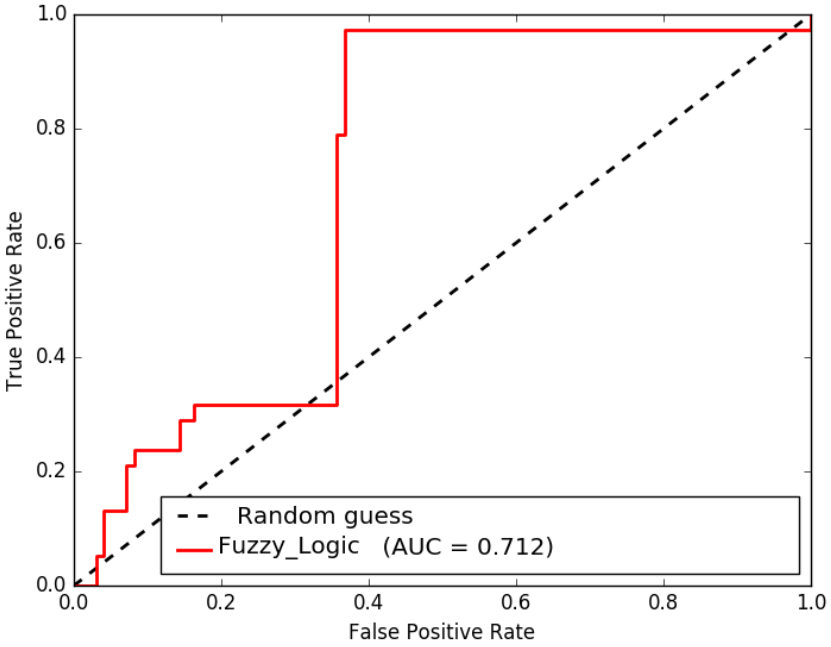

Figure 8.4. AUC simulated for Fuzzy logic

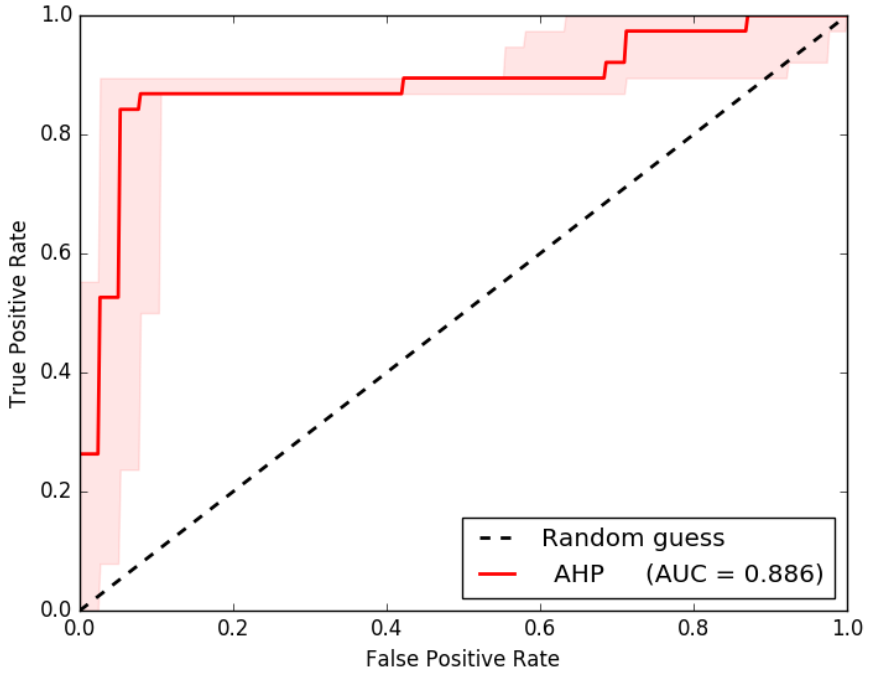

Figure 8.5. AUC simulated for Fuzzy logic

Furthermore, one may argue that the results obtained in this assessment also correlate with previous studies such as those of Gupta and Joshi (1990); Roodposhti et al. (2014); Zhou et al. (2016); Abedini and Tulabi (2018); Roy and Saha (2019) and El Jazouli et al. (2019). Nevertheless, numerous approaches to mapping the susceptibility of landslides have been well documented in the literature in the last few decades, including inventory, statistical analysis, heuristic, semi-quantitative, quantitative, probabilistic, and multi-criteria decisions, the accuracy of all these methods has not been accepted universally (El Jazouli et al., 2019) due to the accuracies associated with the method. Therefore, the use of the geotechnical method invalidating the results of the study was introduced. Numerous studies in susceptibility mapping recommended that the results of the susceptibility can be accurate, provided the geotechnical properties of the material and material behaviour are known (Ozturk et al., 2020).

It has been evidenced in studies by Van Den Eeckhaut et al. (2005); Galli et al. (2008); Korup (2008); Schulz et al. (2018); Dou et al. (2015); Reichenbach et al. (2018); Braun et al. (2015); Provost et al. (2017); Kalantar et al. (2018); Corominas et al. (2013) and Golovko et al. (2015) that much of landslide susceptibility research is more concerned about predicting and mapping susceptibility to slope failure. As a result, many of these studies use similar models to validate the accuracy of the prediction yet the research on merging these models with geotechnical models or advanced geotechnical methods has been avoided or remains largely untested. Therefore, a detailed numerical simulation verifying the estimated susceptibility is presented in the next section using the rigorous upper and lower bound solutions of the limit analysis.

8.3.3 Numerical simulation on stability analysis of the selected slopes

Further analysis of the accuracy of the susceptibility estimates was conducted using geotechnical numerical simulations looking into the slope number of the slopes based on rigorous upper and lower bound solutions of the limit analysis. As already indicated the rigorous upper and lower bound solutions of limit analysis are governed by finite element theorems, which incorporate stress and strain interacting with the material. In fact, the finite element theorems enable us to incorporate both the physical and mechanical properties of the solid mass to identify the stability of the slope.

Six cases were selected which are based on susceptibility estimates across the area, the selected areas were therefore modelled using the geotechnical method as a way of generating the correlation or verification of the assessments. The results in cases one (a) and six (f) have shown that both AHP and fuzzy logic classify the area as highly susceptible (Table 8.3), one may argue that the similarity between the two methods was due to overlapping the susceptibility factor implemented in this study.

Furthermore, the factors were based on observations, and geotechnical and geological properties of the slopes. One may argue that the models were sufficient to classify the area. On the other geotechnical modelling using the bounds theorems have shown that the slope in the case can be classified as unstable due to a strength reduction factor of less than 1.5. One may say that the stability estimate by geotechnical modelling has many details in terms of the mechanical behaviour of the solid mass. In this case, the model also confirmed that the slope is susceptible to failure; however, the upper bound of the limit analysis appeared to relate closely to susceptible estimates presented by AHP and fuzzy logic, while the lower bound presents a much lower stability number indicating that the slope is extremely unstable. Furthermore, based on field observation (Figure 8.7), one may agree with the lower bound solution (Figure 8.8) that in case A, the slope has collapsed which then agrees with the simulation. Though the results of the two techniques are closely related, it is argued that the lower bound can be used for design and reinforcement purposes while the upper bound can be used to benchmark with the GIS-based approach and machine learning tools of slope susceptibility estimates.

Table 8.3. Results on the comparison between AHP and fuzzy logic with lower and upper bound solutions of limit analysis for slope susceptibility estimates.

Case studies	**Methods**			
	GIS-based approach	Machine Learning	Limit Analysis Solutions	
	AHP	Fuzzy logic	Lower bound	Upper bound
Case 1 (a)	Highly Susceptible	Highly Susceptible	Unstable (SRF=1.001)	Unstable (SRF=1.027)
Case 2 (b)	Low Susceptible	Low Susceptible	Stable (SRF=1.744)	Stable (SRF=1.804)
Case 3 (c)	Moderately Susceptible	Moderately Susceptible	Imminent-stable (SRF=1.253)	Imminent-stable (SRF=1.274)
Case 4 (d)	Low Susceptible	Low Susceptible	Stable (SRF=1.725)	Stable (SRF=1.754)
Case 5 (e)	Moderately Susceptible	Moderately Susceptible	Imminent-stable (SRF=1.207)	Imminent-stable (SRF=1.2283)
Case 6 (f)	Highly Susceptible	Highly Susceptible	Unstable (SRF=1.042)	Unstable (SRF=1.067)

In cases C and E, both fuzzy logic and AHP were also benchmarked with the rigorous lower and upper solutions of limit analysis. Both machine learning and remote sensing-based approaches agreed that the slope could be classified as moderately susceptible to slope failure. Likewise, in benchmarking the results, the lower bound solutions, together with the upper bound solutions estimate a stability number that classifies the slope as imminent stable (see Figure 8.9). This implies that there is still a great agreement between geotechnical modelling and the GIS-based approach to machine learning. Furthermore, similar results obtained in the first cases have been evident in the second cases that the lower bound solutions appeared to be more suitable to be considered as minimum standardized stability of the slope, meanwhile, the upper bound solutions (see Figure 8.10) are closely related to the estimates made by the GIS-based approach and machine learning.

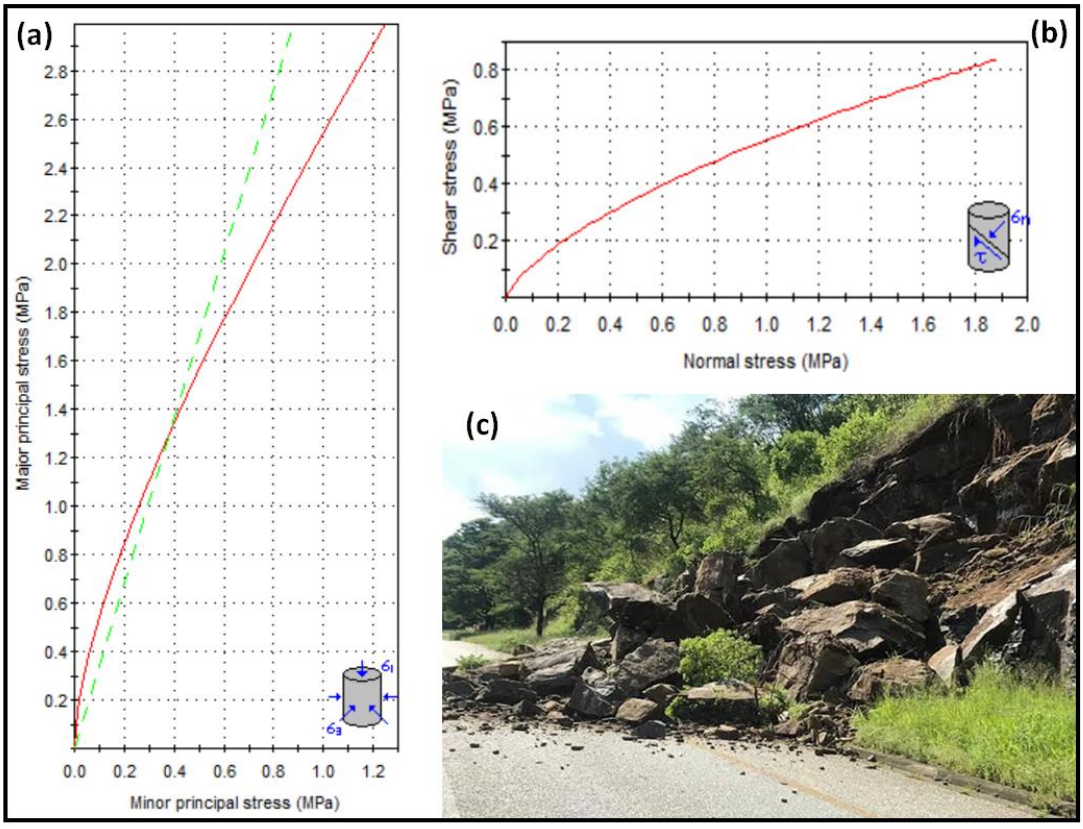

Figure 8.6. Distribution of stresses and material behaviour (a) major principal stresses versus minor principal stresses of the slope material (b)

shear stress versus normal stress and (c) example of existing slope failure along the road.

The last cases (b and d) were also considered, however, the results simulated by both the GIS-based approach and machine learning documented that the slopes are considered low susceptibility, implying that the slopes are not prone to failure, provided the external and internal factors of the slope remain constant. On the other hand, lower and upper bound solutions of the limit analysis documented that the slopes are considered stable (Figure 8.11). In this case, one may argue that the field observation also supports the results simulated by the three techniques implemented while validating the accuracy of the GIS-based approach and machine learning estimates of slope failure.

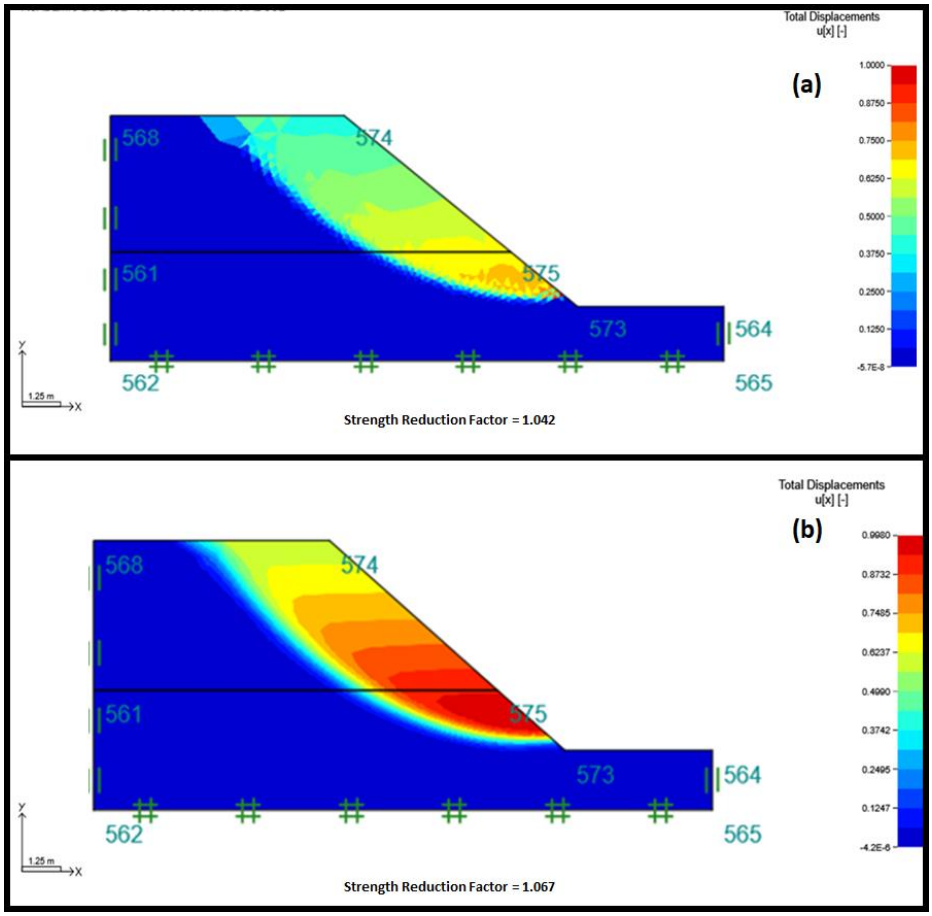

Figure 8.7. Estimated stability number using FEM for the first case study (case 1(a)) (a) Lower bound solution (b) upper bound solution.

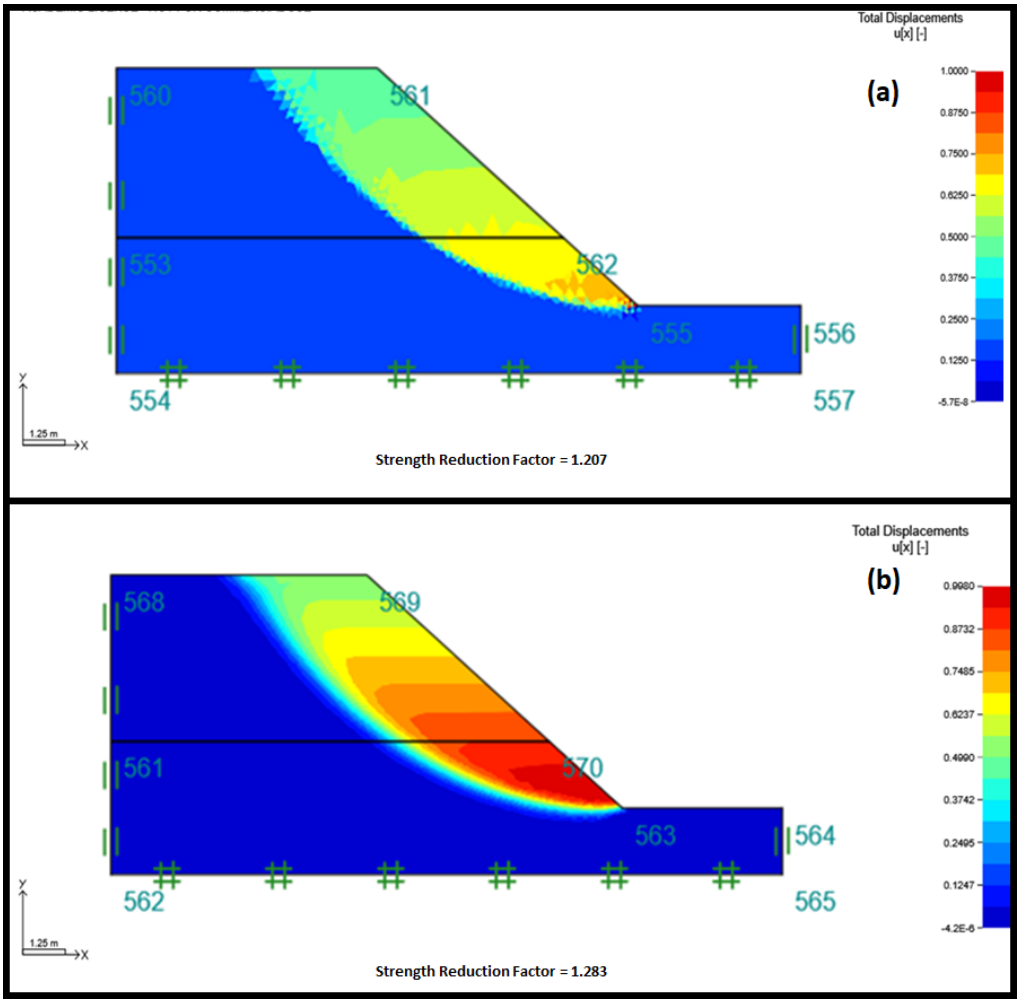

Figure 8.8. Estimated stability number using FEM for the first case study (case 5 (e)) (a) Lower bound solution (b) upper bound solution.

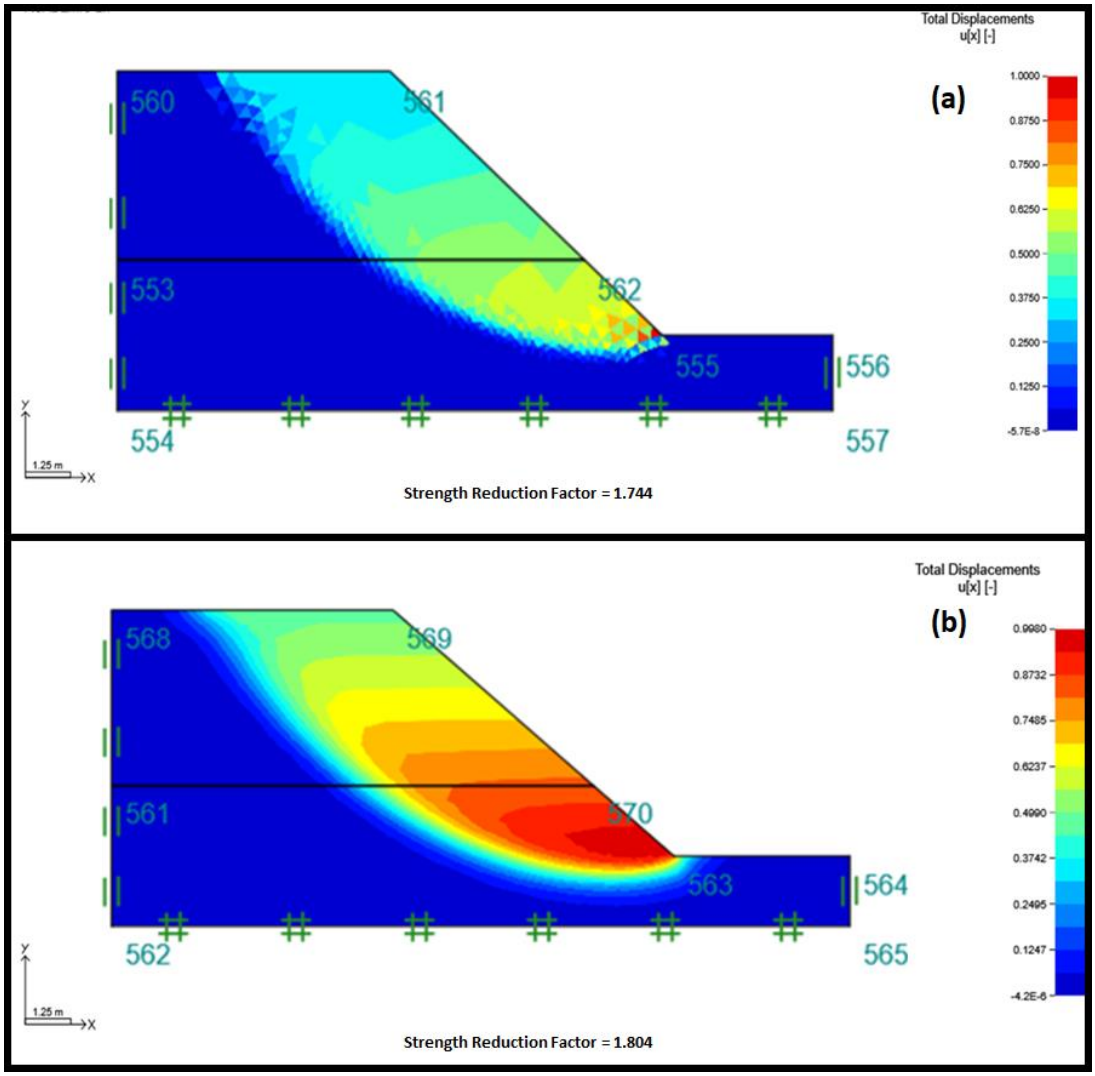

Figure 8.9. Estimated stability number using FEM for the first case study (case 4(d)) (a) Lower bound solution (b) upper bound solution.

8.4 Concluding remarks

The results of the study have shown that the slope susceptibility estimates developed using the GIS-based approach (AHP) were very closely related to those of machine learning tools (Fuzzy logic) in terms of estimating highly susceptible zones. Though a few overlaps (about 0.3%) were denoted across the analysis. In terms of low and moderately susceptible, the two models were found to differ greatly, in fact, their results were versus, and it is believed that such differences were induced by the algorithms among the methods. However, in terms of the accuracy of the models, the AHP was found to produce about 88%, while the fuzzy logic produced about 71%.

One may argue that the high percentage produced by AHP may be due to the allocation of slope susceptibility factors which were controlled by field observations and mechanical and physical properties of the solid material (soil and rocks), while the fuzzy logic is mostly based on expert knowledge among others. In general, the accuracy of the two models was sufficient. In terms of validation, the geotechnical model of the rigorous lower and upper bound solutions of limit analysis was utilized. Sections of the study areas denoting highly susceptible, moderate, and low susceptible were modelled to generate a comparison. The model also confirms that the estimate from both models was closely related to the upper bound solutions, while the lower bound solutions were a bit lower than what was expected but they could be used for design and reinforcement purposes. However, it was noted that if appropriate geotechnical properties of the solid mass across the slope are known, then both the GIS-based approach and machine learning may be able to produce accurate results of slope susceptibility estimates. It is, therefore, argued that the combination of three tools may be used for future research to develop a more reliable robust model for slope susceptibility. Furthermore, it is also argued that in bridging the knowledge gap on how robust landslide susceptibility estimates are, geotechnical modelling can be a useful tool in validating the estimates. Lastly, it is recommended that the sharp drop in the moderate susceptible zones of the two techniques may be further investigated.

Chapter 9 Conclusion and recommendations for future work

The aim of this research study was to perform advanced reliability analysis of road-slope stability in soft rock geological terrain. Selected sites along the N1 highway and R71 roads in Limpopo Province were used as a case study. This chapter presents the summarised findings of the research study, detailed findings per objective, the overall conclusion, and recommendations for future work.

9.1 Summary of the research study

The purpose of the research study was to conduct an advanced reliability analysis of road slope stability in soft rock geological terrain with the national road (N1) and its tributary (R71) as case studies. The aim of this research study was supported by several objectives as follows: developing a predictive chart on the accuracy of Two-Dimensional Limit Equilibrium Methods in Predicting Stability of Homogenous Road Cut Slopes, developing a new method for stability analysis in a multi-faulted rock slope and performing the numerical study on the flow evolution process of slope failure, to conduct a reliability analysis of slope stability using probabilistic analyses compared with deterministic analysis and to apply the GIS-based approach, machine learning and finite element formulation of the bound theorems in developing reliable slope susceptibility along the R71 road in Limpopo.

To achieve the aim and objectives of the research study, field observations and measurements, structural mapping, limit equilibrium, limit analysis, Monte Carlo Simulation, fuzzy inference analysis, GIS digitization, and analysis were performed. Software packages such as SLIDE, FLACslope, Optimum 2G, DIPS, RocLab and ArcGIS were used.

The accuracy classification chart for LEMs, a new method for performing stability analysis in multiple faulted slopes, a reproduction of failure evolution of slope was developed. Monte Carlo Simulation has established the most reliable technique to analyze slope stability effectively. The steepness of the slope, rock and soil properties, extreme rainfall, and geological features were demonstrated to influence slope instability based on an integrated approach as stated above. The above-mentioned major findings, concluded that the developed accuracy error classification chart of LEMs, the new method of slope stability in multi-faulted slopes and the slope susceptibility map are useful. Though the reproduction of failure evolution of slope was successfully achieved, for material to flow for a longer distance, high kinetic energy and more shearing of material are expected to take place during this process. It is recommended that other sophisticated methods could be utilized to further the results

9.2 Development of an error accuracy classification chart for LEMs

The accuracy of the Limit Equilibrium method in terms of estimating the stability number of soil or rock slope has been questioned or debated. Alternative methods were used rather than addressing the problem at hand. On the other hand, the Limit Equilibrium methods were preferred over other methods such as Limit Analysis due to their simplicity. The concern which is often voiced by many engineers and scientists has motivated the present research study. Therefore, this research study strived to address the following to identify the most appropriate LEM, in terms of predicting the stability of the slope with a solution that is close to those of SRM/SRF, secondly to identify which of the bound solutions (lower and upper) is closely related to LEM solutions in homogenous soil and rock slope. Several practical examples were used to establish a reliable LEM by comparing the slope stability analysis and bounding solutions to limit equilibrium methods (eight methods). Six case studies were utilized to establish the above mentioned, and two computer codes (SLIDES used for LEM solutions and

Optum G2 used for bounding solutions of limit analysis) using finite element formulations were used.

Based on the six case studies considered, it was found that the exact stability solutions produced by Janbu Simplified and Ordinary Methods of limit equilibrium in most cases are bracketed within 2 to 10% accuracy error as compared to the rigorous upper bound solutions of the limit analysis. However, these conditions of lower accuracy error were noted in loose sand, medium sand, dense sand and stiff clay soil slope, with the consideration of the effect of the increase in strength of material with depth. Therefore, it can be concluded that the implementation of the Janbu Simplified and Ordinary methods of limit equilibrium are best in the above-mentioned cases of soil slope material.

Furthermore, the detailed comparison of the bounding solutions with limit equilibrium methods has also demonstrated that the prediction of stability numbers by the Spencer and Morgenstern Price method are similar throughout, though the methods were not producing closely related solutions to those of upper bound solutions. This implies that the use of these two methods simultaneously is not required since they give similar solutions.

It was also observed that the Corp Engineering number two method of limit equilibrium produced the highest accuracy error percentages throughout the case studies provided, however, its error accuracy was also found to differ from those of Janbu Simplified with a bracket within 10 to 12%. In simple terms, the method has been found to overestimate the stability number in all cases.

Though the focus was to benchmark the limit equilibrium solutions with the upper and lower bound solutions of limit analysis, all the lower bound solutions were found to be a bit smaller than those of limit equilibrium solutions in all cases. It is, therefore, concluded the lower bound solutions can be used for designing stable excavation, in other words, the lower

bound solutions are closely related to the realistic stability number of the slope.

A simple accuracy classification chart was developed based on the results of the chapter. The chart shows various methods of LEMs and their accuracy error percentage per material or soil slope material. It is believed that the chart is useful to engineers who prefer to apply LEMs in classifying the stability of soil slope. Furthermore, the chart also provides room to explore other sophisticated methods that can improve the prediction of error accuracy of the LEMs in stability analysis.

9.3 Development of a new method for slope stability analysis in multi-faulted slopes

This research study also presents the development of a new method for stability analysis of a multi-faulted rock slope using a ubiquitous joint. The development of this new method was motivated by the fact that in most slopes there is a clear interaction between lithology and geological structures, however, the stability analysis of such slopes has been generalized without the consideration of the sensitivity properties of the faults and the composition of the surrounding rock mass. It is well documented in several previous studies; that the overestimation of the stability number presented in several studies has imposed several design challenges while increasing the potential of failure among the slopes.

As such detailed studies were conducted and the study commences with the evaluation of the sensitivity analysis of fault properties on the stability number of the slope (FoS). This sensitivity analysis incorporated fault geometry, thickness, shear strength properties and mesh densities with a comparison of several ubiquitous joints. After establishing the sensitivity of fault properties, a new method was proposed to capture all these sensitivity properties of faults and rock mass into the stability analysis. The new method introduced the so-called zone of influence, it also analyzed each

fault as a case study and lastly, the overall stability number of the slope can be identified.

A practical application of both current practice and the proposed method was demonstrated based on a slope composed of three faults (planar and two undulated planar faults filled with dolerite dyke while the planar fault is filled with quartz). The results of the study have shown that the current practice tends to overestimate the stability number of the slope. Furthermore, the current practice also generalizes the composition of the slope which jeopardized the accuracy of the estimated stability number. The proposed method was implemented and it was discovered that the current practice overestimates the stability number of a multi-faulted slope by 37%. This implies if all sensitivity properties of faults and joints orientation are well captured in the analysis the estimated stability number is reduced by 37% compared to the current practice. It is maintained that if the proposed method can be implemented in jointed and multi-faulted rock slopes, an accurate stability number of the slope can be achieved. However, it is crucial to mention the proposed method requires extra inputs such as structural properties of the joints and faults in order to achieve the accurate stability number. One may argue that capturing the actual size of the fault in a model has been a concern to many authors but the proposed method strives to look into the details of each fault in order to acquire the accurate stability number of the slope.

9.4 Numerical simulation on the reproduction of flow evolution process of slope failure

A numerical simulation that describes the failure evolution of a slope dominated by faults along with a road cut was used for the purpose. A finite element method associated with an elastoplastic model with strain softening was adopted to provide a failure evolution of R71 road cut slope instabilities. The numerical simulation follows the finite element theorems of the upper

and lower bounds solutions, yet their governing equations are those of finite element methods following the stain-softening theory.

The results have demonstrated that the present computational framework is capable of quantitatively reproducing the failure evolution process and the final run-out distance of the slope material. The simulation has evidenced that the flow evolution of material during extreme rainfall is expected to extend to the final deposit of 4.5m, which is also confirmed by the field measurements and observations. Furthermore, the simulations also demonstrated that the distance in which material can reach is largely controlled by the composition and phases the material undergoes during flow evolution. Owing to that, the resistance of material has a major role in the run-out of the material; this resistance of the material is also controlled by shearing and absorbed kinetic energy during the process. The overall conclusion is that, for material to flow for a longer distance, high kinetic energy and more shearing of material are expected to take place during this process.

9.5 Reliability analysis of road cuts slopes

The N1 highway road in Limpopo Province, South Africa has been reported to experience multiple slope instabilities along the road slope cut. Yet, few studies have been conducted to understand the mechanism and classify the slope based on stability number. However, these studies were more concerned with the overall FoS of the slope using deterministic methods. Regardless of these studies, slope instabilities along road cuts have been reported continuously. Yet this research study attempted to present a reliability analysis approach to the slope stability along this national road.

In this regard, a deterministic approach with different methods of stability analysis, namely the ordinary method, Bishop’s method, Janbu's method and Morgenstern Price method using the iterative capabilities of software SLIDEs have been used to assess the stability number. The deterministic

analysis was followed by the probabilistic analysis of the similar slopes using mean safety factor, probability failure and reliability index methods.

Knowing that the deterministic approach yields conservative values of factors of safety because assigned input parameters are single-valued and the spatial variation of the input parameters is not accounted for. The results from deterministic analysis denoted that slope in location one is stable and the slope in location two is unstable, these results were validated by all deterministic approach techniques. Nevertheless, the results obtained from probabilistic approach denoted that the mean safety factor of the slopes was closely related to deterministic solutions, furthermore, the probability failure shows that 70% of the slope in location one was stable meanwhile, 9 to 13% of the slope in location two was declared stable. Furthermore, results on probability analysis using the reliability index have shown that both slopes are not reliable though the slope in location one presents a reliable index closer to 1. The probability analysis approach declared that though deterministic analysis may declare the slope stable, a detailed analysis of the slope points has to be analyzed to acquire a reliable stability number. One may argue that a single stability number that has been used on the N1 highway road could have been the main issue that contributed to reoccurring slope stability since the slopes were declared stable but they were not. It can therefore be concluded that the probability of failure corresponding to a particular factor of safety and an allowable risk criterion can be used to establish a consistent target for the design process of slopes along the N1 road.

9.6 Developing a reliable slope susceptibility hazard map

The development of a reliable slope susceptibility map of a regional road (R71) which is an important route in connecting several areas as well as towns, malls, and farms has been found significant. GIS-based tools, machine learning, and geotechnical modelling were used to develop and

validate the results of the study. Though it has been well established that most slope susceptibility models aim to predict and map the degree to which the landscapes are prone to slope failure, these models were mostly developed using GIS and machine learning and validated using similar techniques. As a result, the accuracy of the results entirely depends on accurate input parameters of geotechnical properties of soil and rock. Nevertheless, most studies are not able to acquire the accurate values and behaviour of solid materials, yet the accuracy of the prediction is always expressed. It is proposed that the use of geotechnical modelling invalidates the estimates of slope susceptibility estimates since this model can analyse the mechanical and physical behaviour of solid mass.

The results have shown that the slope susceptibility estimates developed using the GIS-based approach (AHP) were very closely related to those of machine learning tools (fuzzy logic) in terms of estimating highly susceptible zones, though there were a few overlaps (about 0.3%) denoted across the analysis. The low and moderately susceptible models were found to differ greatly, in fact, their results were opposites. It is believed that such differences were induced by the algorithms among the methods. However, in terms of the accuracy of the models, the AHP was found to produce about 88% accuracy while the fuzzy logic produced about 71%. One may argue that the high percentage produced by AHP may be due to the allocation of slope susceptibility factors which were controlled by field observations and mechanical and physical properties of the solid material (soil and rocks), while the fuzzy logic is mostly based on expert knowledge among others. In general, the accuracy of the two models was sufficient. In terms of validation, the geotechnical model of the rigorous lower and upper bound solutions of limit analysis was utilized. Sections of the study areas denoting highly susceptible, moderate, and low susceptible were modelled to generate a comparison. The model also confirms that the estimate from both models was closely related to the upper bound solutions, while the lower bound solutions were a bit lower than what was expected but they could be used for design and reinforcement purposes. However, it was

noted that if appropriate geotechnical properties of the solid mass across the slope are known then both the GIS-based approach and machine learning may be able to produce accurate results of slope susceptibility estimates. It is, therefore, argued that the combination of three tools may be used for future research to develop a more reliable robust model for slope susceptibility. Furthermore, it is also argued that in bridging the knowledge gap on how robust are landslide susceptibility estimates? The use of geotechnical modelling can be a useful tool in validating the estimates.

9.7 Overall conclusion of the research study

The research study has shown that its purpose was to apply advanced reliability methods in addressing some of the gaps in knowledge regarding slope stability analysis in soft rock geological terrain. It is well demonstrated that limit equilibrium, limit analysis, machine learning, GIS-based tools, finite element and finite difference methods were applied for the purpose. The results of the research study have shown that the developed accuracy error predictive chart for LEMs is very reliable and assists engineers and scientists in the field of study. Similarly, a new method for stability analysis in a multi-faulted slope was also developed and has been evidenced to be simple to use and very useful. Though it has been reported that the reproduction of failure evolution of a slope is considered a complex process (Sengani and Mulenga, 2020) and has been done in large deformation problems, this research study presented a developed numerical simulation of failure evolution in shallow slope instability, as such narrowing the gap regarding flow evolution in shallow slope failure has been achieved.

It is also crucial to indicate that the majority of slope stability analyses are based on a single stability number to classify the entire slope, yet continuous slope failure has been reported in those stable slopes. The reliability analysis of slope-based Monte Carlo simulation has proven that the deterministic analysis which have extensively utilized by engineers, does

not reliably predict of slope stability, yet the deterministic analysis shows that the slope is stable, and the probabilistic analysis shows that in reality, the slope may not be stable at all. It is therefore concluded that stability analysis should be a comprehensive process that incorporates a stability index, and probability failure among others. Lastly, the research study also demonstrated that the combination of GIS-based tools, machine learning and geotechnical methods provides more insights into the development of accurate slope susceptibility in the study area.

9.8 Recommended future studies

Based on the scope of the work covered in this research study, the following items are suggested for future studies:

- It is recommended that other sophisticated methods (SLIDEs 3D, PFEM, OPTUM G3) could be utilized to extend the results such as establishing the failure mechanism and the kinematics of the slope instability,
- The reliability analysis may be preferred as compared to deterministic analysis which is based on a global mean safety factor of the slope, therefore further study on the possibility of improving deterministic analysis is recommended.
- Lastly, it is recommended that the sharp drop in the moderate susceptible zones of the two techniques may be further investigated.

List of references

Abedini, M., and S. Tulabi. (2018). Assessing LNRF, FR, and AHP models in landslide susceptibility mapping index: A comparative study of Nojian watershed in Lorestan province, Iran. Environmental Earth Sciences 77 (11): 405.

Abramson L.W., Lee T.S., Sharma S., and Boyce G.M (2002). Slope Stability and Stabilization Methods. John Wiley and Sons Inc. 712.

Aleotti, P., and R. Chowdhury. (1999). Landslide hazard assessment: Summary review and new perspectives. Bulletin of Engineering Geology and the Environment 58 (1): 21–44. https://doi.org/10.1007/s100640050066.

Al-Naqshabandy, M.S. (2012). Reliability-based ultimate limit state design of lime-cement columns. Doctoral thesis. KTH Royal Institute of Technology, Stockholm, Sweden.

Althuwaynee, O.F., and Pradhan, B. (2016). Semi-quantitative landslide risk assessment using GIS-based exposure analysis in Kuala Lumpur City. Geomatics Natural Hazards and Risk 8(2): 1–27.

Anderheggen, E., and Knopfel, H. (1972). "Finite element limit analysis using linear programming." Int. J. Solids and Struct., 8, 1413-1431

Ansari, M.K., Ahmad, M., Singh, R., and Singh, T.N. (2014). Rockfall hazard assessment at Ajanta Cave Aurangabad, Maharashtra, India. Arabian Journal of Geoscience, vol. 7, pp.1773 – 1780.

Arabameri, A.; Pradhan, B.; Rezaei, K. (2019). Gully erosion zonation mapping using integrated geographically weighted regression with certainty factor and random forest models in GIS. J. Environ. Manag. 232, 928–942.

Aubry, R., Idelsohn, S.R., and Oñate, , E. (2005). Particle finite element method in fluid mechanics including thermal convection-diffusion. Computer and Structures, vol. 83, pp.1459 – 1475.

Ayalew, L. (1999). The effect of seasonal rainfall on landslides in the highlands of Ethiopia. Bulletin of Engineering Geology and the Environment, 58(1), 9-19.

Ayalew, L., Yamagishi, H., and Ugawa, N. (2004). Landslide susceptibility mapping using GIS-based weighted linear combination, the case in Tsugawa area of Agano River, Niigata Prefecture, Japan. Landslides, 1(1), 73-81.

Azarfar, B.; Peik, B. and Abbasi, B. (2018). A Discussion on Numerical Modeling of Fault for Large Open Pit Mines. 52nd US Rock Mechanics/Geomechanics Symposium held in Seattle, Washington, USA, 17–20 June 2018, pp1-12.

Barton, N.R. (1973). Review of a new shear strength criterion for rock joints. Engng Geol. 7, 287-332.

Barton, N.R. (1976). The shear strength of rock and rock joints. Int. J. Mech. Min. Sci. and Geomech. Abstr. 13(10), 1-24.

Barton, N., and Bandis, S. (1982). Effects of block size on the shear behavior of jointed rock. In the 23rd US symposium on rock mechanics (USRMS). American Rock Mechanics Association.

Barton, N., and Bandis, S. (1990). Review of predictive capabilities of JRC-JCS model in engineering practice. In: Balkema, A.A, (Ed), Proceedings of International Conference on Rock Joints, Leon, Norway, pp.603-610. Rotterdam.

Barton, N.R., and Choubey, V. (1977). The shear strength of rock joints in theory and practice. Rock Mech. 10(1-2), 1-54.

Bieniawski, Z.T. (1973). Engineering classification of jointed rock masses. Transaction of the South African Institution of Civil Engineers, v. 15, pp. 335-344.

Bieniawski, Z.T. (1979). The geomechanics classification in rock engineering applications. In: Proceedings of the 4th international congress on rock mechanics, Montreux, 1979, pp. 41-48.

Bieniawski, Z.T. (1989). Engineering Rock Mass Classifications. Wiley, New York, p.251.

Bishop, A.W. (1955). The use of the slip circle in the stability analysis of slopes. Geotechnique 5 (1): 7-17

Bjerrum L. (1954). Theoretical and experimental investigations on the shear strength of soils. PhD thesis. ETH Zurich.

Bottero, A., Negre, R., Pastor, J., and Turgeman, S. (1980). "Finite element method and limit analysis theory for soil mechanics problems." Computational Methods Appl. Mech. and Engrg., 22, 131-149.

Bouma, N., and A. Imeson. (2000). Investigation of relationships between measured field indicators and erosion processes on badland surfaces at Petrer, Spain. Catena 40 (2): 147–171. https://doi.org/10.1016/s0341-8162(99)00046-6.

Braun, A., Fernandez-Steeger, T., Havenith, H-B., Torgoev, A. (2015) Landslide susceptibility mapping with data mining methods—a case study from Maily-Say, Kyrgyzstan. In Giorgio Lollino, Daniele Giordan, Giovanni B. Crosta, Jordi Corominas, Rafig Azzam, Janusz Wasowski, and Nicola Sciarra, editors, Engineering geology for society and territory - Volume 2, pages 995–998. Springer International Publishing, ISBN 978-3-319-09057-3

Budimir, M.E.A., Atkinson, P.M., and Lewis, H.G. (2015). A systematic review of landslide probability mapping using logistic regression. Landslides 12 (3): 419–436.

Bui, D.T., Lofman, O., Revhaug, I., and Dick O. (2011). Landslide susceptibility analysis in the Hoa Binh province of Vietnam using statistical index and logistic regression. Natural Hazards 59: 1413.

Bureau of Indian Standards (1972), Methods of test for soils, Part XIII, Direct shear test. B.I.S, New Delhi, IS 2720.

Calamak, M. and Yanmaz, A.M. (2014). Probabilistic assessment of slope stability for earth-fill dams having random soil parameters. In: 11th National Conference on Hydraulics in Civil Engineering and 5th International Symposium on Hydraulic Structures: Hydraulic Structures and Society-Engineering Challenges and Extremes. Engineers Australia, p 34

Calderon, A.R. (2000). The Application of Back-Analysis and Numerical Modeling to Design a Large Pushback in a Deep Open Pit Mine (MS thesis). Faculty and Board of Trustees of the Colarodo School of Mines. (Unpublished).

Chandler, D.S. (1996). Monte Carlo simulation to evaluate slope stability. Conference Proceedings on Uncertainty in the Geologic Environment, Wisconsin, USA, vol. 1, 474-493.

Chen R.H. and Chameau, J.L. (1982). “Three-dimensional limit equilibrium analysis of slopes,” Geotechnique, vol. 33, no. 1, pp. 31–40.

Chen, W., M. Panahi, and H.R. Pourghasemi. (2017). Performance evaluation of GISbased new ensemble data mining techniques of adaptive neuro-fuzzy inference system (ANFIS) with genetic algorithm (GA), differential evolution (DE), and particle swarm optimization (PSO) for landslide spatial modelling. CATENA 157: 310–324.

Chen, Z. (1995). Recent developments in slope stability analysis. In: Fujii T, editor. Proceedings of the 8th International Congress of Rock Mechanic, 3(5), pp. 23–51.

Cheng, Y.M., Lansivaara, T., and Wei, W.B. (2007). “Two-dimensional slope stability analysis by limit equilibrium and strength reduction methods,” Computers and Geotechnics, vol. 34, no. 3, pp. 137–150.

Cheng, Y., L. Li, T. Lansivaara, S. Chi and Y. Sun (2008a). An improved harmony search minimization algorithm using different slip surface generation methods for slope stability analysis, Engineering Optimization, vol. 40, No. 2, pp. 95-115.

Cheng, Y., L. Liang, S. C. Chi, and W. B. Wei (2008b). Determination of the critical slip surface using artificial fish swarm’s algorithm, Journal of Geotechnical and Geoenvironmental Engineering, vol. 134, No. 2, pp. 244-251.

Chiwaye, H.T. (2010). A comparison of the limit equilibrium and numerical modelling approaches to risk analysis for open pit mine slopes. Doctoral dissertation. Faculty of Engineering and the Built Environment, University of the Witwatersrand, Johannesburg

Cho, S. (2007). Effects of spatial variability of soil properties on slope stability, Engineering Geology, vol. 92, No. 3-4, pp. 97-109.

Coulson, J.H. (1972). Shear strength of flat surfaces in rock. In Stability of Rock Slopes (pp. 77-105). ASCE.

Corominas J, van Westen. C., Frattini, P., Cascini, L., Malet, J-P., Fotopoulou S, Catani F, Van Den Eeckhaut M, Mavrouli O, Agliardi F, Pitilakis K, Winter MG, Pastor M, Ferlisi S, Tofani V, Hervás J, Smith JT (2013) Recommendations for the quantitative analysis of landslide risk. Bull Eng Geol Environ 1435–9537.https://doi.org/10.1007/s10064-013-0538-8 http://link.springer.com/10.1007/s10064-013-0538-8

Cundall, P.A. (2002). The replacement of limit equilibrium methods in design with numerical solutions for factor of safety. Powerpoint presentation. Itasca Consulting Group, Inc

Dai, F., and Lee, C. (2002). Landslide characteristics and slope instability modeling using GIS, Lantau Island, Hong Kong. Geomorphology 42: 213–228.

Davis RO, Desai CS, Smith NR (1993) Stability of motions of translational landslides. J Geotech Engg ACSE 119:420–432

Dawson E. M., Roth W. H., and Drescher, A. (1999). “Slope stability analysis by strength reduction,” Geotechnique, vol. 49, no. 6, pp. 835–840.

De Blasio, F.V. (2010) Introduction to the physics of landslides. Springer, Berlin

Dehnavi, A., Aghdam, I.N., Pradhan, B., Morshed, V.M.H. (2015). A new hybrid model using stepwise weight assessment ratio analysis (SWARA) technique and adaptive neuro-fuzzy inference system (ANFIS) for regional landslide hazard assessment in Iran. Catena, vol. 135, pp. 122 – 148

Dou J, Bui DT, Yunus AP, Jia K, Song X, Revhaug I, Xia H, Zhu Z (2015) Optimization of causative factors for landslide susceptibility evaluation using remote sensing and GIS data in parts of Niigata. Japan. PLoS One 100(7): e0133262. https://doi.org/10.1371/journal.pone.0133262

Duncan, J.M., and Wright, S.G. (1980). "The accuracy of equilibrium methods of slope stability analysis." Engineering Geology, 16, 5-17.

Duncan, J.M. (1996). State of the art: limit equilibrium and finite-element analysis of slopes. Journal of Geotechnical Engineering (ASCE), vol. 122, pp. 577 – 596.

Duncan, J.M. (1996). State of the art: limit equilibrium and finite-element analysis of slopes. Journal of Geotechnical Engineering (ASCE), vol. 122, pp. 577 – 596

Eberhardt, E. (2003). Rock slope stability analysis- utilization of advanced numerical techniques. Vancouver, Canada: University British Columbia.

Eckhardt, R. (1987). "Stan Ulam, John von Neumann, and the Monte Carlo method," Los Alamos Science, Special Issue (15): 131–137.

El Jazouli, A., Barakat, A., and Khellouk, R. GIS-multicriteria evaluation using AHP for landslide susceptibility mapping in Oum Er Rbia high basin (Morocco). Geoenviron Disasters 6, 3 (2019). https://doi.org/10.1186/s40677-019-0119-7

Einstein, H.H., and Baecher, G.B. (1982). Probabilistic and statistical methods in engineering geology I. Problem statement and introduction to solution. In: Ingenieurgeologie und Geomechanik als Grundlagen des Felsbaues/Engineering Geology and Geomechanics as Fundamentals of Rock Engineering.

Erzin, Y., Cetin, T. (2013). The prediction of the critical factor of safety of homogeneous finite slopes using neural networks and multiple regressions. Comput Geosci 51:305–313

Fan, X., G. Scaringi, G. Domènech, F. Yang, X. Guo, L. Dai, et al. (2019). Two multitemporal datasets that track the enhanced landsliding after the 2008 Wenchuan earthquake. Earth System Science Data 11 (1): 35–55.

Fishman, G.S. (1995). Monte Carlo: Concepts, Algorithms, and Applications. New York: Springer. ISBN 0-387-94527-X.

Fleurisson, J.A. (2012). "Slope Design and Implementation in Open Pit Mines: Geological and Geomechanical Approach." The first Int. Symp. on Innovation and Technology in the Phosphate Industry 46: 27-38.

Franz, J. (2009). An investigation of combined failure mechanisms in large-scale open pit slopes. Ph.D. Thesis, University of New South Wales, Australia.

Fredlund, D.G., and Krahn, J. (1977). "Comparison of slope stability methods of analysis." Can. Geotech. J., Ottawa, Canada, 14, 429- 439.

Gao, W. (2015). Stability analysis of rock slope based on an abstraction ant colony clustering algorithm. Environ. Earth Sci. 73 (12), 7969–7982.

Galli, M., Ardizzone, F., Cardinali, M., Guzzetti, F., Reichenbach, P. (2008) Comparing landslide inventory maps. Geomorphology 940(3–4):268–289. https://doi.org/10.1016/j.geomorph.2006.09.023

Gavin, K. and Xue, J. (2010). Design Charts for the Stability Analysis of Unsaturated Soil Slopes," Geotechnical and Geological Engineering, vol. 28, No. 1, pp. 79-90.

Ghavidel, Alireza, S. Roohollah Mousavi, and Mohsen Rashki. (2017). "The effect of FEM mesh density on the failure probability analysis of structures." KSCE J. of Civil Eng. 1-13.

Ghosh, K., Bandyopadhyay, S., De, S.K. (2017). A comparative evaluation of weight-rating and analytical hierarchical (AHP) for landslide susceptibility mapping in Dhalai District, Tripura. In Hazra, S., Mukhopadhyay, A., Ghosh, A., Mitra, D. and Dadhwal, V. (Eds.), Environment and Earth Observation, Remote Sensing/Photogrammetry, Springer, pp. 175 – 193

Göktepe, I., Keskin, F. (2018). A comparison study between traditional and finite element methods for slope stability evaluations. Journal Geological Society of India, vol. 91, pp. 373 – 379.

Golovko, D., Roessner, S., Behling, R., Wetzel, H-U., Kleinschmit, B. (2015). Development of multi-temporal landslide inventory information system for Southern Kyrgyzstan using GIS and satellite remote sensing. Photogrammetrie - Fernerkundung – Geoinformation 20150(2):157–172. https://doi.org/10.1127/pfg/2015/0261

Gordan B, Jahed Armaghani D, Hajihassani M, Monjezi M (2015) Prediction of seismic slope stability through combination of particle swarm optimization and neural network. Eng Comput. doi:10.1007/s00366-015-0400-7

Griffiths D. V. and Lane P. A., (1999). “Slope stability analysis by finite elements,” Geotechnique, vol. 49, no. 3, pp. 387–403.

Griffiths D. V. and Marquez R. M. (2007). “Three-dimensional slope stability analysis by elasto-plastic finite elements,” Geotechnique, vol. 57, no. 6, pp. 537–546.

Gupta, R., and B. Joshi. (1990). Landslide hazard zoning using the GIS approach—A case study from the Ramganga catchment, Himalayas. Engineering Geology 28 (1–2): 119–131. https://doi.org/10.1016/0013-7952(90)90037-2.

Gupta, S.K., Shukla, D.P., and Thakur, M. (2018). Selection of weightages for causative factors used in preparation of landslide susceptibility zonation (LSZ). Geomatics, Natural Hazards and Risk, vol. 9, no. 1, pp. 471 – 487.

Guzzetti F, Reichenbach P, Wieczorek GF (2003). Rockfall hazard and risk assessment in the Yosemite Valley, California, USA. Nat Hazards Earth Syst Sci 3:491–503.

Hammond, C.J., Prellwitz, R.W., and Miller, S.M. (1991). Landslide hazard assessment using Monte Carlo simulation. Proceedings of the 6th International Symposium on Landslide, Rotterdam, Netherlands, vol. 2, 959-964.

Hasanipanah M, Jahed Armaghani D, Monjezi M, and Shams S (2016) Risk assessment and prediction of rock fragmentation produced by blasting operation: a rock engineering system. Environ. Earth Sci 75:808

Hasofer, A.M., and Lind, N.C. (1974). Exact and invariant second—moment code format. Journal of the Engineering Mechanics Division of American Society of Civil Engineers 100, 111–121

Helmstetter A, Sornette D, Grasso J-R, Andersen JV, Gluzman S., and Pisarenko V. (2004) Slider block friction model for landslides: application to Vaiont and La Clapie´ re landslides. J Geophys Res 109: B02409

Hoek E, and Bray J.W. (1981). Rock slope engineering, Institution of Mining and Metallurgy. London.

Hoek, E., and Diederichs, M. (2006). Empirical estimates of rock mass modulus. Int. J Rock Mech. Min. Sci., 43, 203–215

Hoek, E. (1994). Strength of rock and rock masses, ISRM News J, 2(2), 4-16. Hoek, E., and Brown, E.T. 1980a. Underground excavations in rock. London: Instn Min. Metall.

Hoek, E., and Brown, E.T. (1997). Practical estimates or rock mass strength. Int. J. Rock Mech. Min.g Sci. and Geomech. Abstr. 34(8), 1165-1186.

Hoek, E., Kaiser, P.K., and Bawden. W.F. (1995). Support of underground excavations in hard rock. Rotterdam: Balkema.

Hoek, E., Marinos, P., and Benissi, M. (1998). Applicability of the Geological Strength Index (GSI) classification for very weak and sheared rock masses. The case of the Athens Schist Formation. Bull. Engng. Geol. Env. 57(2), 151-160.

Hoek, E., Marinos, P., and Marinos, V. (2005). Characterization and engineering properties of tectonically undisturbed but lithologically varied sedimentary rock masses. Int. J. Rock Mech. Min. Sci., 42/2, 277-285

Huang, J, Griffiths, DV and Fenton, GA. (2010). System Reliability of Slopes by RFEM. Soils and Foundations 50(3): 343-353.

Idelsohn, S., Oñate , E., and Del Pin, F.D. (2003b). A Lagrangian meshless finite element method applied to fluid structure interaction problems. Computer and Structures, vol. 81, pp. 655 – 671

Idelsohn, S.R., Oñate , E., Pin, F.D. (2004). The particle finite element method: a powerful tool to solve incompressible flows with free surfaces and breaking waves. International Journal for Numerical Methods in Engineering, vol. 61, 964 – 989

l Hamdouni R, Jiménez-Perálvarez, J.D., Fernández P, Chacón J. (2012) Spatial stability of slope cuts in rock massifs using GIS technology and probabilistic analysis. Bull Eng Geol Environ 71:569–578

Ishii, Y., Ota, K., Kuraoka, S., Tsunaki, R. (2012). Evaluation of slope stability by finite element method using observed displacement of landslide. Landslides, vol. 9, pp. 335 – 348

Jahed Armaghani D, Mahdiyar A, Hasanipanah M, Shirani Fara- donbeh R, Khandelwal M, Bakhshandeh Amnieh H. (2016). Risk assessment and prediction of flyrock distance by combined multiple regression analysis and monte carlo simulation of quarry blasting. Rock Mech Rock Eng. doi:10.1007/s00603-016-1015-z

Janbu, N. (1968). Slope Stability Computations. Soil Mechanics and Foundation Engineering Report, Technical University of Norway, Trondheim

Jiang, Q., and Zhou, C. (2017). “A rigorous solution for the stability of polyhedral rock blocks,” Computers and Geotechnics, vol. 90, pp. 190–201.

Jiang, Q, and Zhou, C. (2018). “A rigorous method for three-dimensional asymmetrical slope stability analysis,” Canadian Geotechnical Journal, vol. 55, no. 4, pp. 495–513.

Johnson, R.B., and Degraff, J.V. (1991). Principles of Engineering Geology, John Wiley and Sons, New York, 497 pp.

Kalantar B, Pradhan B, Naghibi SA, Motevalli A, Mansor S. (2018). Assessment of the effects of training data selection on the landslide susceptibility mapping: a comparison between support vector machine (SVM), logistic regression (LR) and artificial neural networks (ANN). Geomatics Nat Hazards Risk 90(1):49–69. https://doi.org/10.1080/19475705.2017.1407368.

Kalkani, E.C. (1975). “Two-dimensional finite element analysis for the design of rock slopes." 16th Symp. on Rock Mechanics, University of Minnesota. 11-20.

Korup, O. (2008). Rock type leaves topographic signature in landslide-dominated mountain ranges. Geophys Res Lett 350(11): L11402. https://doi.org/10.1029/2008GL034157.

Krahn, J. (2004). Stability Modeling with SLOPE/W. First Ed., Calgary, Alberta, Canada: GEO-SLOPE/W International Ltd.

Lam, L. and Fredlund, D.G. (1993). “A general limit equilibrium model for three-dimensional slope stability analysis,” Canadian Geotechnical Journal, vol. 30, no. 6, pp. 905–919.

Larese, R., Rossi, E., Oñate, S.R., and Idelsohn, S. (2008). Validation of the Particle Finite Element Method (PFEM) for simulation of free surface flows. Engineering Computations, vol. 25, pp. 385 – 425

Li S, Zhao HB, and Ru Z (2013). Slope reliability analysis by updated support vector machine and Monte Carlo simulation. Nat Hazards 65:707–722

Li, C., Sun, C., Li, C., and Zheng, H. (2017). Lower bound limit analysis by quadrilateral elements, Journal of Computational and Applied Mathematics, Volume 315, Pages 319-326, ISSN 0377-0427, https://doi.org/10.1016/j.cam.2016.11.024.

Low, B.K., and Tang, W.H. (1997). Efficient reliability evaluation using spreadsheet. J. Eng. Mech. 123 (7), 749–752.

Lu, R., Wei, W., Shang, K., and Jing, X. (2020). Stability Analysis of Jointed Rock Slope by Strength Reduction Technique considering Ubiquitous Joint Model, Advances in Civil Engineering, Volume 2020, Article ID 8862243, 13 pages https://doi.org/10.1155/2020/8862243.

Lysmer, J. (1970). "Limit analysis of plane problems in soil mechanics. J. Soil Mech. and Found. Div., ASCE, 96(4), 1131-1334.

Maji, V.B. (2017). An insight into slope stability using strength reduction technique. Journal of the Geology Society of India, vol. 89, pp. 77 – 81.

Matsui T. and San K.-C. (1992). “Finite element slope stability analysis by shear strength reduction technique,” Soils and Foundations, vol. 32, no. 1, pp. 59–70.

Miller, S.M., Whyatt, J.K., and McHugh, E.L. (2004). Applications of the Point Estimation Method for Stochastic Rock Slope Engineering, Gulf Rocks 2004, the 6th North America Rock Mechanics (NARMS), 5–9 June. American Rock Mechanics Association, Houston, Texas, Document ID ARMA-04-517.

Mineo S, Pappalardo G, Mangiameli M, Campolo S, Mussumeci G. (2018). Rockfall analysis for preliminary hazard assessment of the cliff of Taormina Saracen Castle (Sicily). Sustainability 10(2):417.

Mineo, S., Pappalardo, G., D’Urso, A., and Calcaterra, D. (2017). Event tree analysis for rockfall risk assessment along a strategic mountainous transportation route. Environ. Earth Sci., vol. 76, pp.620.

Morgenstern, N.R., and Price, V.E. (1965). The analysis of the stability of general slip surfaces. Geotechnique 15 (1): 79-93.

Nash, D. (1987). "Chapter 2: A comparative review of limit equilibrium methods of stability analysis." Slope Stability, M. G. Anderson and K. S. Richards, eds., John Wiley and Sons, Inc., New York, N.Y.

Nilsen, B., 2000. New trends in rock slope stability analyses. Bull. Eng. Geol. Environ. 58, 173–178.

Oka, Y., and Wu, T.H. (1990), System reliability of slope stability. Journal of Geotechnical Engineering, ASCE, vol. 116 (8), pp.1185-1189.

Oliver, J., Cante, J.C., Weyler, R., Gonzalez, C., and Hernandez, J. (2007). Particle finite element methods in solid mechanics problems. In E. Oñate, and D.R.J. Owen (Eds.), Computational Plasticity, Springer. pp. 87 – 103

Oñate , E., Idelsohn, S.R., Celigueta, M.A., and Rossi, R. (2008). Advances in the particle finite element method for the analysis of fluid multibody interaction and bed erosion in free surface flows. Computer Methods in Applied Mechanics and Engineering, vol. 197, pp. 1777 – 1800.

Oñate , E., Idelsohn, S.R., Del Pin, F., and Aubry, R. (2004). The particle finite element method: an overview. International Journal of Computational Methods, vol. 2, pp. 267 – 307.

Optum G2. (2019). Theory of the model. Optum Computational Engineering.

Qian, Q.H. (2012). Challenges faced by underground projects construction safety and countermeasures. Chin. J. Rock Mech. Eng. 31 (10), 1945–1956, (in Chinese).

Pantelidis, L. (2009). Rock slope stability assessment through rock mass classification systems. International Journal of Rock Mechanics and Mining Sciences, 46(2), 315-325.

Parise, M. (2002). Landslide hazard zonation of slopes susceptible to rock falls and topples. Natural Hazards and Earth System Sciences, 2(1/2), pp. 37–49.

Park, S., C. Choi, B. Kim, and J. Kim. (2013). Landslide susceptibility mapping using frequency ratio, analytic hierarchy process, logistic regression, and artificial neural network methods at the Inje area, Korea. Environmental Earth Sciences 68: 1443–1464.

Peric, D., Hochard, C., Dutko, M., and Owen, D.R.J. (1996). Transfer operators for evolving meshes in small strain elasto-plasticity. Computer Methods in Applied Mechanics and Engineering, vol. 137, pp.331–344.

Pourghasemi, H.R., B. Pradhan, and C. Gokceoglu. (2012). Application of fuzzy logic and analytical hierarchy process (AHP) to landslide susceptibility mapping at Haraz watershed, Iran. Natural Hazards 63: 965–996.

Provost F, Hibert C, and Malet J-P (2017) Automatic classification of endogenous landslide seismicity using the random forest supervised classifier: seismic sources automatic classification. Geophys Res Lett 440(1):113–120. https://doi.org/10.1002/2016GL070709

Qing-qing, J. (2009). "Strength reduction method for slope based on a ubiquitous-joint criterion and its application." Mining Sci. and Technology 19 452-456.

Quan, H.C., and Lee, B.G. (2012). GIS-Based Landslide Susceptibility Mapping Using Analytic Hierarchy Process and Artificial Neural Network in Jeju (Korea). Journal of Civil Engineering, vol. 16(7), pp.1258-1266.

Rabie, M. (2014). Comparison study between traditional and finite element methods for slopes under heavy rainfall.” Journal of Housing and Building National Research Center, vol. 10, pp.160-168.

Raghuvanshi, T. (2017). "Plane failure in rock slopes – A review on stability analysis techniques." J. of King Saud University – Science Article in press.

Ramesh, V., Mani, S., Baskar, M., Kavitha, G., and Anbazhagan, S. (2017). Landslide hazard zonation mapping and cut slope stability analyses along

Yercaud ghat road (Kuppanur–Yercaud) section, Tamil Nadu, India. International Journal of Geotechnical Engineering, vol. 8: pp.2.

Ramos-Bernal, R.N., Vázquez-Jiménez, R., and Romero-Rojas, W. (2018). Modeling the Susceptibility to Landslides by Remote Sensing Techniques. Case Study: Central Area of the State of Guerrero in México, Havana, Cuba, Ministerio de Comunicaciones: Havana, Cuba, pp. 1–8.

Rawat, M.S., Uniyal, D.P., Dobhal, R., Joshi, V., Rawat, B.S., Bartwal, A., Singh, D., and Aswal, A. (2015). Study of landslide hazard zonation in Mandakini Valley, Rudraprayag district, Uttarakhand using remote sensing and GIS. Current Science, vol. 109, pp. 158–170.

Read, S., Richards, L., and Cook, G. (2003). Rock mass defect patterns and the Hoek-Brown failure criterion. In 10th ISRM Congress. International Society for Rock Mechanics and Rock Engineering, pp.161–222.

Read, J., Stacey, P. (2009). Guidelines for Open Pit Slope Design. CSIRO Publishing, Australia.

Refahi, H.Gh. (2000). Soil Erosion by Water and Conservation. 2nd ed., Tehran University Publications, Tehran, Iran, pp. 551.

Reichenbach, P., M. Rossi, B.D. Malamud, M. Mihir, and F. Guzzetti. (2018). A review of statistically based landslide susceptibility models. Earth-Science Reviews 180: 60–91.

Renani, H.R., and Martin, C.D. (2020). Factor of safety of strain-softening slopes, Journal of Rock Mechanics and Geotechnical Engineering, Volume 12, Issue 3, Pages 473-483, ISSN 1674-7755, https://doi.org/10.1016/j.jrmge.2019.11.004.Rocscience, (2004). Procedures for DIPS. 1-50

Roodposhti, M.S., S. Rahimi, and M.J. Beglou. (2014). PROMETHEE II and fuzzy AHP: An enhanced GIS-based landslide susceptibility mapping. Natural Hazards 73 (1): 77–95.

Roy, J., Saha, S. (2019). Landslide susceptibility mapping using knowledge driven statistical models in Darjeeling District, West Bengal, India. Geoenviron Disasters 6, 11. https://doi.org/10.1186/s40677-019-0126-8

Rubio, R.H., Florez, J.H., and Zingano, A.C. (2016). Slope stability analysis at highway BR-153 using numerical models. REM: R. Esc. Minas, Ouro Preto, vol. 69, (2), pp.185-191.

Samui, P. and Kothari, D.P. (2011). Utilization of a least square support vector machine (LSSVM) for slope stability analysis. Scientia Iranica, 18(1), pp.53-58.

Sarkar, S., and Kanungo, D.P. (2004). An integrated approach for landslide susceptibility mapping using remote sensing and GIS. Photogrammetric Engineering and Remote Sensing, vol. 70 (5), pp. 617- 625.

Sarma, S.K. (1973). Stability Analysis of Embankment and Slopes. Geotechnique, vol. 23 (3), pp. 423-33.

Schneider-Muntau, B., Medicus, W.G., and Fellin, W. (2018). “Strength reduction method in Barodesy,” Computers and Geotechnics, vol. 95, pp. 57–67.

Schulz WH, Smith JB, Wang G, Jiang Y, Roering JJ. (2018) Clayey landslide initiation and acceleration strongly modulated by soil swelling. Geophys Res Lett 450(4):1888–1896. https://doi.org/10.1002/2017GL076807

Sengani, F., and Mulenga, F. (2020a). Application of Limit Equilibrium Analysis and Numerical Modeling in a Case of Slope Instability. Sustainability, 12, 8870. https://doi.org/10.3390/su12218870

Sengani, F., and Mulenga, F. (2020b). Influence of rainfall intensity on the stability of unsaturated soil slope: Case Study of R523 road in Thulamela Municipality, Limpopo Province, South Africa. Applied Sciences 2020, 10, applsci-982838.

Shamekhi, S.E. (2014). Probabilistic assessment of rock slope stability using response surfaces determined from finite element models of geometric realizations. PhD thesis.

Sharma, S., Raghuvanshi, T. K., and Anbalagan, R. (1995). Plane failure analysis of rock slopes. Geotechnical and Geological Engineering, 13(2), 105-111.

Sharma, S., Raghuvanshi, T., and Sahai, A. (1999). An engineering geological appraisal of the Lakhwar dam, Garhwal Himalaya, India. Engineering geology, 53(3-4), 381-398.

Sharma, R.K. (2022). Reliability Analysis of Slope Stability using Monte Carlo Simulation and Comparison with Deterministic Analysis. National Institute of Technology Hamirpur. Accessed on 02 February 2022.

Shen, H. (2012). Non-deterministic analysis of slope stability based on numerical simulation (Ph.D. thesis). Technische Universität Bergakademie Freiberg, (unpublished).

Singh, R., Forbes, C., Diop S., Musekiwa, C., and Claasen, D. (2011). Landslide geohazards in South Africa. Landslide susceptibility mapping, socio-economic impacts, mitigation, and remediation measure. Pretoria: Council for Geoscience, pp.58.

Sjöberg, J., and Norstrom, U. (2001). "Failure Mechanisms for High Slopes in Hard Rock." In Slope Stability in Surface Mining, edited by W. A. Hustrulid, 71-80. Littleton, Colorado: SME, Inc.

Sjöberg, J., and U Norstrom. (2001). "Failure Mechanisms for High Slopes in Hard Rock." In Slope Stability in Surface Mining, edited by W. A. Hustrulid, 71-80. Littleton, Colorado: SME, Inc.

Sloan, S.W. (1988). "Lower bound limit analysis using finite elements and linear programming." Int. J. Numer. and Analytical Methods in Geomech., 12, 61-77.

Sloan, S. W. (1989). "Upper bound limit analysis using finite elements and linear programming." Int. J. Numer. and Analytical Methods in Geotech., vol. 13, 263-282.

Sloan, S.W. (1995). "Limit analysis in geotechnical engineering." Modem developments in geomechanics, C. M. Haberfield, ed., Monash University, Melbourne, Australia, 167-199.

Sloan, S.W., and Kleeman, P.W. (1995). "Upper bound limit analysis using discontinuous velocity fields." Computational Methods of Appl. Mech. and Engrg., 127, 293-314.

Spencer, E. (1967). A method of analysis of the stability of embankments assuming parallel interslice forces. Geotechnique 17 (1): 11-26.

Sun, J., J. Li and Q. Liu. (2008). Search for critical slip surface in slope stability analysis by spline-based GA method, Journal of Geotechnical and Geoenvironmental Engineering, vol. 134, pp. 252-256.

Tabba, M.M. (1984). Deterministic versus risk analysis of slope stability. 4th International Symposium on Landslides. Toronto, Canada. pp. 491–498.

Turner, A.K., and Jayaprakash, G.P. (2012). Introduction. In Turner, A.K., Schuster, R.L. (Eds.), Rockfall characterization and control, Transportation Research Board, National Academy of Sciences, Washington D.C., pp. 3 – 20.

Tutluoglu, L., I. O¨ge, and CelalKarpuz. (2015). "Two- and three-dimension analysis of a slope failure in a lignite mine." Computers &Geosciences 37 232-240.

Tyodo, Z. (2013). Landslide Susceptibility Mapping: Remote Sensing and GIS Approach. MSc. University of Stellenbosch.

U.S. Army Corps of Engineers. (1970). Engineering and Design - Stability of Earth and Rockfill Dams. Engineer Manual EM 1110-2-1902, Department of the Army, Corps of Engineers, Washington, DC.

Van Den Eeckhaut M, Poesen J, Verstraeten G, Vanacker V, Moeyersons J, Nyssen J, and van Beek LPH. (2005) The effectiveness of hillshade maps and expert knowledge in mapping old deep-seated landslides. Geomorphology 670(3–4):351–363.

Varnes, D.J. (1978) Slope Movement Types and Processes. In: Schuster RL, Krizek RJ (eds.) Landslides: analysis and control. Special Report 176, Transportation and Road Research Board, National Academy of Science, Washington, DC, pp. 11–33.

Wang HB, Xu WY, Xu RC (2005) Slope stability evaluation using back propagation neural networks. Eng Geol 80:302–315

Wang, D., Bienen, B., Nazem, M., Tian, Y., Zheng, J., and Pucker, T. (2015). Large deformation finite element analyses in geotechnical engineering. Computer Geotechnical, vol. 65, pp. 104 – 114.

Wang, Y., Au, S-K., and Cao, Z. (2010). Bayesian approach for probabilistic characterization of sand friction angles. Engineering Geology 114(3-4): 354-363.

Whalley, W.B. (1984). Rockfalls. In Brunsden, D., Prior, D.B. (Eds.), Slope instability, Wiley, New York, pp. 217 – 256.

Woldearegay, K. (2013). Review of the occurrences and influencing factors of landslides in the highlands of Ethiopia: With implications for infrastructural development. Momona Ethiopian Journal of Science, 5(1), 3-31.

Wyllie, D.C., and Mah, C.W. (2004). Rock slope engineering, civil and mining, Fourth Edition. Taylor and Francis, London, and New-York

Yalçin, Y. (2018). Integrated limit equilibrium method for slope stability analysis, Masters dissertation, The Graduate School of Natural and Applied Sciences of Middle East Technical University, pp.8.

Yilmaz, I. (2009) A case study from Koyulhisar (Sivas-Turkey) for landslide susceptibility mapping by artificial neural networks. Bull Eng Geol Environ 68:297–306

Yin, H. (2012). “A three-dimensional rigorous method for stability analysis of landslides,” Engineering Geology, vol. 145–146, pp. 30–40.

Yu, H.S., Salgado, R, Sloan, S.W. and Kim, J.M. (1998). Limit analysis versus limit equilibrium for slope stability, Journal of Geotechnical and Geoenvironmental Engineering, ol. 124, No. 1, January 1998.

Zêzere, J.L., S. Pereira, R. Melo, S.C. Oliveira, and R.A. Garcia. (2017). Mapping landslide susceptibility using data-driven methods. Science of the Total Environment 589: 250–267.

Zhang, X. (2014). Particle finite element method in geomechanics. PhD thesis, University of Newcastle, Australia.

Zhang, X., Krabbenhoft, K., Sheng, D., and Li, W. (2015). Numerical simulation of a flow-like landslide using the particle finite element method. Computer Mechanical, vol. 55, pp.167 – 177.

Zhang, X., Krabbenhoft, K., and Sheng, D. (2014). Particle finite element analysis of the granular column collapse problem. Granular Matter, vol. 16, pp.609 – 619.

Zhang, X., Oñate, E., Torres, S.A.G., Bleyer, J., and Krabbenhoft, K. (2019). Aunified Lagrangian formulation for solid and fluid dynamics and its possibility for modelling submarine landslides and their consequences. Computer Methods in Applied Mechanics and Engineering, vol. 343, pp. 314 – 338.

Zhang, X., Sheng, D., Sloan, S.W., and Bleyer, J. (2017). Lagrangian modelling of large deformation induced by progressive failure of sensitive 25 clays with elastoviscoplasticity. International Journal for Numerical Methods in Engineering, vol. 112, pp. 963 – 989

Zhang, X., Sloan, S.W., and Oñate, E. (2018). Dynamic modelling of retrogressive landslides with emphasis on the role of clay sensitivity. International Journal for Numerical and Analytical Methods in Geomechanics, vol. 42, pp. 1806 – 1822

Zhang, X., Wang, L., Krabbenhoft, K., and Tinti, S. (2019). A case study and implication: particle finite element modelling of the 2010 Saint-Jude sensitive clay landslide. Landslides, vol. 17, pp. 1117–1127. DOI 10.1007/s10346-019-01330-4

Zheng, H., Liu, D. F., and. Li C. G, (2005). “Slope stability analysis based on elasto-plastic finite element method,” International Journal for Numerical Methods in Engineering, vol. 64, no. 14, pp. 1871–1888.

Zhou, X.P., and Cheng, H. (2013). Analysis of stability of three-dimensional slopes using the rigorous limit equilibrium method. Engineering Geology; 160:21e33.

Zhou, S., G. Chen, L. Fang, and Y. Nie. (2016). GIS-based integration of subjective and objective weighting methods for regional landslides susceptibility mapping. Sustainability 8 (4): 334.

Zienkiewicz OC, Humpheson C, and Lewis RW. (1975). Associated and non-associated visco-plasticity and plasticity in soil mechanics. Geotechnique;25(4):671e89.

Zienkiewicz, O.C., and Taylor, R.L. (2000). “The finite element method: solid mechanics”, vol. 2. Butterworth-Heinemann, Oxford.

Appendix

Appendix A: Structural Mapping Data

Dip	Dip Direction		Set	Spacing (m)	Length (m)	Type	Shape	Surface
70	134	1	1	1.6	17	joint	planar	smooth
68	288	1	1	2.3	10	joint	stepped	rough
90	265	1	1	2.1	8	joint	planar	smooth
76	231	1	1	1.8	8	joint	planar	smooth
55	294	1	1	1	8	joint	undulate	smooth
76	58	1	1	2	8	joint	undulate	rough
69	258	1	1	1.5	8	joint	planar	smooth
66	9	1	1	2.1	7	joint	planar	rough
71	246	1	1	1.8	8	joint	planar	rough
37	250	1	1	2.4	16	joint	planar	rough
31	223	1	1	1.9	15	joint	planar	v.rough
64	249	1	1	7	20	shear	planar	slick
75	6	1	1	1.9	7	joint	undulate	smooth
64	219	1	1	1.7	9	joint	planar	rough
38	179	1	1	1.9	13	joint	undulate	smooth
51	249	1	1	6	20	shear	planar	slick

73	272	1	1	1.4	7	joint	undulate	v.rough
26	32	1	1	2.7	8	joint	undulate	rough
54	232	1	1	2.1	12	joint	planar	rough
62	29	1	1	3	9	joint	planar	smooth
90	307	1	1	1.6	7	joint	planar	rough
72	36	1	1	3.8	10	joint	planar	smooth
80	203	1	1	2.3	9	joint	planar	rough
57	338	1	1	1.9	13	joint	undulate	smooth
62	240	1	1	1.6	9	joint	undulate	rough
43	240	1	1	10	23	shear	planar	slick
63	192	1	1	2.1	9	joint	stepped	rough
27	182	1	1	1.9	15	joint	planar	rough
76	231	1	1	2.2	9	joint	undulate	rough
80	230	1	1	2	8	joint	undulate	smooth
75	356	1	1	2.3	11	joint	stepped	rough
67	235	1	1	2.2	10	joint	undulate	smooth
71	146	1	1	2	18	joint	planar	rough
49	140	1	1	1.6	20	bedding	planar	smooth

58	279	1	1	2.8	14	joint	planar	smooth
50	253	1	1	6	23	shear	planar	slick
45	23	1	1	2.3	8	joint	stepped	smooth
58	14	1	1	1.8	7	joint	undulate	rough
46	28	1	1	2	8	joint	planar	v.rough
60	336	1	1	0.7	8	joint	planar	v.rough
76	34	1	1	2.6	8	joint	planar	rough
52	269	1	1	1.9	12	joint	planar	v.rough
33	303	1	1	1.8	15	joint	planar	rough
30	272	1	1	2	16	joint	planar	rough
54	338	1	1	2.2	15	joint	planar	v.rough
39	58	1	1	2.6	10	joint	stepped	rough
30	225	1	1	1.2	11	joint	undulate	smooth
79	62	1	1	5.2	12	joint	undulate	smooth
25	181	1	1	2	16	joint	planar	smooth
59	246	1	1	1.7	10	joint	planar	smooth
52	139	1	1	1.1	17	joint	undulate	smooth
70	117	1	1	1.4	16	joint	planar	smooth

67	349	1	1	1.7	10	joint	planar	smooth
64	1	1	1	2.4	14	joint	undulate	v.rough
14	317	1	1	1.6	13	joint	planar	v.rough
81	36	1	1	3.8	9	joint	planar	smooth
70	102	1	1	1.1	7	joint	planar	smooth
54	153	1	1	1.8	7	joint	planar	rough
52	293	1	1	1.3	10	joint	undulate	smooth
70	266	1	1	1.6	8	joint	planar	rough
62	343	1	1	1.7	11	joint	planar	smooth
57	269	1	1	1.8	11	joint	planar	smooth
70	32	1	1	3.8	10	joint	planar	smooth
36	273	1	1	1.8	14	joint	planar	rough
43	342	1	1	0.7	9	joint	planar	rough
39	266	1	1	10	20	shear	planar	slick
72	272	1	1	2.2	9	joint	undulate	rough
77	218	1	1	1.9	8	joint	undulate	smooth
68	348	1	1	1.6	10	joint	undulate	v.rough
61	221	1	1	1.6	9	joint	planar	polished

60	262	1	1	1.9	10	joint	planar	smooth
64	289	1	1	3	13	joint	planar	smooth
39	264	1	1	6	19	shear	planar	slick
71	98	1	1	0.9	7	joint	planar	smooth
75	24	1	1	1.3	6	joint	undulate	rough
66	9	1	1	2	7	joint	planar	smooth
79	319	1	2	3.8	10	joint	planar	polished
73	319	1	2	4.8	14	joint	undulate	rough
83	319	1	2	1	6	joint	undulate	rough
65	310	1	2	2.6	12	joint	planar	smooth
49	306	1	2	3.8	21	joint	undulate	rough
69	325	1	2	2.2	14	joint	planar	polished
64	334	1	2	3.8	17	joint	planar	smooth
50	316	1	2	3.8	21	joint	undulate	v.rough
64	324	1	2	4.3	13	joint	undulate	smooth
69	323	1	2	1.6	11	joint	undulate	rough

71	309	1	2	3.4	17	joint	stepped	rough
53	321	1	2	1	9	joint	planar	smooth
89	317	1	2	3.8	10	joint	planar	rough
60	302	1	2	2.2	12	joint	planar	smooth
89	311	1	2	3	10	joint	planar	smooth
69	331	1	2	5.3	18	joint	planar	smooth
84	328	1	2	2.2	10	joint	planar	rough
70	320	1	2	2.2	10	joint	planar	smooth
88	316	1	2	3.4	11	joint	undulate	smooth
55	323	1	2	4.3	22	joint	planar	smooth
70	312	1	2	3	16	joint	planar	smooth
73	328	1	2	2.6	10	joint	planar	rough
66	331	1	2	1	9	joint	stepped	smooth
49	319	1	2	1.3	11	joint	planar	rough
64	316	1	2	3.4	15	joint	planar	smooth
66	317	1	2	2.6	12	joint	planar	rough
58	321	1	2	1	8	joint	planar	rough
64	308	1	2	2.6	12	joint	planar	rough
61	322	1	2	0.7	7	joint	planar	rough
76	322	1	2	3.8	16	joint	planar	rough

85	322	1	2	6.8	17	joint	planar	rough
89	317	1	2	3.4	10	joint	planar	smooth
81	331	1	2	1.9	7	joint	planar	rough
65	331	1	2	1.9	11	joint	planar	v.rough
73	331	1	2	1.3	8	joint	stepped	rough
53	323	1	2	3	17	joint	planar	v.rough
53	317	1	2	2.2	14	joint	planar	v.rough
56	333	1	2	6.3	30	joint	planar	v.rough
58	303	1	2	2.6	13	joint	planar	smooth
62	307	1	2	1.3	9	joint	stepped	v.rough
72	320	1	2	1.3	6	joint	planar	polished
89	321	1	2	3	9	joint	planar	smooth
64	321	1	2	2.2	9	joint	undulate	v.rough
73	325	1	2	3	8	joint	planar	v.rough
58	330	1	2	4.3	21	joint	planar	v.rough
64	321	1	2	1.6	8	joint	planar	smooth
89	317	1	2	1.6	7	joint	planar	smooth

66	309	1	2	1	7	joint	planar	smooth
86	322	1	2	3	10	joint	stepped	smooth
72	327	1	2	3.8	13	joint	planar	slick
75	320	1	2	6.3	20	joint	planar	rough
82	332	1	2	1.9	7	joint	planar	v.rough
51	311	1	2	2.6	16	joint	planar	rough
68	319	1	2	4.3	16	joint	undulate	rough
73	331	1	2	1.9	9	joint	undulate	smooth
80	319	1	2	1.9	7	joint	undulate	smooth
73	315	1	2	0.4	6	joint	planar	rough
55	318	1	2	4.3	22	joint	undulate	rough
61	323	1	2	3.8	17	joint	planar	rough
89	326	1	2	3.8	16	joint	undulate	smooth
56	330	1	2	2.2	14	joint	planar	rough
61	327	1	2	3.4	17	joint	planar	rough
73	325	1	2	3.4	14	joint	planar	v.rough
61	306	1	2	3.8	17	joint	planar	smooth
73	328	1	2	1.9	10	joint	planar	smooth
73	318	1	2	2.6	10	joint	planar	smooth

77	322	1	2	3.8	14	joint	planar	smooth
56	308	1	2	3	16	joint	planar	rough
74	332	1	2	2.2	9	joint	undulate	rough
75	319	1	2	3.4	13	joint	planar	smooth
87	327	1	2	4.8	20	joint	planar	smooth
81	332	1	2	3.8	10	joint	undulate	rough
62	321	1	2	6.3	25	joint	planar	smooth
88	327	1	2	2.6	13	joint	undulate	smooth
70	320	1	2	4.3	15	joint	planar	rough
51	312	1	2	5.8	29	joint	planar	smooth
84	313	1	2	0.4	6	joint	planar	smooth
77	311	1	2	1.9	8	joint	planar	smooth
84	313	1	2	3.8	14	joint	planar	polished
68	80	1	3	1.3	7	joint	undulate	v.rough
74	85	1	3	0.7	6	joint	planar	smooth
86	91	1	3	0.9	6	joint	undulate	smooth
62	76	1	3	1.3	7	joint	planar	rough

78	79	1	3	3.4	10	joint	undulate	rough
74	78	1	3	3.3	10	joint	planar	smooth
77	88	1	3	0.9	6	joint	undulate	rough
85	76	1	3	2.1	8	joint	undulate	rough
77	81	1	3	1.2	7	joint	planar	smooth
66	87	1	3	1.1	7	joint	planar	smooth
68	92	1	3	1.1	7	joint	planar	rough
77	95	1	3	0.8	6	joint	undulate	rough
73	87	1	3	0.7	6	joint	planar	smooth
79	89	1	3	3.8	11	joint	planar	rough
89	68	1	3	1.5	7	joint	undulate	rough
82	68	1	3	0.7	6	joint	planar	smooth
63	79	1	3	3	11	joint	planar	smooth
67	86	1	3	0.9	7	joint	planar	rough
65	91	1	3	1.9	9	joint	planar	polished
80	95	1	3	0.9	6	joint	planar	rough
78	90	1	3	1.7	8	joint	planar	smooth
85	78	1	3	0.7	6	joint	undulate	rough

63	97	1	3	2.7	11	joint	stepped	rough
88	69	1	3	5.5	12	joint	planar	smooth
79	83	1	3	0.9	6	joint	planar	rough
83	75	1	3	1	6	joint	planar	rough
75	74	1	3	1.9	8	joint	undulate	v.rough
70	86	1	3	3	11	joint	planar	smooth
67	88	1	3	2.1	9	joint	stepped	smooth
77	93	1	3	0.9	6	joint	planar	polished
72	87	1	3	2.6	10	joint	planar	v.rough
79	85	1	3	5.4	14	joint	planar	v.rough
81	74	1	3	0.8	6	joint	undulate	v.rough
76	83	1	3	0.9	6	joint	planar	rough
82	69	1	3	1.7	7	joint	planar	rough
75	67	1	3	1.1	7	joint	stepped	rough
73	81	1	3	0.9	6	joint	planar	v.rough
72	82	1	3	1.9	8	joint	planar	v.rough
74	73	1	3	2.6	9	joint	planar	rough
67	72	1	3	2.5	9	joint	stepped	smooth

71	82	1	3	0.8	6	joint	planar	smooth
69	94	1	3	1	7	joint	planar	rough
78	72	1	3	1.9	8	joint	planar	smooth
71	85	1	3	3	10	joint	planar	rough
78	80	1	3	2.1	8	joint	stepped	rough
84	83	1	3	0.9	6	joint	planar	smooth
84	154	1	4	1.6	11	joint	planar	rough
87	142	1	4	2.6	9	joint	planar	rough
67	183	1	5	0.9	7	joint	planar	rough
69	181	1	5	0.5	6	joint	planar	rough
78	169	1	5	1.2	7	joint	undulate	rough
59	176	1	5	0.5	6	joint	undulate	rough
74	176	1	5	0.9	7	joint	planar	rough
60	177	1	5	1.9	10	joint	planar	rough
74	183	1	5	2.4	9	joint	undulate	rough
67	187	1	5	1.6	10	joint	planar	smooth
73	166	1	5	0.5	6	joint	undulate	rough
68	171	1	5	1.2	8	joint	planar	rough
76	180	1	5	0.8	7	joint	planar	rough
75	181	1	5	0.8	6	joint	undulate	smooth
72	163	1	5	0.6	6	joint	planar	rough

72	182	1	5	0.6	6	joint	planar	smooth
75	164	1	5	0.4	6	joint	planar	smooth
70	169	1	5	2.1	10	joint	planar	smooth
62	179	1	5	0.4	6	joint	planar	rough
77	175	1	5	2	9	joint	planar	slick
68	169	1	5	0.5	6	joint	stepped	rough
73	168	1	5	1.1	7	joint	stepped	rough
72	168	1	5	0.5	6	joint	planar	v.rough
70	177	1	5	1	7	joint	planar	smooth
76	174	1	5	0.5	6	joint	undulate	rough
57	176	1	5	1.5	9	joint	planar	v.rough
66	160	1	5	2.3	11	joint	undulate	smooth
70	178	1	5	0.6	6	joint	planar	polished
76	166	1	5	0.6	6	joint	planar	v.rough
61	176	1	5	1.1	8	joint	undulate	rough
81	169	1	5	2	8	joint	planar	smooth
79	172	1	5	1.4	7	joint	planar	rough
68	187	1	5	0.4	6	joint	planar	rough

68	176	1	5	1.5	8	joint	planar	v.rough
58	189	1	5	2.4	12	joint	planar	rough
83	164	1	5	3.6	10	joint	planar	smooth
69	158	1	5	0.6	6	joint	planar	smooth
79	164	1	5	0.6	6	joint	planar	smooth
61	162	1	5	0.7	7	joint	stepped	rough
66	178	1	5	0.6	7	joint	planar	rough
65	173	1	5	0.5	6	joint	undulate	rough
63	176	1	5	1	8	joint	planar	rough
66	170	1	5	1.1	9	joint	planar	rough
75	172	1	5	1.6	8	joint	planar	rough
79	164	1	5	0.5	6	joint	planar	rough
64	176	1	5	3	12	joint	planar	polished
66	172	1	5	2	10	joint	planar	smooth
39	136	1	6	1.6	22	bedding	planar	smooth
61	125	1	6	1.3	17	bedding	planar	smooth
66	130	1	6	1.4	16	joint	stepped	smooth
55	122	1	6	1.6	19	bedding	planar	smooth

54	126	1	6	1.6	19	beddi ng	planar	smoot h
62	126	1	6	1.9	19	beddi ng	planar	smoot h
60	133	1	6	1.3	17	beddi ng	planar	smoot h
60	109	1	6	1.4	16	joint	steppe d	rough
54	126	1	6	1.9	20	beddi ng	planar	smoot h
63	129	1	6	1	15	beddi ng	planar	smoot h
63	123	1	6	1.7	18	beddi ng	planar	smoot h
63	115	1	6	1.3	16	beddi ng	planar	smoot h
47	119	1	6	1.5	19	beddi ng	planar	smoot h
56	133	1	6	1	16	joint	undula te	rough
54	119	1	6	0.9	15	joint	undula te	rough
51	119	1	6	1.7	20	beddi ng	planar	smoot h
51	137	1	6	1.7	20	beddi ng	planar	smoot h
53	122	1	6	1	16	joint	planar	v.roug h
53	112	1	6	1.2	16	joint	undula te	rough
54	126	1	6	2.1	21	beddi ng	planar	smoot h

65	53	1	7	8	26	shear	planar	slick
64	40	1	7	1	10	joint	stepped	smooth
76	47	1	7	10	20	shear	planar	slick
69	45	1	7	2.2	8	joint	planar	rough
65	38	1	7	1.9	8	joint	planar	rough
79	38	1	7	8	25	shear	planar	slick
74	48	1	7	1.9	8	joint	planar	smooth
61	38	1	7	1.9	8	joint	planar	v.rough
64	43	1	7	0.4	6	joint	planar	smooth
74	48	1	7	4.3	11	joint	undulate	smooth
67	48	1	7	2.2	8	joint	planar	rough
79	38	1	7	3.4	9	joint	planar	smooth
87	23	1		2.9	8	joint	planar	rough
85	106	1		1.5	11	joint	planar	smooth
84	214	1		1.7	7	joint	planar	v.rough
86	267	1		1.8	7	joint	planar	rough
86	45	1		2.2	7	joint	planar	smooth
87	296	1		1	6	joint	planar	rough
88	1	1		1.5	7	joint	planar	rough
77	322	1	2	3	14	joint	planar	rough

Appendix B: Numerical Modelling Solutions (Example)

Firm-Stiff clay

==========

STAGE: LB Auto

ANALYSIS TYPE: Strength Reduction

ELEMENT TYPE: Lower

TIME SCOPE: Short Term

K0g: K0 ENERGY K0 ERROR SOLVER STATUS

1.800E+03 6.397E-04 Converged

ADAPT ITR REDUCTION STABILITY

STEP FACTOR

---

1 1 1.000E+00 Stable

1 2 2.000E+00 Unstable

1 3 1.500E+00 Unstable

1 4 1.250E+00 Stable

1 5 1.375E+00 Stable

1	6	1.438E+00	Unstable
1	7	1.406E+00	Unstable
1	8	1.391E+00	Unstable
1	9	1.383E+00	Stable
2	1	1.383E+00	Stable
2	2	1.508E+00	Unstable
2	3	1.445E+00	Stable
2	4	1.477E+00	Unstable
2	5	1.461E+00	Stable
2	6	1.469E+00	Unstable
2	7	1.465E+00	Stable
3	1	1.465E+00	Stable
3	2	1.503E+00	Unstable
3	3	1.484E+00	Unstable
3	4	1.474E+00	Unstable
3	5	1.470E+00	Stable

No OF TRIANGLES = 848

No OF EDGES = 1292

No OF NODES = 445

BEST STRENGTH REDUCTION FACTOR = 1.470

==========

==========

==========

==========

STAGE: UB Auto

ANALYSIS TYPE: Strength Reduction

ELEMENT TYPE: Upper

TIME SCOPE: Short Term

K0g: K0 ENERGY K0 ERROR SOLVER STATUS

8.033E+02 2.916E-04 Converged

ADAPT ITR REDUCTION STABILITY

STEP FACTOR

---

1 1 1.000E+00 Stable

1 2 2.000E+00 Unstable

1 3 1.500E+00 Stable

1 4 1.750E+00 Unstable

1	5	1.625E+00	Stable
1	6	1.688E+00	Unstable
1	7	1.656E+00	Unstable
1	8	1.641E+00	Stable
2	1	1.641E+00	Unstable
2	2	1.504E+00	Stable
2	3	1.573E+00	Unstable
2	4	1.539E+00	Unstable
2	5	1.521E+00	Unstable
2	6	1.513E+00	Stable
3	1	1.513E+00	Unstable
3	2	1.475E+00	Stable
3	3	1.494E+00	Unstable
3	4	1.484E+00	Unstable
3	5	1.479E+00	Stable

No OF TRIANGLES = 944

No OF EDGES = 1495

No OF NODES = 496

BEST STRENGTH REDUCTION FACTOR = 1.484

==========
==========

Appendix C: Editor's Report

Sury Bisetty Academic Editing Services –

The pen is mightier than the sword

To whom it may concern,

I have edited the dissertation entitled: **ADVANCED RELIABILITY ANALYSIS OF ROAD-SLOPE STABILITY IN SOFT ROCK GEOLOGICAL TERRAIN** by **FHATUWANI SENGANI** submitted in fulfilment of the academic requirements for the Degree of Doctor of Engineering in the Department of Civil Engineering and Geomatics Faculty of Engineering and the Built Environment at the Durban University of Technology

Sury Bisetty
Professional Language and Technical Editor
22 May 2022

CONTACT DETAILS
Email: surybisetty11@gmail.com
Cell no: 0844932878
Tel.: 031 7622 766

MEMBER OF:
Professional Editor's Guild (BIS002)
South African Council of Educators (222277)

SAMEA (761237008553)

CERTIFICATION:
PEGSA: Critical Reading
Editing Mastery: How to Edit to Perfection
Complete writing, editing master class.
ELSEVIER – Editor's guide to …

Disclaimer: Please note, I provided language and technical editing as per discussion with the client. The **content and structure** of the paper were not amended in any way. The edited work described here may not be identical to that submitted. The author, at his/her sole discretion, has the prerogative to accept, delete, or change amendments/suggestions made by the editor before submission.

NB – in keeping with POPIA regulations all work related to this thesis will be deleted 3 months after completion.